Lim, Fannon Chwee Ning (2003) *A preliminary investigation into the effects of nonlinear response modification within coupled oscillators.* PhD thesis.

http://theses.gla.ac.uk/2106/

Copyright and moral rights for this thesis are retained by the author

A copy can be downloaded for personal non-commercial research or study, without prior permission or charge

This thesis cannot be reproduced or quoted extensively from without first obtaining permission in writing from the Author

The content must not be changed in any way or sold commercially in any format or medium without the formal permission of the Author

When referring to this work, full bibliographic details including the author, title, awarding institution and date of the thesis must be given

Glasgow Theses Service
http://theses.gla.ac.uk/
theses@gla.ac.uk

A PRELIMINARY INVESTIGATION INTO THE EFFECTS OF NONLINEAR RESPONSE MODIFICATION WITHIN COUPLED OSCILLATORS

by

Fannon Chwee Ning Lim

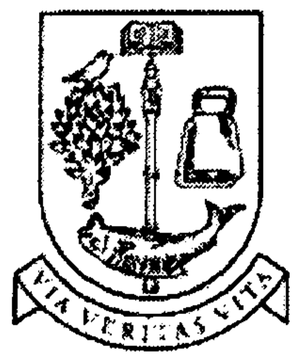

UNIVERSITY
of
GLASGOW

THESIS SUBMITTED IN FULFILLMENT OF THE REQUIREMENTS
FOR THE DEGREE OF DOCTOR IN PHILOSOPHY
TO THE FACULTY OF ENGINEERING
DEPARTMENT OF MECHANICAL ENGINEERING
UNIVERSITY OF GLASGOW

© Fannon C.N. Lim
June 2003

All Rights Reserved.
This work may not be reproduced in whole or in part,
by photocopy or other means, without permission of the author.

This thesis is produced under the accordance of British Standards BS 4821:1990

To My Family

COPYRIGHT

Attention is drawn to the fact that copyright of this thesis rests with its author. This copy of the thesis has been supplied on the condition that anyone who consults it is understood to recognise that its copyright rests with the author and that no quotation from the thesis and no information derived from it may be published, without prior written consent of the author.

This thesis may not be consulted, photocopied or lent by any library without the permission of the author for a period of two years from the date of acceptance of the thesis.

nonlinear (nŏn-lĭn'ē-ər) adj. Not in a straight line; Behaving in an erratic and unpredictable fashion; Unstable; Of or relating to a system of equations whose effects are not proportional to their causes. Such a set of equations can be chaotic; Of or relating to a device whose behaviour is described by a set of nonlinear equations and whose output is not proportional to its input.

response (rĭ-spŏns') n. A reaction, as that of an organism or a mechanism, to a specific stimulus.

modification (mŏd'ə-fĭ-kā'shən) n. The act of modifying or the condition of being modified; An alteration, adjustment or limitation.

Source: http://www.dictionary.com/

ABSTRACT

This thesis provides an account of an investigation into possible dynamic interactions between two coupled nonlinear sub-systems, each possessing opposing nonlinear overhang characteristics in the frequency domain in terms of positive and negative cubic stiffnesses. This system is a two degree-of-freedom Duffing oscillator coupled in series in which certain nonlinear effects can be advantageously neutralised under specific conditions. This theoretical vehicle has been used as a preliminary methodology for understanding the interactive behaviour within typical industrial ultrasonic cutting components. Ultrasonic energy is generated within a piezoelectric exciter, which is inherently nonlinear, and which is coupled to a bar-horn or block-horn to one, or more, material cutting blades, for example. The horn/blade configurations are also nonlinear, and within the whole system there are response features which are strongly reminiscent of positive and negative cubic stiffness effects. The two degree-of-freedom model is analysed and it is shown that a practically useful mitigating effect on the overall nonlinear response of the system can be created under certain conditions when one of the cubic stiffnesses is varied. It has also been shown experimentally that coupling of ultrasonic components with different nonlinear characteristics can strongly influence the performance of the system and that the general behaviour of the hypothetical theoretical model is indeed borne out in practice.

ACKNOWLEDGEMENTS

I am so grateful to those people who have made this research possible and those who have made my experience in the University one that I will always remember fondly.

Firstly, I would like to express my sincere gratitude to my supervisor, Professor Matthew Phillip Cartmell. His advise and guidance throughout the course of my postgraduate studies were invaluable, as was his patience and politeness that never failed during his supervision. I have learnt immeasurable knowledge which will definitely be beneficial to me in future. Wherever I am in life, the skills I learnt from him will serve me well. Thank you for being an advisor and a good friend.

Thanks also extend out to Dr Margaret Lucas and Mr Andrea Cardoni who have been a great advisor and a great colleague respectively. Both of them have been the driving machine with suggestions and useful discussions on the part on ultrasonics.

Also to the Engineering and Physical Sciences Research Council (EPSRC) and Nestlé UK, who provided me with the scholarships for this course of study. Mr Martin Harrop of Nestlé PTC York, UK for collaboration during this research, and the Department of Mechanical Engineering, University of Glasgow for the provision of computing and other facilities; these are greatly appreciated.

Lastly, to my family for their never ending support, understanding and encouragement throughout my courses of study in the University of

Glasgow. Without them, I would not have been able to achieve what I have today.

"Thank you so very much"

LIST OF FIGURES

LIST OF TABLES

TABLE OF CONTENTS

NOMENCLATURE

Symbols	Description	Units
a_1 , a_2	Amplitude responses	(m)
c_1 , c_2	Damping coefficients	(Ns/m)
h_1	Nonlinear cubic hardening spring stiffness	(N/m^3)
h_2	Nonlinear cubic softening spring stiffness	(N/m^3)
k_1 , k_2	Linear spring stiffnesses	(N/m)
m_1 , m_2	Masses	(kg)
t	Nondimensionalised time, $t = \omega_{e1} t^*$	
t^*	Time	(s)
x_1 , x_2	Nondimensionalised displacements, $x_{1,2} = \frac{x^*_{1,2}}{x^*_{ref}}$	
x_1^* , x_2^*	Displacements	(m)
x^*_{ref}	Reference displacement	(m)
A_1 , A_2	Complex amplitudes	(m)
F^* , F_1^* , F_2^*	Excitation force	(N)
F	Nondimensionalised excitation force, $F = \frac{F^*}{m_1 \omega_{e1}^2 x^*_{ref}}$	
T_n	n = 0 : Fast time scale; n = 1 : Slow time scale i.e. $T_0 = t$; $T_1 = \varepsilon t$	(s)
β_1 , β_2	Complex frequencies	(rad/s)
ε	Ordering parameter for method of multiple scales	
εv	External detuning parameter	(rad/s)

$\varepsilon\sigma_i$	Internal detuning parameters $i=1$: Case 1 – Superharmonic resonance $i=2$: Case 2 – Subharmonic resonance $i=3$: Case 3 – Primary Resonance	(rad/s)
$\gamma_1, \gamma_2, \gamma_3$	Nondimensionalised linear spring stiffnesses	
η_1, η_2, η_3	Nondimensionalised nonlinear spring stiffnesses	
$\zeta_1, \zeta_2, \zeta_3$	Nondimensionalised damping coefficients	
ω_{e1}, ω_{e2}	Undamped linear natural frequencies (i.e. Eigenvalues)	(rad/s)
ω_1, ω_2	Nondimensionalised natural frequencies, $\omega_1 = \sqrt{\gamma_1}$, $\omega_2 = \sqrt{\gamma_3}$	
Ω	Nondimensionalised excitation frequency, $\frac{\Omega^*}{\omega_{e1}}$	
Ω^*	Excitation frequency	(rad/s)

ACA	Adaptive control algorithm
ANC	Active noise cancellation
BIFD	No. of iterates (dots plotted) for each bifurcation parameter
BIFPI	Pre-iterates for each bifurcation parameter
BIFV	No. of parameter values in bifurcation diagram
CON	Connect consecutive dots of trajectories
DSP	Digital signal processors
ESPI	Electronic speckle pattern interferometry
IHB	Incremental harmonic balance
IPP	No. of iterates per plot
KB	Krylov-Bogolioubov
KBM	Krylov-Bogolioubov-Mitropolski

LDV	Laser Doppler vibrometer
LP	Lindstedt-Poincaré
MS	Method of multiple scales
NI	Direct numerical integration
ODE	Ordinary differential equation
OPCL	Open-plus-closed-loop
PI	No. of pre-iterates before plotting
SPC	Steps per cycle
1D	One-dimensional
3D	Three-dimensional

CHAPTER 1

INTRODUCTION

1.1 The Rise of Nonlinear Science

The 19th century was the century of classical mechanics but this has recently rather given way to scientific applications and initial technological proposals for relativistic and quantum mechanics in areas as diverse as computing and space craft propulsion. However, in the many technological applications of Newtonian mechanics the various, and complicated effects of *nonlinearity* have been shown to be pervasive in all areas. Nonlinear phenomena genuinely appear everywhere in our daily life and in many of our scientific works, and therefore today they represent one of the most important effects within research in most fields of science and technology. It can still be difficult to solve nonlinear problems, numerically and analytically, and even more difficult to establish high fidelity models for real-world nonlinear problems. Many assumptions have to be made, sometimes artificially, to make practical engineering problems solvable, leading to the potential loss of important information. So, one of our chief aims in general is to establish more reasonable nonlinear models for practical engineering problems, the physical sciences, and for the economic sciences, and so this ensures that nonlinear mechanics is of continuing interest to the

international applied science community. Particular engineering interest will continue to be directed to contributions concerned with the application of variational theory in order to deduce field equations and boundary/initial conditions, and towards the solution of inverse or hybrid problems of identification of optimal aerofoils, cascades, towards the solution of channels, and other important technology based engineering applications.

Most problems in natural sciences are not scale invariant, meaning that the responses of the system to increases in (generic) forces are not proportional to such increments, but rather that they respond to more complex interactions. When the response of a system to the addition of forces or scaled stimuli is not just the simple addition of the responses, or the scaling of the solution, we speak of the problems as being nonlinear.

Nonlinear problems appear almost everywhere within applied science; in lasers, electronics, fluid dynamics, biology, chemistry, medicine, signal processing, vibrations, rigid and flexible body multi-body dynamics, planetary orbits and spacecraft propulsion, as well as taking a role in certain aspects of sociology and economics. The review paper on the nonlinear dynamics of engineering components by Jerrelind and Stensson (2000) gives a comprehensive definition of inherently nonlinear behaviour in a wide range of practical components. Therefore, there exist innumerable potential new possibilities for nonlinear phenomena in all areas of contemporary and future science and technology.

1.2 Background

Mechanical and structural systems are inherently nonlinear with many sources of nonlinearities present in any system under consideration. Nonlinearities necessarily introduce a whole range of phenomena that are not found in linear systems. These include the well-known jump phenomenon, the occurrence of multiple solutions, the presence of modulations, specific shifts in natural frequencies, the generation of combination resonances, evidence of period-multiplying bifurcations and complicated chaotic motions. These various phenomena have all been investigated in many publications and the literature on nonlinear dynamics is huge. Books on nonlinear dynamics have been written by Nayfeh (1973), Nayfeh and Mook (1979), Sanders and Verhulst (1985), Thompson and Stewart (1986), Cartmell (1990), Moon (1992), Strogatz (1994), Nayfeh and Balachandran (1995), Thomsen (1997), Murdock (1999) and Tomlinson and Worden (2000).

One highly specialised, but extremely topical application area is that of high power ultrasonic tooling within modern manufacturing. This has emerged as an interesting and potentially very effective methodology within manufacturing but is largely unexploited due to observed reliability problems associated with the nonlinear behaviour of the systems that have been operated to date. It has recently been accepted that research is required to investigate and model the influence of ultrasonic energy generation, and its interaction with possibly beneficial mechanisms in ultrasonic tooling design in order to formulate solutions to certain observed nonlinear coupling effects which have been shown to be extremely

important (Lucas *et al.*, 2001). This research necessarily impinges on multiple blade ultrasonic cutting tool design, and in doing so attempts to establish a range of high power ultrasonic manufacturing tools within a standardised tool design approach for optimum performance. On that basis this research aims to define a new generation of ultrasonic tools by identifying generic models for practically necessary multi-component tools. Reliability of tuned components in ultrasonically assisted tooling is often poor due to energy leakage into non-tuned modes. The mechanism of energy leakage can be described by nonlinear vibration behaviour, and Lucas *et al.* (1998) have characterised the nonlinear vibration in ultrasonic tools by using a laser Doppler vibrometer and electronic speckle pattern interferometry. The serious reliability limitations imposed by deficiencies in current design practices are tackled in this thesis, by this first attempt to incorporate logically a mechanistic understanding of ultrasonic system nonlinearities. The outcome is a tuned ultrasonic tool design strategy, adaptable to a wide range of manufacturing processes and targeted towards reliability.

In this research, preliminary investigations into vibration response modifications in coupled oscillators are discussed. In order to establish a systematic basis for this, a simple coupled oscillator problem is proposed in which two single degree-of-freedom sub-systems are implemented, with the principal nonlinearity being a hardening and softening cubic stiffness effect, respectively, in each. This hypothesised theoretical vehicle in fact closely reflects the characteristics which emerge from measurements made on actual ultrasonic cutting tooling in which serially coupled components are encountered. Such systems routinely exhibit alternate hardening and

softening effects in this manner, notwithstanding their more complicated structural form. The hypothesised theoretical vehicle is shown to respond in a manner which mirrors that of a typical food-industry ultrasonic cutting system. Specifically, serially coupled structural components with different nonlinearities (i.e. hardening or softening) are shown to work together in response-modifying ways that are closely predicted by the simplified theoretical model. Although this model is not intended to define literally a typical ultrasonic cutting system it is still of use in that it consolidates a major phenomenon which is readily observable in such systems, and on that basis has intrinsic value.

This research explores the behaviour of the hypothesised theoretical model and then attempts to show that judicious attention to the same class of principal nonlinearities in the experimental system can lead to improved designs for applications to practical engineering systems such as ultrasonic cutting systems.

1.3 Objectives

Currently there are already many methods of controlling nonlinearity and Section 2.4 highlights and discusses some of them. However, this research provides a whole new perspective on nonlinear control, different from the widely used feedback control method. This new approach does not use any electronics or constant feedback from the system to achieve stable response behaviour. Instead, it provides an open-loop approach that modifies the nonlinearity of a system to achieve a more linear response. When a system is modified to become apparently more linear, it has the potential to become more predictable, possibly without additional effort directed to the control of stability.

1.4 Scope

Much research has been carried out on nonlinear systems modelled by the Duffing-type problems (Duffing, 1918), the Van Der Pol oscillator (Van Der Pol, 1927a; Van Der Pol and Van Der Mark, 1927b), Lorenz systems (Lorenz, 1963), Rössler attractor based systems (Rössler 1976), Chua's circuit (Chua, 1992), the Goodwin equation, and Hamiltonian systems in general. The research within this thesis stems from attempting to understand the interactions of nonlinear components theoretically; the classical Duffing equation is used to analyse the effect of coupling within a two degree-of-freedom nonlinear oscillator system which closely represents the proposed hypothesised theoretical vehicle.

1.4.1 A review of basic phenomena within systems governed by the Duffing equation

The Duffing equation is frequently cited in a form containing a cubic nonlinearity, linear viscous damping, linear stiffness and a single-frequency excitation.

$$\ddot{x} + 2\zeta\dot{x} \pm h x^3 + \omega_0^2 x = A\cos\Omega t \quad [1] \qquad \textbf{(1.4-1)}$$

---

[1] Note that all notations in Chapters 1 and 2 do not follow those in the nomenclature but of the original papers.

Figure 1-1 shows representative curves for the general cases where $h=0$, $h>0$ and $h<0$. On comparing these frequency response curves it is seen that the nonlinearity bends the curve to the right when $h>0$ and to the left when $h<0$. These are well known as hardening and softening nonlinearities respectively. When $h=0$, the curve is in linear response.

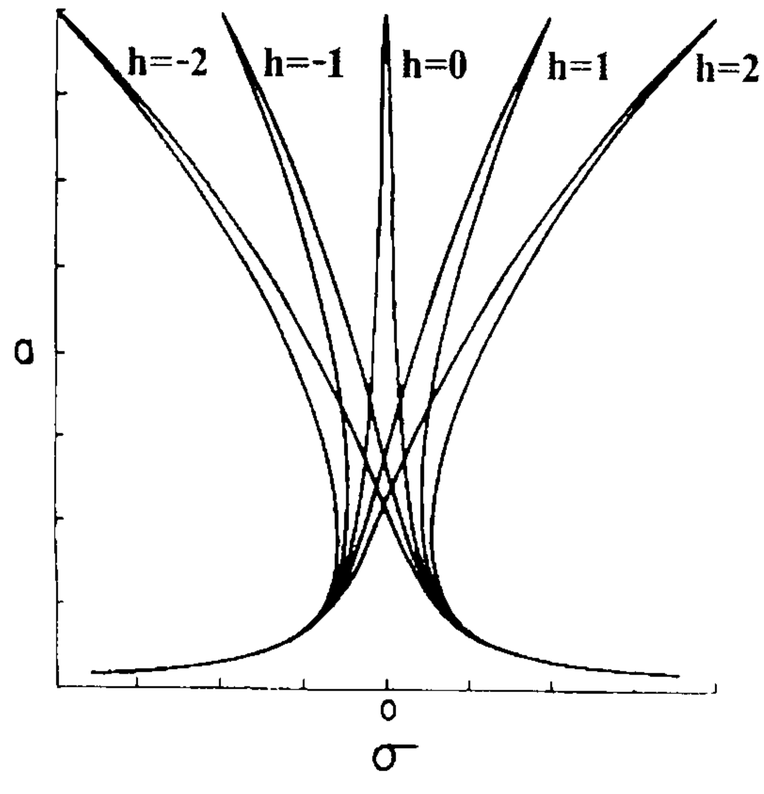

Figure 1-1: Frequency-response curves for different values of coefficient h in a Duffing equation (Effect of nonlinearity) – Nayfeh & Mook (1979)

The well-known 'jump phenomenon' is evident in a nonlinear response of the Duffing system. For a hardening nonlinearity, one can assume that an experiment may be performed in which the amplitude of the excitation is held constant, the frequency of the excitation (i.e. σ) is very slowly varied up and down about the linear natural frequency, and the amplitude (i.e. a) of the harmonic response is observed. The experiment is started at a frequency corresponding to point 1 in Figure 1-2(a). As σ decreases the response travels through point 2 to point 3, and a increases. As σ is decreased further, a jump in a from point 3 to point 4 takes place, after which a decreases smoothly with decreasing σ. Conversely, if

the experiment is started at point 5 and then σ is increased, a increases until point 6 is reached. As σ is increased further, a jump in a from point 6 to point 2 takes place, after which a once again decreases smoothly with increasing σ. The maximum amplitude corresponding to point 6 is only attainable when approached from a lower frequency. The portion of the response curve between points 3 and 6 is unstable and hence cannot be produced experimentally.

In the case of a softening nonlinearity, one could imagine that the experiment is started from point 1 in Figure 1-2(b), and then σ is slowly decreased so that a jump from point 3 to point 4 takes place. For a sweep in the opposite direction starting at point 5 and increasing σ, a jump from point 6 to point 2 occurs. Likewise, the portion between point 3 and 6 is unstable. Thus, these jumps are nonlinear phenomena and take place within hard as well as soft systems.

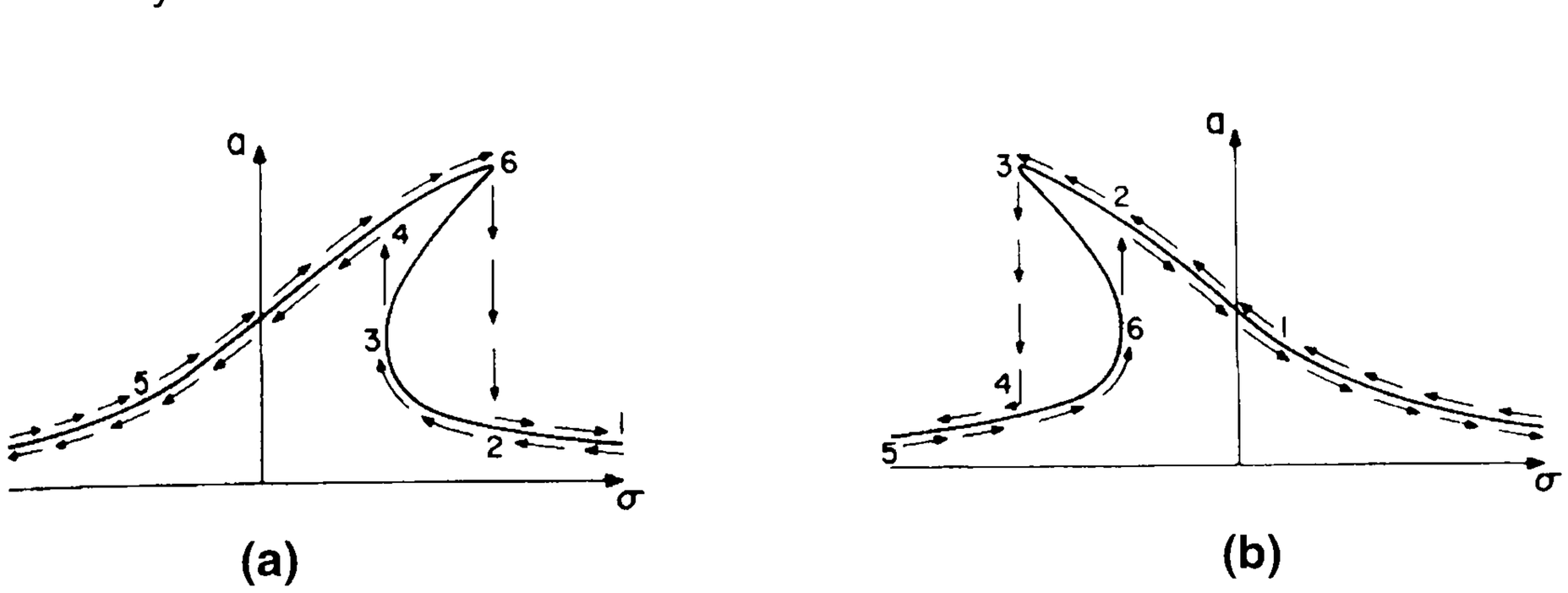

Figure 1-2: Jump phenomena within a typical Duffing system; (a) h > 0; (b) h < 0 – Nayfeh & Mook (1979)

System dynamics within the Duffing equation have been extensively explored by Ueda (1979, 1980a, 1980b). Ueda has shown that however small uncertain factors may be in nonlinear systems, they sometimes bring statistical properties into phenomena, depending on the global structure of the solutions of

the differential equations of the system. The dependence of the attractors on the system's parameters was highlighted by Ueda (1979) when he considered the following Duffing equation,

$$\ddot{x} + k\dot{x} + x^3 = B\cos t \qquad \textbf{(1.4-2)}$$

First he showed the change of attractors through Poincaré maps where the excitation force, B is varied while the damping, k is kept constant at 0.1. Outlines of the attractors in such a case are shown in Figure 1-3. Figure 1-3(a)[2] shows a completely stable period-3 motion, and as B is slightly increased, a fluctuation is brought into the process. This state is shown in Figure 1-3(b). Further increase in B results in the abrupt growth of the fluctuation and a randomly transitional process develops. This motion continues until B reaches 13.3 and the attractors in such cases are shown in Figure 1-3(c) to (g). A catastrophe occurs at some value of B between 13.3 to 13.4, and the randomly transitional process is replaced by a harmonic oscillation as in Figure 1-3(i)[2]. Next, the damping, k is varied while B is kept constant at 12.0. Figure 1-4 shows the effect of varying the damping parameter, and one can conclude that when the damping coefficient k is small, the size of the attractor is large, but as k increases, the attractor decreases.

The same equation was revisited by Ueda (1980a) where he presented 'a picture book of regular and chaotic motions' via phase planes and Poincaré maps for different damping and forcing levels.

---

[2] Permission has been granted for the reproduction of these, and all other, results from the literature, however in this case the periodic points were not clearly reproduced on the available original, and therefore have not transferred successfully into the forms given overleaf. The reader is asked to accept that they are indeed present in the original work.

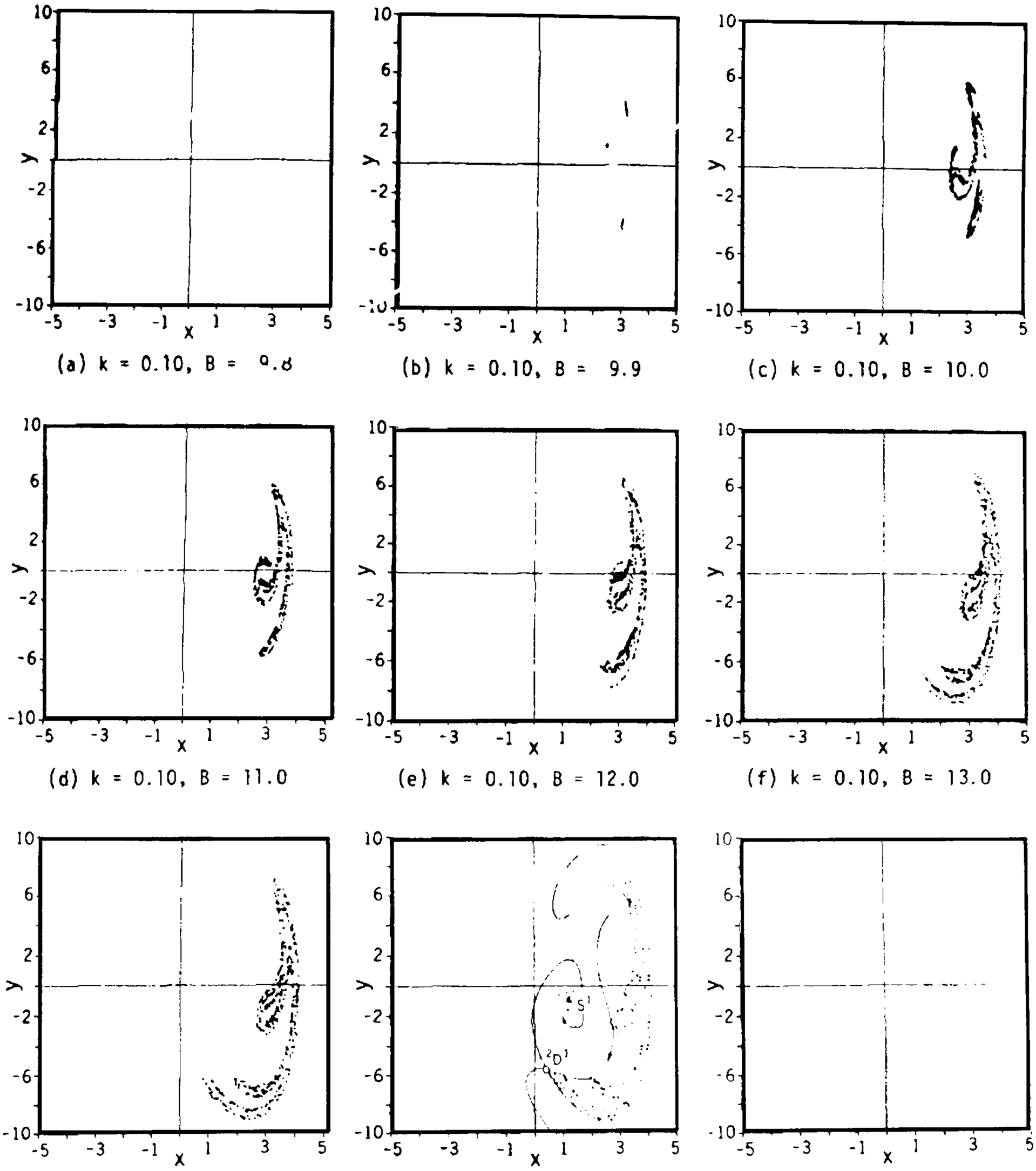

(a) k = 0.10, B = 9.8 (b) k = 0.10, B = 9.9 (c) k = 0.10, B = 10.0

(d) k = 0.10, B = 11.0 (e) k = 0.10, B = 12.0 (f) k = 0.10, B = 13.0

(g) k = 0.10, B = 13.3 (h) Transient state (i) k = 0.10, B = 13.4

Figure 1-3: Poincaré maps of the Duffing oscillator for various values of B; k = 0.10 – Ueda (1979)

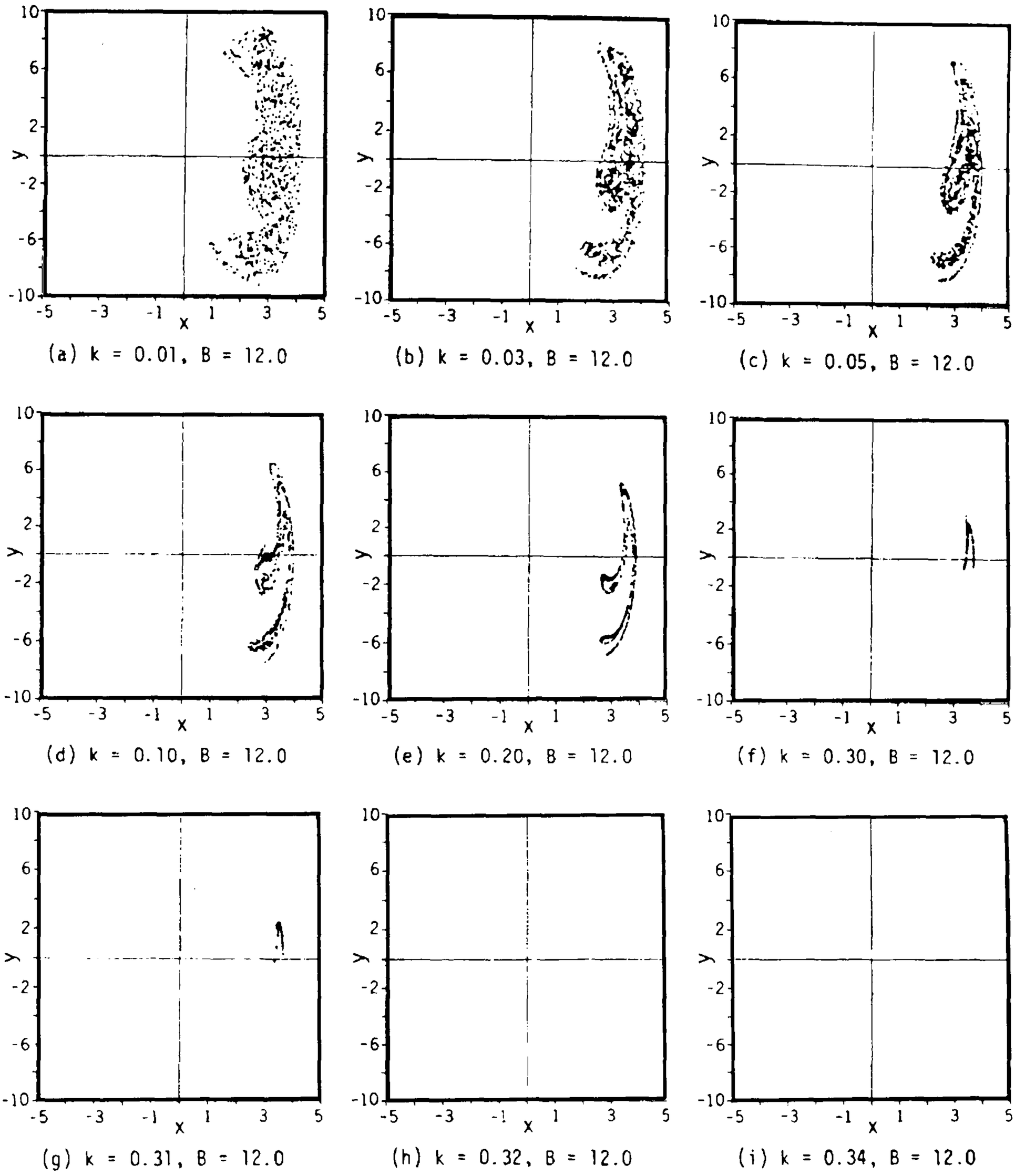

(a) k = 0.01, B = 12.0 (b) k = 0.03, B = 12.0 (c) k = 0.05, B = 12.0

(d) k = 0.10, B = 12.0 (e) k = 0.20, B = 12.0 (f) k = 0.30, B = 12.0

(g) k = 0.31, B = 12.0 (h) k = 0.32, B = 12.0 (i) k = 0.34, B = 12.0

Figure 1-4: Poincaré maps of the Duffing oscillator for various values of k; B = 12.0 – Ueda (1979)

1.4.2 The approach

A preliminary investigation to achieve near linear vibration is presented in this thesis by studying the effect of response modification within coupled nonlinear oscillators. In this research, two single degree-of-freedom systems of opposite nonlinear characteristics are coupled in series. The methodology behind this is based on the premise that modifications to the individual systems' responses may be obtainable in such a way that the overall response behaviour of the two degree-of-freedom model can be shown to exhibit certain key features of a linear system response characteristic. This can be shown to have direct relevance to the ultrasonic cutting systems which are the principal motivations for the whole research programme.

In order to summarise the approach, one may start by assuming a single degree-of-freedom system in which the stiffness is characterised by $(k_1 x_1 + h_1 x_1^3)$. The resonance graph for this system has hardening characteristics as shown in Figure 1-5(a). Another single degree-of-freedom system with an opposite nonlinear stiffness of $(k_2 x_2 - h_2 x_2^3)$ has the characteristic of Figure 1-5(b) in which the resonance graph displays softening characteristics. So, by coupling the above two systems together it is interesting to see if the characteristics of the response of the new two degree-of-freedom system can be modified towards a generally more linear behaviour, as shown in Figure 1-5(c). This proposal is potentially useful

because the effects of nonlinearities can then be reduced, modified, or possibly even eliminated by simply combining appropriate sub-systems together. The theoretical model of this system takes the convenient simplified form of a two degree-of-freedom Duffing oscillator system that will be discussed more in details in Section 3.1.

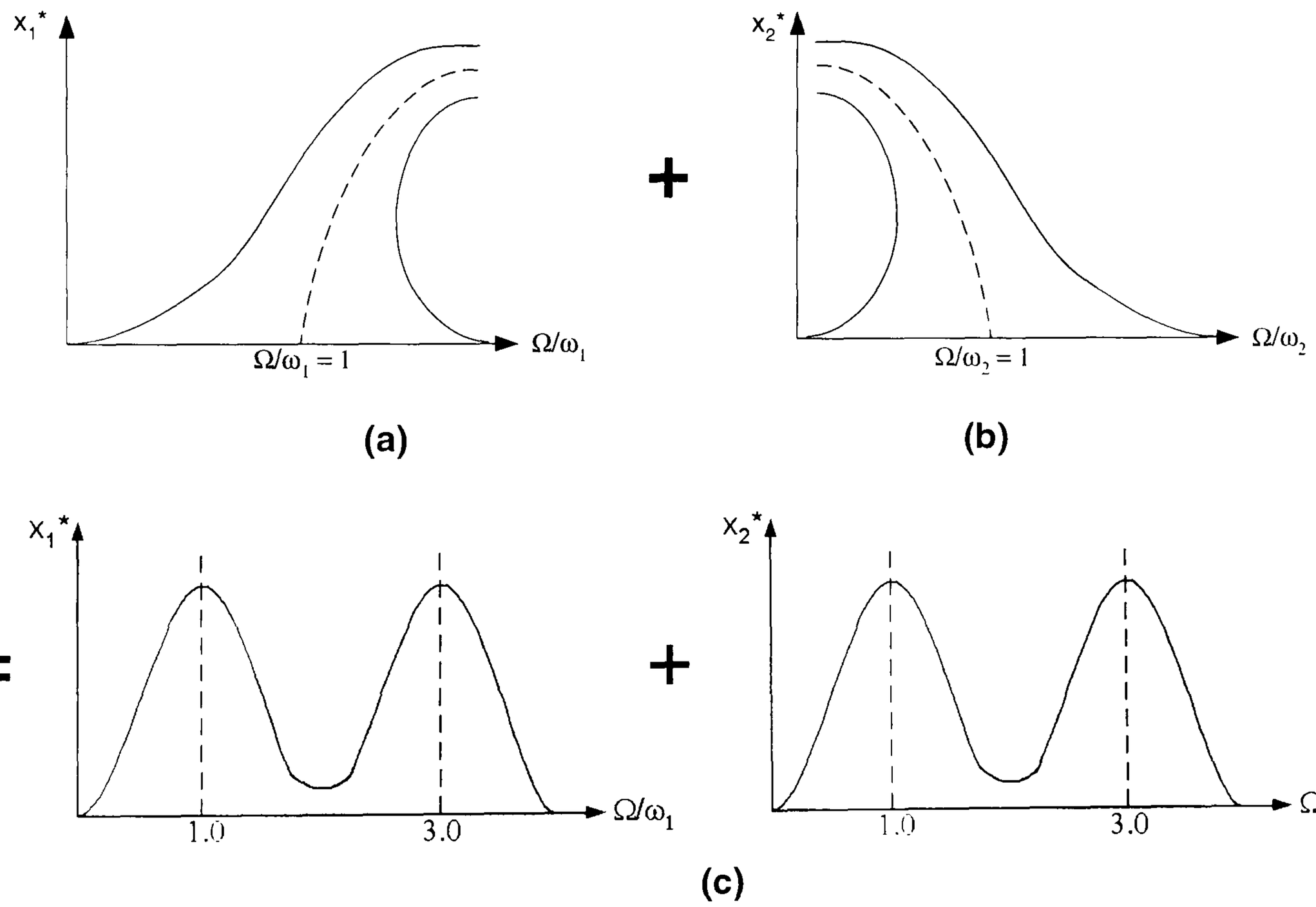

Figure 1-5: Conceptual summary of the nonlinear response modification in the theoretical model
(a) hardening cubic stiffness; (b) softening cubic stiffness;
(c) linear output response of coupling (a) + (b)

1.5 Outline and Methodology

This thesis is divided into seven chapters. It begins off with an introduction in Chapter 1 followed by literature review in Chapter 2. Analytical and numerical methods are used to derive and plot the nonlinear response modification of the hypothesised model in Figure 3-1. Chapter 3 applies the Method of Multiple Scales and Chapter 4 uses a direct numerical integration method.

Chapter 5 strengthens the above results with the numerical investigation of the system dynamics in the form of bifurcation diagrams and calculated Lyapunov exponents. Phase planes, Poincaré maps and time plots are also plotted for more in-depth understanding into the details of the system dynamics. All these will, in turn, provide one with a better comprehension of the overall dynamics of the proposed system.

Besides theoretically understanding the effects of the nonlinear coupling, experiments have been carried out on the coupling of different ultrasonic components to simulate the theory of nonlinear response modifications. These are discussed in Chapter 6.

Chapter 7 presents a discussion and comparison of the results from the four different methods of analysing the coupled system, and the conclusions of the thesis is followed in the next chapter. Recommendations for further work are also suggested in Chapter 9.

A list of journal and conference publications produced during the course of this postgraduate research by the author and others, is given after the References.

CHAPTER 2

LITERATURE REVIEW

2.1 Historical Perspective

The history of Dynamics has progressed considerably since it was recognised formally as a branch of physics in the mid-1600s. Since the invention of differential equations within Europe by Isaac Newton [1643 – 1727], subsequent generations of mathematicians and physicists have proceeded to develop the subject from the bases of quantitative, and then later, qualitative analysis. In the late 1800s, Henri Poincaré [1854 – 1912] introduced the motion of chaos, and this has underpinned the modern subjects of dynamics and dynamical systems. Extensive studies of nonlinear oscillators led to the identification of the cubic phenomenon in the so-called Duffing oscillator (Duffing, 1918), and this system along with several other fundamental nonlinear oscillations has been exhaustively investigated by Ueda, Thompson, Nayfeh, Holmes and other major researchers in the field. Seminal research in nonlinear systems is attributable to Lorenz, Feigenbaum and Mandelbrot and from their pioneering work key constructs within Dynamical systems theory have been defined and explored. Figure 2-1 summarises this history.

Dynamics – A Capsule History

1666	Newton	Invention of calculus, explanation of planetary motion
1700s		Flowering of calculus and classical mechanics
1800s		Analytical studies of planetary motion
1890s	Poincaré	Geometric approach, nightmares of chaos
1920 - 1950		Nonlinear oscillators in physics and engineering, invention of radio, radar, laser
1920 – 1960	Birkhoff Kolmogorov Arnol'd Moser	Complex behaviour in Hamiltonian mechanics
1963	Lorenz	Strange attractor in simple model of convection
1970s	Ruelle & Takens	Turbulence and chaos
	May	Chaos in logistic map
	Feigenbaum	Universality and renormalisation, connection between chaos and phase transitions
		Experimental studies of chaos
	Winfree	Nonlinear oscillations in biology
	Mandelbrot	Fractals
1980s		Widespread interest in chaos, fractals, oscillators, and their applications

Figure 2-1: History of Dynamics - Strogatz (1994)

2.2 Nonlinear Dynamics

Nonlinearity is now recognised as one of the fundamental tenets of dynamics and has been the focus of an enormous research effort in recent years. Many studies have, in particular been based on the Duffing oscillator in different attempts to quantify and map the local and global dynamics of systems in which softening and hardening nonlinearities feature significantly. An early article by Morozov (1976) presented a qualitative study of a softening Duffing equation, viz., the boundedness of the number of resonances and periodic solutions, the existence of heteroclinic solutions and the behaviour of solutions in a neighbourhood of an unperturbed separatrix contour. Over twenty years ago, Ueda (1979, 1980a, 1980b) extensively studied the steady-state chaotic behaviour, and randomly transitional phenomena, in a system governed by a hardening Duffing equation. He showed that the nonlinear system under consideration could exhibit chaotic responses (under harmonic excitation) in certain parameter regimes. By combining second-order perturbation solutions with an assessment of stability by means of Floquet analysis, Nayfeh and Sanchez (1989) developed an approximate procedure for the generation of bifurcation diagrams in a forced softening Duffing oscillator. In a nonlinear system, jump phenomena occur regularly and a hardening system reported by Soliman (1997) showed that for small excitation levels the system exhibited what appeared to be linear behaviour, however this invariably became nonlinear as the excitation levels were increased, and unpredictable jumps *to* and *from* resonance were clearly evident.

Vibration isolators consisting of polymeric materials are used extensively in various forms of vibration control. Nonlinearities in these systems can arise from its geometrical effects, the mode of loading, the material properties or combinations of all three. Harris and Stevenson (1986), Harris (1987), Mallik *et al.* (1999), have experimentally identified that polymeric materials exhibit forms of softening nonlinearity in their stiffness and damping characteristics. They have also shown that the nonlinearity in the damping characteristic is seen to be more pronounced than that in the stiffness for these materials.

Two fundamental nonlinear formulations based on two different strategies have been extended by Majed and Raynaud (2003) for the analysis of a nonlinear structure. The first formulation exploits the eigensolutions of the associated linear system and the dynamic characteristics of each localised nonlinearity, while the second formulation was developed using the linearised eigensolutions which are calculated by means of an iterative process. Their proposed formulations led to coherent results between theoretical and experimental results and was validated for two cases; one being the stiffness nonlinearity effects on transfer functions, and the second one was on the stiffness and damping nonlinearity effects on transfer functions. The strengthening of the stability of the solution around the resonance frequency was found to depend on several parameters particularly the sine-sweep frequency, the weighting coefficient, and the convergence criteria.

2.3 Nonlinear Coupling

The dynamics of coupled anharmonic oscillators are of considerable general interest due to the fact that such models are good candidates for the description of various physical and electromechanical systems. Among the reported coupled anharmonic oscillators, the most intensively studied examples are typically the Duffing oscillators (Umberger *et al.*, 1989; Dressler and Lauterborn, 1990; Asfar, 1992; Kapitaniak, 1993; Kozlowski *et al.*, 1995; Woafo *et al.* 1998), and the Van Der Pol oscillators (Rand and Holmes, 1980; Chakraborty and Rand, 1988; Maccari, 2003).

Woafo *et al.* (1998) used the method of multiple scales to find solutions to a two nonlinearly coupled oscillators subjected to an external periodic force. Chaotic behaviour emanating from the well-known period-doubling bifurcation was evident in this system. However, the coupling in the system of Woafo *et al.* (1998) is fundamentally different to that reported in this thesis because of the predominant presence of quadratic coupling terms and the non-existence of nonlinear cubic coupling. The pair of nonlinear differential equations analysed by Woafo *et al.* (1998) are as follows,

$$\ddot{x} + \lambda_{10}x + \omega_0^2 x + \gamma_0 x^3 - \alpha_{10}q - \beta_{10}q^2 = F\cos(\omega t) \qquad \textbf{(2.3-1)}$$

$$\ddot{q} + \lambda_{20}\dot{q} + \omega_1^2 q - \alpha_{20}x - \beta_{20}qx = 0 \qquad \textbf{(2.3-2)}$$

where x and q are the coordinates, λ_{10} and λ_{20} are the viscous damping coefficients, ω_0 and ω_1 the natural frequencies, and γ_0 the cubic nonlinearity coefficient. The coupling between the oscillators is characterised by the coefficients α_{10}, α_{20}, β_{10} and β_{20}. Oscillatory states of the model were analysed by the method of multiple scales, and the effects

of equal coupling between the oscillators ($\alpha_1 = \alpha_2 = \alpha$) on the amplitudes a_1 and a_2 are shown for different values of external detuning parameter σ in Figure 2-2. The behaviour of the coupling-resonance curves show that when the oscillator move away (σ increases) from the exact external resonance point ($\sigma = 0$), their amplitude may be singled-valued or multi-valued depending on the coupling coefficient α. This theoretically represents an electrostatic microphone, where the acoustic waves may be converted into an electrical signal with minimal distortion, and the parameters of both electrical and mechanical parts must be chosen properly to satisfy this condition. Thus, the amplitude of the oscillators must be single-valued in order to avoid distortion.

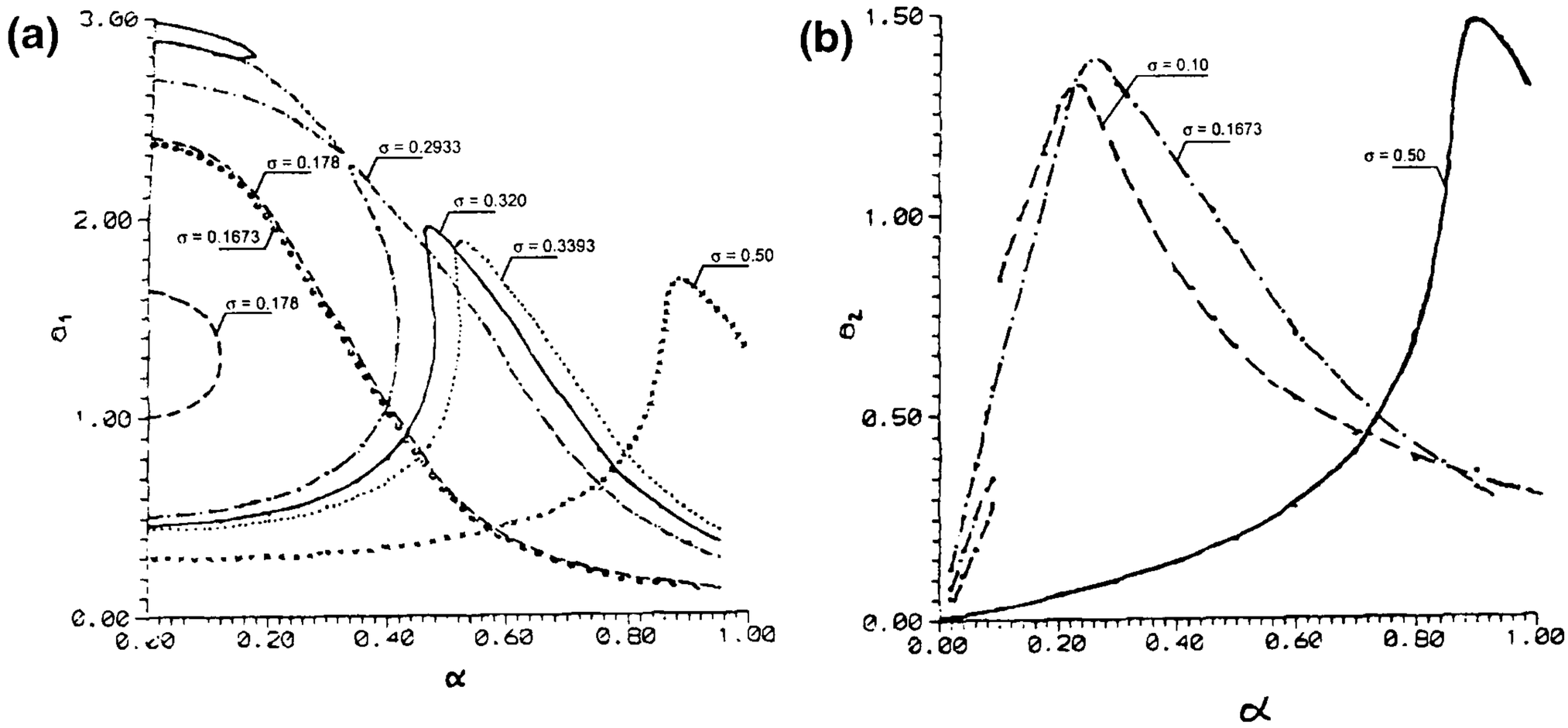

Figure 2-2: Coupling-resonance curves with $\lambda_1 = \lambda_2 = 0.1$; $\gamma = 0.1$; $F = 0.3$; $\sigma_0 = 0$; (a) $a_1(\alpha)$; (b) $a_2(\alpha)$ - Woafo *et al.* (1995)

The local and global bifurcations of a two mutually coupled, identical Duffing oscillators that are driven by an external sinusoidal force have been investigated by Kozlowski *et al.* (1995). The equations for the investigated system were,

$$\ddot{y}_1 + d\dot{y}_1 + y_1 + y_1^3 - c(y_3 - y_1) = f\cos\omega t \qquad \textbf{(2.3-3)}$$

$$\ddot{y}_3 + d\dot{y}_3 + y_3 + y_3^3 + c(y_3 - y_1) = 0 \qquad \textbf{(2.3-4)}$$

where f is the amplitude of the driving force, the frequency ω is used as the control parameter in the bifurcation diagrams, the damping parameter, d and coupling constant c, are fixed at 0.1 and 5 respectively. Note that this system is different from the one analysed in this thesis as it is coupled merely by the linear stiffness, whereas the thesis model is coupled via the linear damping, the linear stiffnesses and also by the cubic nonlinear stiffnesses. The bifurcation sequence of this system shows aspects of recurrence for different frequency regions. Figure 2-3 compares that for different frequency regions, the same structure consisting of symmetry-breaking (sb) and Hopf bifurcations (H) are shown; i.e. (sb-sb)-(sb-sb) for Figures 2-3(a) and (c), and (sb-sb)-(H-H)-(sb-sb) for Figures 2-3(b) and (d). These repeated subpatterns are similar to the structure observed for single, periodically driven, Duffing oscillators (Sato *et al.*, 1983; Scheffczyk *et al.*, 1991), but in a more complicated way and show additional occurrences of Hopf bifurcations.

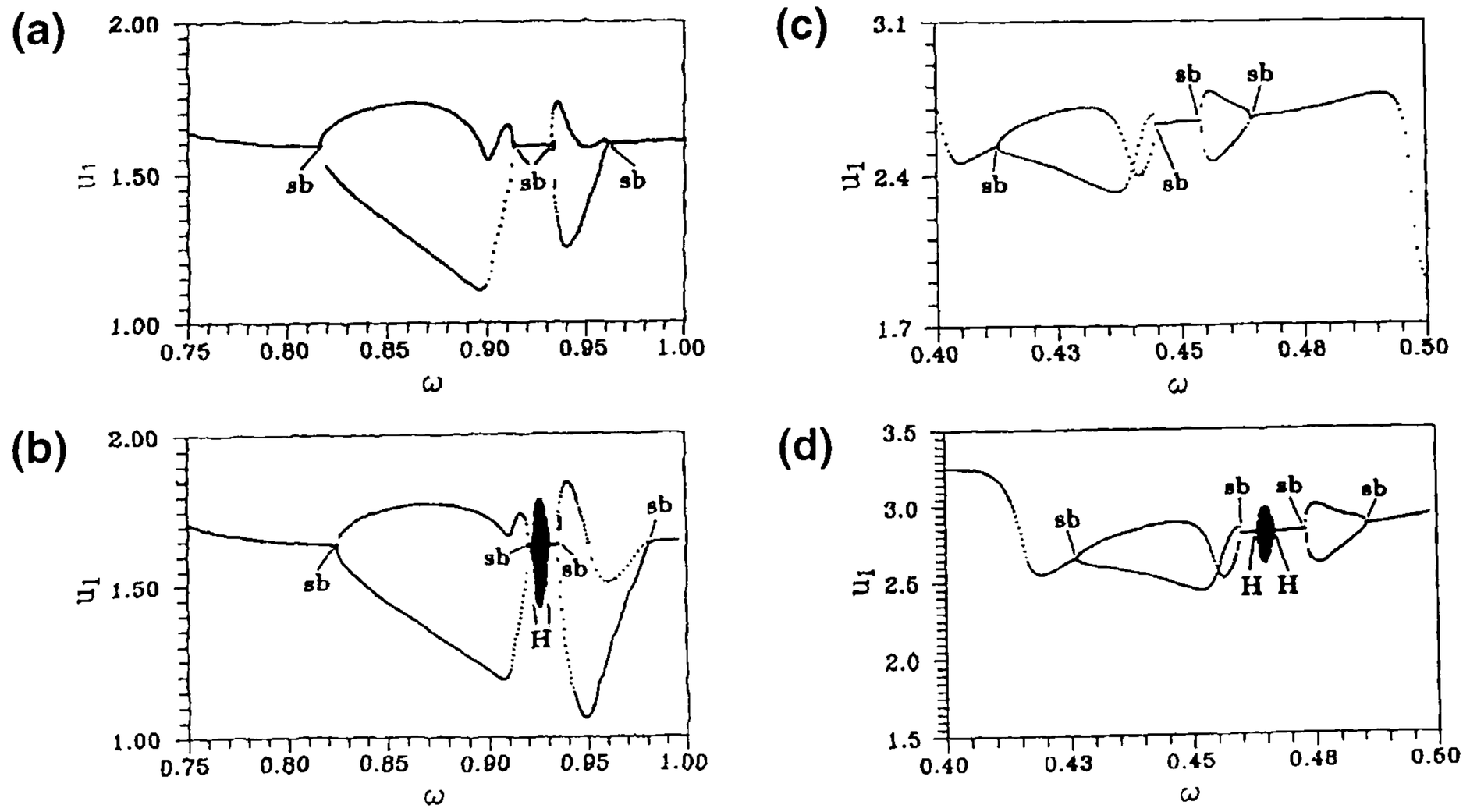

Figure 2-3: Bifurcation diagrams for different driving amplitudes; (a) f =4.5; (b) f =4.8; (c) f =20; (d) f =25 – Kozlowski *et al.* (1995)

2.4 Nonlinear Control

Nonlinearity is generally reckoned to be undesirable in most practical engineering systems, not least because of the analytical difficulties that are perceived to go with it. However, it is a fact that most, if not all, real physical systems exhibit significant nonlinear behaviour. Control of nonlinear structural systems has received considerable attention, and various control methods have been proposed and studied for applications in different discipline areas. These include different algorithms for pulse control (Masri *et al.*, 1981, 1982; Reinhorn *et al.*, 1987a, 1987b), combining passive control with an active control (Abdel-Rohman and Nayfeh, 1987), stochastic dynamic programming (Shefer and Breakwell, 1987), optimal control based on a numerical approach (Kamat, 1988), acceleration control (Nagarajaiah *et al.*, 1993; Reinhorn *et al.*, 1993; Riley *et al.*, 1993), dynamic linearisation (Reinhorn *et al.*, 1993; Yang *et al.*, 1994a), nonlinear control (Yang *et al.*, 1994b; Shing *et al.*, 1995), and neural networks (Nerves *et al.*, 1995).

In addition to general 'nonlinearity', chaos is a robust phenomenon exhibited by the majority of nonlinear systems and leads to potential behaviour patterns of extreme complexity. Recent investigations have clearly shown that chaotic motion can be controlled or directed towards a desired regular orbit by means of preassigned, and small, perturbations, either to the system parameters or through the addition of weak external forces. The associated control methods can be broadly classified into (i) feedback and (ii) non-feedback methods.

Recent research on the response of systems exhibiting nonlinear cubic damping have been reported by Shekhar *et al.*(1998) who studied the

effect of nonlinear damping on the performance of a single degree-of-freedom shock isolator system and showed that this appreciably affects the response. Specifically, a small negative coefficient for the damping term is more favourable than a positive coefficient in generating a considerable reduction in the peak of the acceleration response. In a follow-up paper, Shekhar *et al.* (1999) proposed that three-element and two-stage isolators are more effective when in the presence of nonlinear cubic damping. In another publication, Ravindra and Mallik (1995) showed how nonlinear damping can be used as a passive mechanism to suppress chaos. Besides interpreting the behaviour of nonlinear cubic damping by Shekhar *et al.*, and Ravindra and Mallik, the principal aim of this thesis is to give a detailed discussion of the coupling of two opposite nonlinear stiffnesses, and their effects on the nonlinearity of the coupled system.

In the well-known publication of Ott *et al.* (1990), chaos is controlled by careful choice of a small perturbation parameter in order to create a variety of attracting periodic motions, from which the most desirable attractor can be selected. Since this postulation was made interest in such approaches has increased, and it has been applied in a variety of physical experiments such as a gravitationally buckled amorphous magnetoelastic ribbon, an externally driven nonlinear oscillator, a pendulum, an elastic panel subjected to a combination of supersonic gas flow and quasistatic loading, and a periodically excited nonlinear elastic panel near a buckled state, discussed by Ditto *et al.* (1990), Pyragas and Tamaševičius (1993), Hubiger *et al.* (1994), Bolotin *et al.* (1998) and Chow and Maestrello (2001), respectively.

High frequency parametric vibration and amplitude modulation of the forcing function have both been used by Chow and Maestrello (2001) as the basis for a general method of vibrational control for a certain class of nonlinear evolution equations. The use of high frequency parametric vibration introduces a change in some system parameter in order to ensure static stability, whilst modulation of the forcing amplitude, if needed, can be used to stabilise an unstable periodic motion. Maestrello (2001) used a method that requires knowledge of the initial unstable disturbances in terms of frequency, amplitude and phase, or their equivalent temporal values, to cancel growth after several bifurcations from periodic to chaotic states.

Singer *et al.* (1991) suppressed chaos in a simple dynamical system (i.e. a thermal convection loop) by making small adjustments to the heating rate in response to events detected inside the loop (feedback control).

The Duffing oscillator has been a traditionally useful model for the nonlinear behaviour of certain systems. Suhardjo *et al.* (1992) presented a method of optimal polynomial control, based on the series expansion of the cost function and the indicial notation of tensor algebra (O'Sullivan and Sain, 1985) for the control of Duffing systems. Recently, Agrawal *et al.* (1998) studied the applications of two control strategies to Duffing oscillators; namely an optimal polynomial control (Agrawal and Yang, 1995) and robust sliding mode control (Yang *et al.* 1994c).

Raj and Rajasekar (1997) have studied the transfer from one attractor to another coexisting attractor in two coupled Duffing oscillators by means of an open-plus-closed-loop (OPCL) method and adaptive control algorithm (ACA). Interestingly, migration from chaos to periodic motion is possible by both OPCL and ACA methods. In contrast to the linear

feedback methods, where the control function must be on constantly, the advantage of these two methods (OPCL and ACA) is that control can be switched off once the system trajectory reaches the basin of attraction of the goal dynamics. Figure 2-4 shows the transfer of the system dynamics from the limit cycle X_+ to X_-, and Figure 2-5 illustrates the migration from chaotic motion to the chosen goal orbit by the OPCL and ACA method.

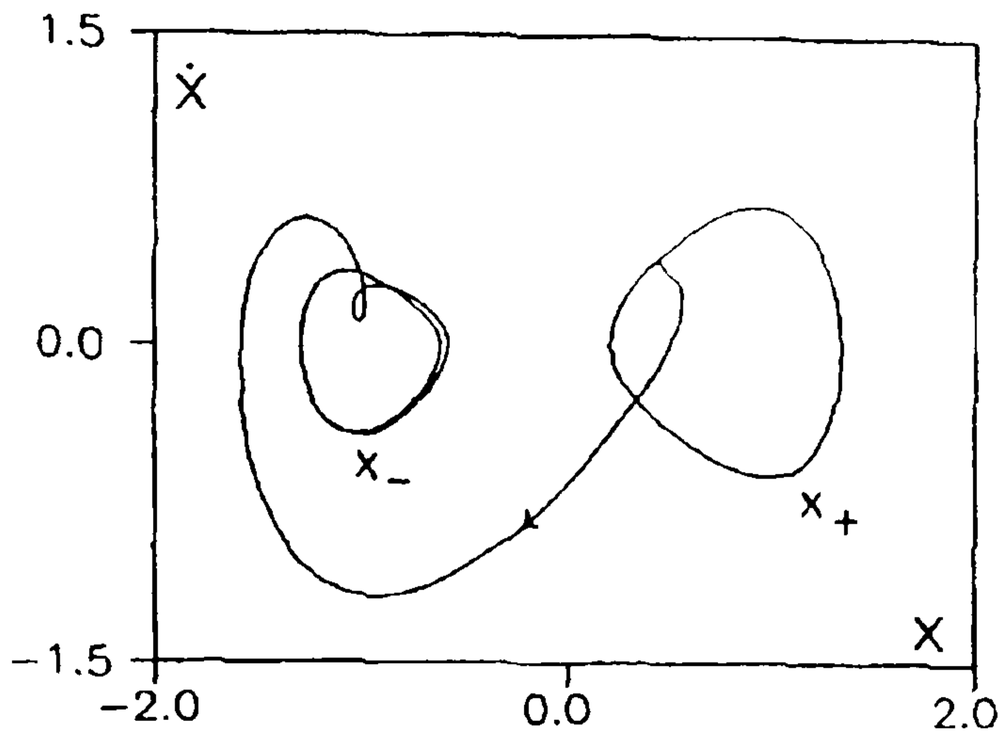

Figure 2-4: Migration dynamics from the limit cycle X_+ to X_- of the two coupled Duffing oscillators by OPCL method - Raj and Rajasekar (1997)

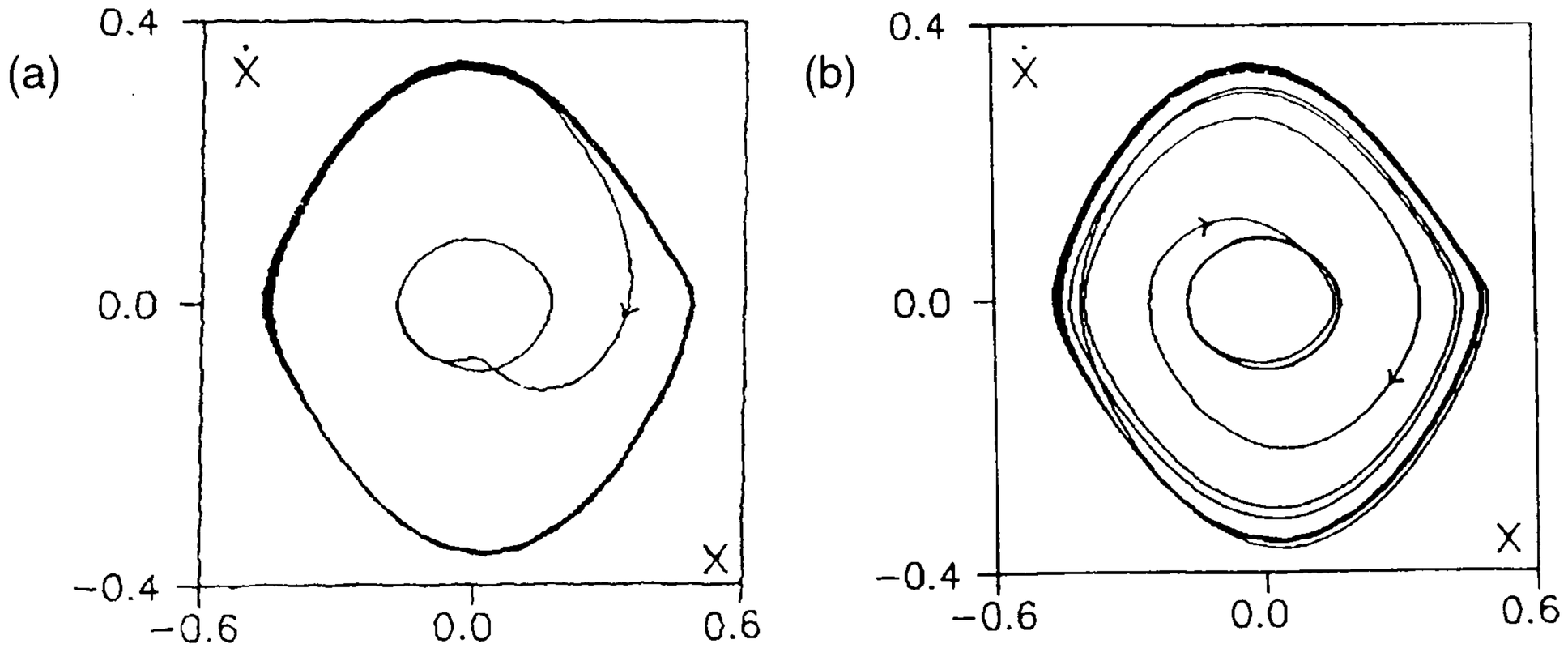

Figure 2-5: Migration from chaotic motion to a coexisting periodic orbit by the (a) OPCL method; (b) ACA method - Raj and Rajasekar (1997)

The proposed nonlinear response modification in the context of this thesis is largely relevant to acoustic systems. Acoustic problems in the environment have gained attention due to the tremendous growth of

technology that has led to noisy engines, heavy machinery, pumps, and a myriad other noise sources. Hence, exposure to high decibels of sound proves damaging to humans from both a physical and a psychological aspect. Although the classical technique of using a passive acoustic approach in order to cancel noise, such as sound absorption and isolation, both of which are inherently stable and effective over a broad band of frequencies, these systems are limited to fixed structures and prove to be impractical where space is at a premium and the added bulk can be a hindrance. Various signal processing techniques have been proposed over the years for noise reduction. Digital Signal Processors (DSPs) have shrunk tremendously in size and cost while their processing capabilities have grown exponentially. The use of DSPs include applications within hearing aids, headsets, and hearing protectors, for example.

Besides these techniques, one worthy of particular mention is the concept of Active Noise Cancellation (ANC). ANC is an electroacoustic methodology that cancels the primary unwanted noise by generating an 'antinoise' of equal amplitude but opposite phase, thus resulting in an attenuated residual noise signal, as shown in Figure 2-6. The design of ANC systems was first conceived in a patent by Lueg (1936), and an overview can be found in the book and tutorial paper of Kuo and Morgan (1996, 1999). ANC systems are based either on *feedforward* control where a coherent reference noise input is sensed, or *feedback* control where the controller does not have the benefit of a reference signal. Figure 2-7 shows a *feedforward* ANC where an integral amplifier drives a set of loudspeakers to insert the 'antinoise' into the noise stream.

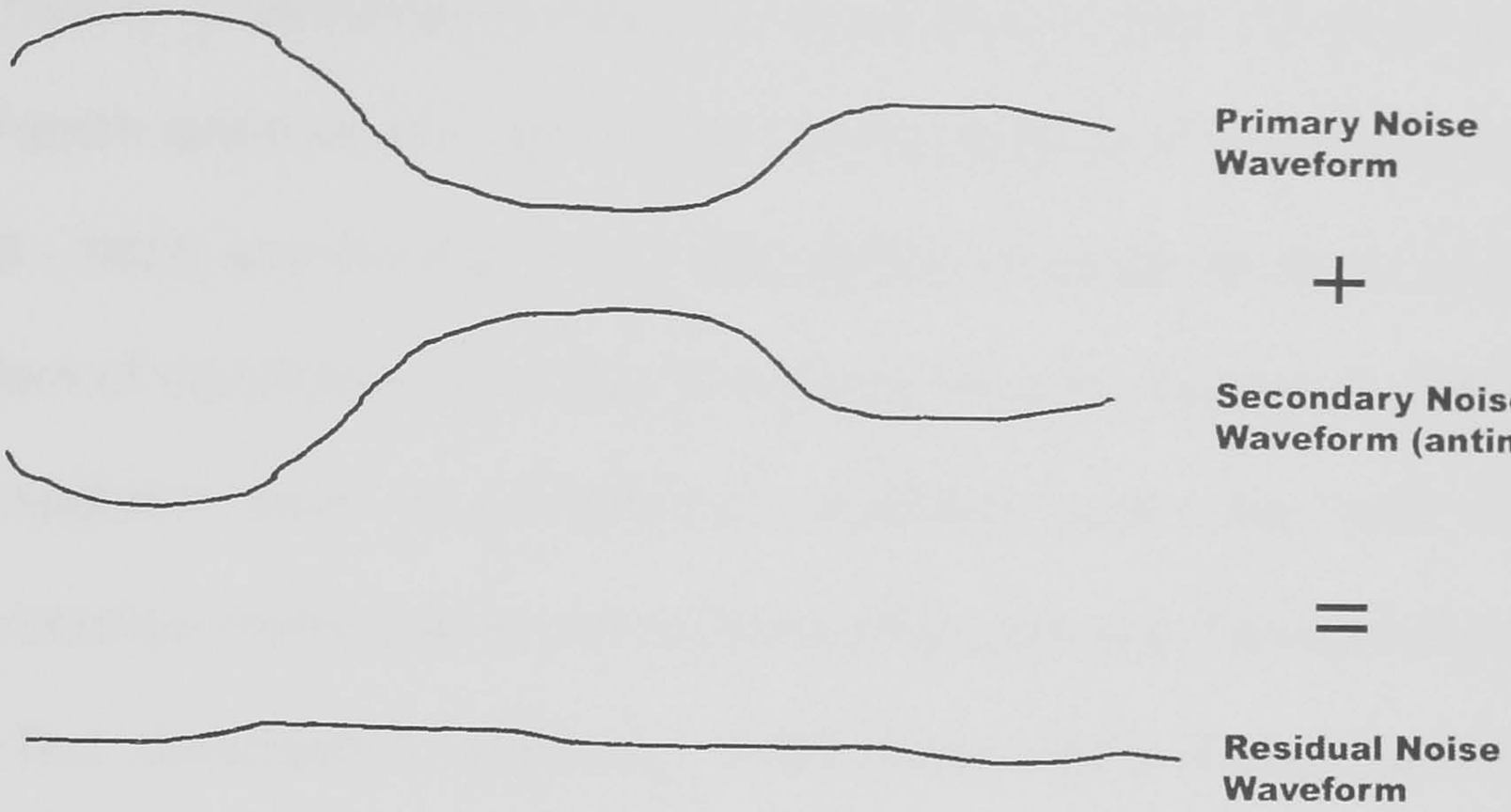

Figure 2-6: Physical concept of Active Noise Control

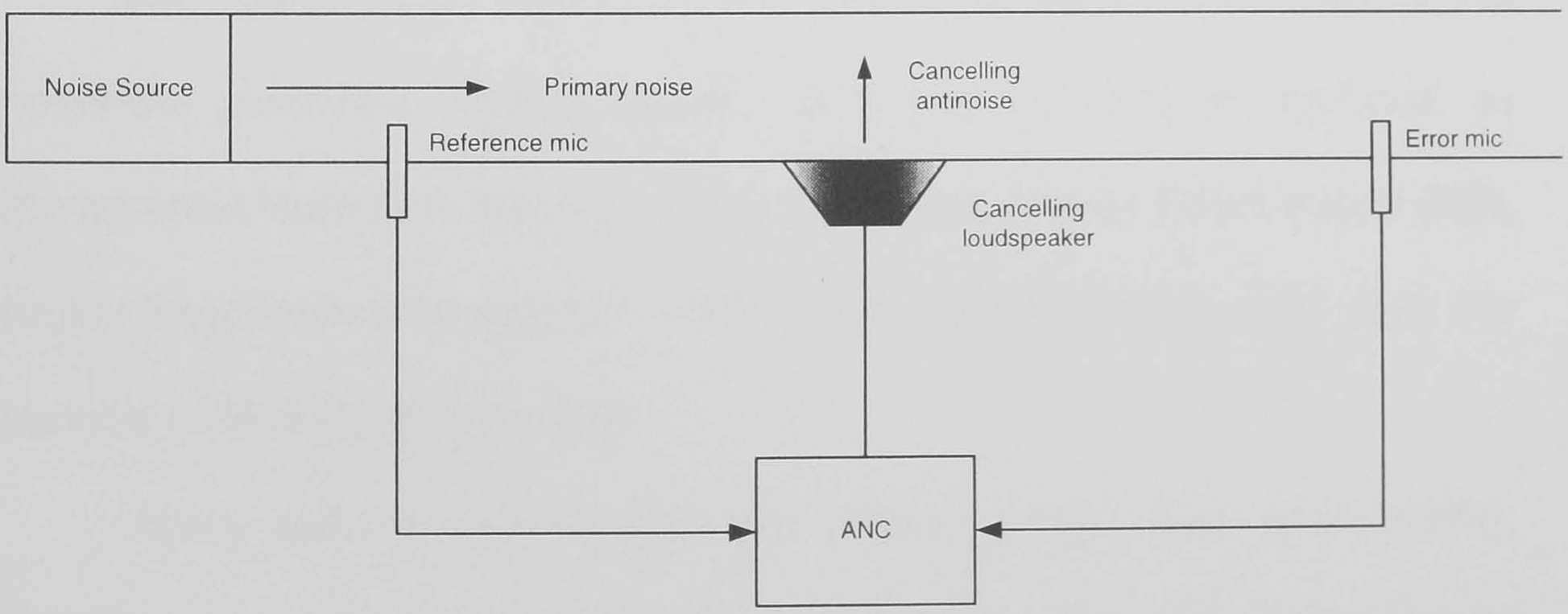

Figure 2-7: Signal channel broadband *feedforward* Active Noise Control

2.5 Perturbation Methods

The history of perturbation methods dates back to the 18th century, when the French astronomer, mathematician and physicist Pierre Simon Laplace [1749 - 1827] was the first to use perturbation methods when he solved the problem of equilibrium of a large weightless drop on a plane. Laplace gave an insightful view of perturbation methods when he said that "a mathematical method is the more precise the greater is the need for it".

The perturbation methods, which have many similar qualities to asymptotic methods, are a collection of techniques that may be used to simplify, and to solve, a wide variety of mathematical problems involving small or large parameters. The solutions may often be constructed in explicit analytical form or, when it is impossible, the original equation may be reduced to a more simple one that is much easier to solve numerically.

Many perturbation methods have been envisaged in the resolution of nonlinear problems. These include such well established methods as Incremental Harmonic Balance (IHB), Averaging, Krylov-Bogolioubov (KB), Krylov-Bogolioubov-Mitropolski (KBM), Lindstedt-Poincaré (LP) and the Method of Multiple Scales (MS).

Many authors such as Lau and Cheung (1981), Lau *et al.* (1982), and Pierre and Dowell (1985) have all applied the IHB method to various problems in nonlinear dynamics. In addition, Pierre *et al.* (1985) proposed a multi-harmonic analysis of a dry, friction-damped, system using the IHB method, where he found that the IHB method can yield very accurate results over the time domain methods. Ferri (1986) showed the equivalence of the IHB method and the harmonic balance Newton-

Raphson method. Cheung and Iu (1988) presented a development of a simple algorithm for the implementation of the harmonic balance method for solving a nonlinear dynamic system. The versatility of this algorithm is demonstrated on a variety of nonlinear vibration responses, namely, the combination resonances of a hinged-clamped beam, the nonlinear effect on the degenerate vibration modes of a square plate and the nonlinear oscillation of thin rings. Jezequel *et al.* (1990) proposed a nonlinear synthesis in the frequency domain by using the Ritz-Galerkin-Newton-Raphson method and also the IHB method. Friswell and Penny (1994) proposed the iterative Newton-Raphson method for solving sets of nonlinear equations from the Duffing equation, where the series solution is composed of sine and cosine functions,

$$x(t) = a_0 + a_1 \cos(\omega_f t) + a_2 \sin(\omega_f t) + a_3 \cos(2\omega_f t) + a_4 \sin(2\omega_f t) + \cdots \quad \textbf{(2.5-1)}$$

where ω_f is the fundamental frequency in the response.

In the analysis of the machining dynamics of tool chatter, Nayfeh *et al.* (1997) used the MS method to obtain the normal form of the Hopf bifurcation, a six-term harmonic balance solution to generate a bifurcation diagram, and a combination of Floquet theory and Hill's determinant to ascertained the stability of the periodic solutions. Lately, Warmiński *et al.* (2003) have taken this application further in the multiple scales analysis of non-resonant machining vibrations.

2.6 The Method of Multiple Scales

The perturbation method of multiple scales has been associated primarily with the names of Sturrock (1957, 1963), Frieman (1963), Cole and Kevorkian (1963), Nayfeh (1965a, 1965b, 1968, 1973) and Sandri (1965, 1967). The method of multiple scales is now so popular that it is applied to a very wide variety of problems in physics, engineering and applied mathematics. The underlying principal behind this method is that the dependent variables are uniformly expanded in terms of two, or more, independent variables, or scales, instead of a single variable, thus taking better account of slow and fast oscillations within the system, this being a commonly occurring feature within nonlinear systems.

In terms of useful, generic, engineering applications, Lee and Park (1999) investigated a weakly nonlinear, harmonically excited, spring-pendulum system, which is known to be a good model for a variety of engineering systems, including ship motions. The analysis was carried out using a second order multiple scales expansion, with the zeroth order term neglected. Resonances relating the spring and pendulum modal frequencies, ω_1 and ω_2, namely $2\omega_2 = \omega_1 + \varepsilon\hat{\sigma}_1$ and $\Omega = \omega_2 + \varepsilon\hat{\sigma}_2$, led to the identification of regions of periodic and chaotic motions, as well as a route to chaos. The modulation equations were used to generate Poincaré maps for bifurcation analysis and to obtain the Lyapunov exponent. It was shown that the Lyapunov exponent is quantitatively and qualitatively quite different for the first order and second order approximations, with the authors suggesting that the latter agrees better with the original system.

In another important work, Rahman and Burton (1989) proposed a version of the method of multiple scales which can be used to determine the periodic, steady-state, primary response of a single degree-of-freedom, lightly damped, weakly nonlinear, forced oscillator. The usual ordering of damping and external excitation and the conventional expansion of external frequency produces extra non-physical results for some cases, and this approach is referred to as *MMS version I* in Rahman and Burton, 1989. In order to eliminate the conditions which can sometimes generate unwanted, and physically dubious results, Rahman and Burton then recommended the alternative *MMS version II* for ordering and expansion of the damping and external excitation frequency. The version I method starts from the point of steady-state conditions where the slow-time variations in amplitude and phase have been set to zero after annulling the secular generating terms. The steady-state value of the complex amplitude, A, is given in the usual form of $A_0 = \frac{1}{2} a_0 e^{i\phi_0}$ and so this leads to computation of the second order solutions from,

$$\varepsilon f_1\left(A_0, \bar{A}_0\right) + \varepsilon^2 f_2\left(A_0, \bar{A}_0\right) = 0 \qquad \textbf{(2.6-1)}$$

Version II requires that, in the steady-state, each function $f_1\left(A_0, \bar{A}_0\right)$, $f_2\left(A_0, \bar{A}_0\right)$ vanish separately, ensuring that the steady-state solutions u_0, u_1 and u_2 do not explicitly depend on ε. Rahman and Burton (1989) also point out that this divergence in the approach cannot be used for first order expansions because in such cases the only possibility is $f_1\left(A_0, \bar{A}_0\right) = 0$. The reason given for the inadequacy of version I of the second order expansion method is that this approach accommodates possible violations of the

ordering requirements (as opposed to ε not being 'sufficiently small'), where terms that are neglected because they appear to be of too high an order are actually contributing at a similar level to those that remain. Rahman and Burton suggest that version I is inconsistent, and that version II is generally better. Similar proposals and discussions have been advanced by Luongo *et al.* (1986), Hassan (1994a, 1994b, 1995), Boyaci and Pakdemirli (1997) and Luongo and Paolone (1999).

As the preceding discussion points out certain fundamental difficulties can be encountered in the application of perturbation techniques to the study of strongly nonlinear problems. One of the most pervasive difficulties centres around the fact that all classical perturbation techniques rely strongly on the assumption of a small parameter. Many novel techniques have been proposed to overcome this particular limitation. For example, Cheung *et al.* (1991) proposed a modified Lindstedt-Poincaré method, and He (1999, 2000) proposed a homotopy perturbation technique. The homotopy technique embeds a parameter p that typically ranges from zero to one. When the embedding parameter is zero, the equation is of a linear system, when it is one, the equation is the same as the original one. So the embedded parameter $p \in [0,1]$ can be considered as a small parameter which globally controls the prevailing nonlinear nature of the problem. He (2000) illustrates this method with a nonlinear differential equation:

$$A(u) + f(r) = 0, \quad r \in \Omega \qquad \textbf{(2.6-2)}$$

with boundary conditions,

$$B(u, \partial u/\partial n) = 0, \quad r \in \Gamma \qquad \textbf{(2.6-3)}$$

where A is a general differential operator, B is a boundary operator, $f(r)$ is a known analytic function, Γ is the boundary of the domain Ω. The operator A can be divided into two parts L and N, where L is linear, while N is nonlinear, so equation (2.6-2) can therefore be written as follows,

$$L(u)+N(u)-f(r)=0 \qquad \textbf{(2.6-4)}$$

A homotopy $v(r,p):\Omega\times[0,1]\to\Re$ is then constructed which satisfies,

$$h(v,p)=(1-p)\left[L(v)-L(u_0)\right]+p\left[A(v)-f(r)\right]=0\text{, or} \qquad \textbf{(2.6-5)}$$

$$h(v,p)=L(v)-L(u_0)+pL(u_o)+p\left[N(v)-f(r)\right]=0 \qquad \textbf{(2.6-6)}$$

where $p\in[0,1]$, $r\in\Omega$ and u_0 is an initial approximation of equation (2.6-2). Equations (2.6-5) and (2.6-6) are called the perturbation equations with an embedding parameter, and it can be solved by a traditional perturbation technique using the embedding variable p as a 'small parameter'

A comprehensive review of the method of multiple scales has recently been completed by Cartmell *et al.* (2003), in which they examined the rôle of term ordering, the integration of the small perturbation parameter within system constants, nondimensionalisation and time-scaling, series truncation, inclusion and exclusion of higher order nonlinearities, and typical problems in the handling of secular terms. In that paper, Cartmell *et al.* (2003) showed in a comparative example that the form of the adopted power series and the ordering terms can have a major bearing on the structure of the solution, with clear connotations for accuracy and physical relevance. They then gave suggestions on how one can deal with ordering by basing it on some sort of physical appreciation of

the problem in terms of 'hard' and 'soft', or 'strong' and 'weak' quantities within the equation of motion such as damping mechanisms, excitation amplitudes, and the coefficients of nonlinear terms.

In a recent advancement, the method of multiple scales has been computerised by means of specialised packages within *Mathematica* code constructs, by Khanin and Cartmell (1999), Khanin *et al.* (2000) and Khanin and Cartmell (2001), with parallelisation strategies introduced for reasons of optimisation. This work is still at the stage of a research tool but is entering a final stage in which issues of visualisation of large and complicated symbolic solutions are to be explored, and so it will enter the public domain in the next few years.

2.7 Ultrasonics

Ultrasound comprises mechanical vibrations of sound waves in a solid or fluid, but at a frequency higher than the range audible to humans - the lowest ultrasonic frequency is normally taken to be 20 kHz. The top end of the frequency range is limited only by the ability to generate the signals - frequencies in the gigahertz range have been used (Sittig *et. al.,* 1969; Brereton and Bruno, 1994).

Ultrasound has been used for a huge variety of applications, and can be divided into two broad categories: low and high power ultrasound. Low power applications are usually used where the ultrasound does not have any significant effects on the subject of the scan, and these include medical imaging (e.g. scanning the unborn foetus) and non-destructive testing (e.g. regular crack-testing for aircraft structures). By contrast, high power applications tend to use frequencies at the low end of the spectrum (i.e. from 20 kHz to about 100 kHz). This is because the power available is limited by mechanical stress in the vibrating parts. To maximise the effects, high power applications often use as much amplitude as possible. Typical amplitudes range from about 5 to 50 microns. These appear to be small amplitudes, but an ultrasonic system operating at 20 kHz and 50 microns is moving with a cyclic acceleration of 80,000 g! Some high power applications include cutting, machining, welding, cleaning, etc.

The application of high power ultrasonic tooling to manufacturing processes is a well-established area of research and one which has shown great potential. However, ultrasonic machining and cutting processes have been rather under-exploited in industry due to reliability problems

associated with the nonlinear behaviour of the various components that are used. These processes generally require the use of specifically designed ultrasonic components to transmit the energy correctly from the exciter (known incorrectly, but generally, as the *transducer*) to the tool interface. In the design of ultrasonic components, three primary performance indicators are the vibration amplitude, the uniformity of vibration amplitude at the vibration transmission surface, and the acceptable stresses in the block horns or blades.

Studies of high power ultrasonic components by Lucas *et al.* (1996) have relied upon 1D Laser Doppler Vibrometer (LDV) analysis to monitor the out-of-plane component of vibration. However, verification of modal behaviour is difficult with this method because ultrasonic components are designed to exhibit a predominantly longitudinal response, hence measurable out-of-plane motion can be easily misidentified as a flexural mode response. Further work in providing a complementary technique to 1D LDV measurements was undertaken by Graham *et al.* (1999a, 1999b). In these studies, ultrasonic bar- and block-horns were analysed by using electronic speckle pattern interferometry (ESPI). ESPI is the name given to several laser speckle-based techniques which are used for measuring discrete displacement components. Shellabear and Tyrer (1989, 1991) have successfully used ESPI to measure wholefield vibration displacement of structures in the low ultrasonic frequency range and thus provides an opportunity to incorporate in-plane measurement data into the modal analysis of ultrasonic horns. With the advent of 3D LDV, Cardoni and Lucas (2002) have accurately characterised the modal analysis of block horns from both in-plane and out-of-plane measurements.

With the advancement of experimental measurements by the use of 3D LDV, design strategies such as ensuring vibrational uniformity and acceptable stresses in the block horns, or blades, really have to be implemented for reliable tuned ultrasonic systems.

One main source of nonlinearities in ultrasonics equipment emanates from the primary component – the ultrasonic transducer. Transducers consist of piezoelectric ceramics, which when driven at high electrical levels rapidly reach their nonlinear response domain. By describing the transducer as a lumped system, Aurelle *et al.* (1996) have highlighted the influence of a nonlinear coefficient, α, in a nonlinear piezoelectric constitutive equation as stated below,

$$-\Omega^2\sum_{n=-\infty}^{n=+\infty} n^2 C_n e^{jn\Omega t} + w^2\sum_{n=-\infty}^{n=+\infty} C_n e^{jn\Omega t} + \alpha\sum_{n=-\infty}^{n=+\infty}\sum_{m=-\infty}^{m=+\infty} C_n C_m e^{j(n+m)\Omega t}$$
$$+\frac{\gamma\Sigma E_0}{2lM}\left(\sum_{n=-\infty}^{n=+\infty} C_n e^{j(n+1)\Omega t} + \sum_{n=-\infty}^{n=+\infty} C_n e^{j(n-1)\Omega t}\right) + 2\lambda w j\Omega\sum_{n=-\infty}^{n=+\infty} nC_n e^{jn\Omega t} = \frac{-e\Sigma E_0}{2M}\left(e^{j\Omega t} + e^{-j\Omega t}\right) \qquad \textbf{(2.7-1)}$$

where M is the mass of each tail mass (at each end of the transducer), Σ the ceramic surface, l the half length of the ceramic stack, e the linear piezoelectric coefficient, α and γ the nonlinear piezoelectric coefficients, E_0 the excitation level, Ω the driving pulsation, λ the damping coefficient, and w the pulsation associated with the natural frequency of the linear system. Equation (2.7-1) was derived by seeking a solution of the tail mass displacement u, in the form,

$$u(t) = \sum_{n=-\infty}^{n=+\infty} C_n e^{jn\Omega t} \qquad \textbf{(2.7-2)}$$

and together with the stress T given by the piezoelectric constitutive equations extended to the nonlinear domain, equation (2.7-1) is primarily structured from equation (2.7-3), $M\ddot{u} = -T\Sigma$ **(2.7-3)**

where the primes specify time differentiation. In Figure 2-8, as α is increased from 1×10^{15} to 2×10^{15}, it is obvious that the effect of increasing it manifests as a more accentuated softening behaviour. Aurelle *et al.* (1996) have shown how these coefficients affect the nonlinearity of a transducer which is predominantly of a softening characteristic. Different excitation levels were also investigated, and when the excitation was small, a symmetrical curve was generated, whose maximum amplitude is at the natural resonant frequency of the system and is represented in Figure 2-9. As the excitation level increases, it is evident that the curve changes and becomes nonlinear; together with unstable regions. Therefore, the performance of ultrasonic systems is strongly affected by these nonlinearities and instabilities which originate partly within the transducers themselves.

However, by investigating and modelling the influence of ultrasonic energy generation and its interaction with the beneficial mechanisms in ultrasonic tooling, other potentially useful solutions related to the measured nonlinear coupling effects can be formulated. The state of the art in ultrasonic system design is not by any means entirely clear-cut and so reliability limitations imposed by deficiencies in current design practices are treated in this research by a new attempt to exploit a mechanistic understanding of ultrasonic system nonlinearities. The outcome is a reliable

tuned ultrasonic tool design strategy which is potentially adaptable to a wide range of manufacturing processes involving ultrasonics.

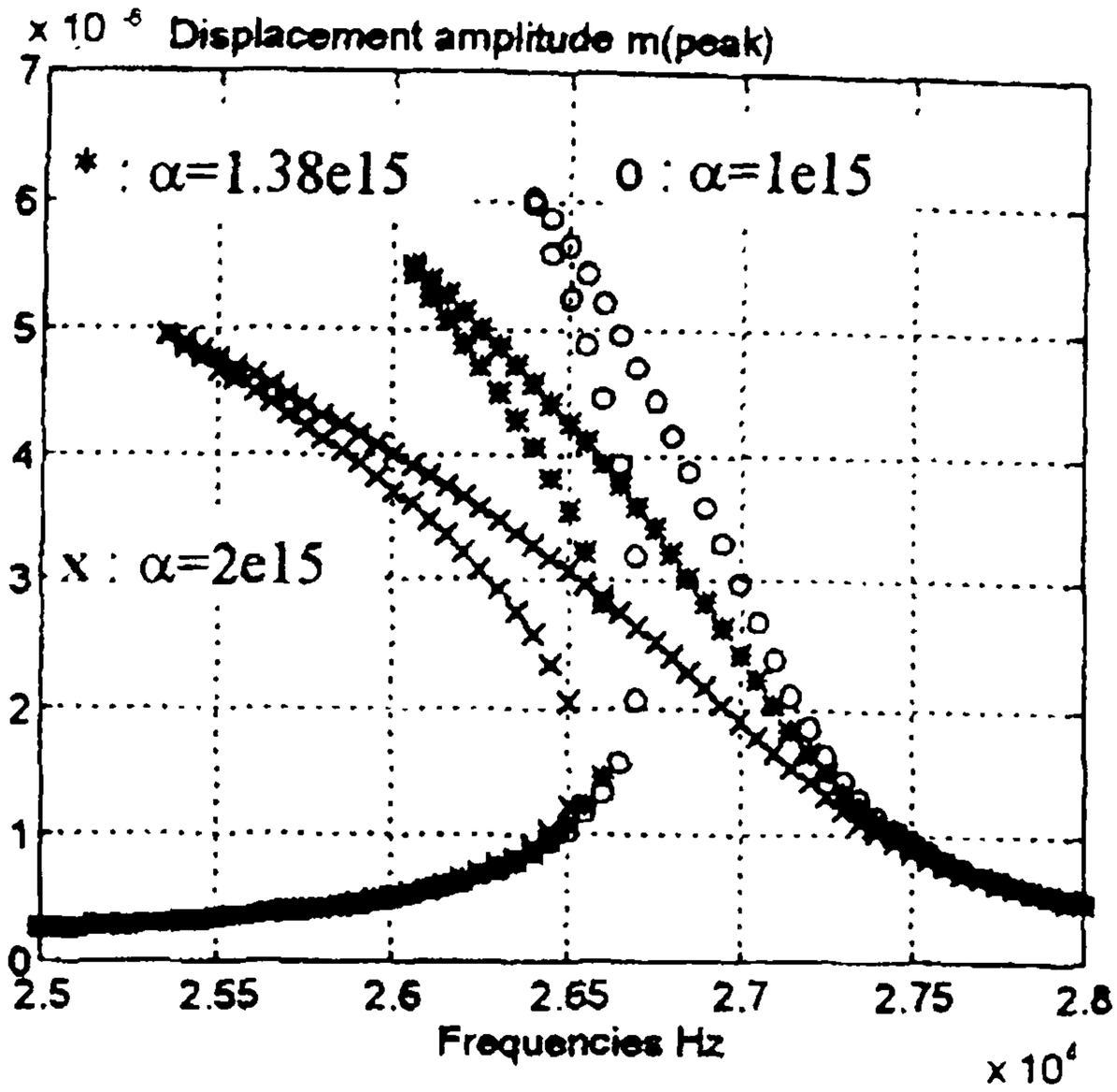

Figure 2-8: Influence of nonlinear parameter α – Aurelle *et al.* (1996)

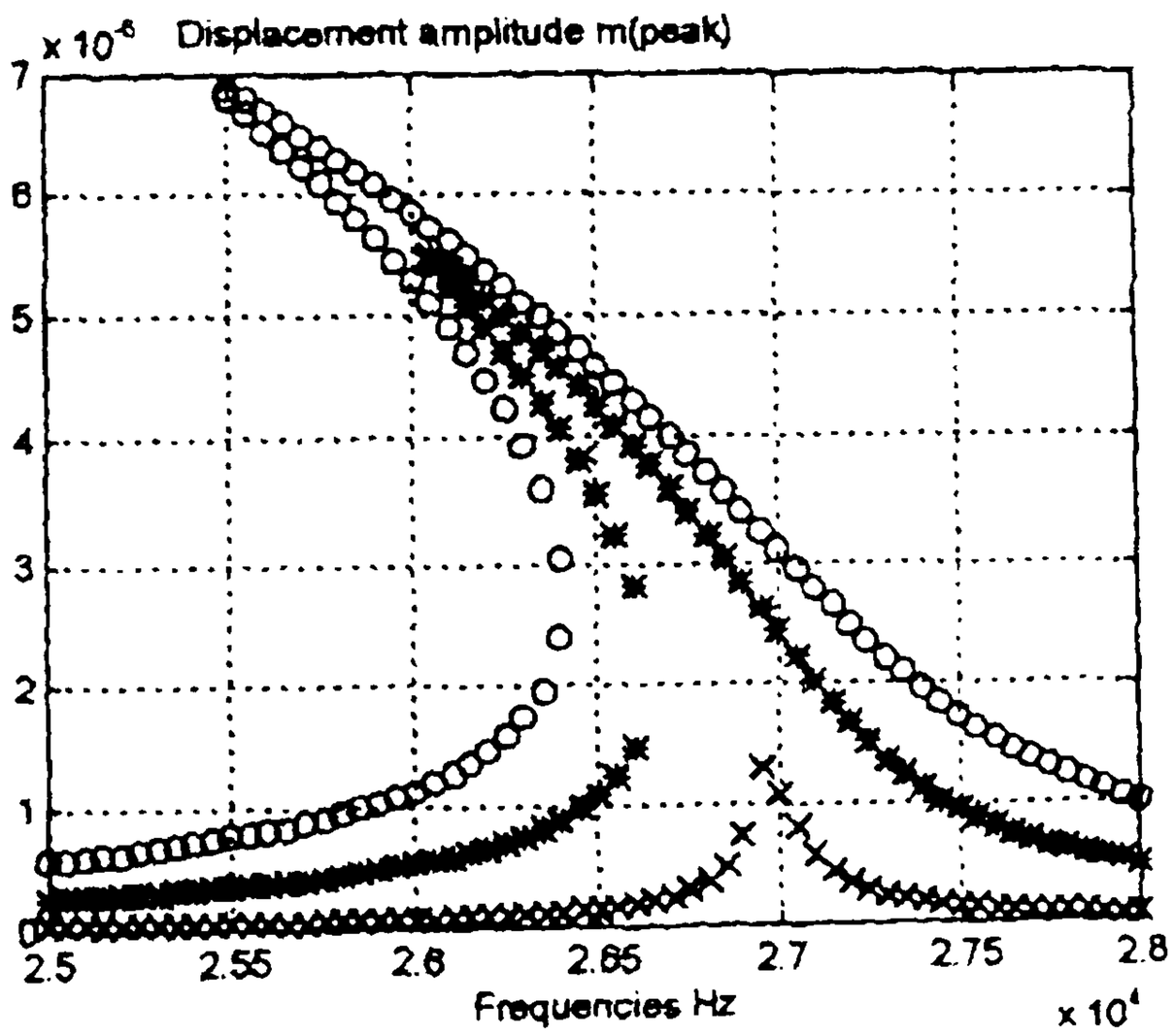

Figure 2-9: Influence of excitation levels, U – Aurelle *et al.* (1996)

CHAPTER 3

MODELS OF COUPLED NONLINEAR SYSTEMS

3.1 Introduction

The approach of achieving nonlinear response modification is proposed by coupling two Duffing oscillators in series as introduced in Section 1.4.2. The theoretical model of this system takes the convenient simplified form of a two degree-of-freedom Duffing oscillator system as shown in Figure 3-1(a). The model is taken to have predominantly linear damping, as defined by coefficients c_1 and c_2, and linear spring stiffnesses, together with attendant nonlinear cubic stiffnesses, k_1, k_2 and h_1, h_2 respectively. The nonlinear stiffness quantity h_1 relates to a hardening spring defined by $+h_1 x_1^{*3}$ and h_2 controls a softening spring defined by $-h_2 x_2^{*3}$. A harmonic excitation force $F_1^*(t) = F^* \cos \Omega^* t^*$ is applied to the first sub-system, whereas there is no applied force on the second sub-system $F_2^*(t) = 0$. Note that the stars define physical, dimensional, quantities. This line of thinking very much emanates from the serially coupled nature of the ultrasonic cutting tool upon which this modelling concept is based as shown in Figure 3-1(b).

(a)

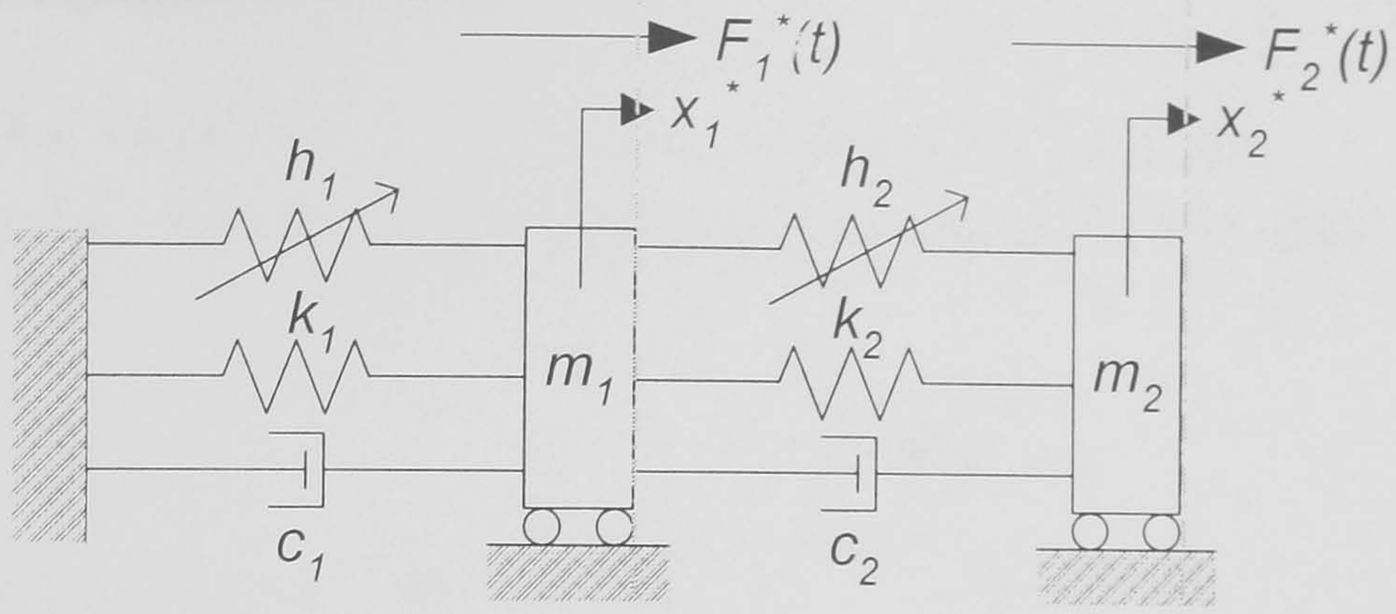

(b)

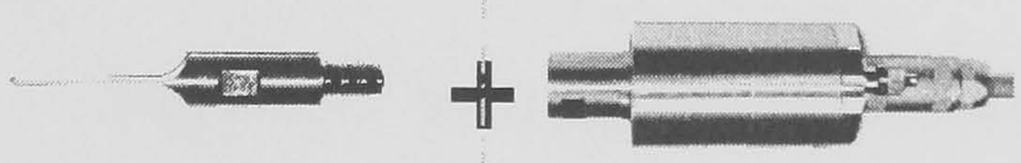

Figure 3-1: (a) Theoretical representation of the hypothesised model; (b) A practical representation of an ultrasonic cutting tool

3.2 System 1 : Stiffness Coupled Translating System Modelled In Physical Coordinates

3.2.1 Equations of Motion

The governing differential equations for the sub-systems in Figure 3-2 and Figure 3-3 are directly derived from the free body diagrams using Newton's laws of motion,

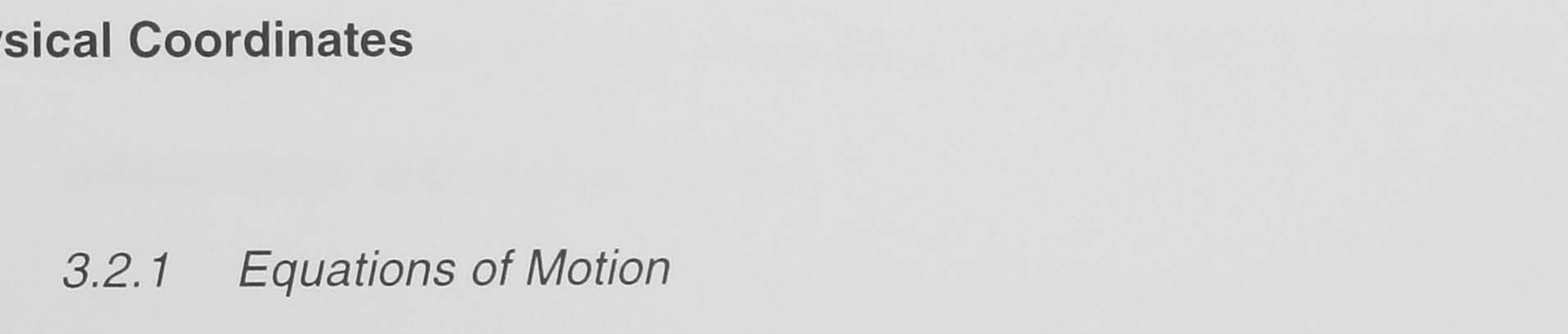

Figure 3-2: Free Body Diagram of m_1

The equation in x_1^* is as follows,

$$m_1\ddot{x}_1^* + c_1\dot{x}_1^* + k_1x_1^* + h_1(x_1^*)^3 - c_2(\dot{x}_2^* - \dot{x}_1^*) - k_2(x_2^* - x_1^*) + h_2(x_2^* - x_1^*)^3 = F_1^*(t^*)$$

$$m_1\ddot{x}_1^* + c_1\dot{x}_1^* + c_2\left(\dot{x}_1^* - \dot{x}_2^*\right) + k_1x_1^* + k_2\left(x_1^* - x_2^*\right) + h_1(x_1^*)^3 + h_2(x_2^* - x_1^*)^3 = F^*\cos\Omega^* t^* \quad \textbf{(3.2-1)}$$

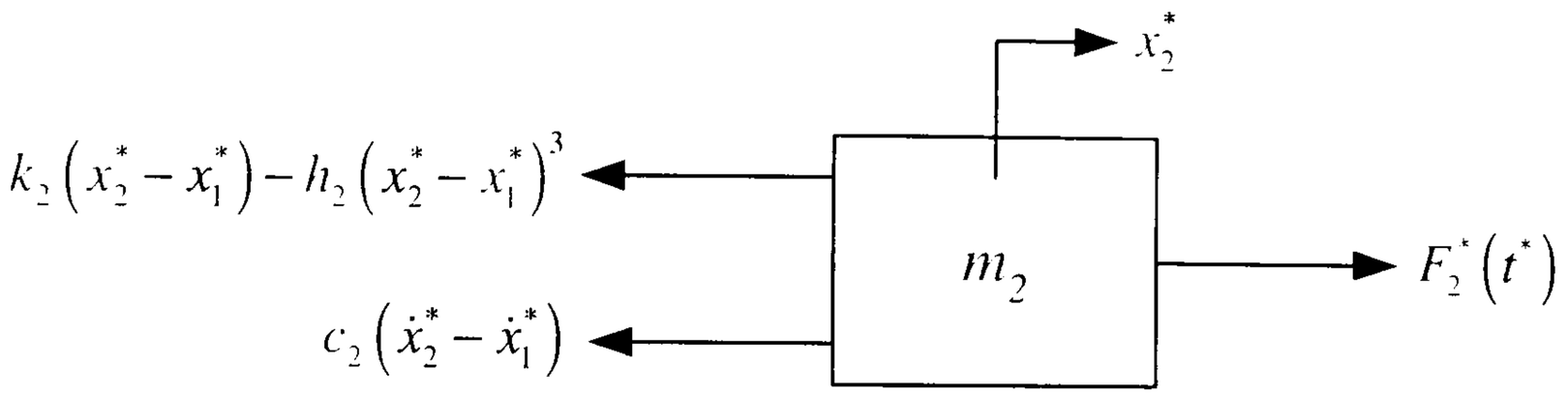

Figure 3-3: Free Body Diagram of m_2

The other equation for x_2^* is also directly obtained, thus,

$$m_2\ddot{x}_2^* + c_2(\dot{x}_2^* - \dot{x}_1^*) + k_2(x_2^* - x_1^*) - h_2(x_2^* - x_1^*)^3 = F_2^*(t^*)$$

$$m_2\ddot{x}_2^* + c_2\left(\dot{x}_2^* - \dot{x}_1^*\right) + k_2\left(x_2^* - x_1^*\right) - h_2(x_2^* - x_1^*)^3 = 0 \quad \textbf{(3.2-2)}$$

where $x_{1,2}^* = x_{1,2}^*\left(t^*\right)$ and the star (*) represents variables which still, at this stage, possess physical dimensions, and the dot ($\dot{}$) represents differentiation with respect to time, t^*.

3.2.2 Derivation of the Natural Frequencies (Eigenvalues) of this 2 Degree-of-Freedom System

The undamped linear natural frequencies (i.e. eigenvalues) of the two degree-of-freedom system are derived and are used as reference frequencies for non-dimensionalisation. Appendix A summaries the derivation of these two natural frequencies. Therefore, equations (A.1-7) and (A.1-8) are the first and second

linear natural frequencies of undamped vibration respectively, and are re-stated below as,

$$\omega_{e1} = \sqrt{\frac{1}{2}\left[\frac{k_1}{m_1}+\frac{k_2}{m_1}+\frac{k_2}{m_2}-\sqrt{\left(\frac{k_1}{m_1}\right)^2+\frac{2k_1}{m_1}\left(\frac{k_2}{m_1}-\frac{k_2}{m_2}\right)+\left(\frac{k_2}{m_1}+\frac{k_2}{m_2}\right)^2}\right]} \qquad \textbf{(3.2-3)}$$

$$\omega_{e2} = \sqrt{\frac{1}{2}\left[\frac{k_1}{m_1}+\frac{k_2}{m_1}+\frac{k_2}{m_2}+\sqrt{\left(\frac{k_1}{m_1}\right)^2+\frac{2k_1}{m_1}\left(\frac{k_2}{m_1}-\frac{k_2}{m_2}\right)+\left(\frac{k_2}{m_1}+\frac{k_2}{m_2}\right)^2}\right]} \qquad \textbf{(3.2-4)}$$

3.2.3 Non-Dimensionalisation of Equations

By introducing dimensionless time, $t = \omega_{e1}\, t^*$ **(3.2-5)**

And non-dimensional response coordinates in the form of,

$$x_{1,2} = \frac{x^*_{1,2}}{x^*_{ref}} \qquad \textbf{(3.2-6)}$$

where ω_{e1} is the first eigenvalue as stated in Equation (3.2-3) and x^*_{ref} can be an arbitrary reference displacement.

Therefore,

$$\Rightarrow \quad \ddot{x}^*_{1,2}\left(t^*\right) = \frac{d^2 x^*_{1,2}}{d\left(t^*\right)^2} \quad ; \quad \dot{x}^*_{1,2}\left(t^*\right) = \frac{dx^*_{1,2}}{dt^*}$$

$$= \frac{d^2 x^*_{1,2}}{d\left(\frac{t}{\omega_{e1}}\right)^2} \qquad = \frac{dx^*_{1,2}}{d\left(\frac{t}{\omega_{e1}}\right)}$$

$$= \omega_{e1}^2\left(\frac{d^2 x^*_{1,2}}{dt^2}\right) \qquad = \omega_{e1}\left(\frac{dx^*_{1,2}}{dt}\right)$$

$$\therefore \quad \ddot{x}_{1,2}\left(t^*\right) = \omega_{e1}^2\, x^{*\prime\prime}_{1,2}(t) \quad ; \quad \dot{x}_{1,2}\left(t^*\right) = \omega_{e1}\, x^{*\prime}_{1,2}(t) \qquad \textbf{(3.2-7)}$$

In dimensionless time, equations (3.2-1) and (3.2-2) become,

$$m_1\omega_{e1}^2 x_1^{*\prime\prime} + c_1\omega_{e1} x_1^{*\prime} + c_2\omega_{e1}\left(x_1^{*\prime} - x_2^{*\prime}\right) + k_1 x_1^{*} + k_2\left(x_1^{*} - x_2^{*}\right) + h_1\left(x_1^{*}\right)^3 + h_2(x_2 - x_1^{*})^3 = F^{*}\cos\frac{\Omega^{*}}{\omega_{e1}}t \quad \textbf{(3.2-8)}$$

$$m_2\omega_{e1}^2 x_2^{*\prime\prime} + c_2\omega_{e1}\left(x_2^{*\prime} - x_1^{*\prime}\right) + k_2\left(x_2^{*} - x_1^{*}\right) - h_2(x_2^{*} - x_1^{*})^3 = 0 \quad \textbf{(3.2-9)}$$

where the prime (′) represents differentiation now with respect to dimensionless time, t .

Non-dimensionalising equations (3.2-8) and (3.2-9) with respect to the reference displacement, x_{ref}^{*} ,

$$\frac{x_1^{*\prime\prime}}{x_{ref}^{*}} + \frac{c_1}{m_1\omega_{e1}}\frac{x_1^{*\prime}}{x_{ref}^{*}} + \frac{c_2}{m_1\omega_{e1}}\left(\frac{x_1^{*\prime}}{x_{ref}^{*}} - \frac{x_2^{*\prime}}{x_{ref}^{*}}\right) + \frac{k_1}{m_1\omega_{e1}^{\,2}}\frac{x_1^{*}}{x_{ref}^{*}} + \frac{k_2}{m_1\omega_{e1}^{\,2}}\left(\frac{x_1^{*}}{x_{ref}^{*}} - \frac{x_2^{*}}{x_{ref}^{*}}\right) + \frac{h_1 x_{ref}^{*\,2}}{m_1\omega_{e1}^{\,2}}\left(\frac{x_1^{*}}{x_{ref}^{*}}\right)^3 + \frac{h_2 x_{ref}^{*\,2}}{m_1\omega_{e1}^{\,2}}\left(\frac{x_2^{*} - x_1^{*}}{x_{ref}^{*}}\right)^3 = \frac{F^{*}}{m_1\omega_{e1}^{\,2} x_{ref}^{*}}\cos\frac{\Omega^{*}}{\omega_{e1}}t \quad \textbf{(3.2-10)}$$

$$\frac{x_2^{*\prime\prime}}{x_{ref}^{*}} + \frac{c_2}{m_2\omega_{e1}}\left(\frac{x_2^{*\prime}}{x_{ref}^{*}} - \frac{x_1^{*\prime}}{x_{ref}^{*}}\right) + \frac{k_2}{m_2\omega_{e1}^2}\left(\frac{x_2^{*}}{x_{ref}^{*}} - \frac{x_1^{*}}{x_{ref}^{*}}\right) - \frac{h_2 x_{ref}^{*\,2}}{m_2\omega_{e1}^2}\left(\frac{x_2^{*} - x_1^{*}}{x_{ref}^{*}}\right)^3 = 0 \quad \textbf{(3.2-11)}$$

results in,

$$x_1'' + 2\zeta_1 x_1' + 2\zeta_2\left(x_1' - x_2'\right) + \gamma_1 x_1 + \gamma_2\left(x_1 - x_2\right) + \eta_1\left(x_1\right)^3 + \eta_2\left(x_2 - x_1\right)^3 = F\cos\Omega t \quad \textbf{(3.2-12)}$$

$$x_2'' + 2\zeta_3\left(x_2' - x_1'\right) + \gamma_3\left(x_2 - x_1\right) - \eta_3\left(x_2 - x_1\right)^3 = 0 \quad \textbf{(3.2-13)}$$

where the non-dimensional parameters are,

$$\zeta_1 = \frac{c_1}{2m_1\omega_{e1}} \quad ; \quad \zeta_2 = \frac{c_2}{2m_1\omega_{e1}} \quad ; \quad \zeta_3 = \frac{c_2}{2m_2\omega_{e1}}$$

$$\gamma_1 = \frac{k_1}{m_1\omega_{e1}^{\ 2}} \quad ; \quad \gamma_2 = \frac{k_2}{m_1\omega_{e1}^{\ 2}} \quad ; \quad \gamma_3 = \frac{k_2}{m_2\omega_{e1}^{\ 2}}$$

$$\eta_1 = \frac{h_1\, x_{ref}^{*\ 2}}{m_1\omega_{e1}^{\ 2}} \quad ; \quad \eta_2 = \frac{h_2\, x_{ref}^{*\ 2}}{m_1\omega_{e1}^{\ 2}} \quad ; \quad \eta_3 = \frac{h_2\, x_{ref}^{*\ 2}}{m_2\omega_{e1}^{\ 2}}$$

$$F = \frac{F^*}{m_1\omega_{e1}^{\ 2} x_{ref}^*} \quad ; \quad \Omega = \frac{\Omega^*}{\omega_{e1}} \qquad \textbf{(3.2-14)}$$

3.2.4 Solution to the Equations of Motion

The classical perturbation method of multiple scales has been chosen for the analysis of these equations because the solution is a function of multiple independent time-scales, so the fast scale can be used for capturing motions at frequencies comparable to the linear natural frequency of the system, whilst the slow scale accounts for slow modulations of amplitudes and phases. Nayfeh (1973), Jordan and Smith (1977), Nayfeh and Mook (1979), Cartmell (1990), Thomsen (1997), Murdock (1999) and Warmiński (2001) have all authored books discussing and applying this method to engineering systems.

3.2.4.1 Ordering of terms

Motions in the neighbourhood of the static equilibrium position are considered so that the amplitude of the response is assumed to be of the order of some small parameter ε, $0 < \varepsilon \ll 1$. All the terms in equations (3.2-15) and (3.2-16) are re-formulated in terms of this small parameter, ε, with the exception of the linear inertia terms, and the linear stiffness terms containing γ_1 and γ_3. This ensures that all other effects only appear within the higher order perturbation equations, whereas the aforementioned terms appear in the zeroth order perturbation equations from which generating solutions are obtained [Asfar (1992)]. This philosophy is pragmatic and realistic in that it permits the pre-ordained generation of linear, homogeneous, generating solutions for each coordinate.

Multiplying the appropriate terms in equations (3.2-12) and (3.2-13) by ε :

$$x_1'' + 2\varepsilon\tilde{\zeta}_1 x_1' + 2\varepsilon\tilde{\zeta}_2\left(x_1' - x_2'\right) + \gamma_1 x_1 + \varepsilon\tilde{\gamma}_2\left(x_1 - x_2\right) + \varepsilon\tilde{\eta}_1\left(x_1\right)^3 + \varepsilon\tilde{\eta}_2\left(x_2 - x_1\right)^3 = \varepsilon\tilde{F}\cos\Omega t \qquad \textbf{(3.2-15)}$$

$$x_2'' + 2\varepsilon\tilde{\zeta}_3\left(x_2' - x_1'\right) + \gamma_3\left(x_2 - x_1\right) - \varepsilon\tilde{\eta}_3\left(x_2 - x_1\right)^3 = 0 \qquad \textbf{(3.2-16)}$$

where:

$$\zeta_1 = \varepsilon\tilde{\zeta}_1 \quad ; \quad \zeta_2 = \varepsilon\tilde{\zeta}_2 \quad ; \quad \zeta_3 = \varepsilon\tilde{\zeta}_3 \quad ; \quad \eta_1 = \varepsilon\tilde{\eta}_1 \quad ; \quad \eta_2 = \varepsilon\tilde{\eta}_2 \quad ; \quad \eta_3 = \varepsilon\tilde{\eta}_3$$

$$\gamma_2 = \varepsilon\tilde{\gamma}_2 \quad ; \quad F = \varepsilon\tilde{F} \qquad \textbf{(3.2-17)}$$

3.2.4.2 Introducing time scales

As required by the method of multiple scales, the co-ordinates of $x_{1,2}(t)$ are stated in power series form, as are the total derivatives with respect to time. Assuming a uniformly valid expansion for the solution of equations (3.2-15) and (3.2-16) as:

$$x_j(t;\varepsilon) = x_{j0}(T_0, T_1) + \varepsilon\, x_{j1}(T_0, T_1) + O(\varepsilon^{\geq 2}) \qquad \textbf{(3.2-18)}$$

where j : 1,2 and,

$$T_n = \varepsilon^n t \quad \text{where} \quad \varepsilon \ll 1 \qquad \textbf{(3.2-19)}$$

n : 0 = fast time, 1 = slow time (independent time scales)

Taking uniform expansions as:

$$x_1 = x_{10} + \varepsilon\, x_{11} + O(\varepsilon^{\geq 2}) \quad , \quad x_2 = x_{20} + \varepsilon\, x_{21} + O(\varepsilon^{\geq 2}) \qquad \textbf{(3.2-20, 3.2-21)}$$

and for the derivatives:

$$\frac{d}{dt} = D_0 + \varepsilon D_1 + O(\varepsilon^{\geq 2}) \quad ; \quad \frac{d}{dt^2} = D_0^{\,2} + 2\varepsilon D_0 D_1 + O(\varepsilon^{\geq 2}) \qquad \textbf{(3.2-22, 3.2-23)}$$

where x_{1n} and x_{2n} in equations (3.2-20) and (3.2-21) represent functions of timescales T_n (i.e. $T_0 = t$ and $T_1 = \varepsilon t$). The partial derivatives of equations (3.2-22) and (3.2-23) are stated in the standard D operator notation where $D_i^j \equiv \partial^j / \partial T_i^{\,j}$. Series (3.2-20) – (3.2-23) inclusive are truncated after the first order ε terms, because this perturbation analysis is limited to first order level.

3.2.4.3 Coefficients of order, ε

Applying the method of multiple scales in the conventional manner by substituting equations (3.2-20) to (3.2-23) into equations (3.2-15) and (3.2-16), the equations of motion become,

$$\begin{aligned}&\left[D_0^2+2\varepsilon D_0D_1\right]\left[x_{10}+\varepsilon x_{11}\right]+2\varepsilon\tilde{\zeta}_1\left[D_0+\varepsilon D_1\right]\left[x_{10}+\varepsilon x_{11}\right]+2\varepsilon\tilde{\zeta}_2\left[D_0+\varepsilon D_1\right]\left\{\left[x_{10}+\varepsilon x_{11}\right]-\left[x_{20}+\varepsilon x_{21}\right]\right\}\\&+\gamma_1\left[x_{10}+\varepsilon x_{11}\right]+\varepsilon\tilde{\gamma}_2\left\{\left[x_{10}+\varepsilon x_{11}\right]-\left[x_{20}+\varepsilon x_{21}\right]\right\}+\varepsilon\tilde{\eta}_1\left[x_{10}^3+3\varepsilon x_{10}^2x_{11}+3\varepsilon x_{10}x_{11}^2+\varepsilon x_{11}^3\right]\\&+\varepsilon\tilde{\eta}_2\left[-x_{10}^3+3x_{10}^2x_{20}-3x_{10}x_{20}^2+x_{20}^3+O\left(\varepsilon^{\geq 1}\right)\right]=\varepsilon\tilde{F}\cos\Omega t\end{aligned}\qquad \textbf{(3.2-24)}$$

$$\begin{aligned}&\left[D_0^2+2\varepsilon D_0D_1\right]\left[x_{20}+\varepsilon x_{21}\right]+2\varepsilon\tilde{\zeta}_3\left[D_0+\varepsilon D_1\right]\left\{\left[x_{20}+\varepsilon x_{21}\right]-\left[x_{10}+\varepsilon x_{11}\right]\right\}\\&+\gamma_3\left\{\left[x_{20}+\varepsilon x_{21}\right]-\left[x_{10}+\varepsilon x_{11}\right]\right\}-\varepsilon\tilde{\eta}_3\left[-x_{10}^3+3x_{10}^2x_{20}-3x_{10}x_{20}^2+x_{20}^3+O\left(\varepsilon^{\geq 1}\right)\right]=0\end{aligned}\qquad \textbf{(3.2-25)}$$

Then, collecting the coefficients of like order of ε^n and equating them to zero leads to,

Order ε^0

$$D_0^2x_{10}+\gamma_1x_{10}=0 \qquad \textbf{(3.2-26)}$$

$$D_0^2x_{20}+\gamma_3x_{20}-\gamma_3x_{10}=0 \qquad \textbf{(3.2-27)}$$

Order ε^1

$$\begin{aligned}&D_0^2x_{11}+2D_0D_1x_{10}+2\tilde{\zeta}_1D_0x_{10}+2\tilde{\zeta}_2D_0x_{10}-2\tilde{\zeta}_2D_0x_{20}+\gamma_1x_{11}+\tilde{\gamma}_2x_{10}-\tilde{\gamma}_2x_{20}\\&+\tilde{\eta}_1x_{10}^3+\tilde{\eta}_2\left(x_{20}^3+3x_{10}^2x_{20}-3x_{10}x_{20}^2-x_{10}^3\right)=\tilde{F}\cos\Omega t\end{aligned}\qquad \textbf{(3.2-28)}$$

$$\begin{aligned}&D_0^2x_{21}+2D_0D_1x_{20}+2\tilde{\zeta}_3D_0x_{20}-2\tilde{\zeta}_3D_0x_{10}+\gamma_3x_{21}-\gamma_3x_{11}\\&-\tilde{\eta}_3\left(x_{20}^3+3x_{10}^2x_{20}-3x_{10}x_{20}^2-x_{10}^3\right)=0\end{aligned}\qquad \textbf{(3.2-29)}$$

Arranging equations (3.2-28) and (3.2-29) into conventional ODE structure for further analysis,

$$D_0^2 x_{11} + \omega_1^2 x_{11} = \tilde{F}\cos\Omega t - 2D_0D_1x_{10} - 2\tilde{\zeta}_1 D_0 x_{10} - 2\tilde{\zeta}_2 D_0 x_{10} + 2\tilde{\zeta}_2 D_0 x_{20} - \tilde{\gamma}_2 x_{10} + \tilde{\gamma}_2 x_{20} - \tilde{\eta}_1 x_{10}^{\,3} - \tilde{\eta}_2 (x_{20}^{\,3} + 3x_{10}^{\,2}x_{20} - 3x_{10}x_{20}^{\,2} - x_{10}^{\,3}) \quad \textbf{(3.2-30)}$$

$$D_0^2 x_{21} + \omega_2^2 x_{21} = 2\tilde{\zeta}_3 D_0 x_{10} - 2D_0D_1x_{20} - 2\tilde{\zeta}_3 D_0 x_{20} + \omega_2^2 x_{11} + \tilde{\eta}_3 (x_{20}^{\,3} + 3x_{10}^{\,2}x_{20} - 3x_{10}x_{20}^{\,2} - x_{10}^{\,3}) \quad \textbf{(3.2-31)}$$

where, $\omega_1^2 = \gamma_1$, $\omega_2^2 = \gamma_3$ **(3.2-32, 3.2-33)**

It is clear that each perturbation order requires explicit solutions to x_{10} and x_{20}, and then appropriate treatment of the emergent structures on the right hand sides.

3.2.4.4 Terms in x_{11} which are always seen to be *secular*

Harmonic solutions of equations (3.2-26) and (3.2-27) are appropriate; and stated in convenient polar forms, respectively, these are,

$$x_{10} = A_1(T_1)\, e^{i\omega_1 T_0} + \overline{A}_1(T_1)\, e^{-i\omega_1 T_0} \quad \textbf{(3.2-34)}$$

$$x_{20} = A_2(T_1)\, e^{i\omega_2 T_0} + \overline{A}_2(T_1)\, e^{-i\omega_2 T_0} + A_3(T_1)\, e^{i\omega_1 T_0} + \overline{A}_3(T_1)\, e^{-i\omega_1 T_0} \quad \textbf{(3.2-35)}$$

Reference to Appendix B provides a validation of the above equations, and so re-stating equations (B.2-2) and (B.2-3) appropriately, gives,

$$A_3(T_1) = \Gamma\, A_1(T_1) \qquad , \qquad \Gamma = \frac{\omega_2^2}{\omega_2^2 - \omega_1^2} \qquad \textbf{(3.2-36, 3.2-37)}$$

The overbar denotes complex conjugacy and $i = \sqrt{-1}$. It is assumed that the system parameters are such that none of the internal resonances is activated, and the system is under a form of external resonance, as stated in Section 3.2.5.1. Substituting equations (3.2-34) and (3.2-35) into the right-hand side of equation (3.2-30), then removing the 'always secular' terms at the first perturbation order yields the following equation. Appendix C.1 shows the detailed analytical calculation, and so re-stating *In[11]*[1] from it as follows, shows the predominance of cubic structures that are present.

$$\frac{1}{2}e^{i(\Omega-\omega_1)T_0}\tilde{F} - \tilde{\gamma}_2 A_1 - i2\omega_1\tilde{\zeta}_1 A_1 - i2\omega_1\tilde{\zeta}_2 A_1 - 3\tilde{\eta}_1 A_1^2\overline{A}_1 + 3\tilde{\eta}_2 A_1^2\overline{A}_1 - 3\tilde{\eta}_2 A_1^2\overline{A}_3 + 6\tilde{\eta}_2 A_1 A_2\overline{A}_2$$
$$+\tilde{\gamma}_2 A_3 + i2\omega_1\tilde{\zeta}_2 A_3 - 6\tilde{\eta}_2 A_1 A_3\overline{A}_1 + 6\tilde{\eta}_2 A_1 A_3\overline{A}_3 - 6\tilde{\eta}_2 A_2 A_3\overline{A}_2 + 3\tilde{\eta}_2 A_3^2\overline{A}_1 - 3\tilde{\eta}_2 A_3^2\overline{A}_3 - i2\omega_1 A_1' + \text{c.c.}$$

(3.2-38)

As usual, c.c. denotes the complex conjugates of the preceding terms, whilst the prime indicates differentiation with respect to the slow time scale T_1 .

[1] Input line 11 from the *Mathematica* program in Appendix C.

3.2.5 Identification of the External and Internal Resonances

3.2.5.1 External resonance

Since the primary system is excited at Ω, which is going to be synchronous with ω_1, or nearly so, then one can state,

$$\Omega = \omega_1 + \varepsilon\nu \qquad \textbf{(3.2-39)}$$

3.2.5.2 Internal resonances

In Appendix C.2, three internal resonances are identified in the system. They are superharmonic, subharmonic and primary resonances, and are defined as the following specific cases of interest,

- Case 1 (Superharmonic Resonance) : $\omega_2 = \frac{1}{3}\omega_1 + \varepsilon\sigma_1$ **(3.2-40)**
- Case 2 (Subharmonic Resonance) : $\omega_2 = 3\,\omega_1 + \varepsilon\sigma_2$ **(3.2-41)**
- Case 3 (Primary Resonance) : $\omega_2 = \omega_1 + \varepsilon\sigma_3$ **(3.2-42)**

$\varepsilon\nu$ and $\varepsilon\sigma_1, \varepsilon\sigma_2, \varepsilon\sigma_3$ are conveniently defined as external and internal detuning parameters respectively, in common with literature style conventions for such quantities.

The theoretical analyses of Chapters 3 to 5 investigate a simple discrete physical system which is a vehicle for the phenomena of interest but is not a direct model of the ultrasonic system that will be discussed in Chapter 6. The resonance conditions predicted theoretically in these chapters do not, therefore, explicitly define the resonant behaviour of the experimental system. However the theoretical model does indeed encapsulate the phenomena, which can be observed and discussed here, within the experimental system. For this purpose the superharmonic resonance condition is examined first because of the particularly clear-cut manifestation of the phenomena of interest. These phenomena are also present in the subharmonic case and despite some algebraic complexities will also be present in the primary resonance case.

3.2.6 Case 1 (Superharmonic Resonance) : Method of Multiple Scales $\omega_2 = \frac{1}{3}\omega_1 + \varepsilon\sigma_1$

3.2.6.1 Secular terms from the first order perturbation equations

As usual, the system dynamics become more involved when internal resonances are activated. For instance, in the case of the superharmonic resonance ($1:{}^{1}\!/_{3}$), extra terms from *In[1]* of Appendix C.2 are required,

$$-e^{iT_0(3\omega_2-\omega_1)}\tilde{\eta}_2 A_2^3 + \text{c.c.} \qquad \textbf{(3.2-43)}$$

These need to be added to the 'always secular' terms of equation (3.2-38), to result in the following secular terms for perturbation x_{11} for this superharmonic resonance condition,

$$\begin{aligned}&-e^{iT_0(3\omega_2-\omega_1)}\tilde{\eta}_2 A_2^3 + \frac{1}{2}e^{i(\Omega-\omega_1)T_0}\tilde{F} - \tilde{\gamma}_2 A_1 - i2\omega_1\tilde{\zeta}_1 A_1 - i2\omega_1\tilde{\zeta}_2 A_1 - 3\tilde{\eta}_1 A_1^2\overline{A}_1 + 3\tilde{\eta}_2 A_1^2\overline{A}_1\\ &-3\tilde{\eta}_2 A_1^2\overline{A}_3 + 6\tilde{\eta}_2 A_1 A_2\overline{A}_2 + \tilde{\gamma}_2 A_3 + i2\omega_1\tilde{\zeta}_2 A_3 - 6\tilde{\eta}_2 A_1 A_3\overline{A}_1 + 6\tilde{\eta}_2 A_1 A_3\overline{A}_3 - 6\tilde{\eta}_2 A_2 A_3\overline{A}_2\\ &+3\tilde{\eta}_2 A_3^2\overline{A}_1 - 3\tilde{\eta}_2 A_3^2\overline{A}_3 - i2\omega_1 A_1' + \text{c.c.}\end{aligned} \qquad \textbf{(3.2-44)}$$

In Appendix C.3, the secular and complex conjugate terms in equation (3.2-44) are removed from the inhomogeneous part of equation (3.2-30) and so x_{11} is then derived as equation *In[19]* of Appendix C.3, as re-stated below,

$$x_{11} = e^{i\omega_2 T_0}\left(\frac{1}{\omega_1^2-\omega_2^2}\left(\tilde{\gamma}_2 A_2 + i2\omega_2\tilde{\zeta}_2 A_2 - 6\tilde{\eta}_2 A_1 A_2 \bar{A}_1 + 6\tilde{\eta}_2 A_1 A_2 \bar{A}_3 - 3\tilde{\eta}_2 A_2^2 \bar{A}_2 + 6\tilde{\eta}_2 A_2 A_3 \bar{A}_1 - 6\tilde{\eta}_2 A_2 A_3 \bar{A}_2\right)\right)$$

$$+ \text{terms proportional to } e^{i(2\omega_2+\omega_1)T_0}, e^{i3\omega_1 T_0}, e^{i(\omega_2-2\omega_1)T_0}, e^{i(\omega_2+2\omega_1)T_0}, e^{i(2\omega_2-\omega_1)T_0} + \text{c.c.} \qquad \textbf{(3.2-45)}$$

Perturbation x_{11} is then substituted into the inhomogeneous part of equation (3.2-31), and the 'always secular' terms of x_{21} (from *In[12]* of Appendix C.4) are then identified as follows (refer to Appendix C.4 for intermediate analysis),

$$\frac{\omega_2^2\tilde{\gamma}_2 A_2}{\omega_1^2-\omega_2^2} + \frac{i2\omega_2^3\tilde{\zeta}_2 A_2}{\omega_1^2-\omega_2^2} - i2\omega_2\tilde{\zeta}_3 A_2 - \frac{6\omega_2^2\tilde{\eta}_2 A_1 A_2 \bar{A}_1}{\omega_1^2-\omega_2^2} + \frac{6\omega_2^2\tilde{\eta}_2 A_1 A_2 \bar{A}_3}{\omega_1^2-\omega_2^2} + 6\tilde{\eta}_3 A_1 A_2 \bar{A}_1 - 6\tilde{\eta}_3 A_1 A_2 \bar{A}_3$$
$$- \frac{3\omega_2^2\tilde{\eta}_2 A_2^2 \bar{A}_2}{\omega_1^2-\omega_2^2} + 3\tilde{\eta}_3 A_2^2 \bar{A}_2 + \frac{6\omega_2^2\tilde{\eta}_2 A_2 A_3 \bar{A}_1}{\omega_1^2-\omega_2^2} - \frac{6\omega_2^2\tilde{\eta}_2 A_2 A_3 \bar{A}_3}{\omega_1^2-\omega_2^2} - 6\tilde{\eta}_3 A_2 A_3 \bar{A}_1 + 6\tilde{\eta}_3 A_2 A_3 \bar{A}_3 - i2\omega_2 A_2' + \text{c.c.}$$

(3.2-46)

Again, extra terms for the superharmonic resonance need to be added to equation (3.2-46) as follows,

$$e^{i(\omega_1-3\omega_2)T_0}\left(-3\tilde{\eta}_3 A_1 \bar{A}_2^2 + 3\tilde{\eta}_3 A_3 \bar{A}_2^2 + \frac{3\omega_2^2\tilde{\eta}_2 A_1 \bar{A}_2^2}{4\omega_1\omega_2-4\omega_2^2} - \frac{3\omega_2^2\tilde{\eta}_2 A_3 \bar{A}_2^2}{4\omega_1\omega_2-4\omega_2^2}\right) + \text{c.c.}$$

(3.2-47)

This results in the following secular terms for perturbation x_{21} for the superharmonic resonance case,

$$e^{i(\omega_1-3\omega_2)T_0}\left(-3\tilde{\eta}_3 A_1 \bar{A}_2^2 + 3\tilde{\eta}_3 A_3 \bar{A}_2^2 + \frac{3\omega_2^2\tilde{\eta}_2 A_1 \bar{A}_2^2}{4\omega_1\omega_2-4\omega_2^2} - \frac{3\omega_2^2\tilde{\eta}_2 A_3 \bar{A}_2^2}{4\omega_1\omega_2-4\omega_2^2}\right) + \frac{\omega_2^2\tilde{\gamma}_2 A_2}{\omega_1^2-\omega_2^2} + \frac{i2\omega_2^3\tilde{\zeta}_2 A_2}{\omega_1^2-\omega_2^2}$$
$$- i2\omega_2\tilde{\zeta}_3 A_2 - \frac{6\omega_2^2\tilde{\eta}_2 A_1 A_2 \bar{A}_1}{\omega_1^2-\omega_2^2} + \frac{6\omega_2^2\tilde{\eta}_2 A_1 A_2 \bar{A}_3}{\omega_1^2-\omega_2^2} + 6\tilde{\eta}_3 A_1 A_2 \bar{A}_1 - 6\tilde{\eta}_3 A_1 A_2 \bar{A}_3 - \frac{3\omega_2^2\tilde{\eta}_2 A_2^2 \bar{A}_2}{\omega_1^2-\omega_2^2}$$
$$+ 3\tilde{\eta}_3 A_2^2 \bar{A}_2 + \frac{6\omega_2^2\tilde{\eta}_2 A_2 A_3 \bar{A}_1}{\omega_1^2-\omega_2^2} - \frac{6\omega_2^2\tilde{\eta}_2 A_2 A_3 \bar{A}_3}{\omega_1^2-\omega_2^2} - 6\tilde{\eta}_3 A_2 A_3 \bar{A}_1 + 6\tilde{\eta}_3 A_2 A_3 \bar{A}_3 - i2\omega_2 A_2' + \text{c.c.}$$

(3.2-48)

Appendix C.5 identifies the 3 internal resonances of x_{21}, and they are identical to those in Section 3.2.5.2.

3.2.6.2 Modulation equations

The general approach in multiple scales is to equate the secular terms of equations such as (3.2-44) and (3.2-48) to zero, so as to preserve the uniformity of the expansion. The complex amplitudes A_1 and A_2 can be expressed here in polar form, in common with conventional practice based on algebraic expediency,

$$A_n = \frac{1}{2} a_n \, e^{i \beta_n} \quad , \quad \overline{A}_n = \frac{1}{2} a_n \, e^{-i \beta_n} \qquad \textbf{(3.2-49)}$$

Clearly, a_n and β_n are real and are functions of T_1. Substituting them into equations (3.2-44) and (3.2-48) and separating out the real and the imaginary parts of the resulting relations, leads to a set of modulation equations (also known as slow-time equations). Appendix C.6 shows the derivation of the four modulation equations; *In[18]*, *In[19]*, In*[26]* and *In[27]*, and they are re-stated here as ,

$$\frac{\tilde{F}}{2}\cos[\Lambda_1] - \frac{1}{2}\tilde{\gamma}_2 a_1 + \frac{1}{2}\Gamma\tilde{\gamma}_2 a_1 - \frac{3}{8}\tilde{\eta}_1 a_1^3 + \frac{3}{8}\tilde{\eta}_2 a_1^3 - \frac{9}{8}\Gamma\tilde{\eta}_2 a_1^3 + \frac{9}{8}\Gamma^2\tilde{\eta}_2 a_1^3 - \frac{3}{8}\Gamma^3\tilde{\eta}_2 a_1^3$$
$$+\frac{3}{4}\tilde{\eta}_2 a_1 a_2^2 - \frac{3}{4}\Gamma\tilde{\eta}_2 a_1 a_2^2 - \frac{1}{8}\cos[\Phi_1]\tilde{\eta}_2 a_2^3 + \omega_1 a_1 \beta_1' = 0$$

(3.2-50)

$$\frac{\tilde{F}}{2}\sin[\Lambda_1] - \omega_1\tilde{\zeta}_1 a_1 - \omega_1\tilde{\zeta}_2 a_1 + \Gamma\omega_1\tilde{\zeta}_2 a_1 - \frac{1}{8}\sin[\Phi_1]\tilde{\eta}_2 a_2^3 - \omega_1 a_1' = 0$$

(3.2-51)

$$\frac{\omega_2^2\tilde{\gamma}_2 a_2}{2\omega_1^2-2\omega_2^2}-\frac{3\omega_2^2\tilde{\eta}_2 a_1^2 a_2}{4\omega_1^2-4\omega_2^2}-\frac{3\Gamma^2\omega_2^2\tilde{\eta}_2 a_1^2 a_2}{4\omega_1^2-4\omega_2^2}+\frac{3\Gamma\omega_2^2\tilde{\eta}_2 a_1^2 a_2}{2\omega_1^2-2\omega_2^2}+\frac{3}{4}\tilde{\eta}_3 a_1^2 a_2-\frac{3}{2}\Gamma\tilde{\eta}_3 a_1^2 a_2$$

$$+\frac{3}{4}\Gamma^2\tilde{\eta}_3 a_1^2 a_2+\frac{3\cos[\Phi_1]\omega_2^2\tilde{\eta}_2 a_1 a_2^2}{32\omega_1\omega_2-32\omega_2^2}-\frac{3\Gamma\cos[\Phi_1]\omega_2^2\tilde{\eta}_2 a_1 a_2^2}{32\omega_1\omega_2-32\omega_2^2}-\frac{3}{8}\cos[\Phi_1]\tilde{\eta}_3 a_1 a_2^2$$

$$+\frac{3}{8}\Gamma\cos[\Phi_1]\tilde{\eta}_3 a_1 a_2^2-\frac{3\omega_2^2\tilde{\eta}_2 a_2^3}{8\omega_1^2-8\omega_2^2}+\frac{3}{8}\tilde{\eta}_3 a_2^3+\omega_2 a_2\beta_2'=0$$

(3.2-52)

$$\frac{\omega_2^3\tilde{\zeta}_2 a_2}{\omega_1^2-\omega_2^2}-\omega_2\tilde{\zeta}_3 a_2-\frac{3\sin[\Phi_1]\omega_2^2\tilde{\eta}_2 a_1 a_2^2}{32\omega_1\omega_2-32\omega_2^2}+\frac{3\Gamma\sin[\Phi_1]\omega_2^2\tilde{\eta}_2 a_1 a_2^2}{32\omega_1\omega_2-32\omega_2^2}+\frac{3}{8}\sin[\Phi_1]\tilde{\eta}_3 a_1 a_2^2$$

$$-\frac{3}{8}\Gamma\sin[\Phi_1]\tilde{\eta}_3 a_1 a_2^2-\omega_2 a_2'=0$$

(3.2-53)

where $\Lambda_1=\nu_1 T_1-\beta_1$, $\Phi_1=3\sigma_1 T_1-\beta_1+3\beta_2$ **(3.2-54 , 3.2-55)**

and the primes indicate differentiation with respect to the slow time scale T_1. The form of equations (3.2-50) - (3.2-53) renders the system autonomous because of the use of equations (3.2-54) and (3.2-55).

For steady state, the condition is required for this autonomous system whereby,

$$a_1'=a_2'=\Lambda_1'=\Phi_1'=0 \qquad \textbf{(3.2-56)}$$

noting that the dependence on slow time scale T_1 provides a reasonable justification for doing this.

In order to apply the steady-state conditions, it is necessary to differentiate equations (3.2-54) and (3.2-55) with respect to T_1 leading to,

$$\Lambda_1' = \nu_1 - \beta_1' = 0 \quad ; \quad \beta_1' = \nu_1 \qquad \textbf{(3.2-57)}$$

$$\Phi_1' = 3\sigma_1 - \beta_1' + 3\beta_2' = 0 \quad ; \quad \beta_2' = \frac{1}{3}\nu_1 - \sigma_1 \qquad \textbf{(3.2-58)}$$

Substituting equations (3.2-56) to (3.2-58) into equations (3.2-50) to (3.2-53) generates the following four algebraic equations,

$$\frac{\tilde{F}}{2}\cos[\Lambda_1] = \frac{1}{8}\cos[\Phi_1]\tilde{\eta}_2 a_2^3 + \frac{1}{2}\tilde{\gamma}_2 a_1 - \frac{1}{2}\Gamma\tilde{\gamma}_2 a_1 + \frac{3}{8}\tilde{\eta}_1 a_1^3 - \frac{3}{8}\tilde{\eta}_2 a_1^3$$
$$+\frac{9}{8}\Gamma\tilde{\eta}_2 a_1^3 - \frac{9}{8}\Gamma^2\tilde{\eta}_2 a_1^3 + \frac{3}{8}\Gamma^3\tilde{\eta}_2 a_1^3 - \frac{3}{4}\tilde{\eta}_2 a_1 a_2^2 + \frac{3}{4}\Gamma\tilde{\eta}_2 a_1 a_2^2 - \omega_1 a_1 \nu_1$$

(3.2-59)

$$\frac{\tilde{F}}{2}\sin[\Lambda_1] = \frac{1}{8}\sin[\Phi_1]\tilde{\eta}_2 a_2^3 + \omega_1\tilde{\zeta}_1 a_1 + \omega_1\tilde{\zeta}_2 a_1 - \Gamma\omega_1\tilde{\zeta}_2 a_1$$

(3.2-60)

$$\left(\frac{3\omega_2^2\tilde{\eta}_2 a_1 a_2^2}{32\omega_1\omega_2 - 32\omega_2^2} - \frac{3\Gamma\omega_2^2\tilde{\eta}_2 a_1 a_2^2}{32\omega_1\omega_2 - 32\omega_2^2} - \frac{3}{8}\tilde{\eta}_3 a_1 a_2^2 + \frac{3}{8}\Gamma\tilde{\eta}_3 a_1 a_2^2\right)\cos[\Phi_1]$$
$$= -\frac{\omega_2^2\tilde{\gamma}_2 a_2}{2\omega_1^2 - 2\omega_2^2} + \frac{3\omega_2^2\tilde{\eta}_2 a_1^2 a_2}{4\omega_1^2 - 4\omega_2^2} + \frac{3\Gamma^2\omega_2^2\tilde{\eta}_2 a_1^2 a_2}{4\omega_1^2 - 4\omega_2^2} - \frac{3\Gamma\omega_2^2\tilde{\eta}_2 a_1^2 a_2}{2\omega_1^2 - 2\omega_2^2} - \frac{3}{4}\tilde{\eta}_3 a_1^2 a_2$$
$$+\frac{3}{2}\Gamma\tilde{\eta}_3 a_1^2 a_2 - \frac{3}{4}\Gamma^2\tilde{\eta}_3 a_1^2 a_2 + \frac{3\omega_2^2\tilde{\eta}_2 a_2^3}{8\omega_1^2 - 8\omega_2^2} - \frac{3}{8}\tilde{\eta}_3 a_2^3 - \omega_2 a_2\left(\frac{1}{3}\nu_1 - \sigma_1\right)$$

(3.2-61)

$$\left(\frac{3\omega_2^2\tilde{\eta}_2 a_1 a_2^2}{32\omega_1\omega_2 - 32\omega_2^2} - \frac{3\Gamma\omega_2^2\tilde{\eta}_2 a_1 a_2^2}{32\omega_1\omega_2 - 32\omega_2^2} - \frac{3}{8}\tilde{\eta}_3 a_1 a_2^2 + \frac{3}{8}\Gamma\tilde{\eta}_3 a_1 a_2^2\right)\sin[\Phi_1]$$
$$= \frac{\omega_2^3\tilde{\zeta}_2 a_2}{\omega_1^2 - \omega_2^2} - \omega_2\tilde{\zeta}_3 a_2 \qquad \textbf{(3.2-62)}$$

3.2.6.3 Solvability equations

Squaring and adding equations (3.2-59) & (3.2-60) and (3.2-61) & (3.2-62) leads to the so-called *solvability equations* for the superharmonic resonance of Case 1 (See Appendix C.7 for detailed intermediate analytical calculations).

$$
\begin{aligned}
&1296\varepsilon\tilde{F}^2\left(\left(\Gamma-1\right)^2\left(\omega_1+\omega_2\right)^2\left(\omega_2\varepsilon\tilde{\eta}_2+4(\omega_2-\omega_1)\varepsilon\tilde{\eta}_3\right)^2 a_1^2\right)\\
&=\left(\omega_1\left(\varepsilon\tilde{\zeta}_1-(\Gamma-1)\varepsilon\tilde{\zeta}_2\right)a_1-\frac{4\omega_2\left(\omega_2^2\left(\varepsilon\tilde{\zeta}_2+\varepsilon\tilde{\zeta}_3\right)-\omega_1^2\varepsilon\zeta_3\right)\varepsilon\tilde{\eta}_2 a_2^2}{3(\Gamma-1)\left(\omega_1+\omega_2\right)\left(\omega_2\varepsilon\tilde{\eta}_2+4\left(\omega_2-\omega_1\right)\varepsilon\tilde{\eta}_3\right)a_1}\right)^2+\\
&\left(\begin{array}{l}
9(\Gamma-1)\left(\omega_1+\omega_2\right)\left(4\omega_1\varepsilon\tilde{\eta}_3-\omega_2\left(\varepsilon\tilde{\eta}_2+4\varepsilon\tilde{\eta}_3\right)\right)a_1^2\left(8\varepsilon\nu_1\omega_1+4\left(\Gamma-1\right)\varepsilon\tilde{\gamma}_2-3\left(\varepsilon\tilde{\eta}_1+\left(\Gamma-1\right)^3\varepsilon\tilde{\eta}_2\right)a_1^2\right)\\
+2\varepsilon\tilde{\eta}_2\left(8\omega_2\left(2\left(\varepsilon\nu_1-3\varepsilon\sigma_1\right)\left(\omega_1^2-\omega_2^2\right)+3\omega_2\varepsilon\tilde{\gamma}_2\right)-9\left(\Gamma-1\right)^2\left(\omega_2\left(\omega_2-3\omega_1\right)\varepsilon\tilde{\eta}_2+8\left(\omega_1^2-\omega_2^2\right)\varepsilon\tilde{\eta}_3\right)a_1^2\right)a_2^2\\
-36\varepsilon\tilde{\eta}_2\left(\omega_2^2\left(\varepsilon\tilde{\eta}_2+\varepsilon\tilde{\eta}_3\right)-\omega_1^2\varepsilon\tilde{\eta}_3\right)a_2^4
\end{array}\right)^2
\end{aligned}
\qquad \textbf{(3.2-63)}
$$

$$
\begin{aligned}
&\left(\omega_1-\omega_2\right)^2\left(576\omega_2^2\left(\frac{\omega_2^2\varepsilon\tilde{\zeta}_2}{\omega_2^2-\omega_1^2}+\varepsilon\tilde{\zeta}_3\right)^2+\frac{1}{\left(\omega_1^2-\omega_2^2\right)^2}\left(\begin{array}{l}
4\omega_2\left(2\left(\varepsilon\nu_1-3\varepsilon\sigma_1\right)\left(\omega_2^2-\omega_1^2\right)-3\omega_2\varepsilon\tilde{\gamma}_2\right)+\\
9\left(\omega_2^2\left(\varepsilon\tilde{\eta}_2+\varepsilon\tilde{\eta}_3\right)-\omega_1^2\varepsilon\tilde{\eta}_3\right)\left(2\left(\Gamma-1\right)^2 a_1^2+a_2^2\right)
\end{array}\right)^2\right)\\
&=\frac{81}{16}\left(\Gamma-1\right)^2\left(\omega_2\varepsilon\tilde{\eta}_2+4\left(\omega_2-\omega_1\right)\varepsilon\tilde{\eta}_3\right)^2 a_1^2 a_2^2
\end{aligned}
\qquad \textbf{(3.2-64)}
$$

From the standpoint of these two *solvability equations*, the next section shows the results of the frequency-response plots for the superharmonic resonance under appropriately varying conditions and parameters.

3.2.7 Case 1 (Superharmonic Resonance) : Multiple Scales Results

Four autonomous, slow-time, modulation equations (3.2-50 to 3.2-53) were derived from the real and imaginary parts of the secular terms equations for perturbations x_{11} and x_{21}. The function of the secular terms equations is to remove those terms from the right hand sides of the perturbation equations that will otherwise invalidate the uniformity of the power series. The secular terms equations are then processed separately in order to find the steady-state amplitudes of the solutions. After this, a return is made to the main analysis to find the particular solutions for the system variables (i.e. co-ordinates), into which the analytical forms that have been found for the steady state amplitudes can be substituted to give the complete solutions.

In order to make progress, the *Mathematica* code was then used to solve numerically for a_1 and a_2 within equations (3.2-63) and (3.2-64). Graphs of Amplitudes versus Forcing Frequency (i.e. a_1 versus Ω) were plotted for different cubic stiffness values.

Table 3-1 represents the values of the constants for the graphs plotted for Figure 3-4. These values are obtained from the experimental set-up and experimental testing of an elastomer spring in Section 9.1 and Appendix F.1, respectively. Figure 3-4(a) and 3.4(b) shows the nondimensionalised response plots of amplitudes a_1 and a_2 respectively for the case of the superharmonic resonance

of equation (3.2-40). In these plots, the hardening cubic stiffness coefficient h_1, the excitation level, and all system quantities other than the softening cubic stiffness coefficient h_2, are kept constant.

Dimensional Parameters

Mass [kg]	Damping [Ns m^{-1}]	Stiffness (Linear) [Nm^{-1}]	Stiffness (Cubic) [Nm^{-3}]	Force [N]	Eigenvalues [rad s^{-1}]
$m_1 = 2$	$c_1 = 0.05$	$k_1 = 847,776$	$h_1 = 1200\times10^6$	$F^* = 10$	$\omega_{e1} = 209.828$
$m_2 = 1.125$	$c_2 = 0.05$	$k_2 = 52,986$	$h_2 =$ see below		$\omega_{e2} = 673.388$

Softening cubic stiffness coefficient, h_2 varies within the following range:

10×10^6 ; 20×10^6 ; 50×10^6 ; 100×10^6 [Nm^{-3}]

Reference displacement : $x^*_{ref} = 0.1$ m

Non-Dimensional Parameters

Damping	Stiffness (Linear)	Stiffness (Cubic)	Force
$\zeta_1 = 0.0000596$	$\gamma_1 = 9.6277$	$\eta_1 = 136.277$	$F = 0.0001136$
$\zeta_2 = 0.0000596$	$\gamma_2 = 0.601731$	$\eta_2 =$ varies	
$\zeta_3 = 0.0001059$	$\gamma_3 = 1.06974$	$\eta_3 =$ varies	

Table 3-1: Data of graphs plotted for Case 1

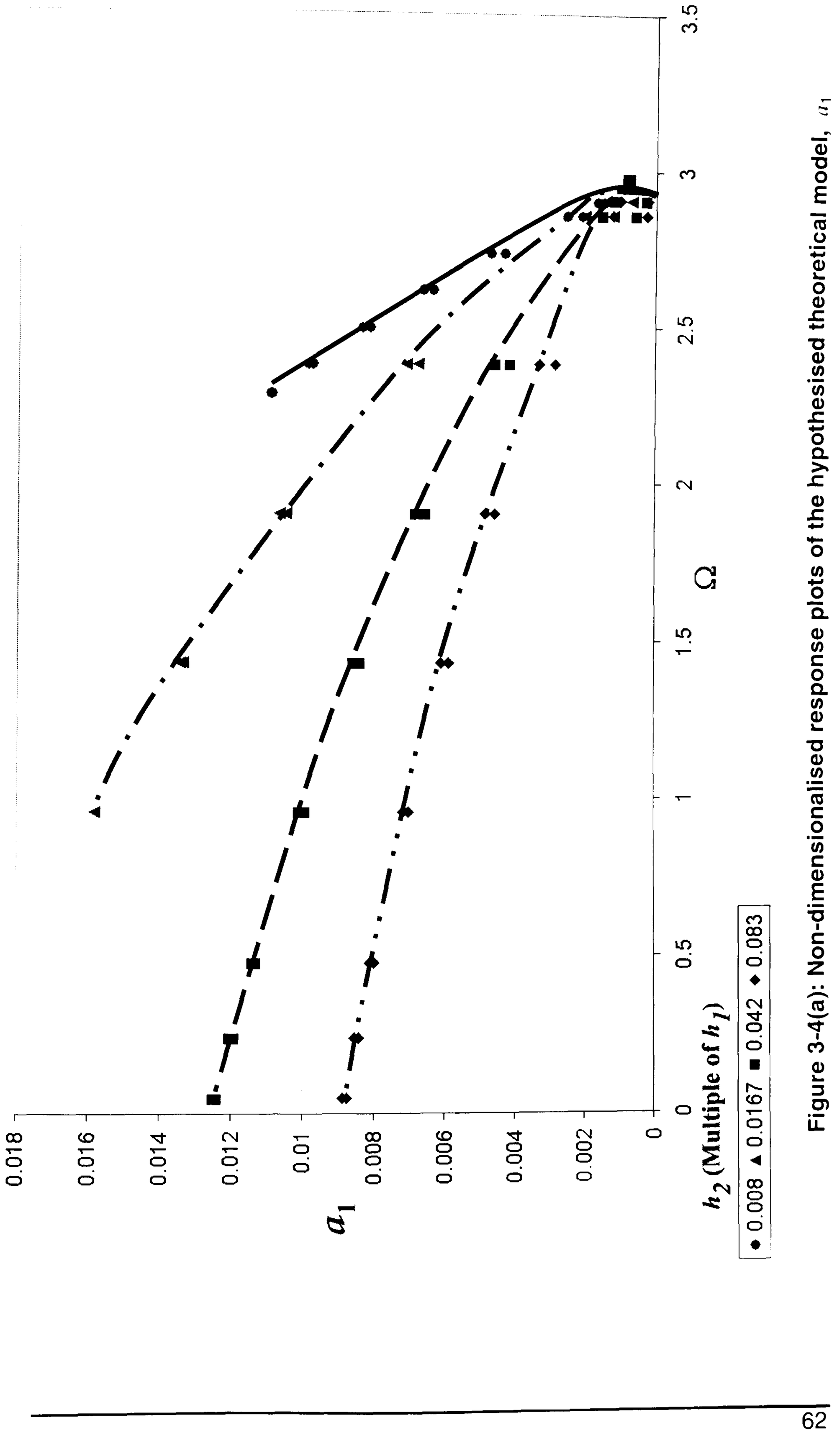

Figure 3-4(a): Non-dimensionalised response plots of the hypothesised theoretical model,

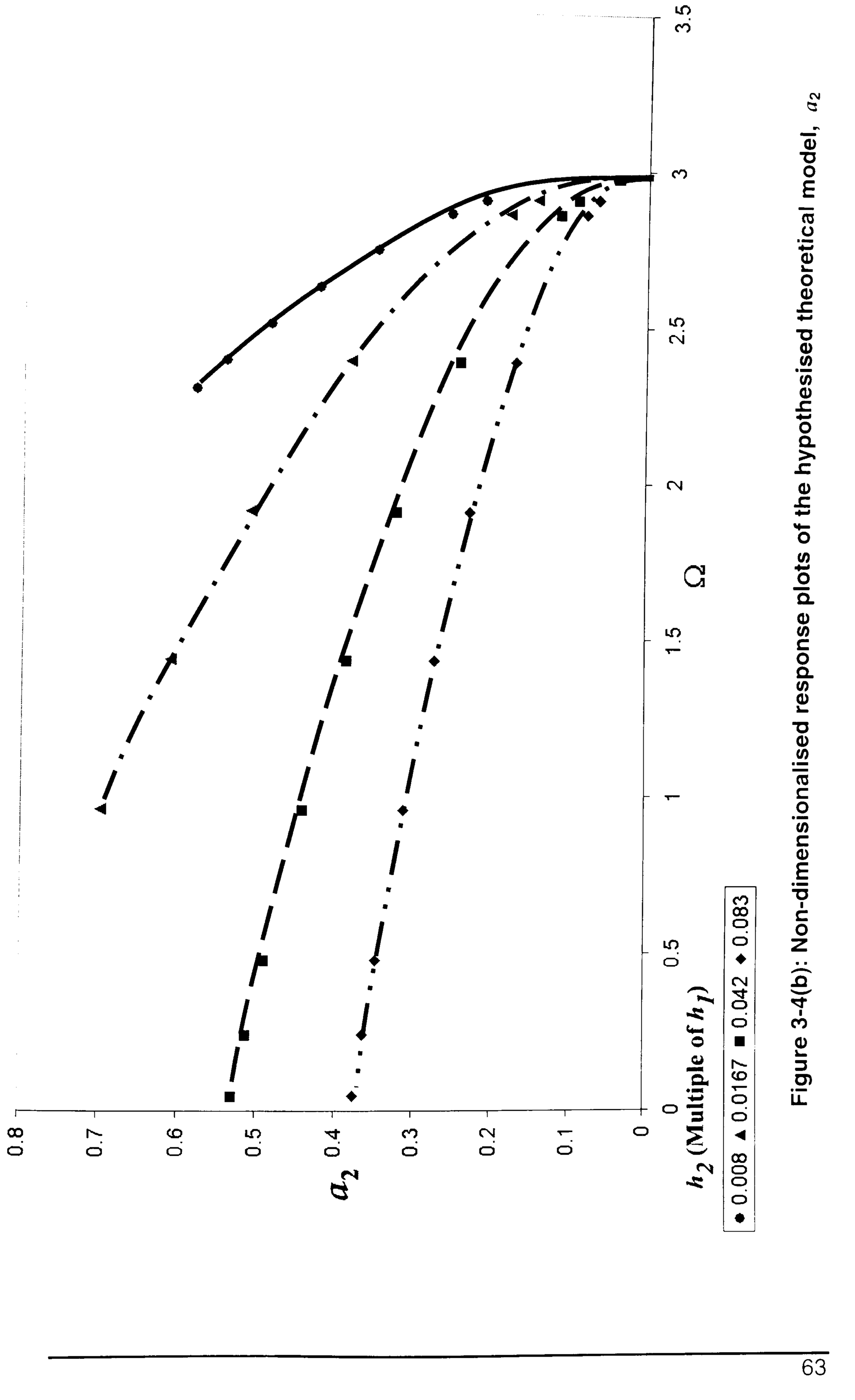

Figure 3-4(b): Non-dimensionalised response plots of the hypothesised theoretical model, a_2

3.2.8 Case 1 (Superharmonic Resonance) : Discussion of Results

Figure 3-4 presents the nondimensionalised response plots of the hypothesised theoretical model of Figure 3-1. Using the method of multiple scales, the effects of coupling an opposite nonlinear cubic stiffness to an initial nonlinear system have been accommodated for the superharmonic resonance. By varying only the softening cubic coefficient h_2, it is evident from Figures 3-4(a) and 3-4(b) that h_2 affects the general characteristic behaviour of the system.

The effect of increasing h_2 manifests as more accentuated softening behaviour by bending both responses towards the left. In both graphs, it is shown that as h_2 is increased from $0.008h_1$ to $0.083h_1$, both responses become more softening in nature, thus suggesting that the softening cubic coefficient does contribute significantly to the nonlinear properties of the overall system.

Conversely, a decrease in h_2 will cause the system to be less softening and bend towards a more linear response. The most desirable response is when $h_2 = 0.008h_1$ for which both responses a_1 and a_2 are distinctly linear in appearance.

Both graphs also show that the resonance curves are centred approximately at $\Omega \approx 3$ reflecting that this analysis is indeed representing the superharmonic resonance of the system.

CHAPTER 4

DIRECT NUMERICAL INTEGRATION

4.1 Introduction

The most general approach for the solution of the dynamic response of systems is direct numerical integration of the governing equations of motion in the time domain. The solution is initially defined at time zero and then convergence is sought thereafter at discrete points in time. Many methods use equal time steps at $\Delta t, 2\Delta t, 3\Delta t ..... N\Delta t$, however highly nonlinear systems benefit from more sophisticated alternatives where variable step size is employed in an attempt to achieve convergence.

The methods for integrating ordinary differential equations can be classified as the predictor-corrector method, multi-step methods and single-step methods. Predictor-corrector methods proceed by extrapolating a polynomial fit to the derivative from the previous points to the new point (the predictor step), then using this to interpolate the derivative (the corrector step). Press *et al.* (1992) opine that predictor-corrector methods have been largely supplanted by the Bulirsch-Stoer and Runge-Kutta methods, but predictor-corrector schemes are still in common use.

Multi-step methods include the Adams method and the Gear method. The principle behind a multi-step method is to utilise the past values of y and/or y' to construct a polynomial that approximates the derivative function, and extrapolate this into the next interval. Most methods use equispaced past values to make the construction of the polynomial easy, and the Adams method is typical. Referring to Figure 4-1, the Adams-Bashforth method uses the 0, -1, -2 and -3 data point to calculate the +1 value. Thus, quite large step sizes can be used accurately. A further advantage is that only one additional calculation is needed for each new step. The earlier points must be calculated using another technique, such as the Runge-Kutta method. A refinement of this approach is the Adams-Moulton method which includes a back calculation step to confirm the accuracy of the first step. These methods are called predictor-corrector methods (forward-backward calculations). These methods work well with ordinary differential equations, however, there are occasions where these methods become very inefficient, particularly for stiff systems.

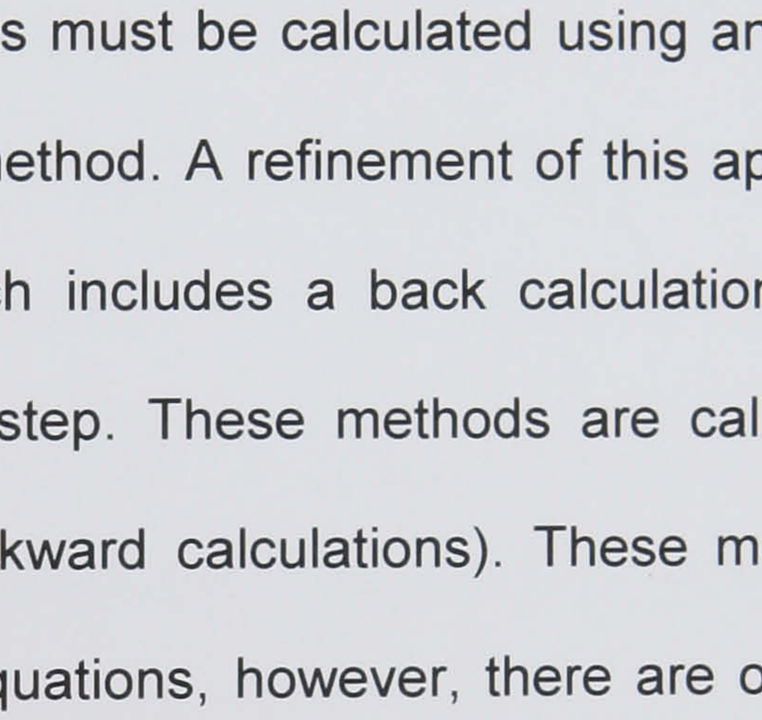

Figure 4-1: Illustrating a multi-step method

Stiff systems are distinguished from non-stiff systems in that they have interacting components that vary on widely different scales. Stiff systems are models where the ratio between the slowest and fastest rate constants is greater than 500 (stiffness ratio > 500). An answer to this problem is the Gear method (Gear, 1971). The Gear method, a predictor-corrector method, is very efficient for stiff systems. It is quite capable of efficiently working with systems with a stiffness ratio greater than 10^6.

The Newton-Raphson method is one of the most popular technique used by engineers for solving nonlinear equations. This method is distinguished from the others by the fact that it requires the evaluation of both the function $f(x)$ and the derivative $f'(x)$, at arbitrary points x. The Newton-Raphson formula consists geometrically of extending the tangent line at a current point x_i until it crosses zero, then setting the next guess x_{i+1} to the abscissa of that zero-crossing. The general iterative formula for this method is,

$$x_{n+1} = x_n - \frac{f(x_n)}{f'(x_n)} \qquad \textbf{(4.1-1)}$$

Another technique that has been applied to the dynamic analysis of many practical engineering structures is the Newmark method. Newmark (1959) presented a family of single-step integration methods for the solution of structural dynamic problems for both blast and seismic loading. Since then, it has been modified and improved by many other researchers such as Wilson and Clough (1962), Wilson *et al.* (1973) and Hughes (1987). In 1962, Wilson and Clough (1962) formulated Newmark's method in matrix notation, added stiffness and mass proportional damping, and

eliminated the need for iteration by introducing the direct solution of equations at each time step. Then Wilson *et al.* (1973) made the general Newmark method unconditionally stable with the introduction of a 'θ factor'. The introduction of the 'θ factor' is motivated by the observation that an unstable solution tends to oscillate about the true solution. Therefore, if the numerical solution is evaluated within the time increment, the spurious oscillations are minimised. Hughes (1987) then proposed the 'α method' and used the Newmark method to solve the following modified equations of motion,

$$M\ddot{u}_t + (1+\alpha)C\dot{u}_t + (1+\alpha)Ku_t = (1+\alpha)F_t - \alpha F_t + \alpha C\dot{u}_{t-\Delta t} + \alpha Ku_{t-\Delta t} \quad \textbf{(4.1-2)}$$

With α equal to zero, the method reduces to the constant acceleration method. It produces numerical energy dissipation in the higher modes; however, it cannot be predicted as a damping ratio as in the use of stiffness proportional damping. Also, it does not solve the fundamental equilibrium equation at time t. The performance of this method appears to be very similar to the use of stiffness proportional damping.

In this chapter, the Runge-Kutta technique is used to integrate numerically the equations of motion so that these can be compared with the results from Chapter 3 that were generated by the Method of Multiple Scales. The *Mathematica* program (Version 4.1.0.0) developed by Wolfram Research [Wolfram (1996)], has been used to carry out this analysis. The function used within this *Mathematica* code to solve the set of differential equations is *NDSolve[ ]*. *NDSolve[ ]* can handle a wide range of ordinary differential equations as well as some partial differential equations. In a system of ordinary differential equations there can be any number of

unknown functions y_i, but all of these functions must depend on a single "independent variable" x, which is the same for each function. *NDSolve[ ]* represents solutions for the functions y_i as *InterpolatingFunction* objects. The *InterpolatingFunction* objects provide approximations to the y_i over the range of values *xmin* to *xmax* for the independent variable x.

The integrator method selected within the function *NDSolve[ ]* is the fourth order Runge-Kutta (i.e. $Method \rightarrow RungeKutta$). This is because the relevant equations of motion are non-stiff. The Runge-Kutta method numerically integrates ordinary differential equations by using a trial step at the midpoint of an interval to cancel out lower-order error terms. The fourth order Runge-Kutta method requires four gradient or 'k' terms to calculate for y_{n+1},

$$y_{n+1} = y_n + \frac{1}{6}(k_1 + 2k_2 + 2k_3 + k_4) \qquad \textbf{(4.1-3)}$$

where h is the incremental independent variable and,

$$k_1 = hf(t_n, y_n) \quad ; \quad k_2 = hf\left(t_n + \frac{h}{2}, y_n + \frac{k_1}{2}\right)$$
$$k_3 = hf\left(t_n + \frac{h}{2}, y_n + \frac{k_2}{2}\right) \quad ; \quad k_4 = hf(t_n + h, y_n + k_3) \qquad \textbf{(4.1-4)}$$

4.2 System 1 : Stiffness Coupled Translating System Modelled In Physical Coordinates

In order to provide another theoretical basis for the comparison with the results from the multiple scales analysis, a direct numerical integration of the differential equations is carried out in this section.

4.2.1 Program Code

The code that numerically integrates the governing equations of motion (3.2-1) and (3.2-2) can be found in Appendix D.1. It is written in *Mathematica* and this code is for an upward frequency sweep. A definition of the program code follows next in Appendix D.2.

4.2.2 Sample Results from Mathematica

Some sample results from the bespoke *Mathematica* integrator are given from a frequency sweep up and down between Ω^* = 205 to 215, with a frequency step of Ωstep = 0.2, (units in rad/s). A superposition of the sweep up and sweep down graphs, together, for x_1 and x_2 can be found in Figures 4-4(b) and 4-5(b), respectively.

4.2.2.1 Frequency sweep up from $\Omega^* = 205$ to 215 rad/s

The program code in Section 4.2.1 took approximately 17576.4 seconds (about 5 hours) on a Pentium 4 - 2.4GHz - 512 Mb RAM computer to produce the following results,

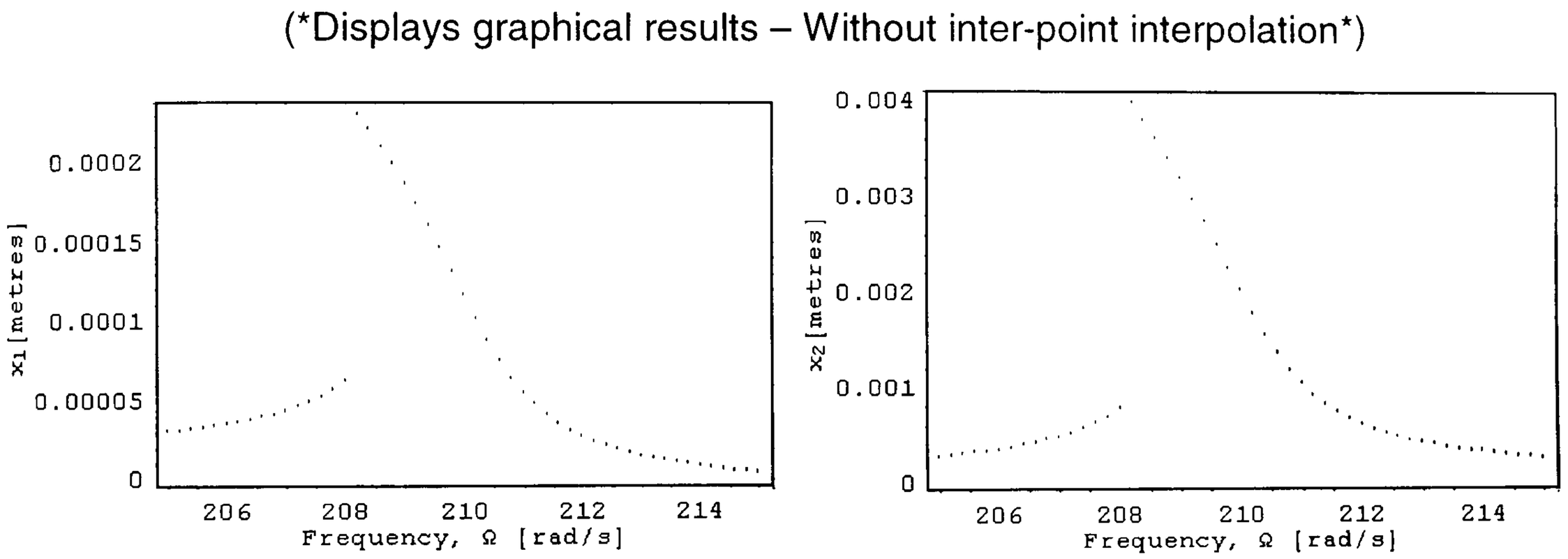

Figure 4-2: Numerical integration frequency sweep up

4.2.2.2 Frequency sweep down from Ω^* = 215 to 205 rad/s

Next, the results are presented for the downward sweep between Ω^* = 215 to 205 rad/s

(*Displays graphical results – Without inter-point interpolation*)

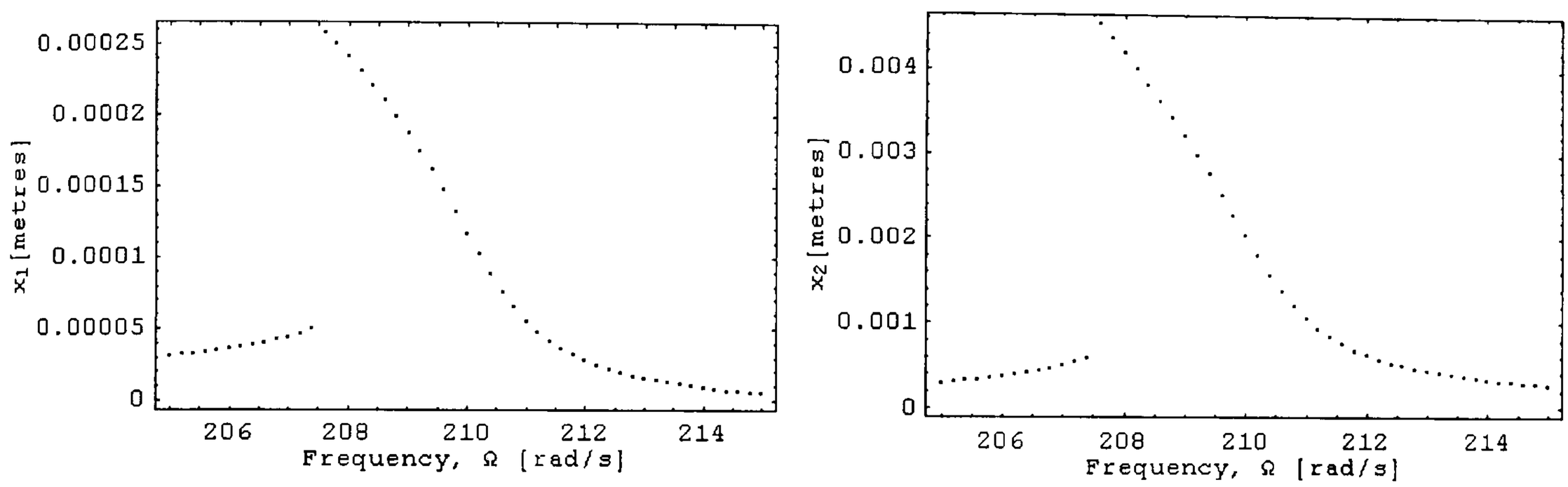

(*Displays graphical results – With inter-point interpolation*)

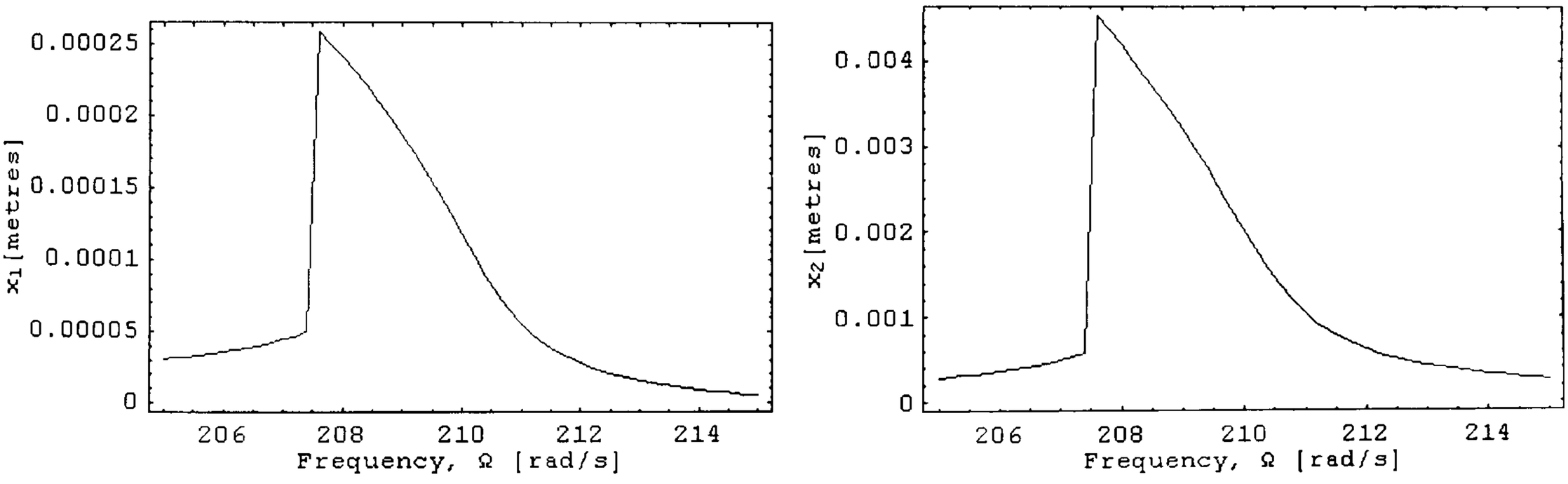

Figure 4-3: Numerical integration frequency sweep down

4.2.3 Case 1 (Superharmonic Resonance)

In order to provide a theoretical benchmark for comparison with the results from the multiple scales analysis, results from direct numerical integration of the differential equations are presented in this section. With certain modifications to some of the program control parameters within the general code summarised in Section 4.2.1 and Appendix D, non-dimensionalised frequency-response graphs are plotted for x_1 and x_2. In a similar approach as taken for the multiple scales analysis the softening cubic stiffness, h_2, is varied, but the rest of the constants remain the same as in Table 3-1. Figures 4-4(a) and 4-5(a) show the non-dimensionalised linear-logarithmic plot of the amplitude responses x_1 and x_2, with respect to the excitation frequency Ω.

An upward and downward sweep of the excitation frequency has been carried out for each overall iteration. The thicker lines denote the upward sweeps while the thinner lines denote the downward sweeps. A closer look at the first mode and the third order superharmonic is provided in Figures 4-4(b)/4-5(b) and 4-4(c)/4-5(c) respectively. It is clearly seen from Figures 4-4(b)/4-5(b) and 4-4(c)/4-5(c) that the regions between the respective thick and thin lines are multivalued, with at least one unstable solution implied. The familiar jump phenomena, which are evident here for the frequency sweep in both directions are as described in Section 1.4.1. The unstable regions in Figures 4-4(c) and 4-5(c) are approximately

around $\Omega = 3.23$ to 3.27 rad/s, with slight variations for the different values of h_2, however these can only be clearly seen if the diagrams are enlarged.

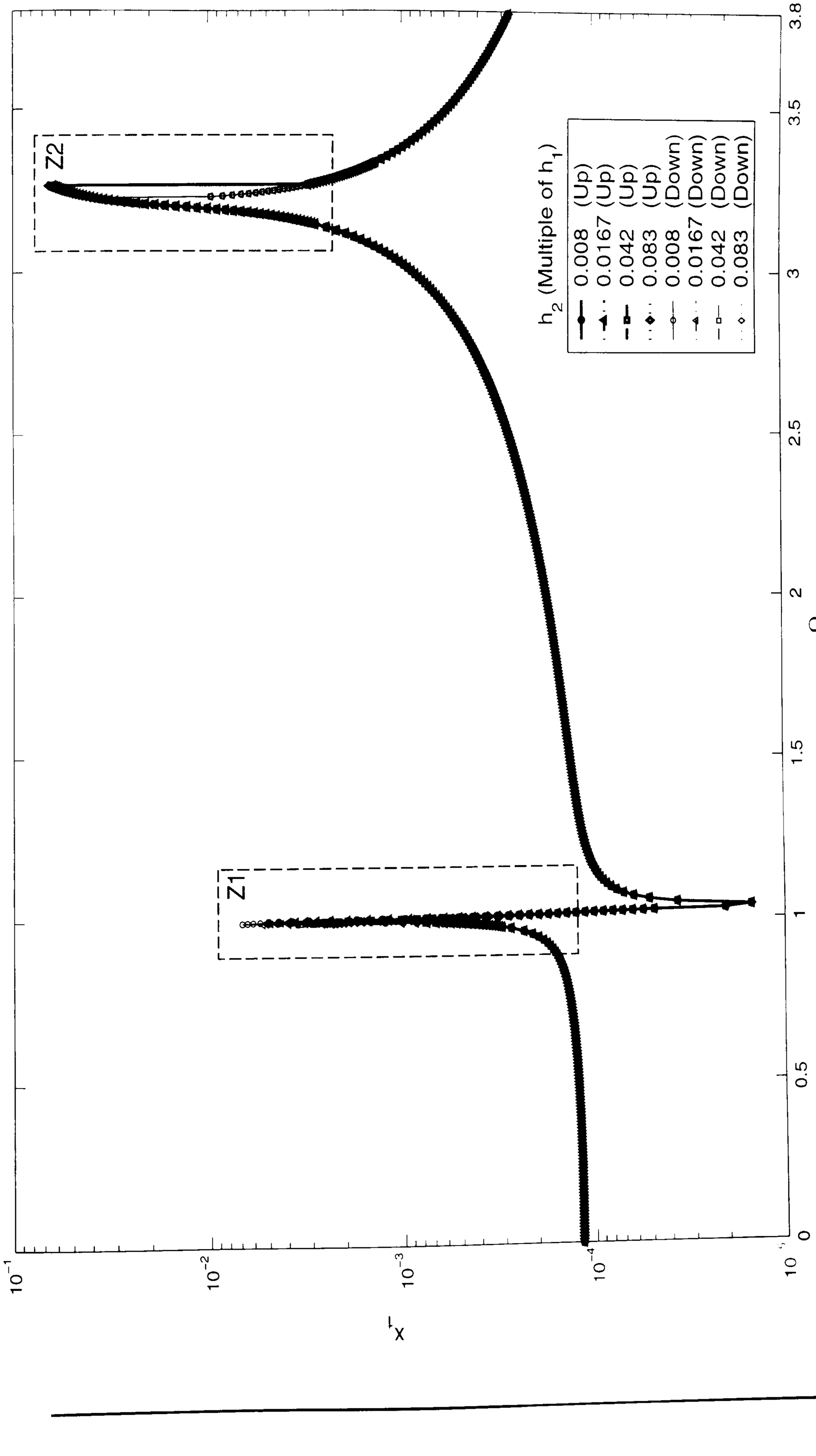

Figure 4-4(a): Direct numerical integration of non-dimensionalised x_1 vs Ω (Logarithmic Scale)

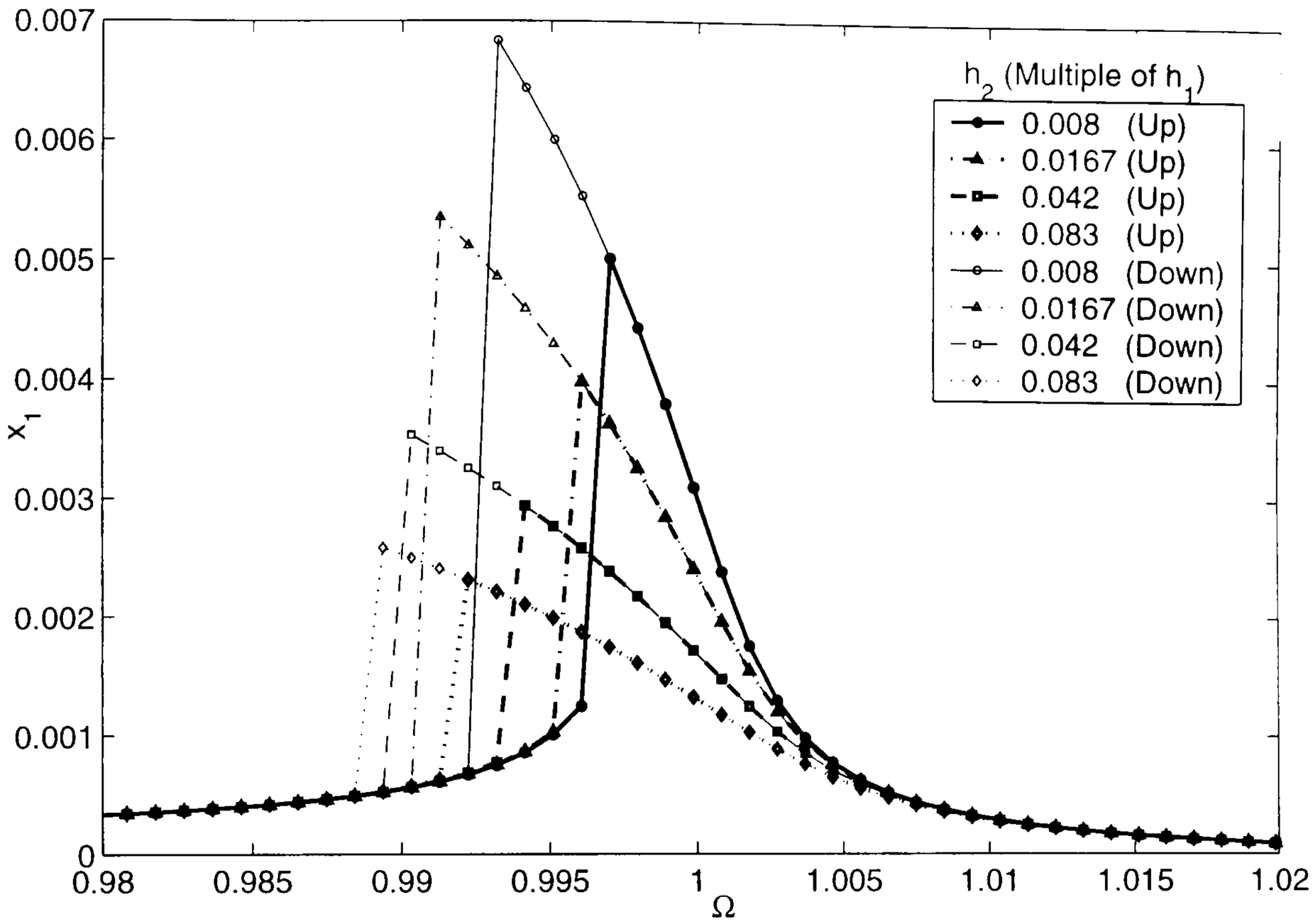

Figure 4-4(b): First mode of response x_1 - Enlarged view of region Z1 in Figure 4-4(a)

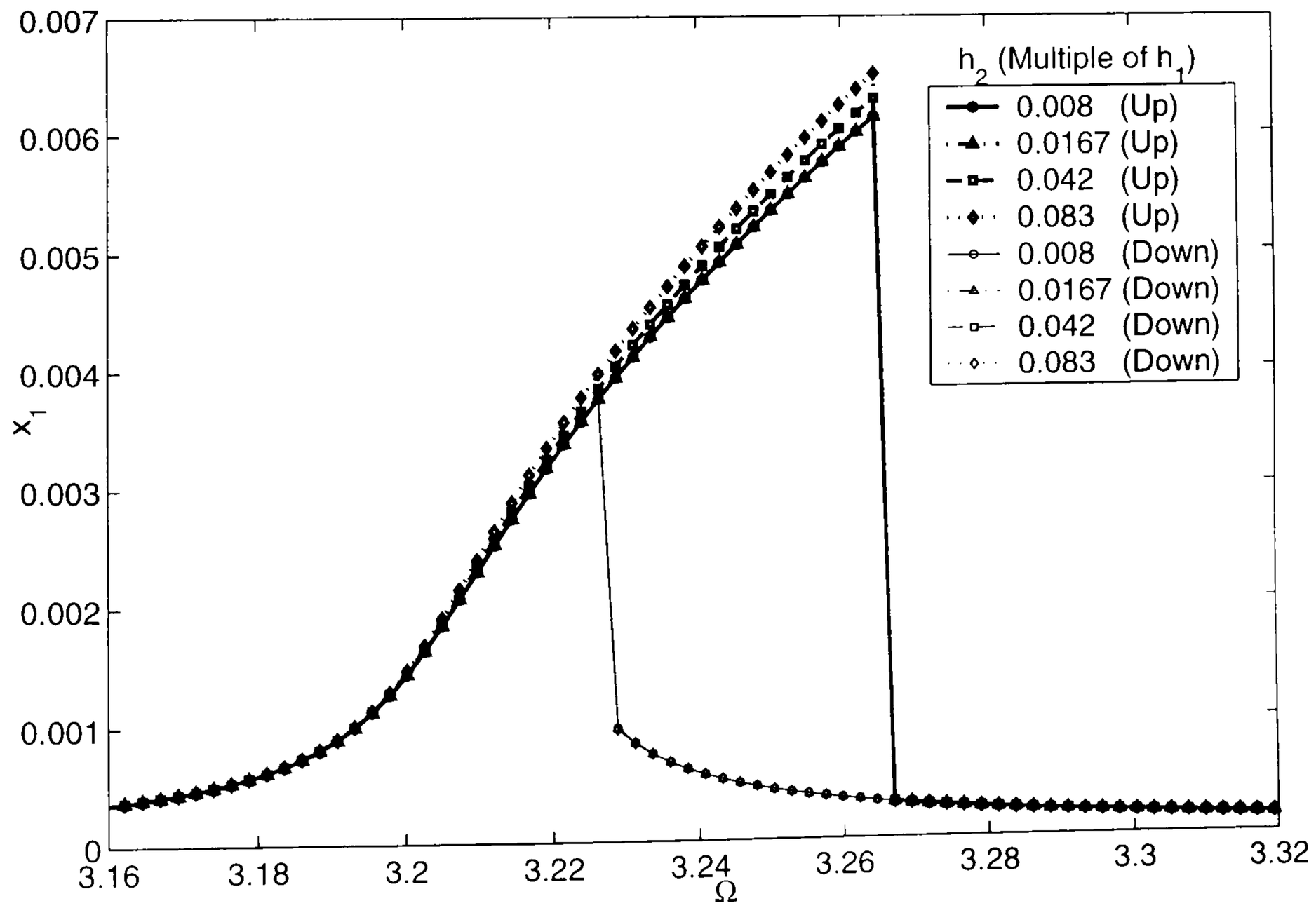

Figure 4-4(c): Third order superharmonic mode of response x_1 - Enlarged view of region Z2 in Figure 4-4(a)

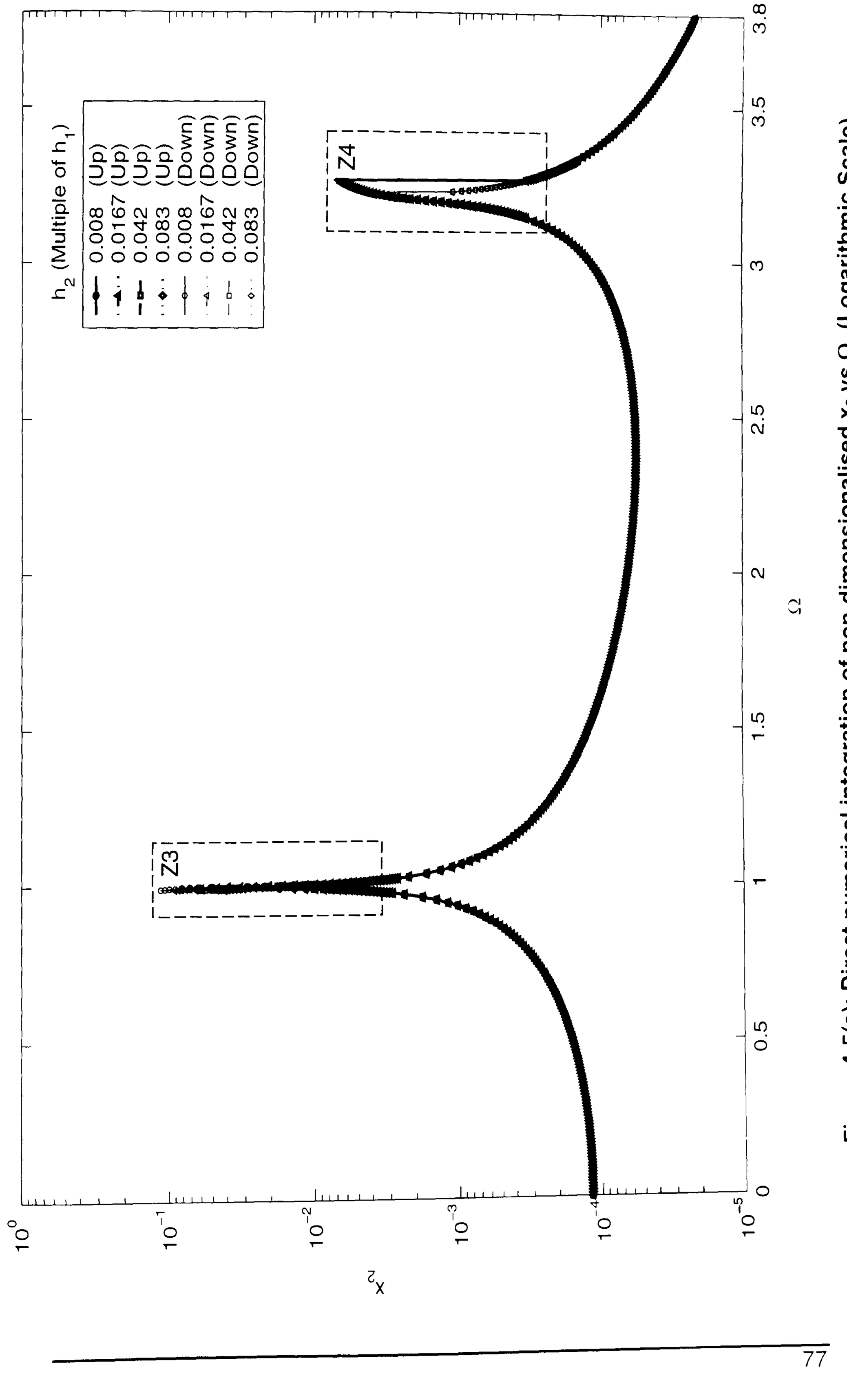
h2 (Multiple of h1)
0.008 (Up)
0.0167 (Up)
0.042 (Up)
0.083 (Up)
0.008 (Down)
0.0167 (Down)
0.042 (Down)
0.083 (Down)
Z4
Z3
3.8
3.5
3
2.5
2
1.5
1
0.5
0
Ω
10^0
10^-1
10^-2
10^-3
10^-4
10^-5
x2
Figure 4-5(a): Direct numerical integration of non-dimensionalised x2 vs Ω (Logarithmic Scale)

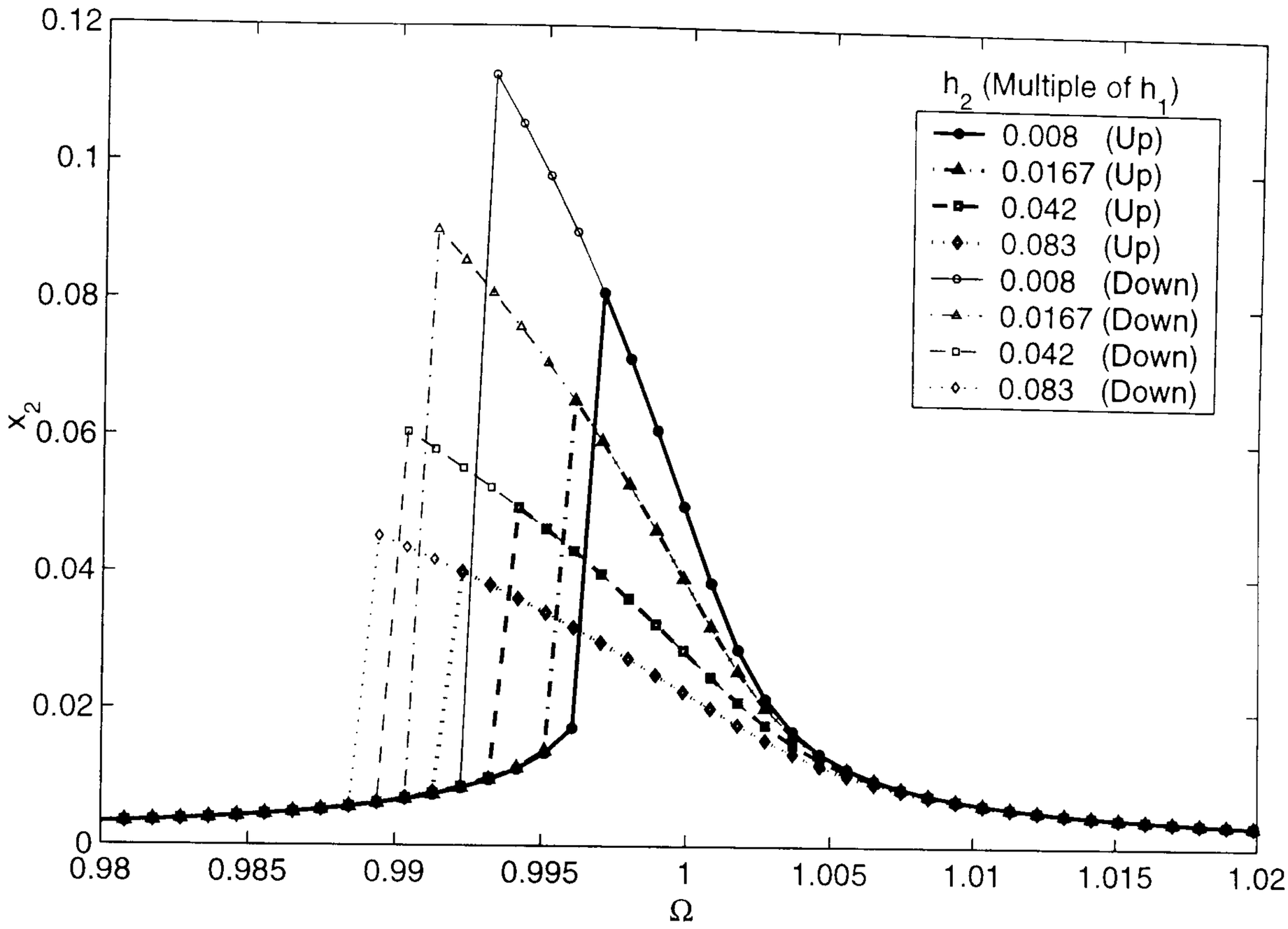

Figure 4-5(b): First mode of response x_2 - Enlarged view of region Z3 in Figure 4-5(a)

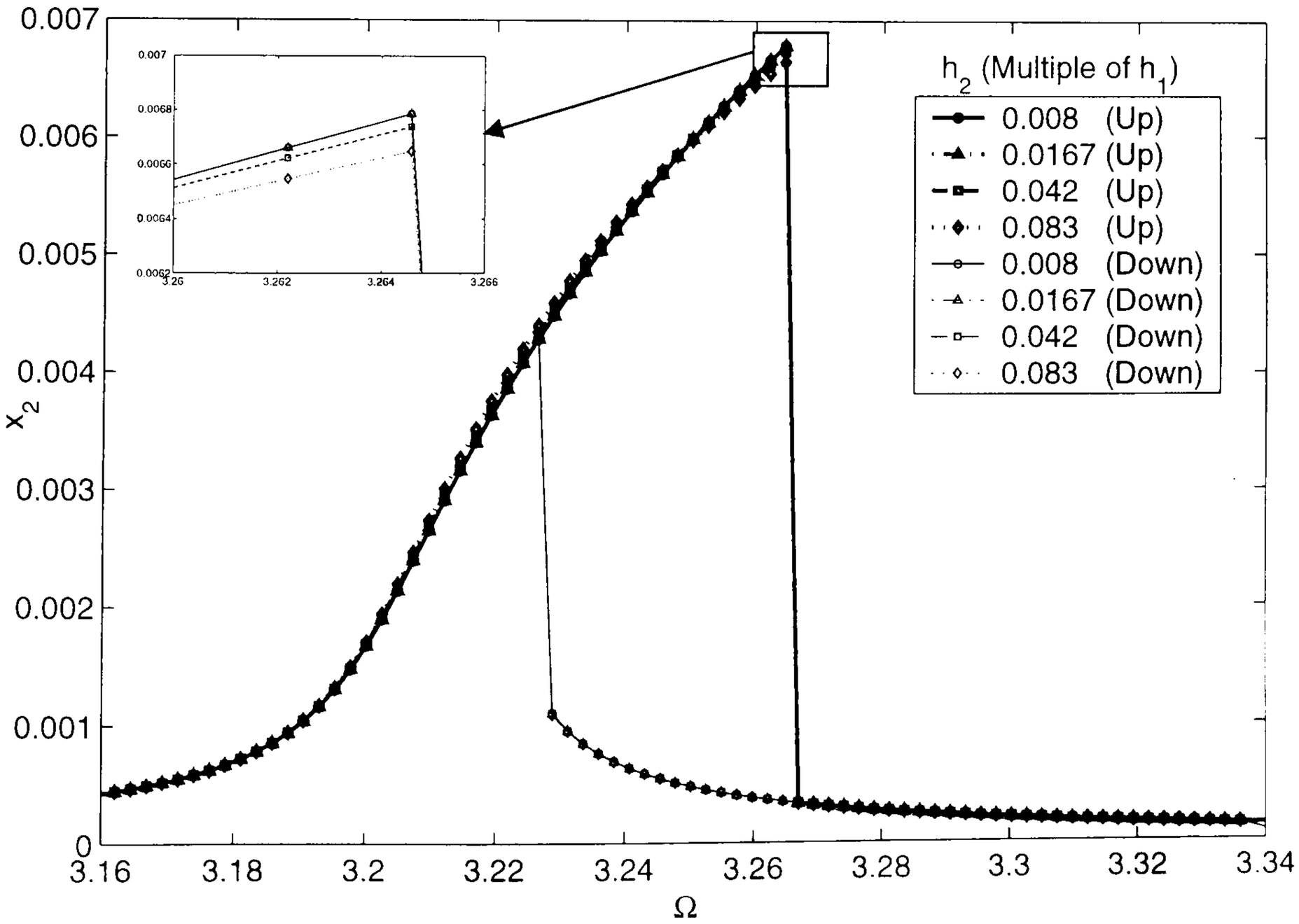

Figure 4-5(c): Third order superharmonic mode of response x_2 - Enlarged view of region Z4 in Figure 4-5(a)

4.2.3.1 Discussion of results

Comparison between the results from the multiple scales analysis in Section 3.2.7 and the numerical integration benchmark summarised here shows evidence of a consistent phenomenon whereby both the responses in the first mode of x_1 and x_2 show accentuated softening as the softening cubic coefficient is increased (see Figures 4-4(b) and 4-5(b)). The amplitudes of both a_2 and x_2 are also marginally higher than a_1 and x_1 for the response of the first mode. The results for the third order superharmonic in Figures 4-4(c) and 4-5(c) cannot be compared to results from the method of multiple scales analysis because the latter only gives results for the first mode around the region close to the external resonance condition where $\varepsilon\nu = 0$, as in equation (3.2-39). However, it is interesting to note that when the softening cubic stiffness coefficient is increased, the overall response characteristic shows a tendency to become more linear in Figure 4-4(c), whilst a more progressive hardening effect is visible in Figure 4-5(c).

CHAPTER 5

NUMERICAL INVESTIGATION OF SYSTEM DYNAMICS

5.1 Introduction

In the study of nonlinear dynamics, exact analytical solutions are hard, if not impossible, to find. Besides relying on precise analytical solutions, emphasis can also be placed on the qualitative behaviour of the system. Bifurications, Lyapunov exponents, manifestations of periodicity, chaotic attractors and fractal structure are all qualitative features which can be observed in solutions obtained from numerical integration. Therefore, understanding the dynamics of an analytically modelled system, or a system defined by a finite element model, can be extended further by recourse to techniques based on specialised numerical investigations. During the last decade, proprietary numerical analysis software, simply entitled *Dynamics* has been developed by Nusse and Yorke (1994) to enable computational numerical investigations of system dynamics. Several authors, Nusse *et al.* (1994), Chin *et al.* (1994) and Nusse *et al.* (1995) have all used the algorithmic approach of this software to plot bifurcation diagrams and basin of attractions for a range of physically interesting systems. Since then, a newer edition, *Dynamics 2*, also by

Nusse and Yorke (1998), has been developed and it is this environment that has been utilised as a computational basis for the qualitative assessments discussed in this chapter.

5.2 Program Code

The *Dynamics 2* programming environment has numerous examples of maps and differential equations built in, in particular the Henon map, Ikeda map, Kaplan/Yorke map, Logistic map, Quasiperiodicity map, Tinkerbell map, Tent map, and the Piecewise linear map, amongst others. Differential equations include Chua's circuit, Goodwin's equation, examples of Hamiltonian systems, the Lorenz system, the Lotka/Volterra equations, forced-damped pendulum equation, a parametrically excited Duffing equation, the Rössler equation, and the forced Van der Pol equation. Some of the defined equations from the program are as follows,

Henon map:

$$H(x, y) = (\rho - x^2 + C_1,\ x)$$

Logistic map:

$$L(x) = \rho\, x(1 - x)$$

Forced-damped pendulum:

$$x'' + C_1\, x' + C_2 \sin x = \rho\left(C_3 + \cos[\Omega t]\right)$$

Parametrically excited Duffing equation:

$$x'' + C_1\, x' - x + C_2\left(1 + \rho \sin[\Omega t]\right) x^2 + C_3\left(1 + \rho \sin[\Omega t]\right) x^3 = 0$$

Forced Van der Pol equation:

$$x'' - C_1 x'\left(1 - x^2\right) + C_2 x + C_3 x^3 = \rho \sin[\Omega t]$$

where ρ is the excitation amplitude, Ω is the excitation frequency, and C_1, C_2 and C_3 are all constants.

Although code is provided for a variety of maps and differential equations, coupled Duffing equations are not pre-defined in this way. However, an option within *Dynamics 2* allows the user to add his/her own mathematical model to the above list. Figure 5-1 shows a screen dump of the code that was created for the analysis of the coupled Duffing system of equations (3.2-1) and (3.2-2). The reader is referred to Appendix E.12 for a brief summary of Nusse and York's (1998) detailed procedures for adding customised differential equations into *Dynamics 2* and also the definition of the program code in Figure 5-1.

```
Enter the documentation and vector field for a differential equation:
 Documentation:   (allowed process parameters: c1,...,c9,phi,rho,sigma,beta)
SYSTEM 1 : CASE 1
Line 1 X''+ (c1+c2)*X'- c2*Y' + (k1+k2)*X - k2*Y + h1*X^3 + h2*(Y-X)^3 = rho*cos(phi*
  2 t)
  3 Y'' + c3*Y' - c3*X' + k3*Y - k3*X - h3*(Y-X)^3 = 0
  4 y[0]=s; y[1]=t; y[2]=X'; y[3]=Y'; y[4]=X; y[5]=Y;
 Vector field: can use p,q,...,x,y,z; phase space: u,v,...,z only; set t':=1
  5 s' := 1 ! This is time
  6 t' := 1 ! This is cycle time mod 2*pi/phi (see Modulo window below)
  7 x' := u
  8 y' := v
  9 u' := rho*cos(phi*t) - (c4+c5)*u + c5*v - (c1+c2)*x + c2*y - c7*x*x*x - c8*(y-
 10 x)*(y-x)*(y-x)  ! EOM1
 11 v' := - c6*v + c6*u - c3*y + c3*x + c9*(y-x)*(y-x)*(y-x) ! EOM2
 Initialize variables & parameters; use only u,v,...,z for phase space
 12 t:=0  x:=0  y:=0  u:=0  v:=0  ! Set initial conditions
 13 XCO := 4  YCO := 2            ! Plot X (x-axis) vs X'(y-axis)
 14 X_upper:= 0.005  X_lower:= -0.005  Y_upper:= 0.15  Y_lower:= -0.15
 15 c1 := 423888    c2 := 26493    c3 := 47098.66667          ! Set k consts
 16 c4 := 0.025     c5 := 0.025    c6 := 0.04444444444        ! Set c consts
 17 c7 := 6e8       c8 := 5e6      c9 := 8.888888889e6        ! Set h consts
 18 rho := 5        phi := 57.1128
 19 spc := 2000  ! Take 2000 steps per 2*pi/phi
 20 ipp := 2000  ! Plot once in 2000 steps / per cycle (Poincare).

 Modulo function: (Optional; this is evaluated once per time step)
Line 21 t := mod(t,0,2*pi/phi) ! Assume period is 2*pi/phi

Esc=Cancel Tab=Next F1=Compile F3=Map CtrlK=EraseLine CtrlW=EraseWindow
```

Figure 5-1: Program code for coupled Duffing equations

5.2.1 Definition of Parameters

Table 5-1 represents the values of the parameters for the program code shown in Figure 5-1. This is for the case of the superharmonic resonance of equation (3.2-40) which corresponds to all the data presented in Chapters 3 and 4. Again, the hardening cubic stiffness coefficient h_1, the excitation level Ω, and all system quantities other than the softening cubic stiffness coefficient h_2, are kept constant.

Parameters for *Dynamics 2* Program

Stiffness (Linear) [s^{-2}]	Damping [s^{-1}]	Stiffness (Cubic) [$m^{-2}s^{-2}$]	Excitation Amplitude [ms^{-2}]
$c_1 = 423,888$	$c_4 = 0.025$	$c_7 = 6\times10^8$	$rho = 5$
$c_2 = 26,493$	$c_5 = 0.025$	$c_8 =$ varies	
$c_3 = 4,7098.66667$	$c_6 = 0.04444$	$c_9 =$ varies	

Because the softening cubic stiffness coefficient, h_2 varies within the following range:

$$h_2 = 10\times10^6 \;;\; 20\times10^6 \;;\; 50\times10^6 \;;\; 100\times10^6 \;\; [Nm^{-3}]$$

Then, $c_8 = 5\times10^6 \;;\; 10\times10^6 \;;\; 25\times10^6 \;;\; 50\times10^6 \;\; [m^{-2}s^{-2}]$

$$c_9 = 8.88889\times10^6 \;;\; 17.77778\times10^6 \;;\; 44.44444\times10^6 \;;\; 88.888889\times10^6 \;\; [m^{-2}s^{-2}]$$

Reference displacement : $x^*_{ref} = 0.1\ \mathrm{m}$

Reference frequency : $\omega_{e1} = 209.828$ rad s^{-1}

Table 5-1: Data for coupled Duffing system parameters used in the *Dynamics 2* program

5.3 Response Bifurcations

Bifurcation is a French word that was introduced into nonlinear dynamics by Poincaré. Its accepted use is as an indicator of a qualitative change in the dynamics of a system, such as the number and type of solutions under the variation of one or more parameters of the system. In bifurcation representations, it is useful to consider a space formed by using the state variable(s) and chosen control parameter(s), called the state-control space. In this space, locations at which bifurcations occur are called bifurcation points.

To understand the dynamics within equations (3.2-1) and (3.2-2), the *Dynamics 2* software was used to plot the bifurcatory behaviour of amplitude responses x_1^* and x_2^* as a function of the excitation frequency Ω^*, and these are illustrated in Figures 5-2 and 5-3 respectively. All the conditions and data variables for these plots are tabulated in Table 5-1. Because the raw graphs plotted using *Dynamics 2* are in dimensionalised coordinates (shown on the inner scale of the graphs), these graphs have subsequently been nondimensionalised (given on the outer scale of the graphs) using the first mode eigenvalue of $\omega_{e1} = 209.828$ rad s^{-1} for the x-axis, and the reference displacement of $x_{ref}^* = 0.1\ \mathrm{m}$ for the y-axis.

In the following pages, all the figures are plotted using certain necessary *Dynamics 2* commands, Table 5-2 below summarises the list of the command values used,

	SPC	IPP	PI	BIFPI	BIFD	BIFV	CON
Time plots	30	1	0	0	200	480	On
Phase planes	30	1	0	0	200	480	On
Poincaré Maps	30	30	0	0	200	480	Off
Bifurcation diagrams	30	30	0	10000	1000	1000	Off
Lyapunov diagrams	30	30	0	10000	1000	1000	On

Table 5-2: Program command values for *Dynamics 2* plotting

Due to the sensitivity of the command values that are necessary to get good plots, the author has included, in Appendix E, a definition of these commands and also a section on tips for using *Dynamics 2*. This represents a significant amount of effort in familiarisation with this very subtle program.

It is evident that for the third order superharmonic, as the cubic softening coefficient is increased from the values of Figure 5-2(a) to that of 5-2(d), the response becomes more linear, hence broadly correlating with results in Figure 4-4(c). The first mode is examined in more detail using a more fine-grained sweep up (see Figures 5-2(e) to 5-2(h)) and a similar sweep down (see Figures 5-2(i) to 5-2(l)) around the resonant region, and it is again evident that the cubic softening coefficient accentuates the softening effect, mirroring the effect noticeable in Figures 3-4(a) and 4-4(b). It is also relevant to note that the single-valued solution for x_1 is not apparent prior to the downward jumps of the downward sweeps in Figures 5-2(i) to 5-2(l) and also at the high frequency end of the upward sweeps in

Figures 5-2(a) to 5-2(c), and possibly in Figure 5-2(d). This could imply chaos and is discussed further in Section 5.4.

Figure 5-3 shows the nondimensionalised bifurcation diagrams of amplitude response x_2 as a function of the excitation frequency Ω. Further evidence of accentuated softening due to the increase of the cubic softening coefficient is highlighted in Figures 5-3(e) to 5-3(l). In the superharmonic responses of Figures 5-3(a) to 5-3(d), the increase in the cubic softening coefficient correlates with the numerical integration of Figure 4-5(c), whereby the response becomes progressively more hardening. However, the results from *Dynamics 2* arbitrarily depict these as negative values, and the analysis is automatically truncated in Figures 5-3(c) and 5-3(d) due to the computational limitations of the program. Despite this effect, both methods still show the same general trends regarding the nonlinear behaviour of the response curves.

Given that necessary and sufficient conditions exists for possible chaos in the form of one stable and one unstable equilibrium then it appears that the presence of chaos in the downward sweep, but not in the upward sweep, is strongly influenced by the effect of the relevant initial conditions. This observation is made in the sense of Pezeshki and Dowell's (1988) proposal that such Duffing systems manifest disconnections in the fractal form of the map of initial conditions and that this leads to chaos, or not, dependent on the precise nature of those initial conditions.

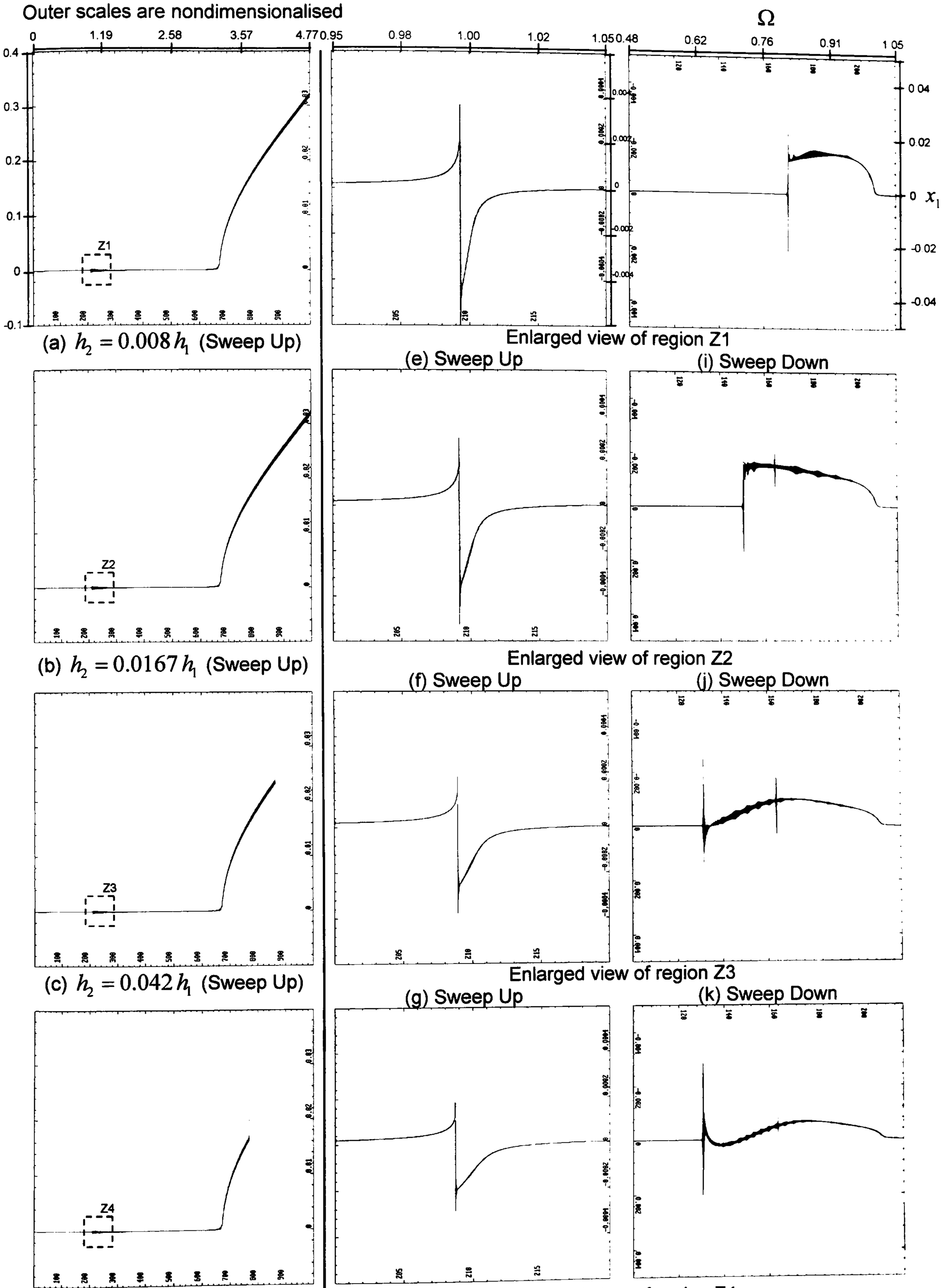

Figure 5-2: Bifurcation diagrams showing x_1 as a function of Ω

(X-axis : Ω Y-axis : x_1)

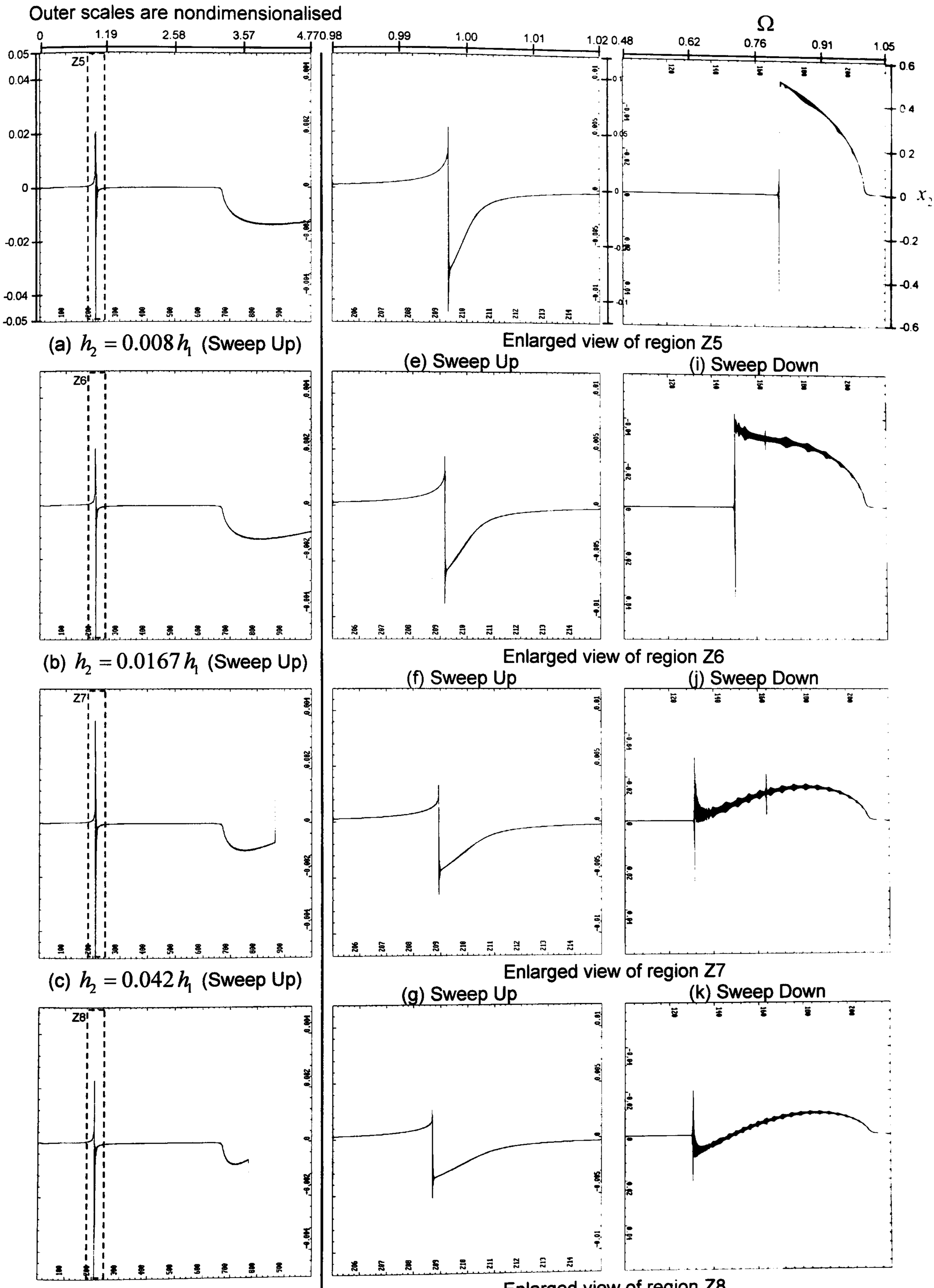

Figure 5-3: Bifurcation diagrams showing x_2 as a function of Ω

(X-axis : Ω Y-axis : x_2)

5.4 Lyapunov Exponents

In 1899 the Russian scientist Aleksandr Mikhailovich Lyapunov [1857 – 1918] introduced a bespoke method for providing ways to determine the stability of sets of ordinary differential equations. His work concentrated on the stability of equilibrium and motion of a mechanical system and the stability of a uniformly rotating fluid. He also devised many important methods of approximation (i.e. Lyapunov's -time, -characteristic exponent, -characteristic number, -equation, -fractal, -function, -stability and -test), which are now better known as Lyapunov methods.[1]

The Lyapunov exponents of a system are a set of invariant geometric measures which describe, in an intuitive way, the dynamical content of the system. In particular, they can serve as a measure of how easy it is to perform prediction on the system. Lyapunov exponents quantify the average rate of convergence or divergence of nearby trajectories generally, in a global sense. A positive exponent implies divergence, a negative one convergence, and a zero exponent indicates the continuous nature of a flow in time. Consequently a system with positive exponents has positive *entropy* in that trajectories that are initially close together move apart over time. The more positive the exponent, the faster they move apart. Similarly, for negative exponents, the trajectories move together. Thus, a positive Lyapunov exponent, is amongst one of the strongest indicators of chaotic motion. The Lyapunov exponent, λ, is defined by

---

1 *Source:* http://www.wikipedia.org/wiki/Aleksandr_Mikhailovich_Lyapunov

taking the natural logarithm of the Lyapunov number (defined by the divergence ratio),

$$\lambda = \lim_{\substack{t\to\infty \\ |\Delta x_0|\to 0}} \frac{1}{t} \ln \frac{|\Delta x(X_0, t)|}{|\Delta x_0|}$$

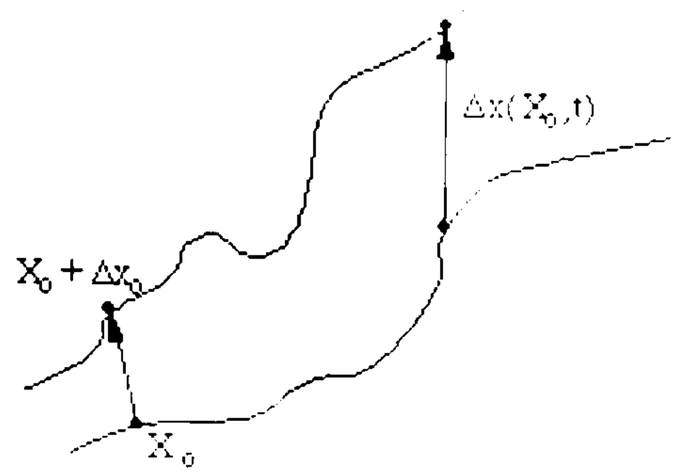

Figure 5-4 shows the Lyapunov exponents plotted for the respective bifurcations of the softening sweep down in Figures 5-2(i) to 5-2(l). In the regions of the softening characteristics, chaotic motions are evident from the positive values of the Lyapunov exponents. And as the cubic softening coefficient is increased, the system gets more softening and correspondingly more chaotic, with a wider region of positive Lyapunov exponents.

Outer scales are nondimensionalised

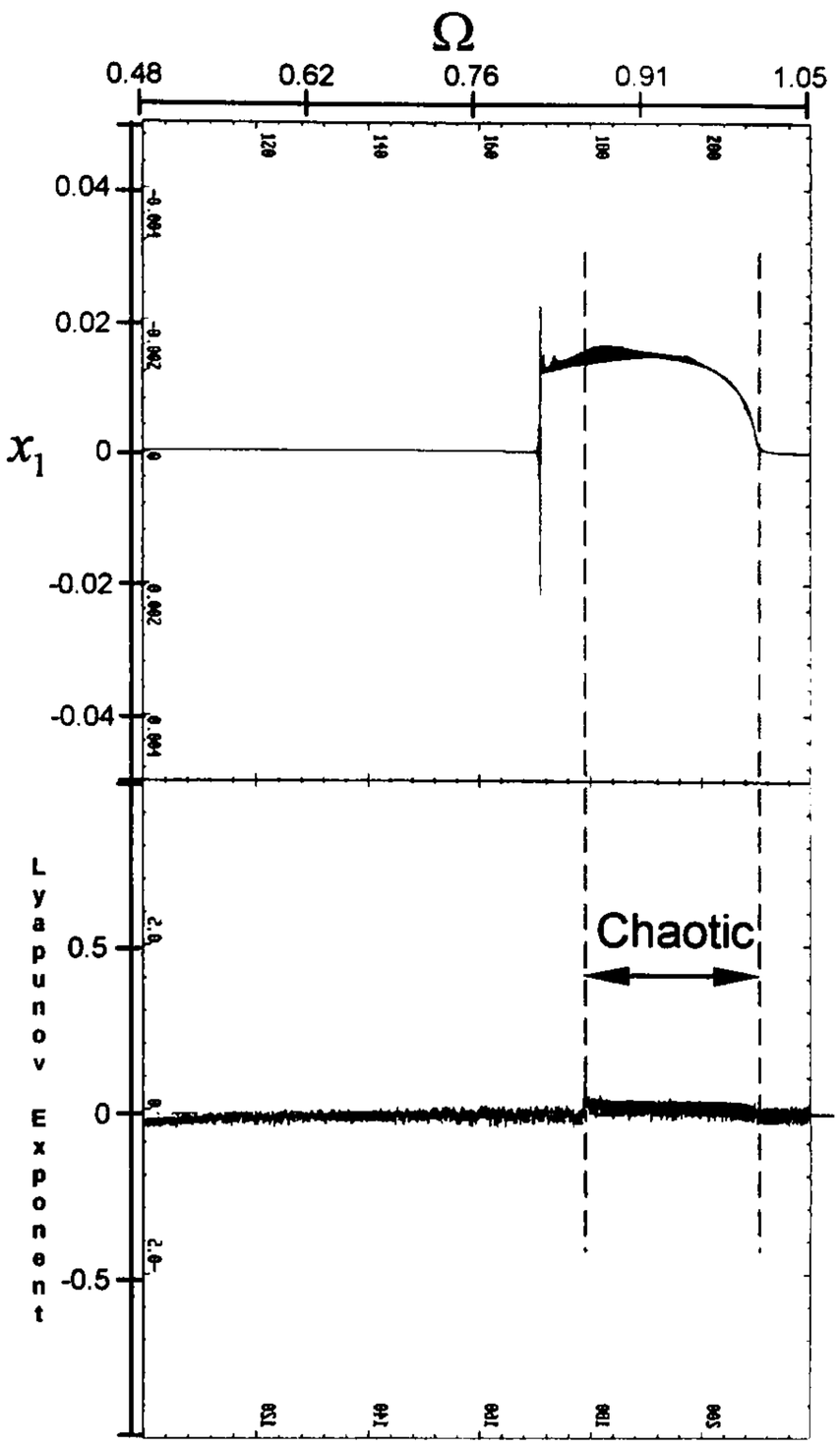

(a) $h_2 = 0.008\,h_1$

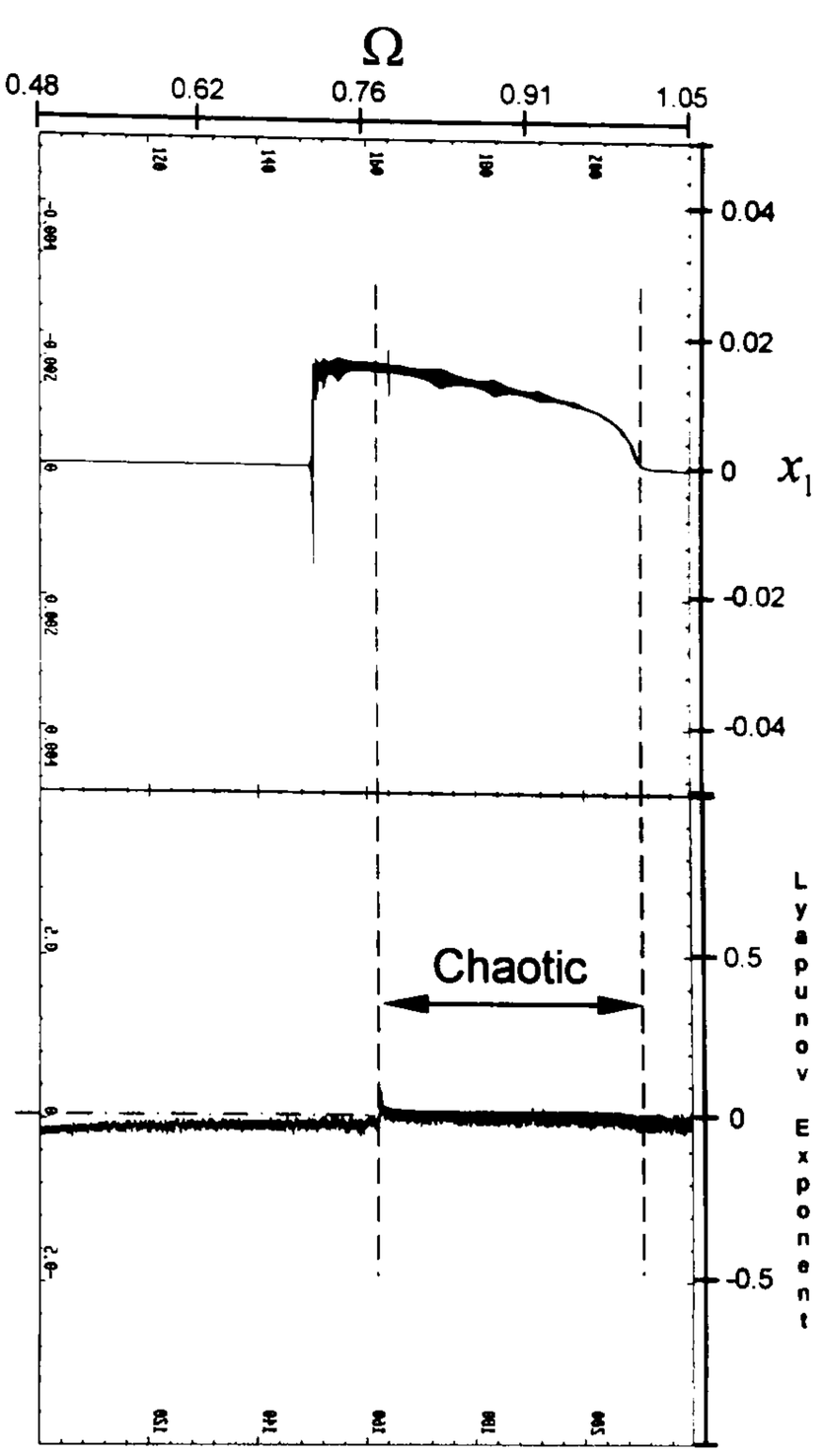

(b) $h_2 = 0.0167\,h_1$

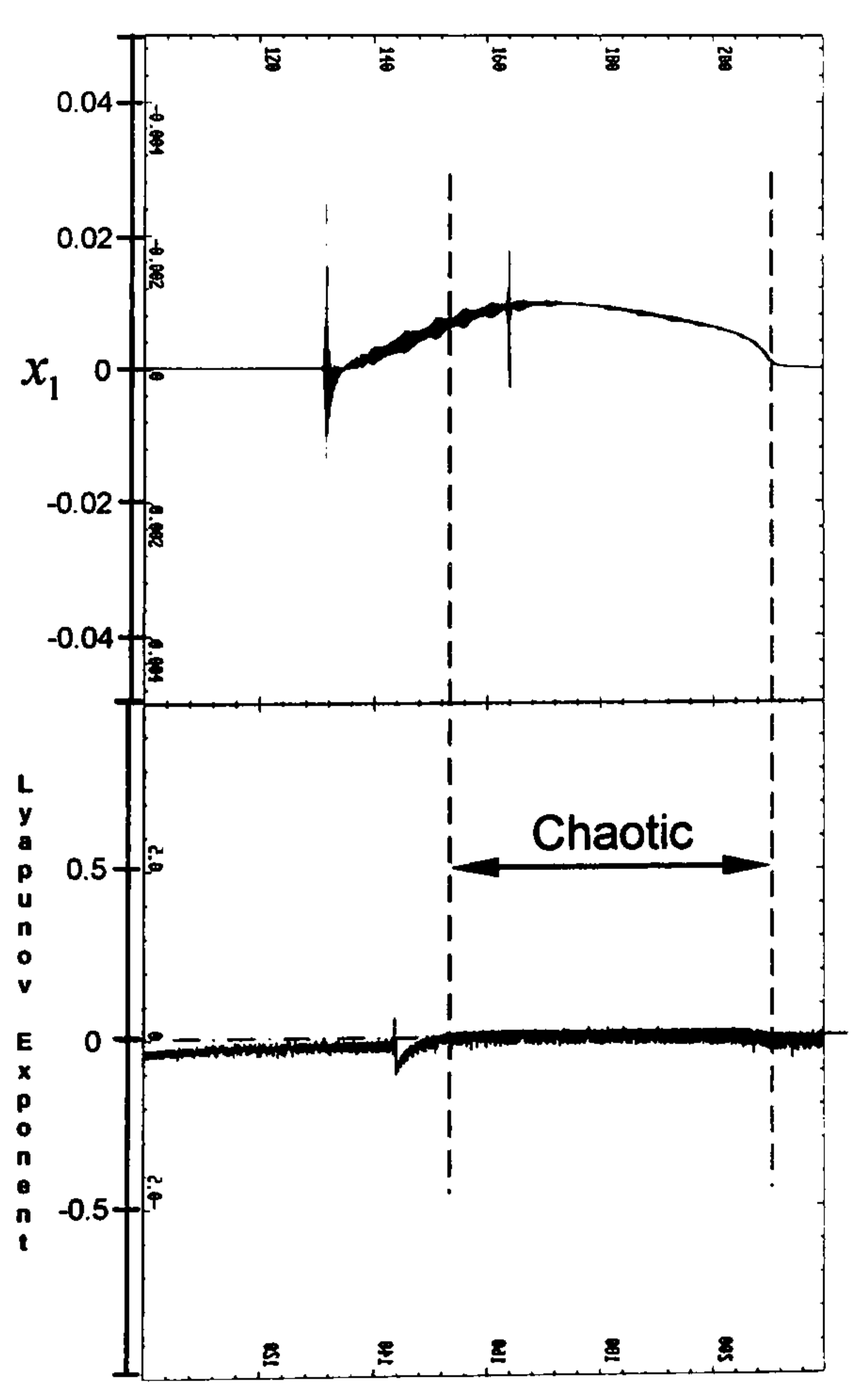

(c) $h_2 = 0.042\,h_1$

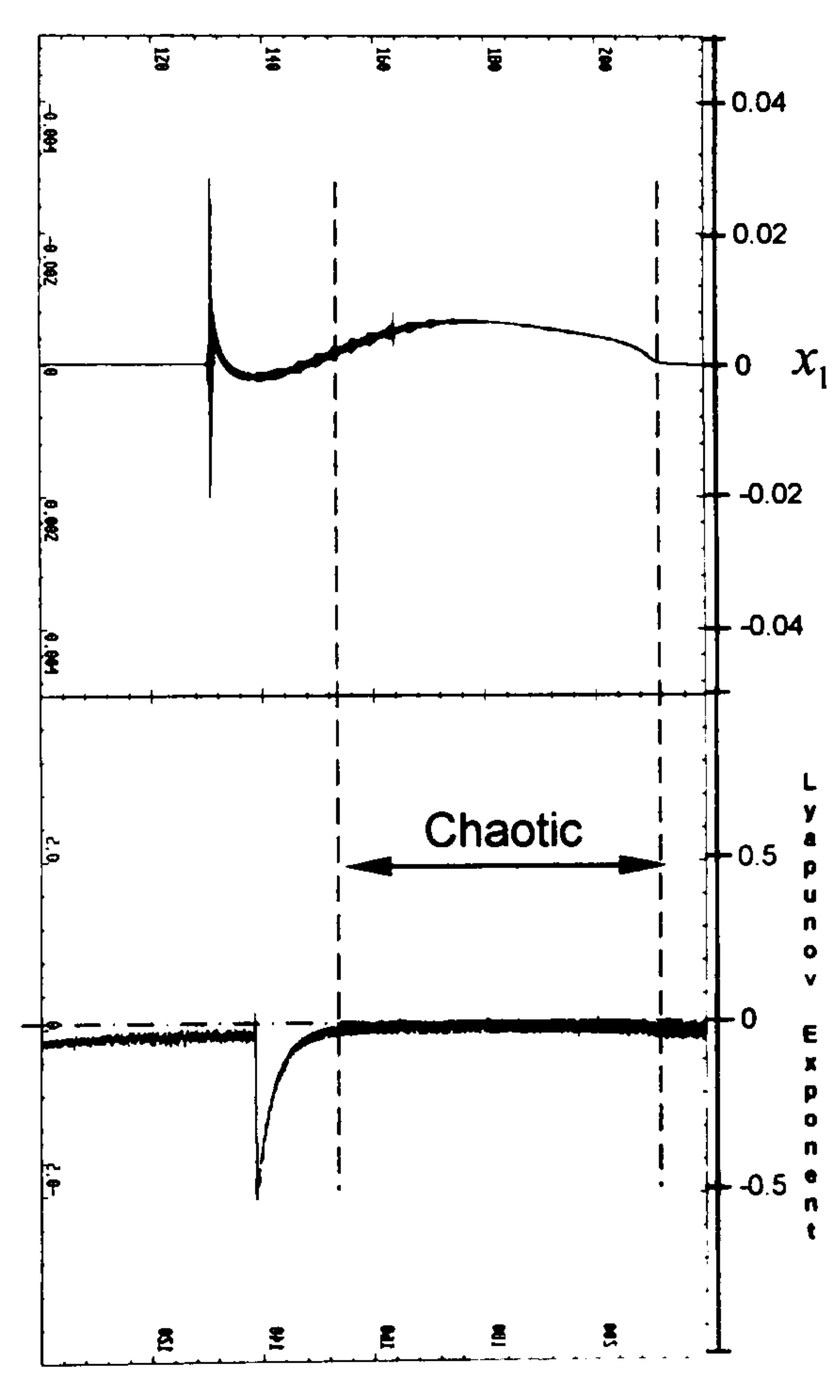

(d) $h_2 = 0.083\,h_1$

Figure 5-4: Lyapunov exponent diagrams for x_1 (i.e. Figures 5-2(i) to 5-2(l))

5.5 Bifurcations as Functions of Excitation Acceleration

Figure 5-5 shows the bifurcation of x_1^* as controlled by the excitation acceleration, when the excitation frequency is set equal to the first mode eigenvalue of $\omega_{e1} = 209.828$ rad/s. By exaggerating the excitation acceleration to a high value, the periodic response for the case based on the smallest cubic softening coefficient in Figure 5-5(a) (i.e. the most linear response in Chapters 3 to 5), bifurcates to chaos as the softening coefficient is increased (see Figure 5-5(b) to 5-5(d)). Positive Lyapunov exponents for these respective figures show clear indication of chaos, while the negative Lyapunov exponents show stable motion. Also from these graphs, as the responses become chaotic, less excitation acceleration is required in each of the four cases, successively. Figure 5-5(d) interestingly shows a period-13 window in the region of F^*/m_1 = 735 to 749 ms^{-2} in between two regions of chaos. Although Figures 5-5(b) and (c) do show a bifurcation to periodic motion after the chaos region, the limitation of *Dynamics 2* has truncated the analyses due to mathematical limits of the program. Discrete excitation acceleration points are selected for the plotting of phase planes, Poincaré maps and time plots for a more detailed understanding of the system's dynamics in the next section.

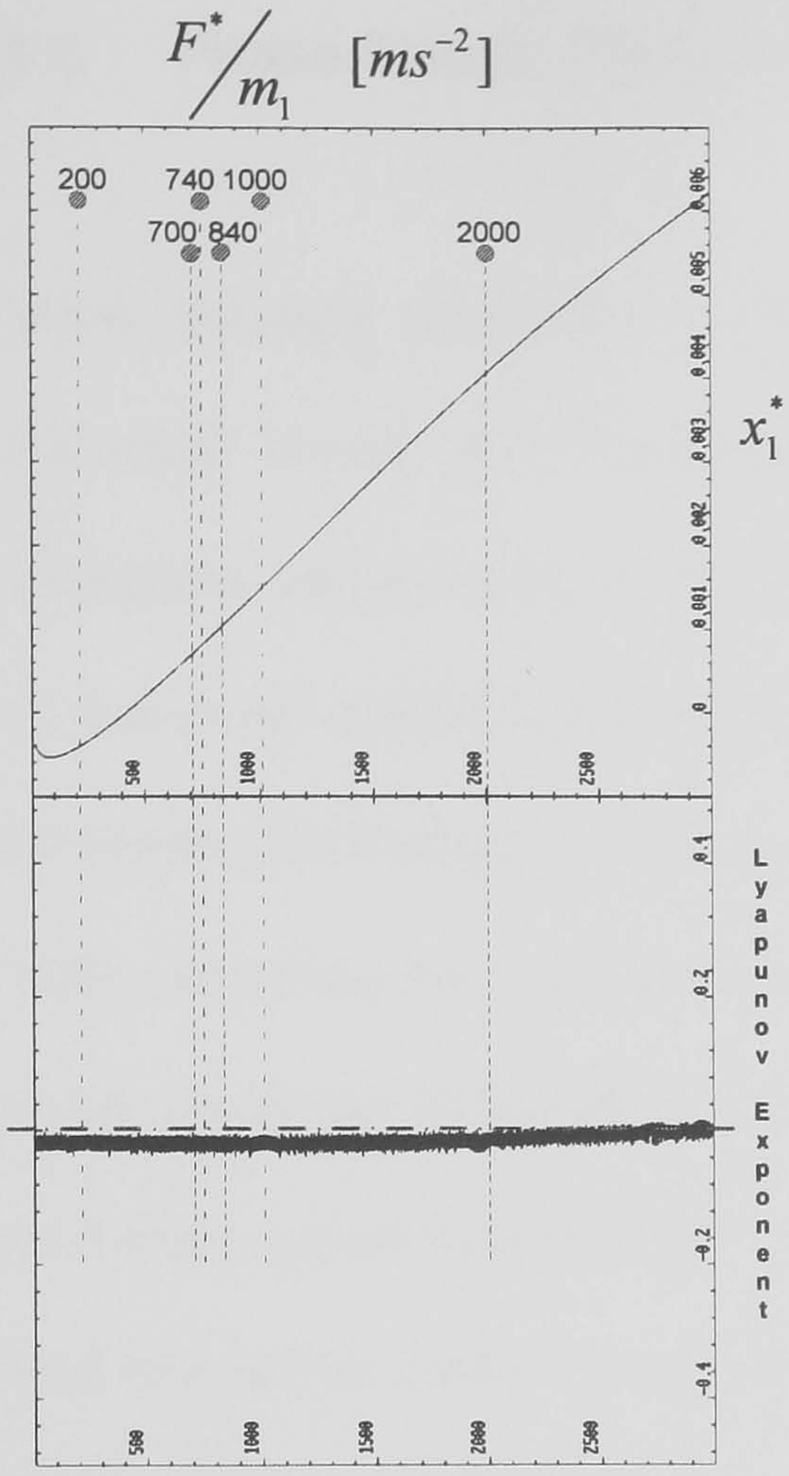

(a) $h_2 = 0.008\,h_1$

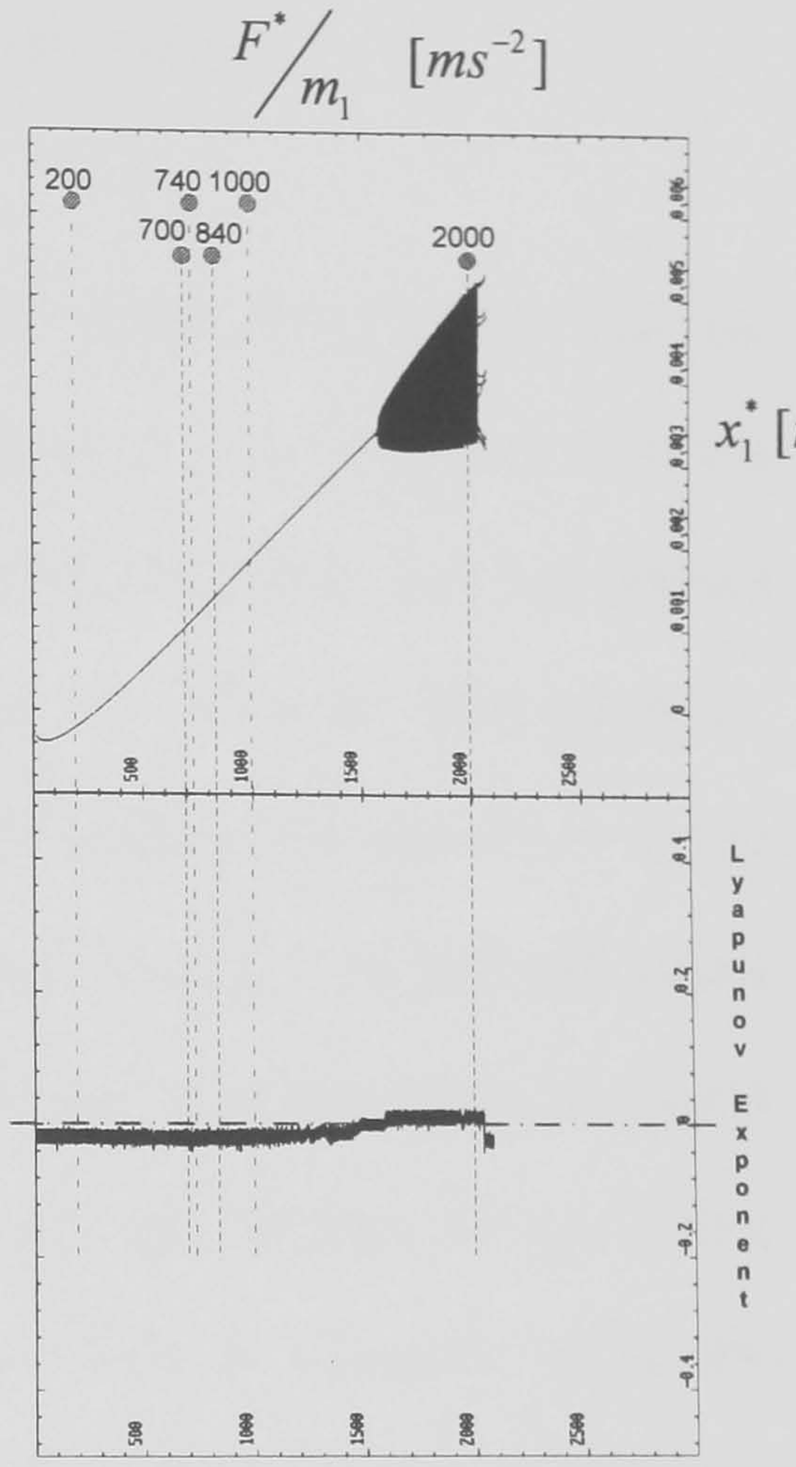

(b) $h_2 = 0.0167\,h_1$

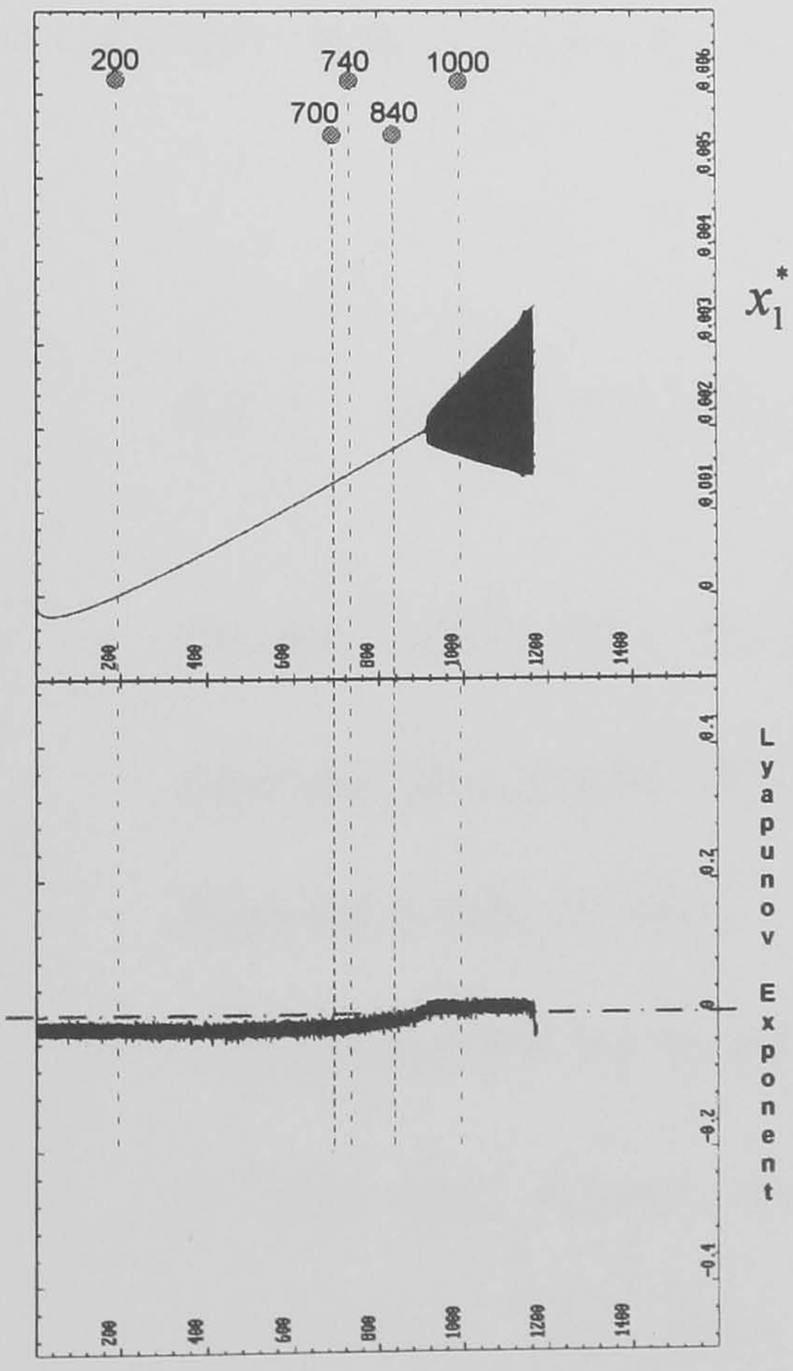

(c) $h_2 = 0.042\,h_1$

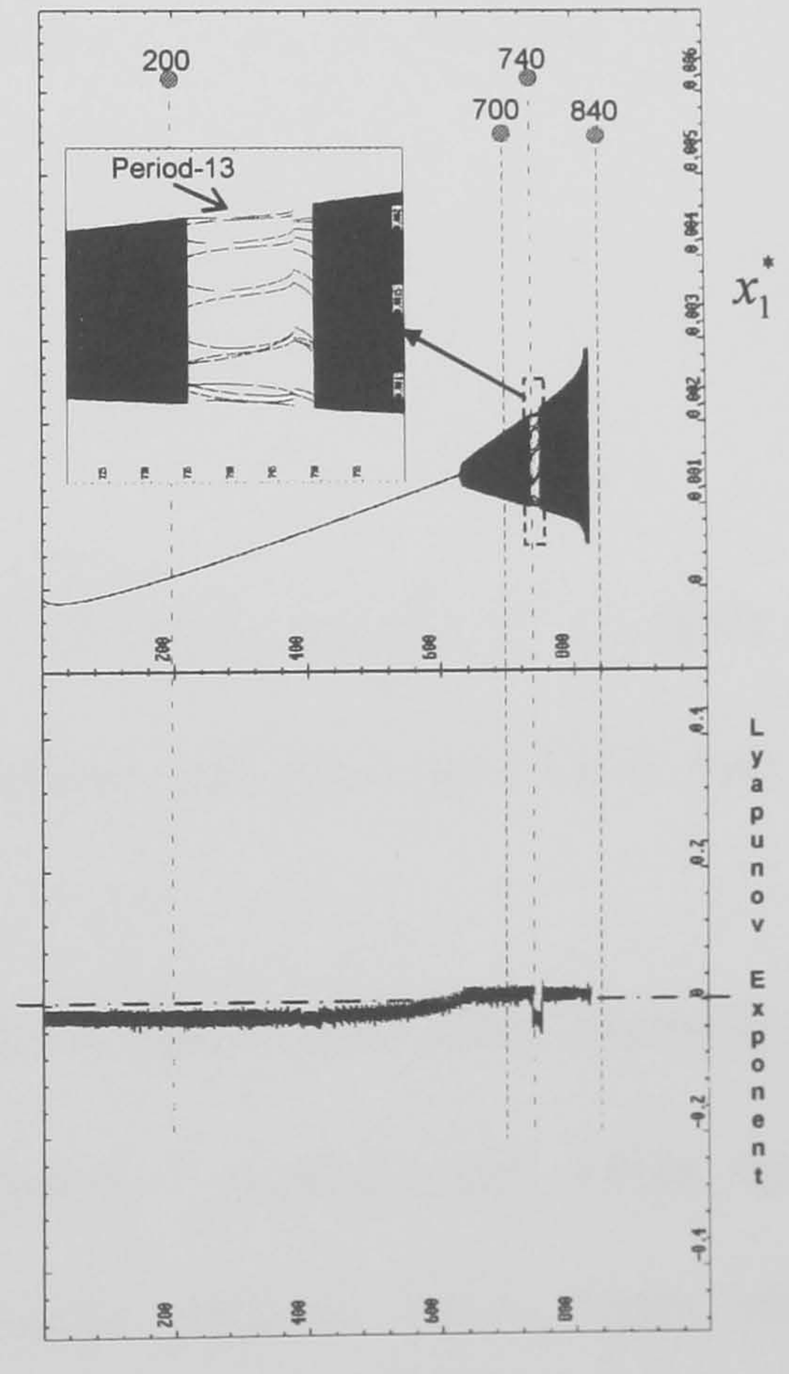

(d) $h_2 = 0.083\,h_1$

Figure 5-5: Bifurcation of x_1 as a function of excitation acceleration

5.6 Phase Planes, Poincaré Maps and Time Plots

More detailed analyses of Figure 5-5 are extended to phase planes, Poincaré maps and time plots (i.e. Figures 5-7 to 5-12) at discrete excitation acceleration points. The phase plane and time plots are plotted at assumed steady-state during the interval t = 999.5 to 1000 seconds. However, the Poincaré maps are plotted from its transient time (i.e. t = 0 to 1000 seconds) as most of them converged to a period-1 motion with just a point, therefore richer diagrams are preferred and so these maps converge to darker areas and finally to a point (indicated with a white cross). Those that are not in period-1 motion have an inset within the diagram where the motion is into a *post-transient* condition. A break-down of the observations for the four different varying softening coefficients, h_2 are as follows,

5.6.1 At $F^*/m_1 = 200\ ms^{-2}$ (Figure 5-7):

- All the bifurcation diagrams for the different values of h_2 show periodic and stable motions with negative Lyapunov exponents (see Figures 5-5(a) to (d)).
- The phase planes show that as h_2 is increased, the orbits decrease in size and move towards the centre, crossing each other at $h_2 = 0.042 h_1$ and then move outwards against each other at $h_2 = 0.083 h_1$. The initial part of the solutions were omitted, so the

figures show only stationary, *post-transient* motion. The orbits are all periodic, corresponding with the bifurcation diagrams.

- All the Poincaré maps converge into a single point at the centre of the darkest region (indicated with a white cross). As the maps consists of a finite number of points, which implies periodic motion, and because there is just one point, it indicates a period-1 motion.
- All the time plots show evidence of a periodic response, and it is observed that as the nonlinearity increases, the peaks of the amplitude in each cycle become further apart, indicating a wider jump in response.

5.6.2 At $F^*/m_1 = 700\ ms^{-2}$ (Figure 5-8):

- The bifurcation diagram for $h_2 = 0.083h_1$, in Figure 5-5(d), shows chaotic motion with positive Lyapunov exponents, whereas the others are all in period-1 motion.
- The phase planes underpin the above, and the periodic orbits now move away from each other as h_2 increases. For the chaotic motion (Figure 5-8(d)), a densely filled phase plane is obtained. Had the simulation been allowed to continue, the central part of the plane would be even more overlaid by repeated orbit cross-overs. A complicated phase plot is *one* indicator of chaotic motion, however motion that rides on a complicated looking orbit may very well be fully-predictable, and thus non-chaotic. For example, a phase plot

with very large numbers of degrees-of-freedom may look similarly complicated, even if the system is in fact linear and thus certainly non-chaotic.

- Here the Poincaré maps again converge into a single point in the darkest region for the periodic motions. The interesting map is that of chaotic motion at $h_2 = 0.083h_1$ (Figure 5-8(d)), where more and more points are added to the map as simulation time marches on. However, they continue to do so in an orderly manner, filling out the details of the strange attractor on which the chaotic motion rides. Inset in the figure is the strange attractor in post-transient motion.
- The time plots are in periodic motion, except for the last one where the oscillations never repeat. This is another qualitative visual indicator of chaotic motion.

5.6.3 At F^*/m_1 = 740 ms^{-2} (Figure 5-9):

- The bifurcation diagram for $h_2 = 0.083h_1$ in the inset of Figure 5-5(d) shows a period-13 motion at F^*/m_1 = 740 ms^{-2}.
- Its corresponding phase plane shows a complicated phase plot, but the orbits repeat its same path as simulation time is continued, unlike chaotic orbits which densely fill the central part.
- The Poincaré map in Figure 5-9(d) shows how the transient motion slowly converges into 13 stationary crosses on the figure inset. This finite number of points implies periodic motion (i.e. Period-13 motion) as corresponding to its bifurcation diagram.

- The time plot for this motion may seem complicated, but a careful observation at it shows that the oscillations repeat itself exactly after every 13 periods.

5.6.4 At $F/m_1 = 840\ ms^{-2}$ (Figure 5-10), $F^*/m_1 = 1000\ ms^{-2}$ (Figure 5-11) and $F^*/m_1 = 2000\ ms^{-2}$ (Figure 5-12) :

- The phase planes, Poincaré maps and time plots for these discrete excitation acceleration display periodic or chaotic motions corresponding with their bifurcation diagrams in Figure 5-5.

5.6.5 Counting number of periods:

For a periodic motion, the informally used term 'period(s)-*n*' can be defined as where *n* is the number of period(s) for a cycle to repeat itself. This can be illustrated with reference to the following forced Duffing equation, from Penney and Edwards (1999)[2]. The phase planes, Poincaré maps and time plots for the equation,

$$x'' + x' - x + x^3 = F_0 \cos t$$

are plotted for two different external forcing levels, $F_0 = 0.6$ and

[2] Can also be found at:
http://www.prenticehallmath.com/epdebvp2/secure/projects/chapt6/proj6.5B/proj6-5B.pdf

$F_0 = 0.7$ in Figure 5-6. At $F_0 = 0.6$, a *period-1* motion is observed which takes exactly one period (i.e. $T = 2\pi$) for the cycle to repeat itself. When $F_0 = 0.7$, the cycle only repeats after $t = 4\pi$ meaning that it is a *period-2* motion because it requires two periods to complete one cycle of oscillation. This definition can be applied to the data of Figures 5-7 to 5-12, where although some of the phase planes and time plots may imply $n > 1$, via a number of peaks apparent in a period, however in actual fact the period for these figures is $T = {2\pi}/{\omega_{e1}} = 0.03 \text{ secs}$ and therefore they are *period-1* motion because the cycle repeats itself after every 0.03 seconds.

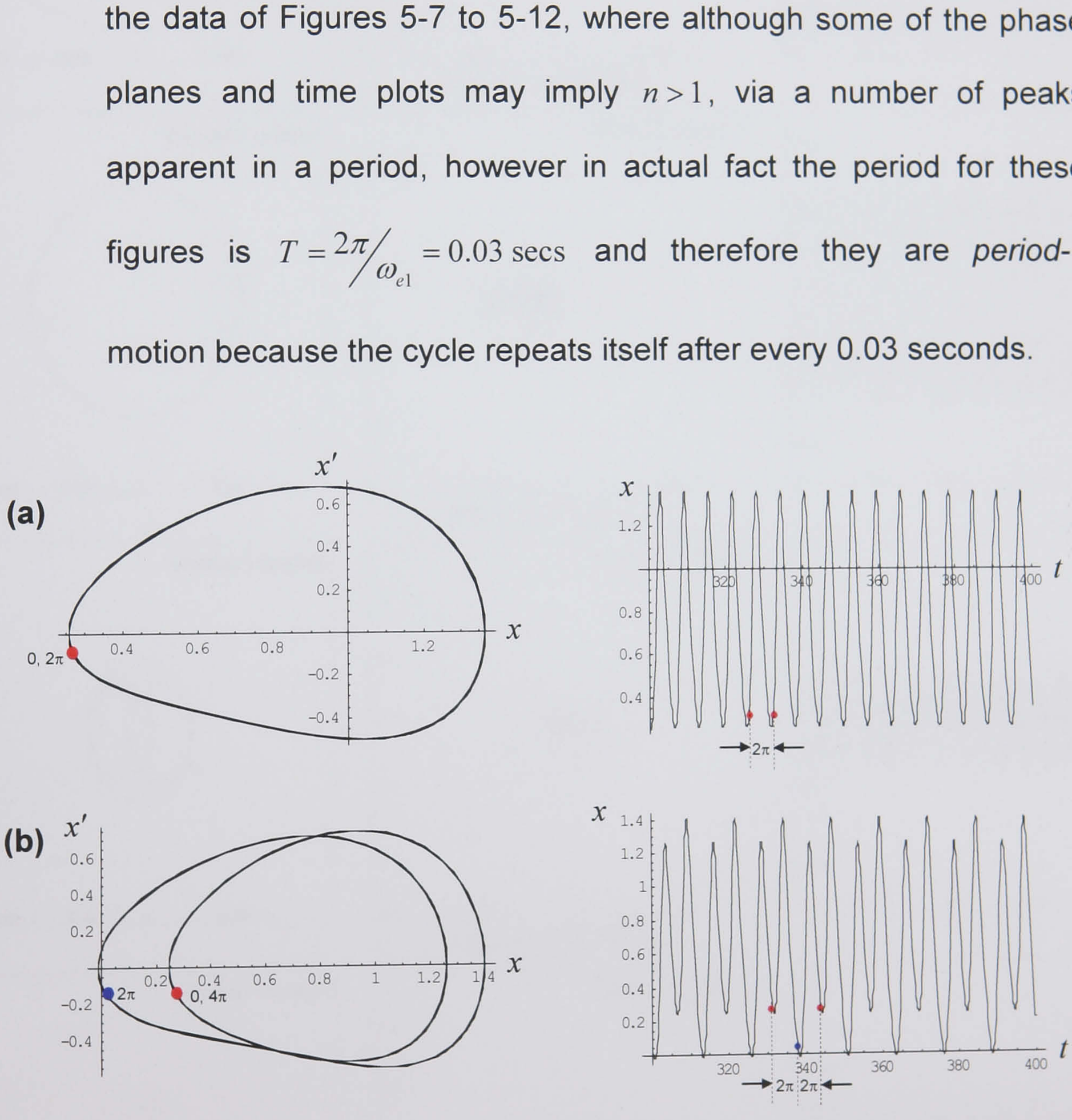

Figure 5-6: Phase plots, Poincaré maps (dots on phase planes) and time plots for forced Duffing equation; (a) $F_0 = 0.6$ and (b) $F_0 = 0.7$

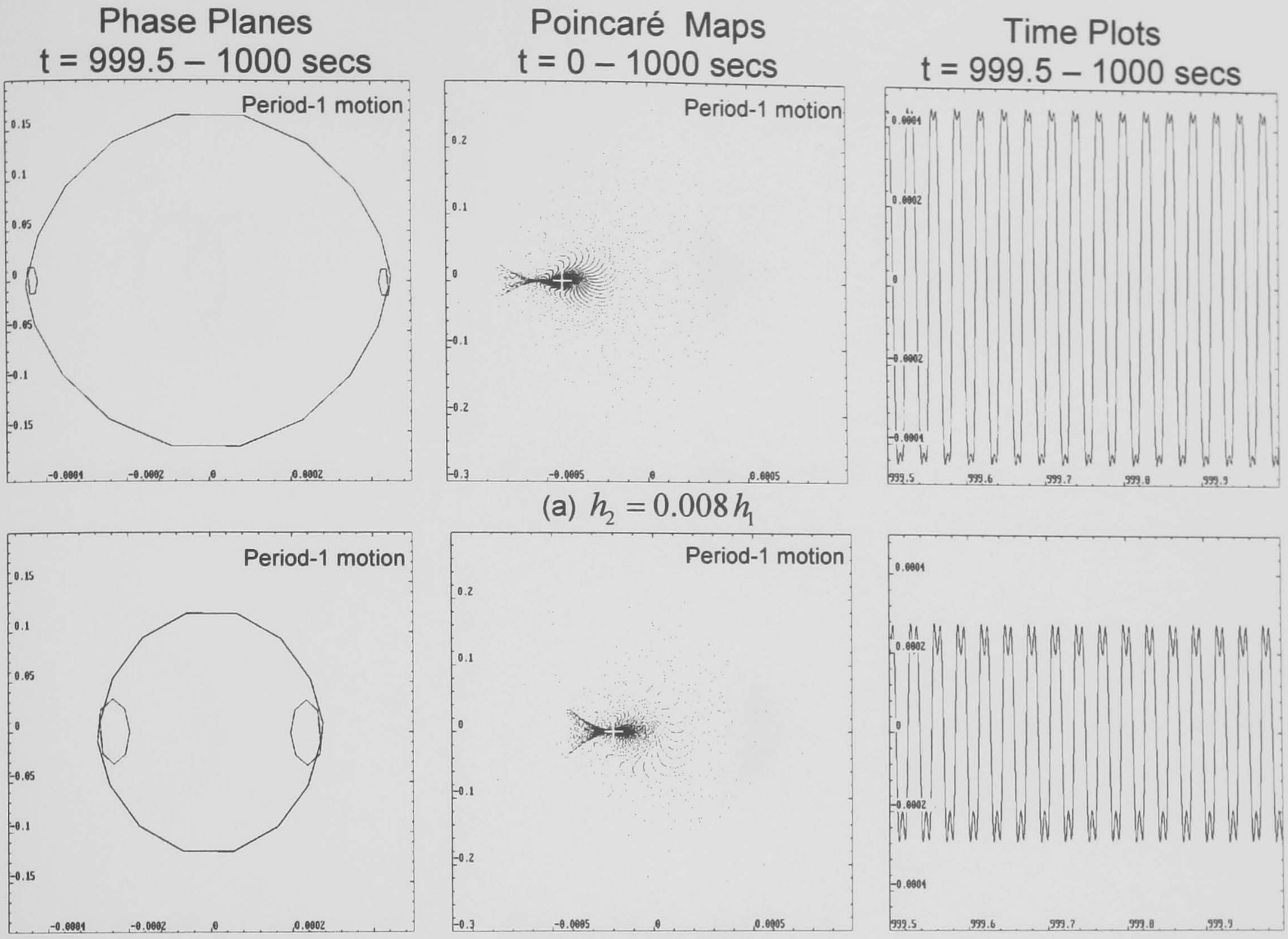

Figure 5-7: Dynamical analysis of excitation acceleration at F^*/m_1 =200 ms^{-2}

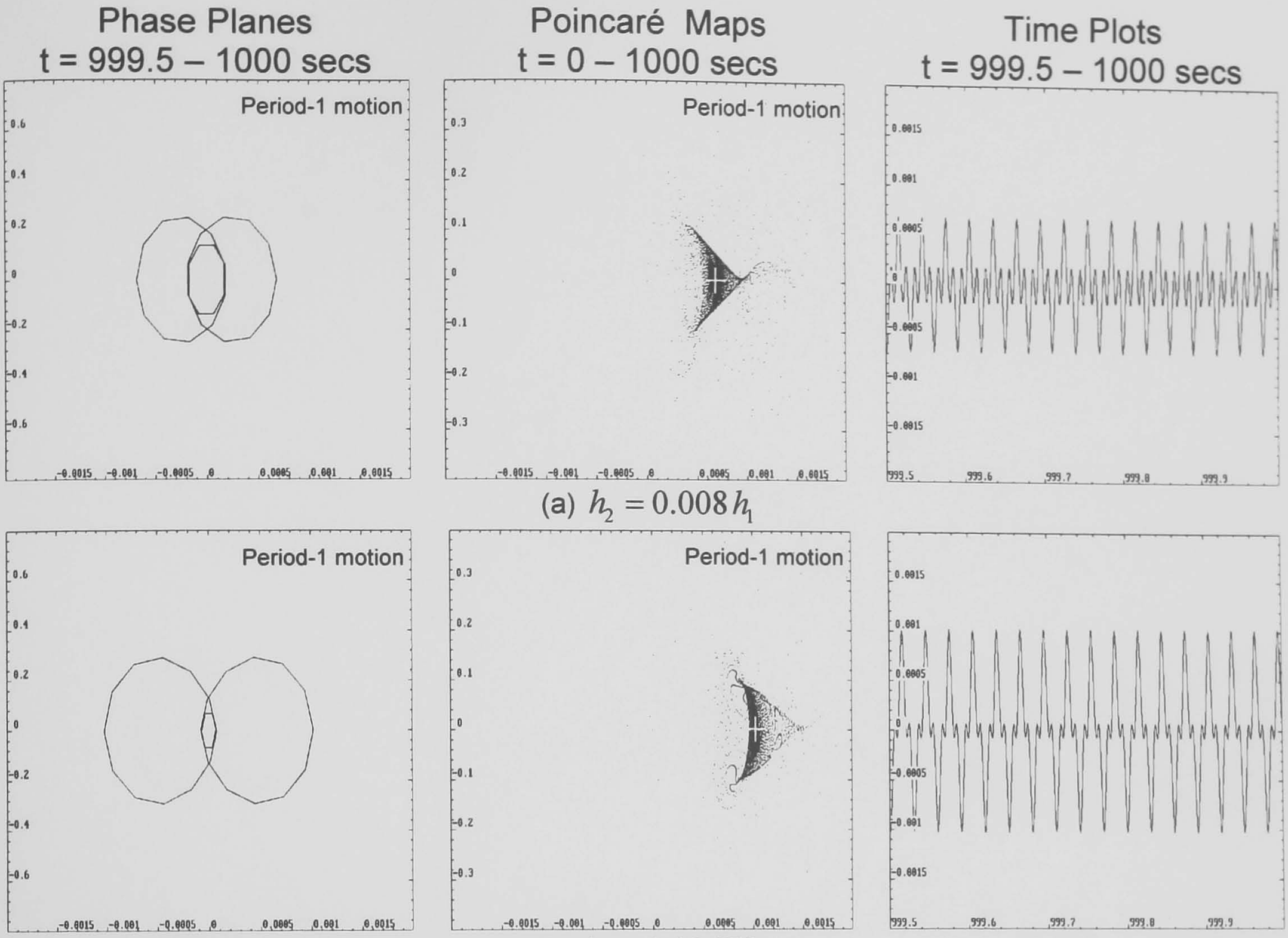

Figure 5-8: Dynamical analysis of excitation acceleration at F^*/m_1 =700 ms^{-2}

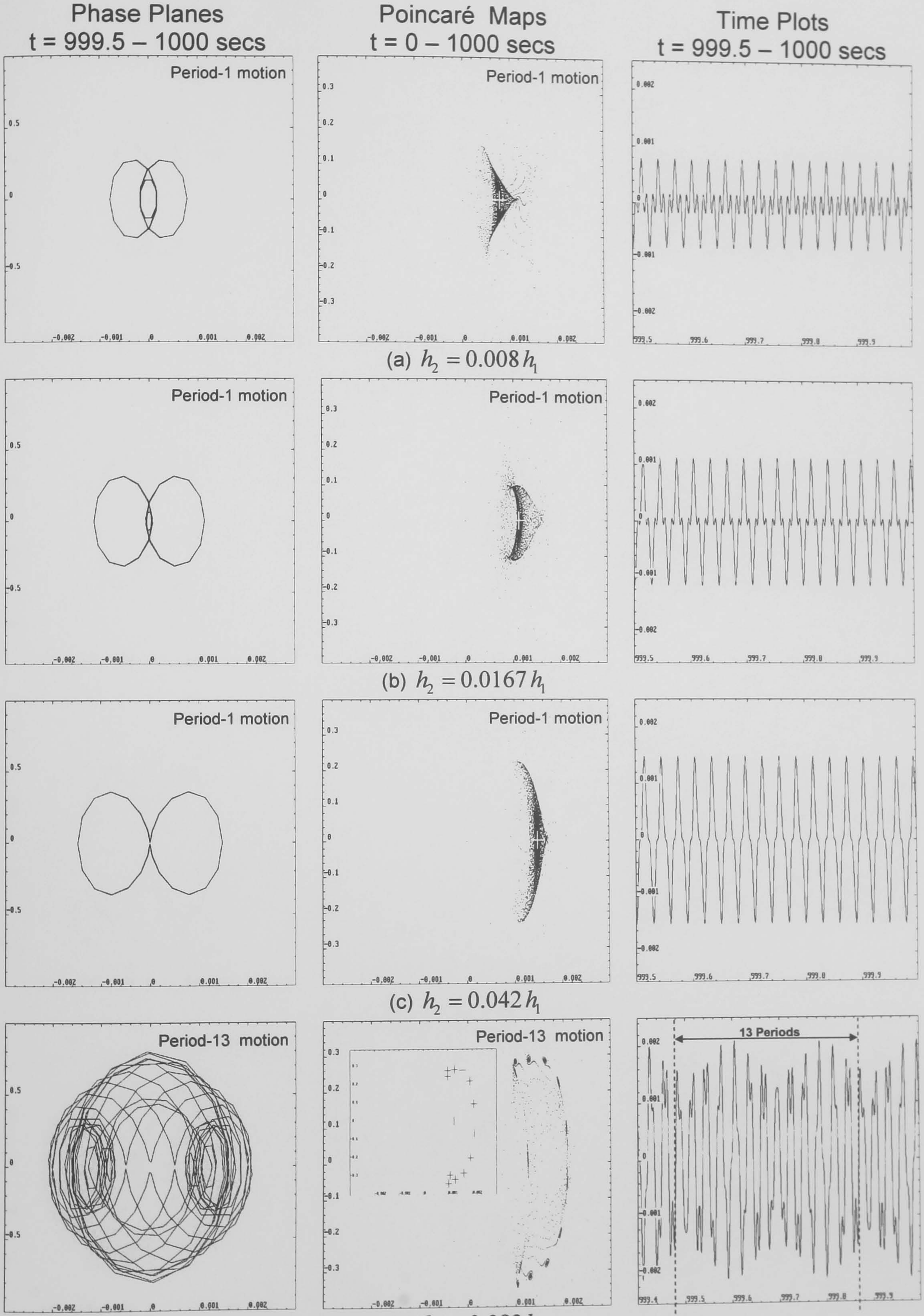

Figure 5-9: Dynamical analysis of excitation acceleration at F^*/m_1 =740 ms^{-2}

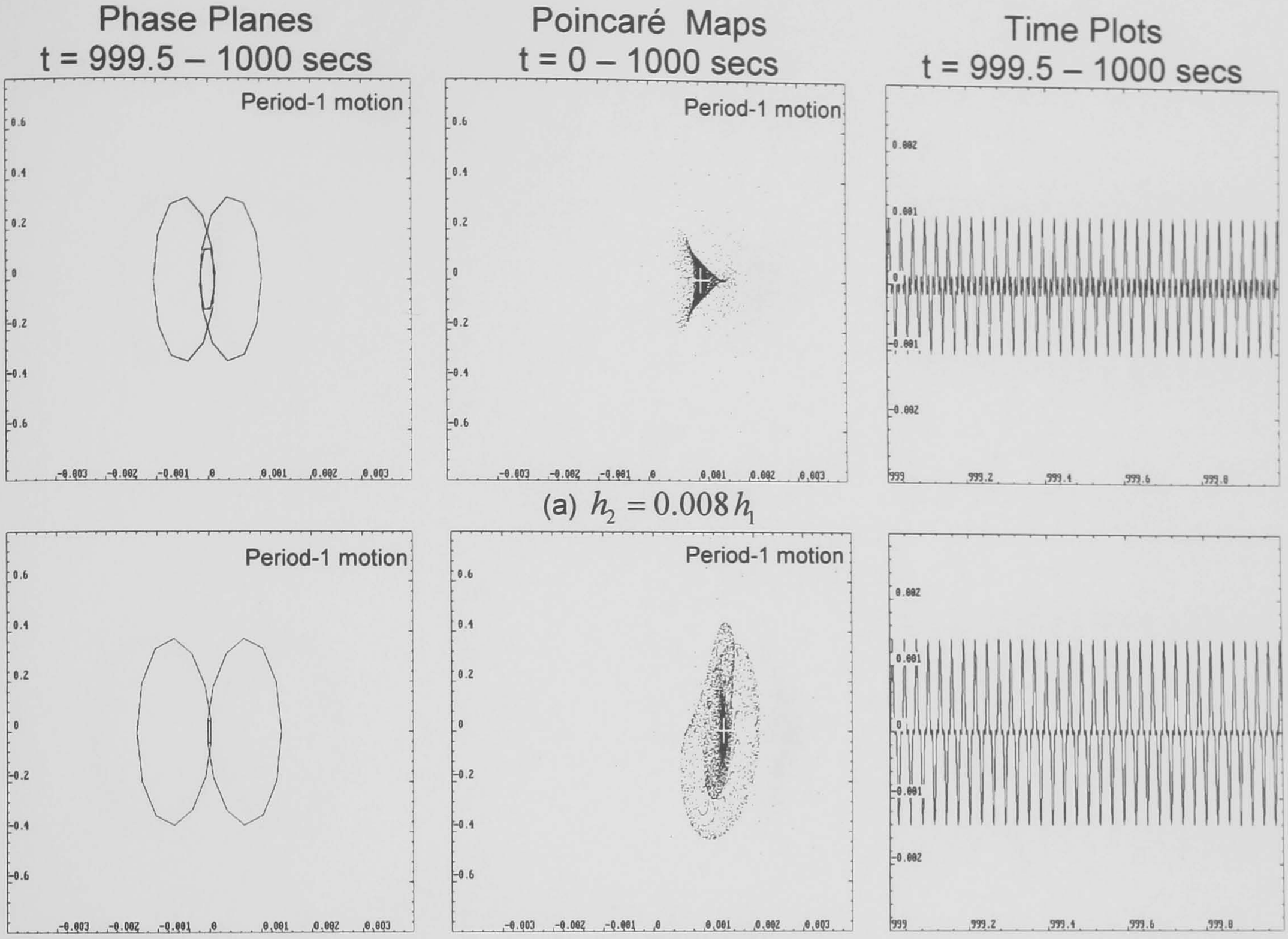

Figure 5-10: Dynamical analysis of excitation acceleration at F^*/m_1 =840 ms^{-2}

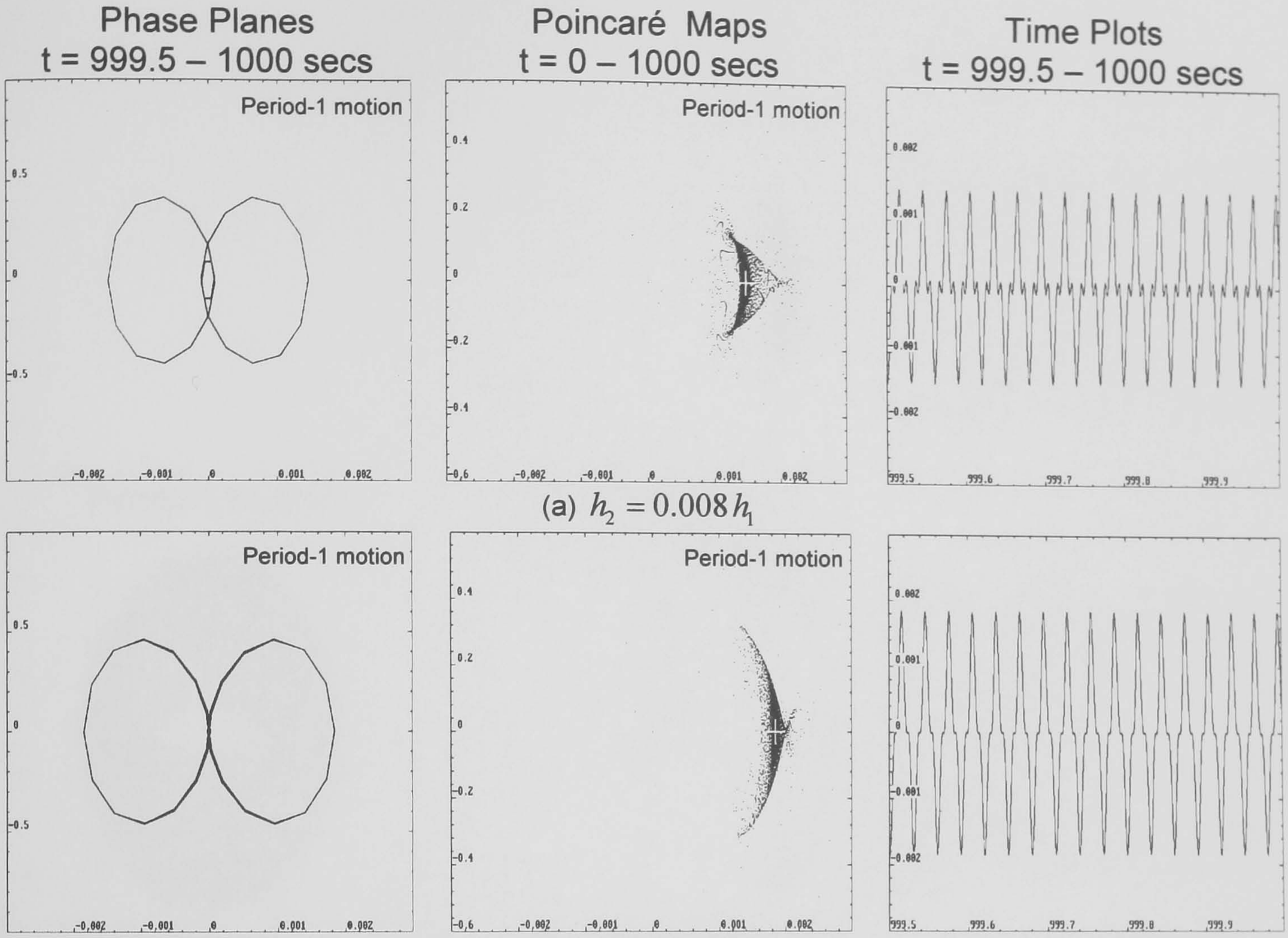

Figure 5-11: Dynamical analysis of excitation acceleration at F^*/m_1 =1000 ms^{-2}

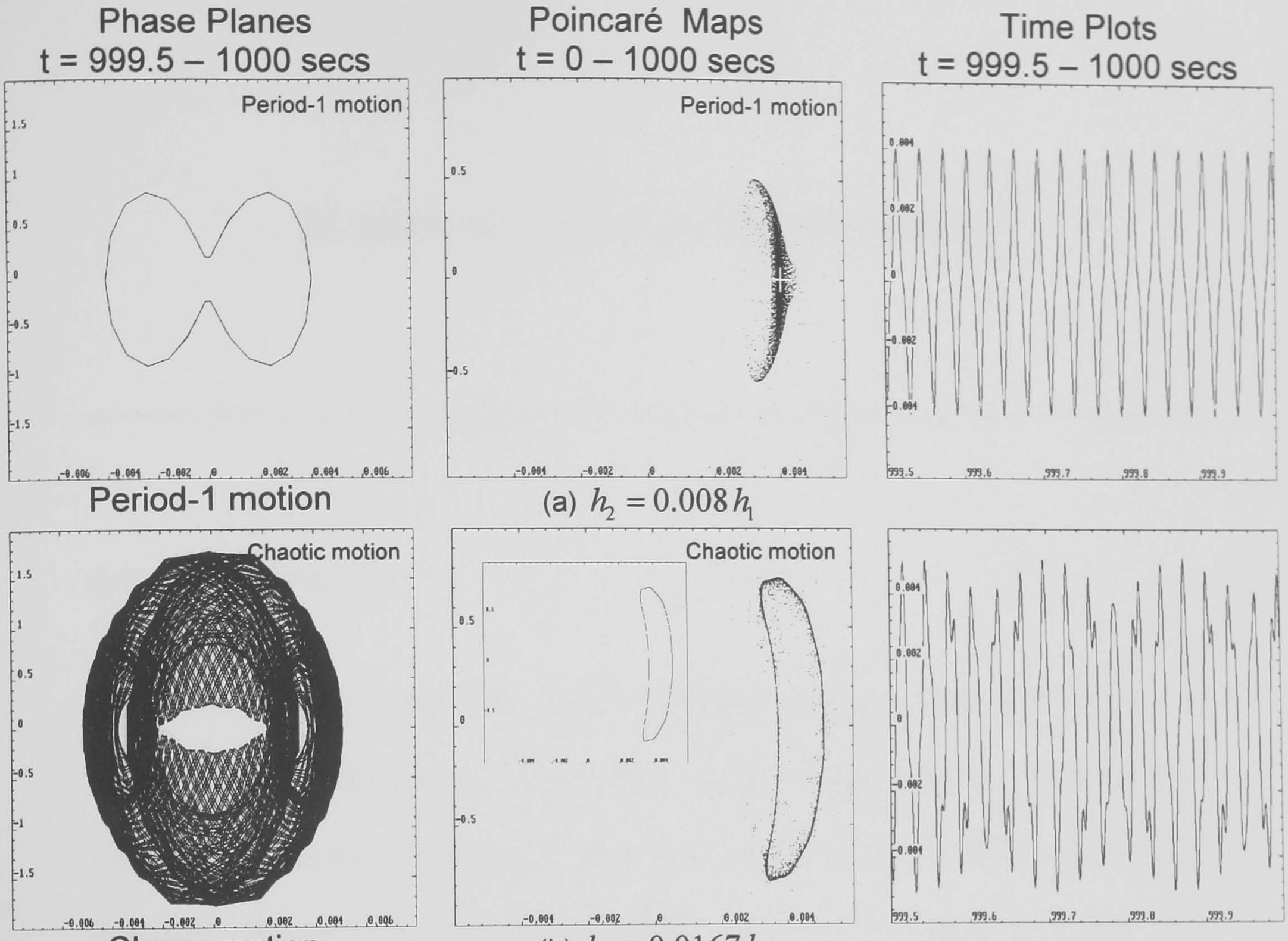

Figure 5-12: Dynamical analysis of excitation acceleration at F^*/m_1 =2000 ms^{-2}

CHAPTER 6

EXPERIMENTAL INVESTIGATIONS

6.1 Introduction

Ultrasonic systems behave in a noticeably nonlinear fashion when run under certain conditions, particularly within high power, continuously operating systems. In the food manufacturing industry, ultrasonic cutting of different products is of considerable interest and this requires the application of high energy, ultrasonic oscillations within the mechanical cutting tools over long operating periods. Because of this, the mechanical cutting tooling is required to be tuned so that modal energy does not leak out into audible lower frequency modes, both for reasons of efficiency, as well as longevity due to the minimisation of fatigue. Nonlinear characteristics within the motion of the cutting tool are not particularly desirable because they can lead to multivalued responses, complex bifurcatory behaviour, unwanted inter-modal coupling, and also other phenomena such as combination resonances and very low cutting efficiency due to high levels of modal spill-over. For these reasons linearisation of the cutting tool response is seen as an important goal, however it has to be realised that nonlinearity within the individual parts of the ultrasonic cutting system cannot necessarily be eradicated at source.

Using the nonlinear modification theory as proposed in the previous chapters, a practically implementable strategy is defined in which the inherent and predominant nonlinearities of the constituent parts of the ultrasonic cutting system are manipulated in such a way that their individual effects on the overall response can be effectively neutralised. In order to justify this work, a programme of experimental research has been conducted in order to identify, and therefore confirm, the precise nature of the predominant nonlinear characteristics in each of the principal parts of an industrial ultrasonic cutting system. The findings of this work supported strongly the notion that such systems could be seen as two serially coupled sub-systems, each with opposing cubic stiffness nonlinearities which strongly predominate.

6.2 Instrumentation

Figures 6-1 and 6-2 show the experimental configuration for measuring the nonlinear response of the ultrasonic system. The exciter (or *transducer*) is driven by a function generator connected to a signal amplifier. The vibration response of the transducer is then measured in the Cartesian x, y and z coordinates by means of a Polytec 3D Laser Doppler Vibrometer (3D LDV), allowing both in-plane and out-of-plane responses to be identified and monitored. A multi-channel data acquisition analyser connected to a portable computer enables the identification of system responses via contemporary signal processing software (DataPhysics SignalCalc 620).

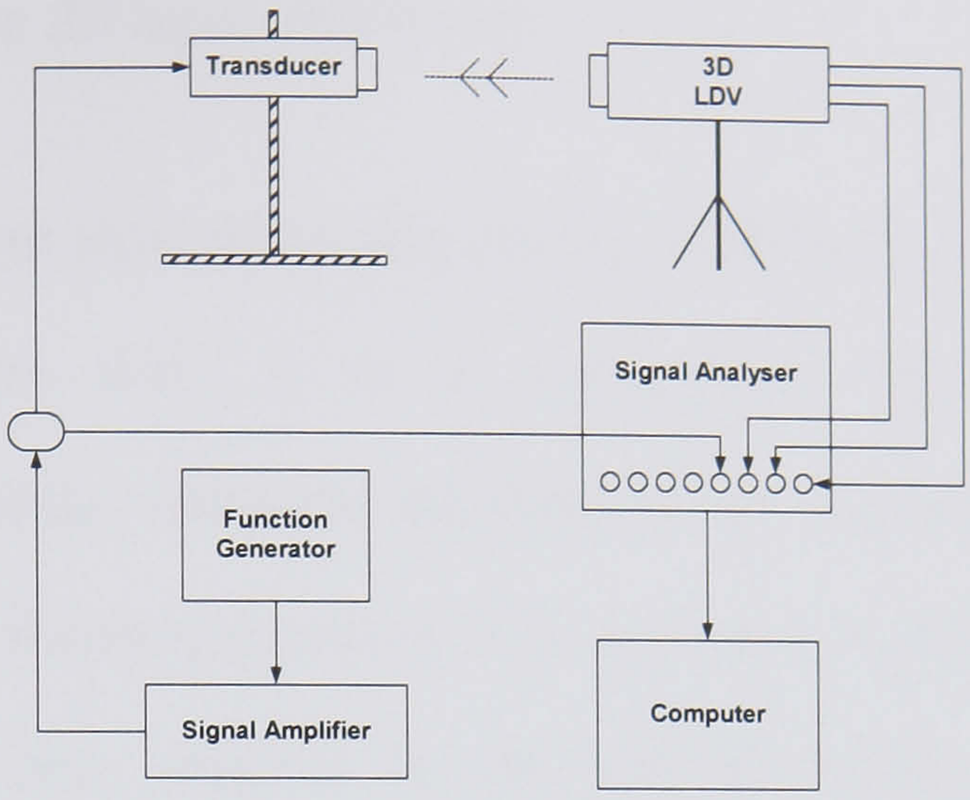

Figure 6-1: Experimental set-up for response measurements

(a)

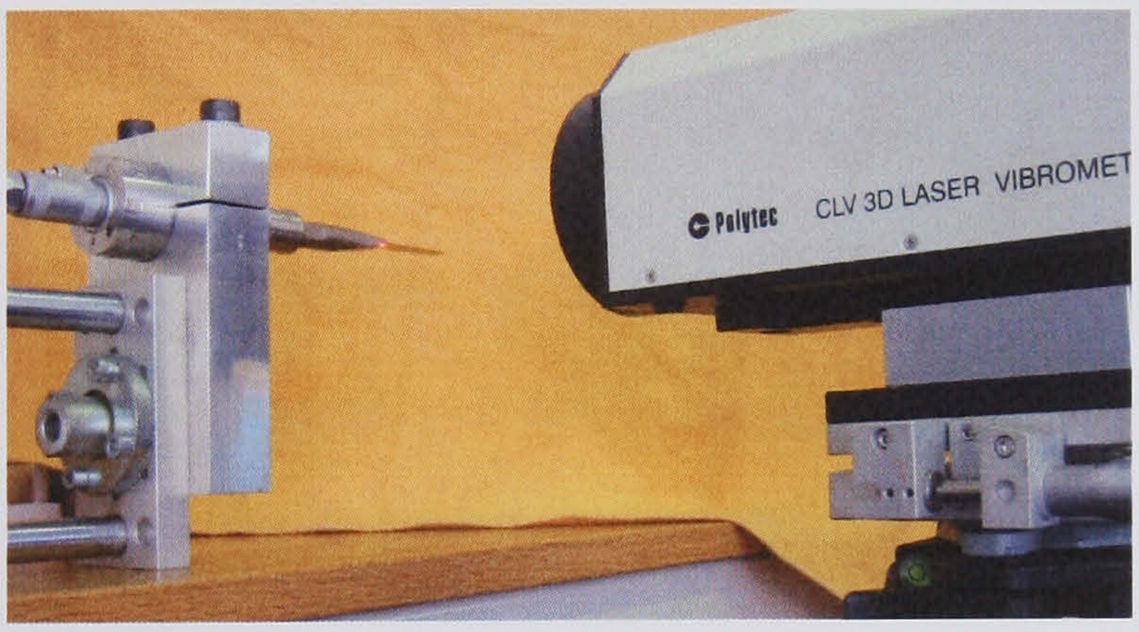

(b)

(c)

(d)

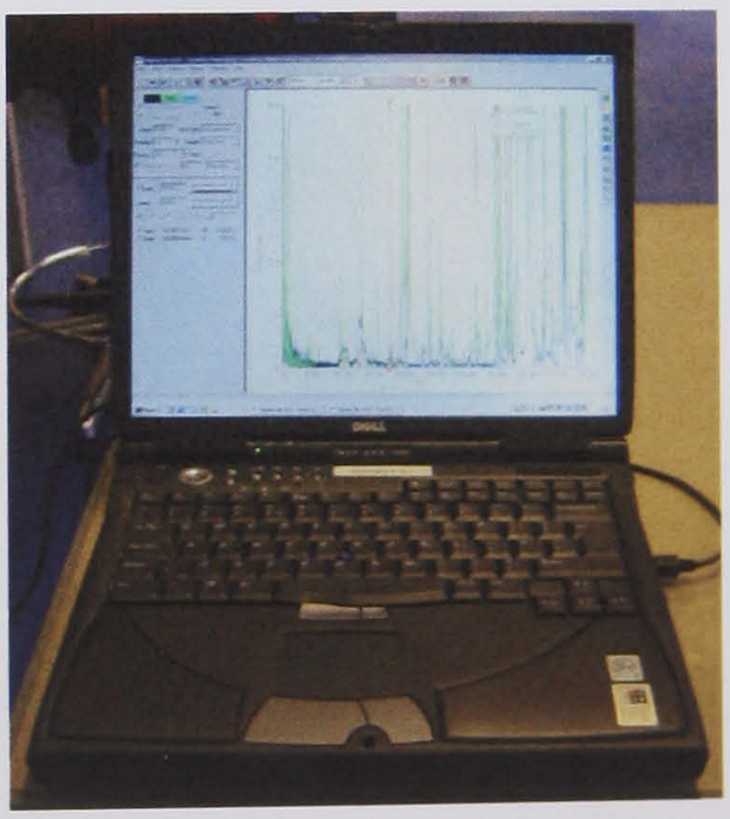

Figure 6-2: Experiment equipment; (a) 3DLDV measuring blade;
(b) Signal generator, amplifier and 3DLDV module;
(c) Signal analyzer and (d) Computer

6.2.1 The 3D laser vibrometer

The 3D laser vibrometer used in the experiment is a Polytec CLV-3D (see Figure 6-3). It is a non-contact vibration sensor that simultaneously measures all three linear velocity components at a point on a vibrating structure. The system comprises a three-channel controller unit coupled to an optical sensor containing three independent optical systems, all focused to the same measurement point. The individual vibration components lying along the three respective laser beams are available as analogue outputs. Most importantly, a geometry-calculation module generates true V_x, V_y and V_z analogue outputs in real time, and can process vibration frequencies as high as 50 kHz.

The optical sensor contains the optical components of three independent sensors. Each output laser beam is inclined at a 12° angle with respect to the surface, but from three slightly different directions. A 12° angle is small enough to allow the sensors to collect enough back-reflected light to make high-quality measurement, but still large enough for good sensitivity to the in-plane vibration components. Further, the narrow cone angle allows the beams to pass through small holes or windows in wind tunnels or environmental test chambers. Figure 6-3 shows how the three beams converges into a measurement point and below outlines the analyses for the measurement geometry.

The CLV-3D sensor generates three laser beams: top, left and right, which measure components V_l, V_t and V_r respectively.

When the sensor is pointed at a surface vibrating in three directions V_x, V_y and V_z, the true x- and z- components can be calculated using these relations with reference to Figure 6-4(a),

$$V_r = V_z \cos\theta + V_x \sin\theta \quad \text{and} \quad V_l = V_z \cos\theta + V_x \sin\theta$$

$$V_z = (V_r + V_l) / 2 \cos\theta \quad \text{and} \quad V_x = (V_r - V_l) / 2 \sin\theta$$

Similarly, viewing the sensor as in Figure 6-4(b), the true y-component is calculated using,

$$V_t = V_z \cos\theta + V_y \sin\theta$$

$$V_y = (V_t - V_z \cos\theta) / \sin\theta$$

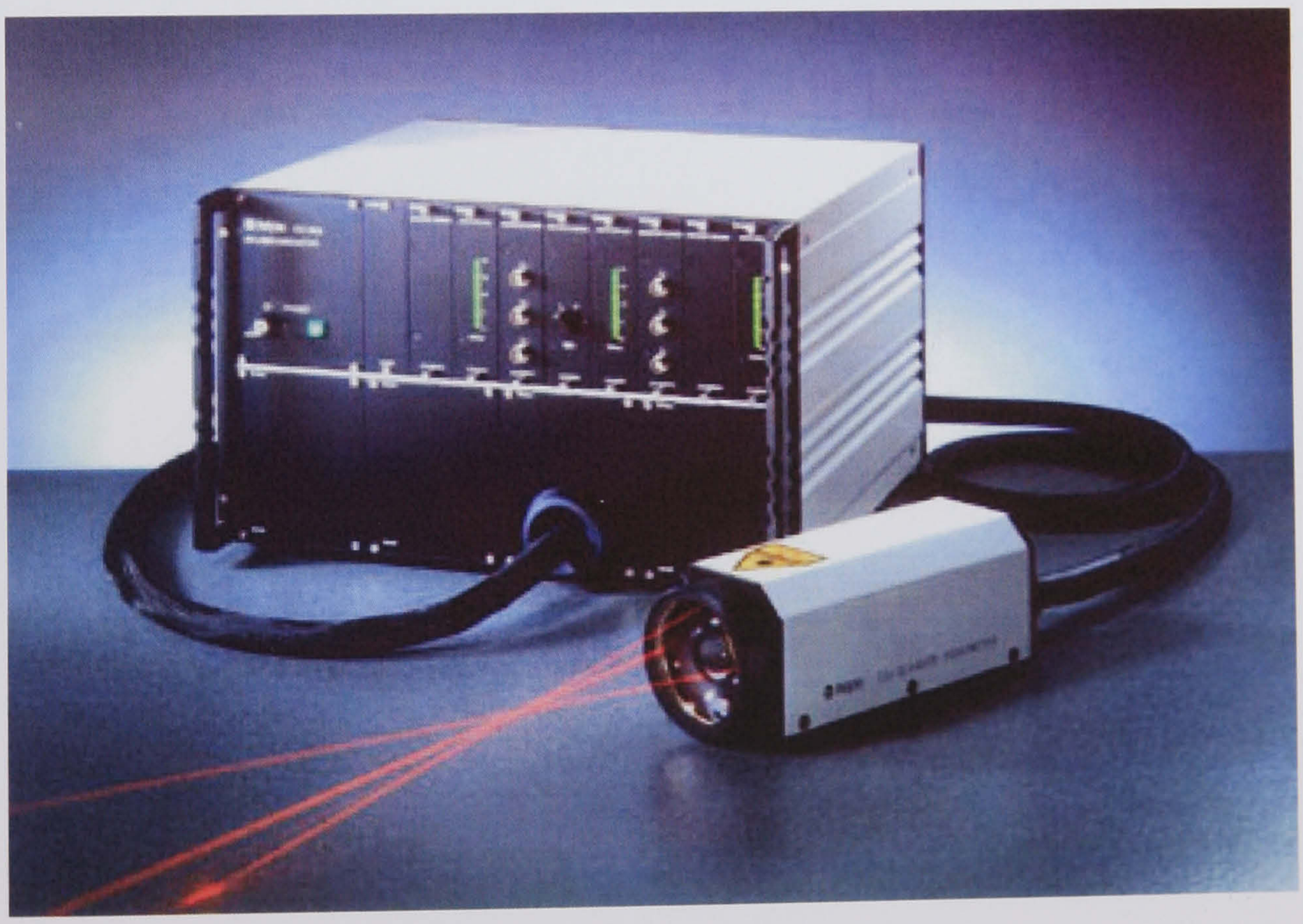

Figure 6-3: The Polytec CLV-3D laser vibrometer and a modular controller unit

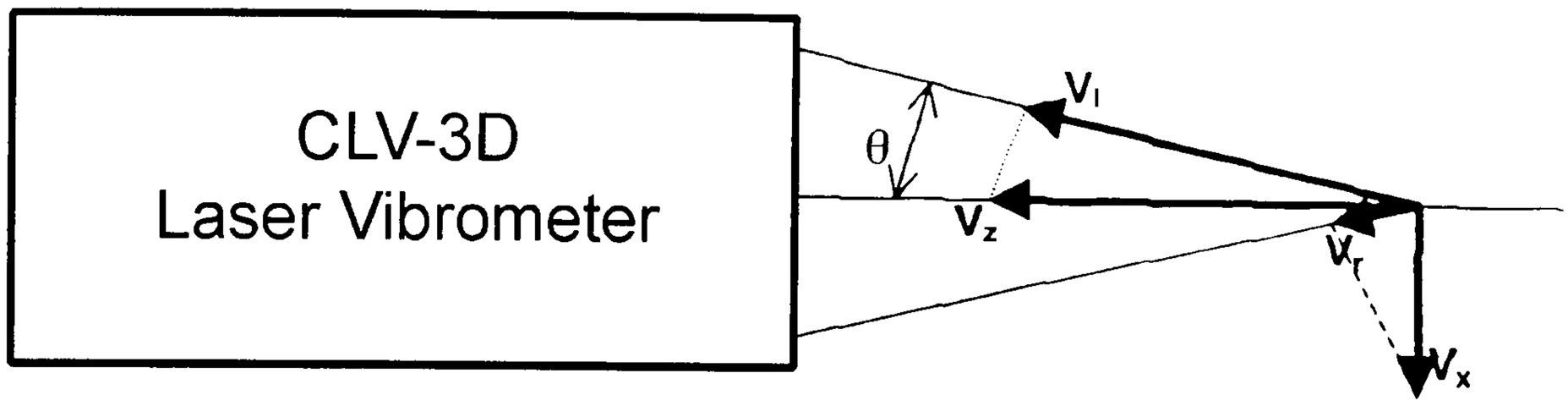

Figure 6-4(a): Top view of the probe beams and the coordinate system

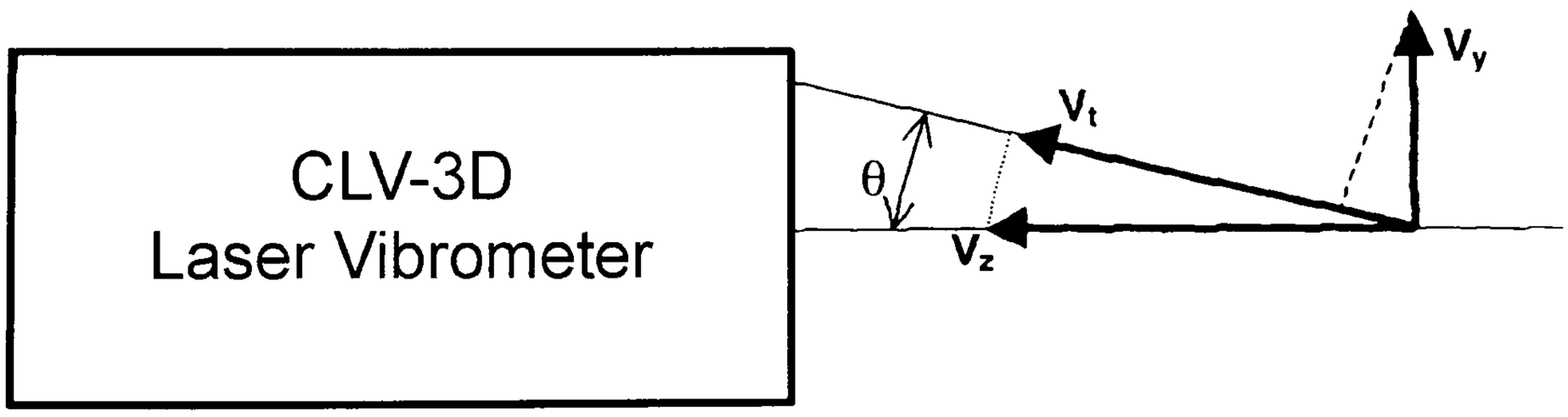

Figure 6-4(b): A different side view of the sensor

6.3 Experimental Results

6.3.1 Nonlinearity of Transducer

The nonlinear response characteristics of a typical industry standard 35 kHz high power ultrasonic transducer, as shown in Figure 6-5(a), can be obtained from an upward and downward stepped-sine sweep about its tuned frequency. The measured longitudinal mode response of the transducer is shown in Figures 6-5(b) and 6-5(c) for two different excitation levels. Figure 6-5(b) shows the transducer's response at an excitation of 30 V. Then, as the excitation is increased to 50 V as in Figure 6-5(c), a region of hysteresis, combined with amplitude jumps and stable and unstable multivalued responses, becomes evident. As the frequency is swept upwards, there is an upward jump at approximately 35.34 kHz. Likewise, as the frequency is swept downwards, there is a downward jump effect at approximately 35.31 kHz. Within this small region hysteretic behaviour is plainly evident. The extremely narrow frequency band over which this occurs is a function of the high Q (i.e. efficiency) of such systems and underlines the importance of very precise design so that these effects can be reduced in such a way that the output of the cutting system to which the transducer is attached is as efficient and robust as possible. The frequency shifts in Figures 6-5(b) and 6-5(c) are considered to be due to the effects of damping and thermal phenomena over the time duration of the experiment.

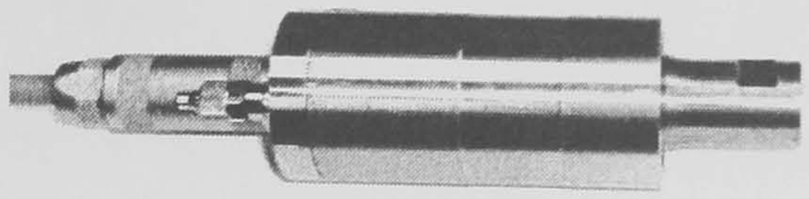

(a) *A 35 kHz* ultrasonic transducer

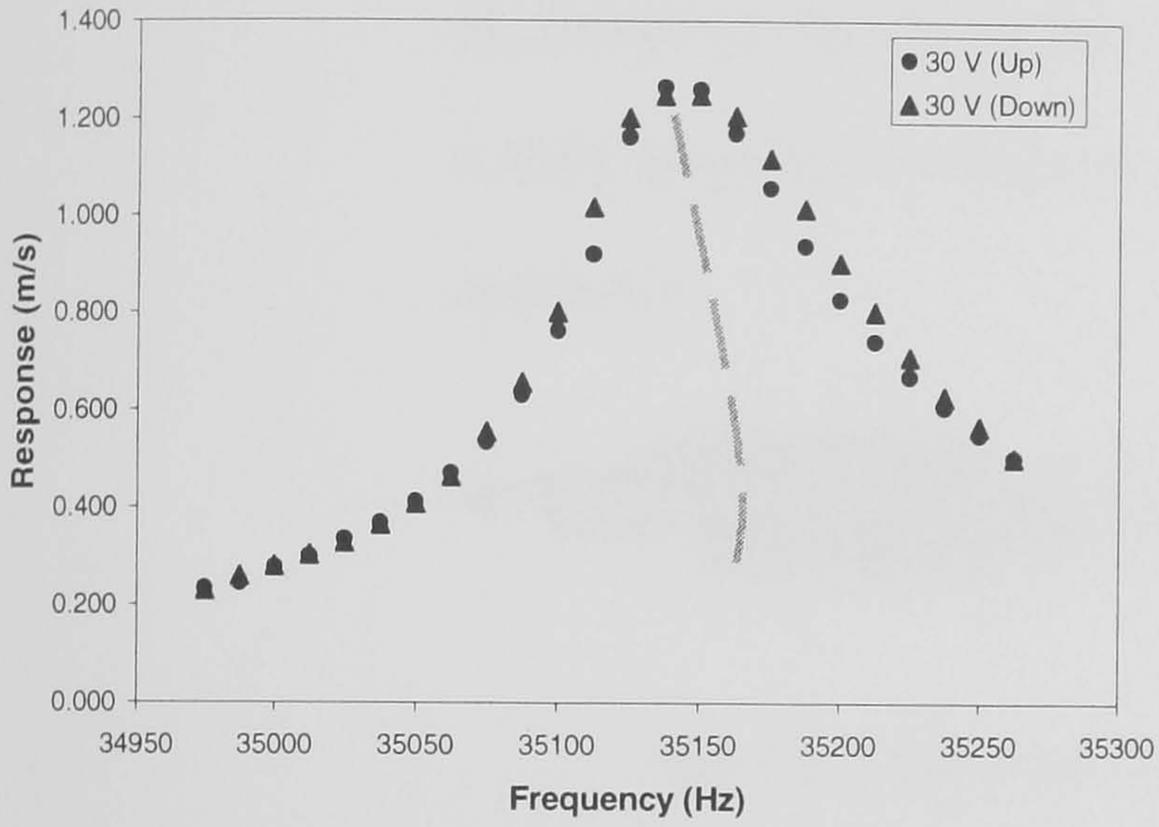

(b) Transducer at 30 V

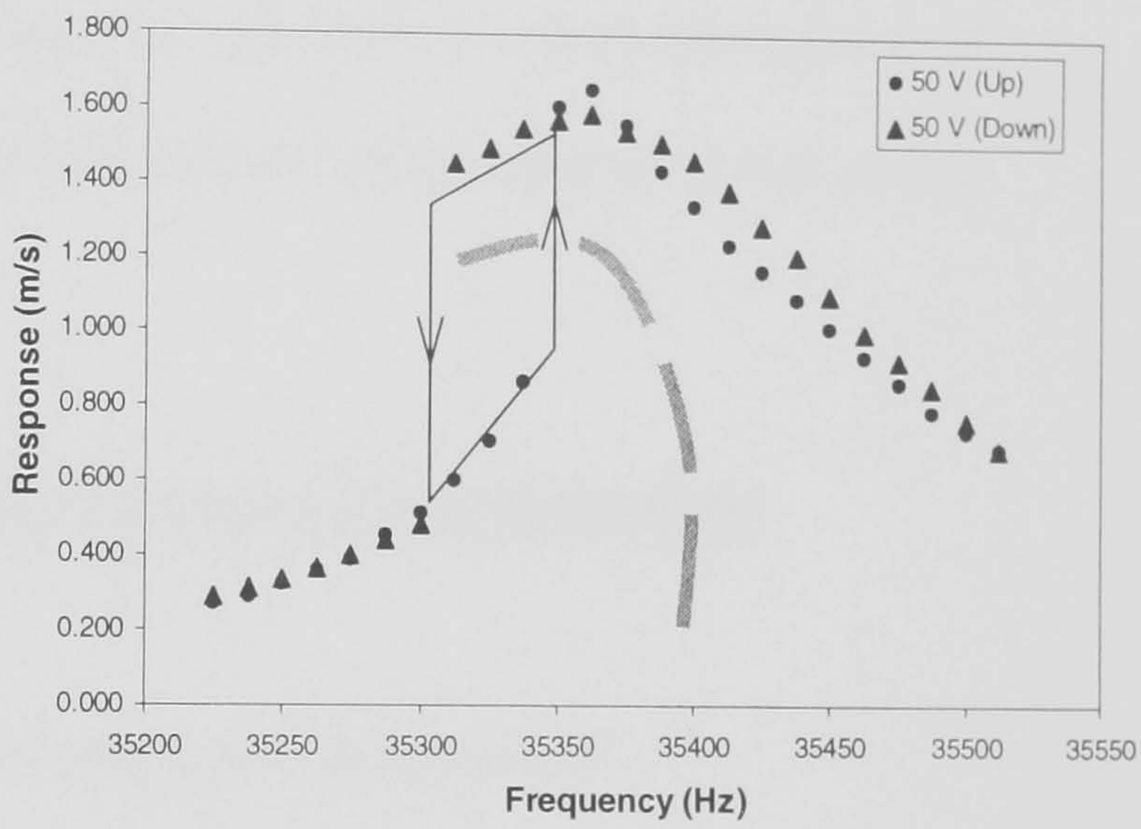

(c) Transducer at 50 V

Figure 6-5: Responses of an industrial ultrasonic transducer for two different excitation levels

6.3.2 Coupling of 1.5 λ Bar Horn

Ultrasonic block and bar horns are specially machined components used to transmit vibration from a transducer to a tool or some other specialised tuned component. In this work, a simple bar horn of aluminium material comprising a solid cylindrical rod (of length 1.5 λ) is attached to the transducer via a threaded stud half-screwed into both components (see Figure 6-6(a)). At the 30 V excitation level, it can be seen that the response in Figure 6-6(b) has less of a softening characteristic compared with that of Figure 6-5(b). A

similar observation applies to the 50 V excitation level, with the characteristic region in Figure 6-6(c) now having reduced in influence. The results obtained for typical industrially relevant equipment suggests that the strongly softening nature of the transducer can only be mitigated to a certain extent by the addition of characteristically hardening bar or block horns, and therefore that a truly linearised response at the output of the system is not easily achieved.

(a) 1.5 λ bar horn screwed into transducer

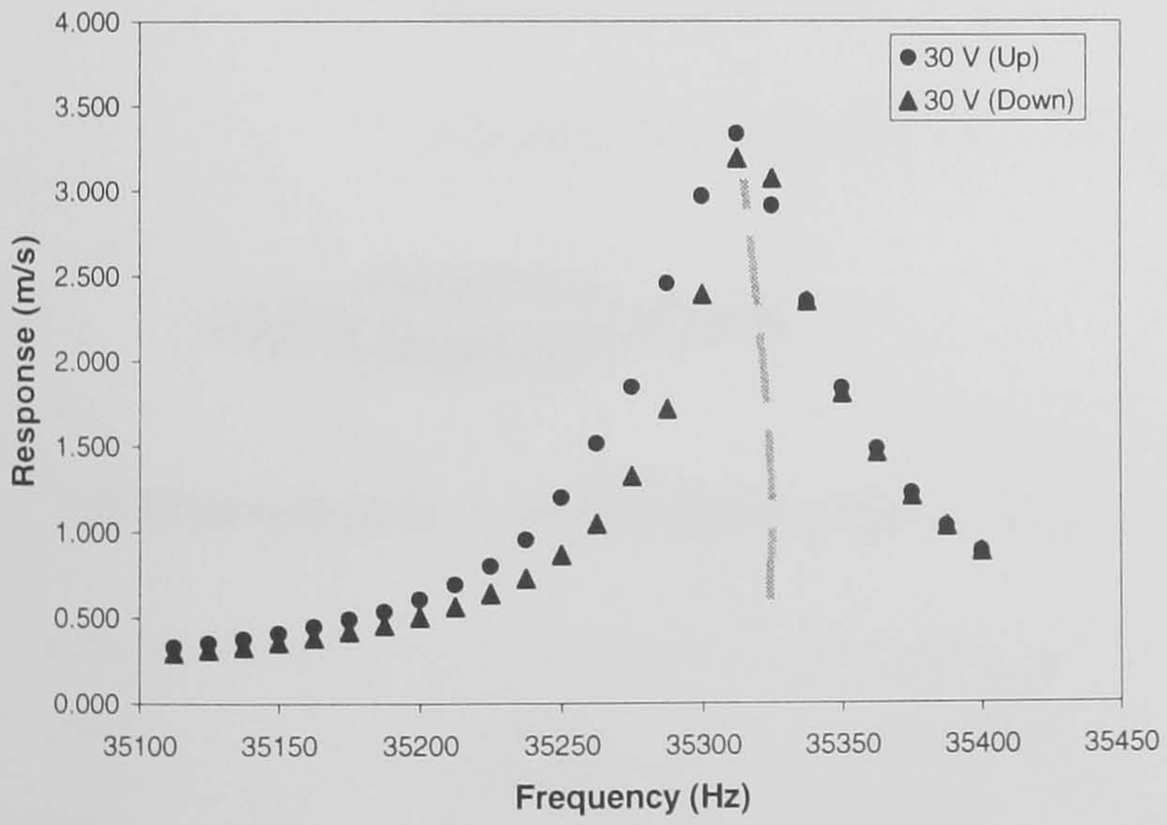

(b) Transducer and bar horn at 30 V

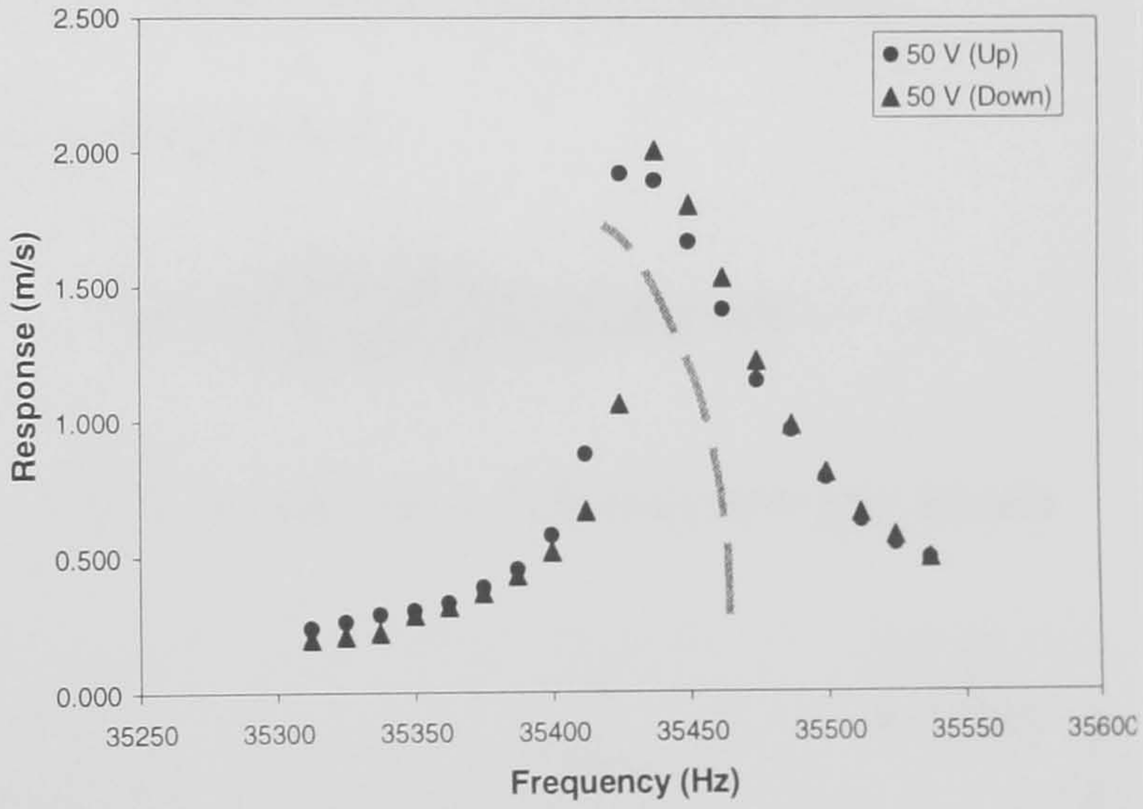

(c) Transducer and bar horn at 50 V

Figure 6-6: Responses of an ultrasonic transducer and 1.5 λ bar horn for two different excitation levels

6.3.3 Coupling of Half- and Full-wavelength Blades

Figure 6-7 compares the nonlinear performance of the same transducer, but attached directly to a 0.5 λ and a λ cutting blade with both blades manufactured from tool steel. In the first case at the 30V excitation level (see Figure 6-7(b)), an even softer response is obtained than that for the transducer by itself. However, the λ blade exhibits a predominantly hardening characteristic and so the combined response is now significantly linearised as depicted in Figure 6-7(d). A supporting theory for the λ blade to have a hardening characteristic is that its geometry is of a 'beam-like' structure, and that Chakraborty *et al.* (1998) have demonstrated that a beam-like structure is a hardening component.

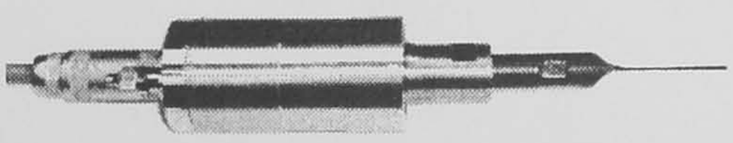

(a) Transducer + half-wavelength blade

(c) Transducer + full-wavelength blade

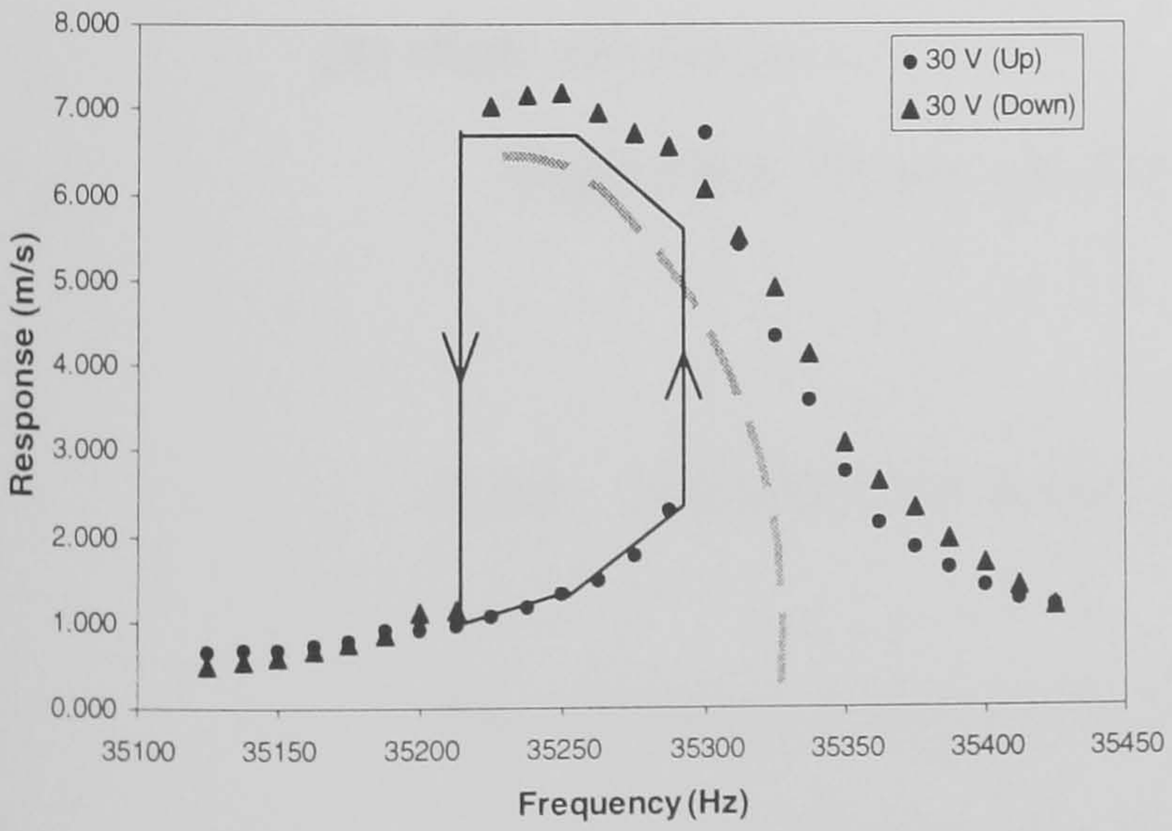

(b) Transducer and 0.5 λ blade

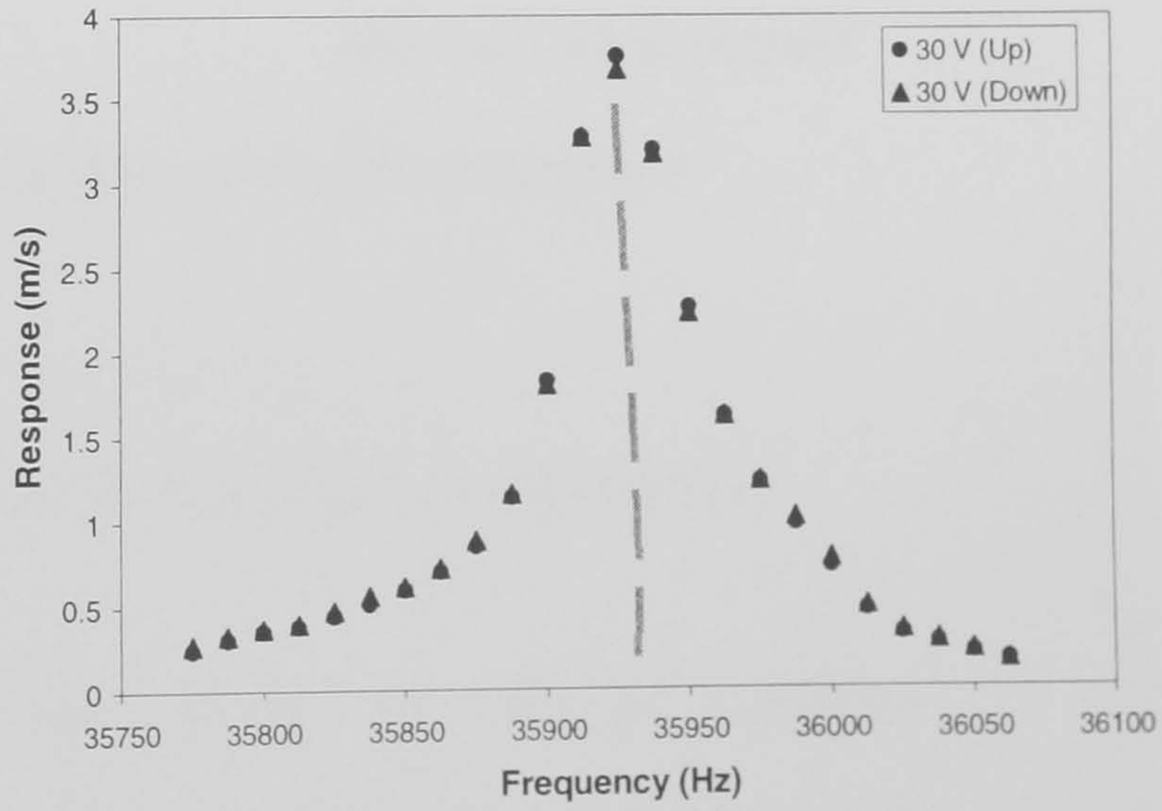

(d) Transducer and λ blade

Figure 6-7: Responses of an industrial ultrasonic transducer and 0.5 λ and λ blades at 30 V excitation level

6.3.4 Influence of Joint Tightness on System Nonlinearity

These experimental investigations have also shown that the tightness of the screwed joints in between the coupled components contributes to the nonlinear characteristics of the system. The joint between the transducer and the 1.5 λ bar horn in Figure 6-6(a) has been tightened with a higher torque and shows a more linearised response in Figure 6-8(a) than that of a lower-torque joint in Figure 6-8(b).

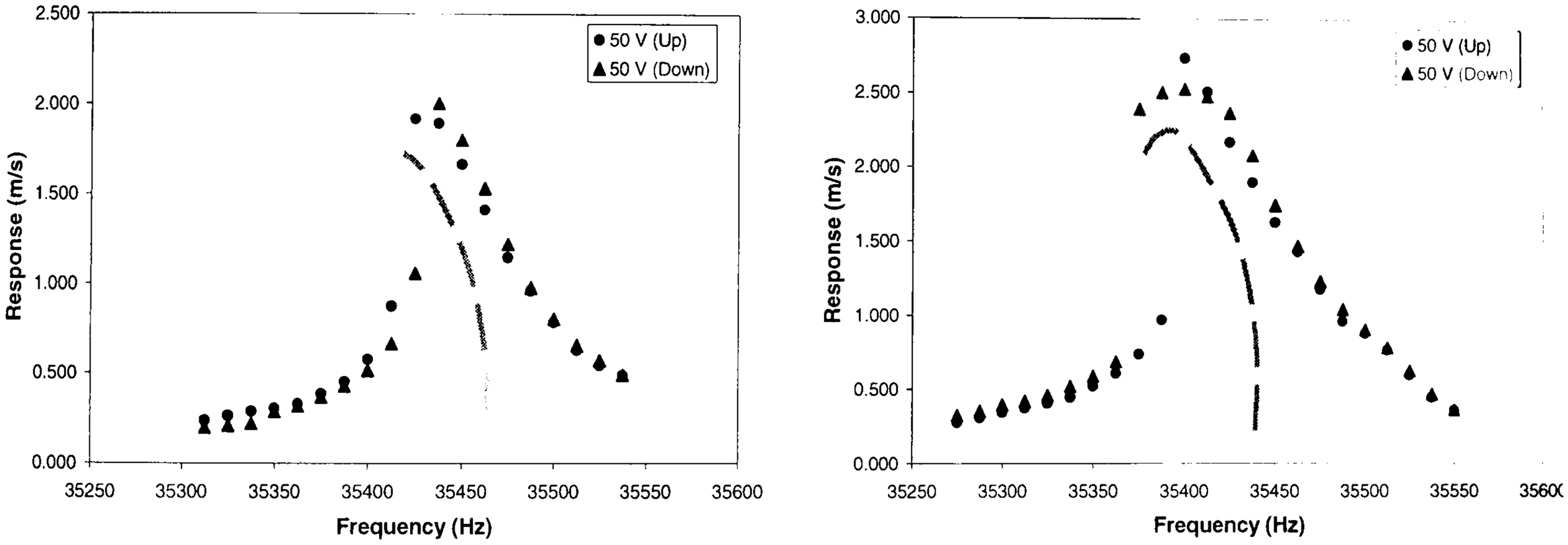

(a) High torque joint **(b) Low torque joint**

Figure 6-8: Effects of joint tightness on the response

6.3.5 Influence of Positioning of Stud on System Nonlinearity

The nonlinear characteristics of the system can also be varied by means of the axial positioning of the stud within the joint. Figure 6-9 shows three different configurations for the position of the threaded stud. It is evident that when the stud is fully-fitted into the transducer-

base (see Figure 6-9(a)), the smallest nonlinear region is evident in the system response at the blade tip compared with a configuration where it is half-fitted into the blade-base (see Figure 6-9(b)). This effect is even more accentuated for the other extreme case where the stud is fully-fitted into the blade-base (see Figure 6-9(c)), for which the widest nonlinear response region can be observed.

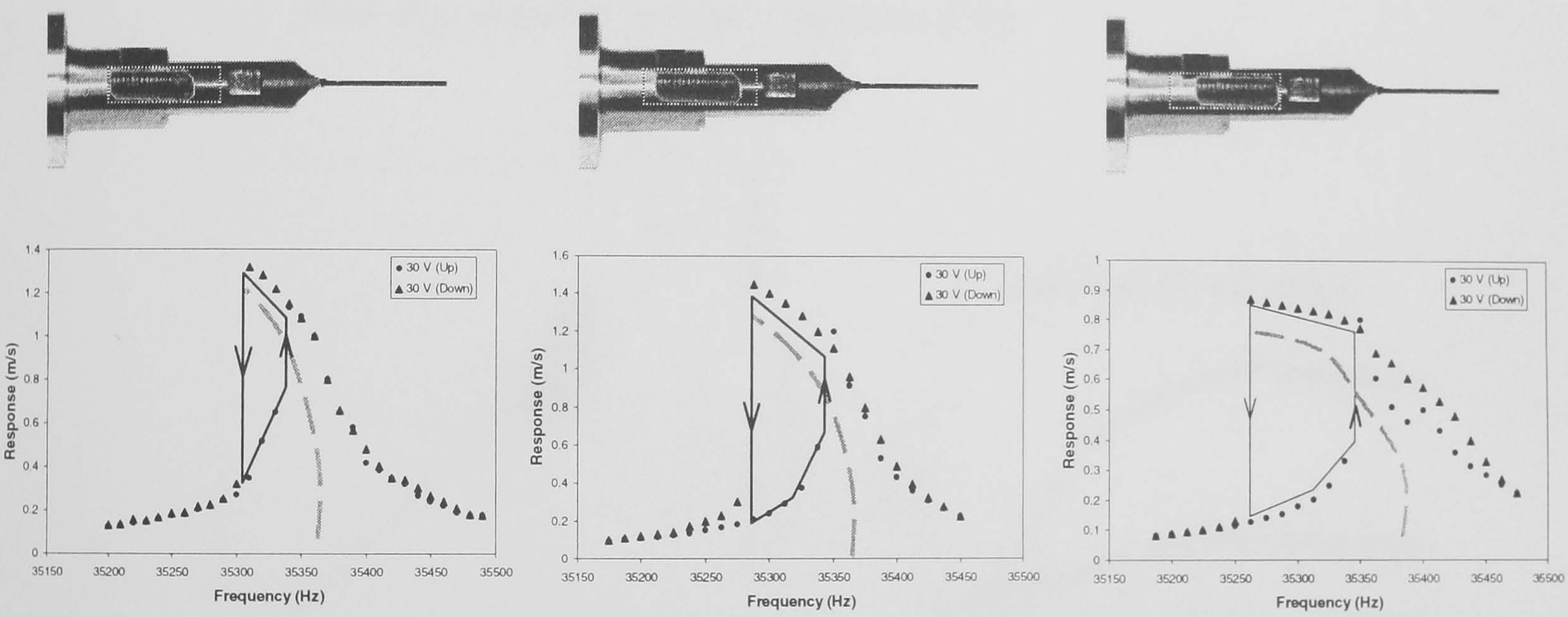

(a) Stud fully-fitted into the transducer-base

(b) Stud half-fitted into the blade-base

(c) Stud fully-fitted into the blade-base

Figure 6-9: Different stud configurations

6.3.6 Relation Between Transducers and the Duffing Oscillator

Further supporting evidence that the transducer behaviour is typical of a Duffing oscillator is presented in Figure 6-10. Figure 6-10(a) is the predicted bifurcation of the response as a function of excitation acceleration when the excitation frequency is at the first mode eigenvalue of the system in Figure 3-1. This phenomenon was

investigated experimentally by measuring the response from the transducer face of two different 35 kHz tuned transducers over a range of excitation levels and the results are presented in Figure 6-10(b). Although the measured response from the transducer face cannot indicate multiple response solutions, the measurements in Figure 6-10(b) seem to exhibit a bifurcation point at higher excitation levels for each transducer, corresponding to the characteristic behaviour outlined in red in Figure 6-10(a) .

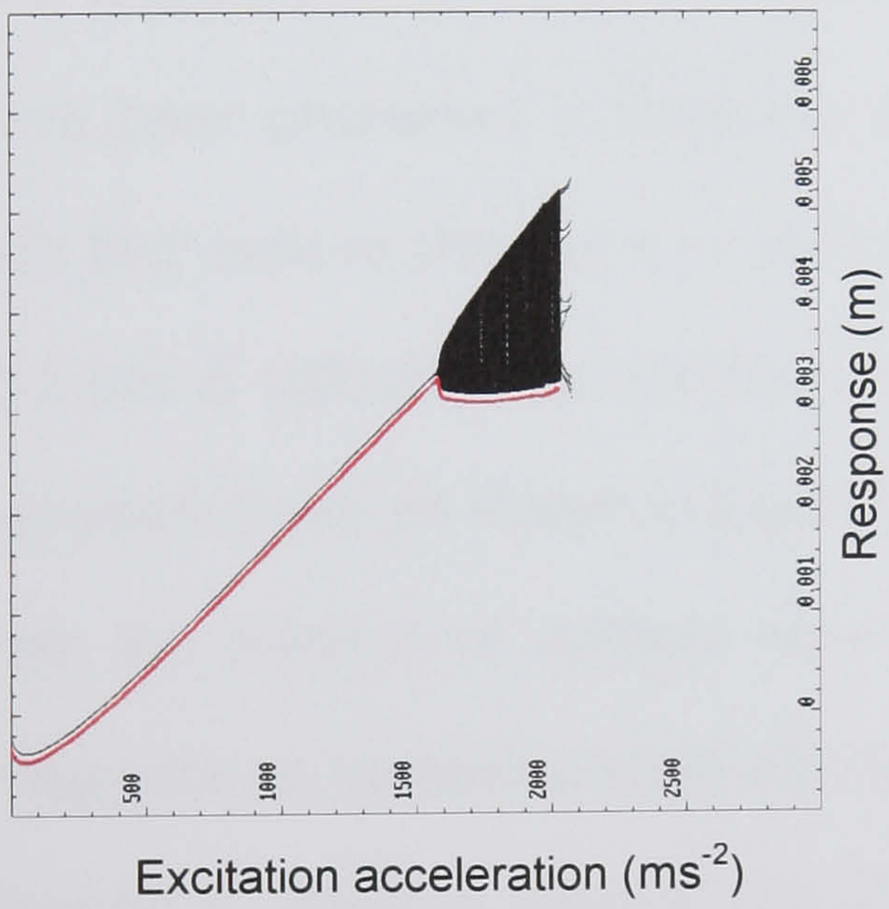

(a) Excitation level plotted against response showing predicted bifurcation for $h_2 = 0.0167\,h_1$

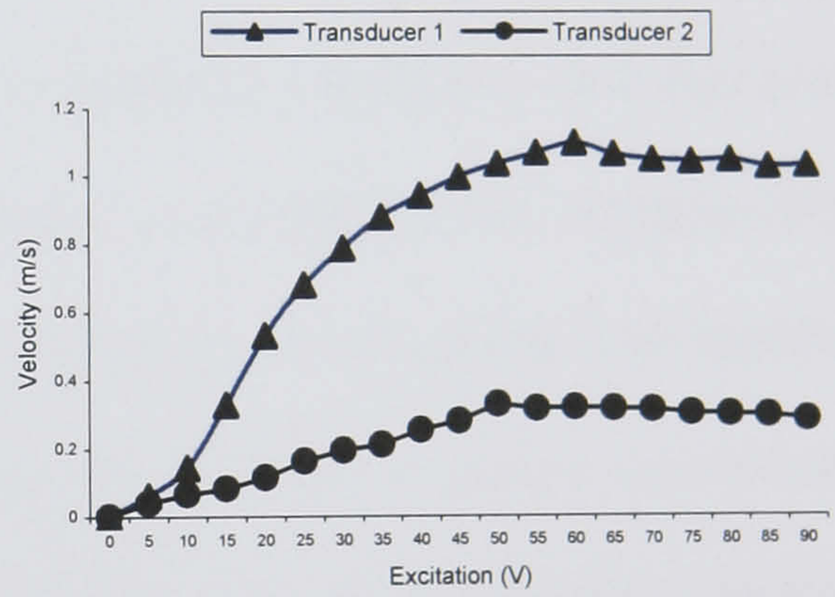

(b) Measured transducer response indicating bifurcation

Figure 6-10: Transducer as a Duffing oscillator

CHAPTER 7

DISCUSSION OF RESULTS

7.1 Introduction

The analyses for the hypothesised nonlinear response modification model have been presented in Chapters 3 to 6. The method of multiple scales was first used in Chapter 3 to derive two solvability equations (3.2-63) and (3.2-64) to calculate the nondimensionalised response of the represented assumed model as shown in Figure 3-1. Chapter 4 corroborated the results from the method of multiple scales with those from a direct numerical integration. A numerical study into the system's dynamics was extended in Chapter 5, where a study of the bifurcations and stability of the solutions via phase planes, Poincaré maps, time plots, bifurcation diagrams and Lyapunov exponents were summarised. Chapter 6 applied this novel method of modifying nonlinear responses to a physical, industrial, application, that is the ultrasonic cutting system.

The purpose of this chapter is to examine the results from Chapters 3 to 6, extending the discussion where appropriate, and allowing conclusions to be derived from the respective results.

7.2 Analytical Results

The analytical developments involved using both the method of multiple scales and direct numerical integration. In the following are summarised points which emerge from these studies:

- The results from the method of multiple scales given in Figures 3-4(a) and 3-4(b) showed good conclusive results that the effect of coupling a softening system to a hardening system does indeed have a global effect on the nonlinear response of the overall system. This is emphasised when increasing the cubic softening stiffness, h_2, and this softens the responses for both amplitudes a_1 and a_2. Similarly, a decrease in h_2 tends to bend the backbone of the nonlinear response further to the right, to a more linear-like response, accentuated when $h_2 = 0.008h_1$.

- Numerically integrating the governing equations of motion (3.2-1) and (3.2-2) has produced results that corroborate those of the method of multiple scales. There is evidence of a consistent phenomenon whereby both the responses in the first mode of x_1 and x_2 show accentuated softening as the softening cubic coefficient is increased (see Figures 4-4(b) and 4-5(b)).

- The amplitudes of both a_2 and x_2 are also marginally higher than a_1 and x_1 for the first mode of response.

- The numerical integration results give two modes of response whereas the method of multiple scales only generates results related

to the chosen resonance condition and around the region of perfect external tuning, $\varepsilon\nu = 0$ (equation 3.2-39).

7.3 Numerical Results

All the subsequent numerical analyses were undertaken by generating problem-specific code within the public-domain software *Dynamics 2*.

- Figures 5-2 and 5-3 give plots of the nondimensionalised bifurcatory behaviour of amplitude responses x_1 and x_2, as a function of the excitation frequency Ω. For the first response mode, as shown in Figures 5-2(i) to (l) and Figures 5-3(i) to (l) respectively, it can be deduced that an increase in the cubic softening coefficient accentuates the softening effect, mirroring the effects noticeable in the results of the method of multiple scales and numerical integration.
- It is evident that in the case of the third order superharmonic when the cubic softening coefficient is increased from the values of Figure 5-2(a) to that of 5-2(d), the response becomes more linear, hence broadly correlating with results in Figure 4-4(c).
- In the superharmonic responses of Figures 5-3(a) to 5-3(d), the increase in the cubic softening coefficient correlates with the numerical integration of Figure 4-5(c), whereby the response becomes progressively more hardening.

- The calculated Lyapunov exponents support the notion that nonlinearities can generate undesirable responses, but only in cases of very high excitation level, as shown in Figure 5-4. As the cubic softening coefficient is increased, the system gets more softening and correspondingly more chaotic, with a wider region of positive Lyapunov exponents, obviously rendering any practical system inefficient.
- Figure 5-5 shows the bifurcatory behaviour of amplitude response x_1^* as a function of the excitation acceleration, accompanied by its respective Lyapunov exponent. For the most linear response from Chapters 3 to 5 (i.e. $h_2 = 0.008h_1$), a periodic response for a wide range of excitation values is achieved. As the softening coefficient is increased, evidence of chaos surfaces, with a lesser excitation acceleration that is subsequently required.

At discrete excitation acceleration points of the above bifurcations, phase planes, Poincaré maps and time plots are given in Figures 5-7 to 5-12. The following are general observations of the coupled Duffing oscillators as the softening cubic coefficient, h_2 is increased from $0.008h_1$ to $0.083h_1$:

- Periodic orbits in the phase planes move away from each other as the effect of the predominant system nonlinearity is increased, either by manipulation of the cubic nonlinear coefficient, or by the excitation acceleration. And therefore, the phenomenon behind this behaviour, as shown on the phase planes, could represent a bifurcation to chaos.

- Complicated phase plots are obtained for the higher values of h_2, indicating likely chaotic motions as the system effectively becomes more nonlinear.
- Strange attractors are also obtained in the Poincaré maps for higher values of h_2, again indicating likely chaotic motions.
- Therefore, certain phenomena, necessary for nonlinear response modifications, are evident, and are also potentially involved in the generation of chaos. In principle such modifications can be achieved by varying the coupled, oppositely configured, nonlinear stiffnesses.

7.4 Experimental Results

The following results were obtained from an experimental programme carried out on an ultrasonic cutting system. An industrial ultrasonic generator (colloquially referred to as a transducer) usually has a softening characteristics, and the following are the resultant effects of coupling different components to such a transducer:

- Attaching a 1.5 λ bar-horn to the transducer results in a more linear response than that provided by the transducer itself. The hardening bar-horn clearly contributes to mitigating the effects of the nonlinearity of the system (see Figure 6-6).
- Attaching a λ blade to the transducer also results in an almost linear response. Thus, once again, hardening characteristics of a coupled

component, this time the blade, modifies the nonlinear response of the system (see Figure 6-7(d))

- However, coupling a 0.5 λ blade to the transducer results in an even more softening response than originally generated by the transducer itself. This shows clearly that this length of blade is, instead of a softening nonlinear characteristic and therefore exaggerates the softening behaviour of the system (see Figure 6-7(b)).

Other ways of influencing the nonlinearity of an ultrasonic system have also been identified in this research:

- Figure 6-8 shows that a higher torque joint is preferred over a lesser torque joint as the former generally results in a more linear overall response than the latter.
- The axial positioning of the stud within the joint can also highly influence the nonlinearity of the system. Figure 6-9(a) shows that when the stud is fully-fitted into the transducer-base, the smallest nonlinear region is evident in the system response at the blade tip compared with a configuration where it is half-fitted into the blade-base (see Figure 6-9(b)). The most undesirable case is where the stud is fully-fitted into the blade-base in Figure 6-9(c), for which the widest nonlinear response region, and accentuated softening can be observed.
- Relationships between the transducers and the Duffing oscillator were also identified by comparing the predicted bifurcation of the latter's response as a function of excitation level in Figure 6-10(a).

with the measured response from the transducer face of two different transducers over a range of excitation levels in Figure 6-10(b). These two figures show some similarities in the bifurcation path.

7.5 Conclusions

The three methods of investigating and identifying the response behaviour of serially coupled Duffing oscillators have all shown similar trends with regards to the effects of increasing the softening cubic coefficient. Numerical studies have also indicated that chaos is evident as the system becomes more nonlinear due to the coupling of the opposite nonlinear cubic stiffness. Experimental results from tests on the coupling of different components within an ultrasonic system conclude that this novel approach to nonlinear response modifications could be successfully applied to an industrial application.

CHAPTER 8

CONCLUSIONS

This thesis has considered the issue of response modifications within an ultrasonic system as used within the food industry. The technique that has been developed is based on the exploitation of the natural mitigating effects of serially coupled nonlinear sub-systems on the overall system response. It has been shown theoretically that certain nonlinear effects can be advantageously neutralised with the novel methodology of coupling another sub-system of opposite nonlinear characteristic. It has been experimentally demonstrated that components with different geometries, materials and wavelengths are shown to possess different nonlinear characteristic. By coupling them together, the overall nonlinear response of the system has been usefully influenced. There are some limited references to such systems in the literature but there have not been many reported phenomena relating to serially-coupled, interacting, oppositely-signed, nonlinear subsystems to date.

In order to gain an understanding of serially-coupled nonlinear oscillators it was decided firstly to investigate the behaviour of a pair of nonlinear single degree-of-freedom sub-systems coupled together via their linear and nonlinear stiffnesses. This approach was seen to be justifiable in order to test the hypothesis that useful response modifications could be

obtained by means of manipulations of the pertinent and dominant nonlinearities. The hypothesised, simplified, system contained springs (linear and nonlinear), masses, and dampers, together with an externally imposed harmonic excitation. The two nonlinear springs were of positive cubic and negative cubic characteristics, respectively, and the equations of motion were derived in the form of two Duffing oscillators coupled in series.

These equations were solved analytically, to first order approximation, using the method of multiple scales, and they were also numerically integrated. Interesting interactive behaviour between the two degree-of-freedom was observed for the synchronous external resonance condition and the superharmonic internal resonance, $\Omega = \omega_1 + \varepsilon\nu$ and $\omega_2 = \frac{1}{3}\omega_1 + \varepsilon\sigma_1$, where $\varepsilon\nu$ and $\varepsilon\sigma_1$ are the external and internal detuning parameters respectively. In this research it has been shown conclusively by using a first order multiple scales approximation that the nonlinear characteristics of the steady-state responses to the nonautonomous modulation equations can be manipulated by altering the two, oppositely-signed, nonlinear cubic stiffness coefficients. In particular it was shown that the effect of increasing the softening quantity, h_2 was to soften the amplitude for the responses of both subsystems, a_1 and a_2. In addition to this, certain specific numerical relationships between the raw nonlinear coefficients (i.e. $h_2 = 0.008h_1$, for example), can be determined that effectively linearise the two sub-system response amplitudes (Figures 3-4(a) and 3-4(b)), notwithstanding the fact that such numerical relationships are necessarily system-data specific. These effects were corroborated numerically and a further study of the bifurcations and stability of the

solutions via phase planes, Poincaré maps, time plots, bifurcation diagrams and Lyapunov exponents showed that additional, and highly complex, dynamics could be observed, particularly in more strongly excited systems. A range of numerical results was obtained for both the first order analytical approximation and the numerical integrations for the principal, stiffness-coupled, model in the physical co-ordinate space, and these underpinned the general finding that response amplitude characteristics could be effectively linearised for different combinations of data. This suggests that the useful mitigating effect might also be realisable in the more complex ultrasonic system and so a parallel programme of experimental tests on an ultrasonic cutting system was carried out to test this hypothesis.

The nonlinear response characteristic of a physical industrial application was thus determined. Ultrasonic transducers are inherently nonlinear at high power and tend to exhibit a cubic softening characteristic, with a jump phenomenon typical of a Duffing oscillator. To find a practical design solution to the effects of nonlinear responses, it was first necessary to measure the linear regime and nonlinear response for a range of input voltages to the transducer. The effect on this response of attaching different tuned components was also assessed, as well as the effects of the attachment method. It was found that some tuned components, including certain blades and block-horns of particular wavelength, tended to reduce the softening response when attached to the transducer, and would therefore result in the system increasing its linear threshold, and operating with a near linear response. In other cases, including those of half-wavelength blades, the blade transducer system response was softer than that of the transducer alone, had a lower linear threshold, and a wider

instability region. A bank of experimentally obtained information on the nonlinear characteristics of transducers, bar-horns, block-horns and blades has been compiled, providing valuable data for understanding serially-coupled multi-component system configurations, and which assists the control of the nonlinear response in the design of ultrasonic devices.

Additionally, the width of the instability region could be manipulated by altering the tightness of the joints, and by altering the position of the stud between the attached components. It has always been understood in the high power ultrasonics community that careful assembly of system components is critical for good system performance. There have been many "rules of thumb" applied, concerned with stud sizes, stud position and torque requirements for joining components, although there are inconsistencies between manufacturers' recommendations. The work carried out in this project has clarified this issue and has related the nonlinear responses to the undesirable audible noise problems associated with poor assembly. As an illustrative example, Figure 6-9 shows the effect of stud position on the response of a single blade attached to a transducer, from a sweep up/down measurement around the longitudinal mode frequency using the 3D laser vibrometer. The stud position has a marked effect on the nonlinear response, offering a practical method for manipulating the softening characteristic.

The results of this work have showed that serially-coupled elements within a typical ultrasonic cutting system do indeed exhibit alternately softening and hardening nonlinear cubic stiffness characteristics, and that these can be mutually ameliorated by individual characteristic manipulations. So, although the two degree-of-freedom models did not

directly model the ultrasonic cutting system, they provided a phenomenologically relevant test-bed through which the important interactions could be investigated. From this, robust indicators were obtained for obtaining linearised responses of the cutting blades, and therefore the capability of showing preferential modal characteristics. These indicators were in the form of experimentally derived data defining the principal nonlinearities within the components of the system that was tested, and the relationship between these and the various practical settings and configurations of the cutting system itself. It is intended that reduced order dynamical models of practical ultrasonic cutting systems will be derived in future spin-off work, and that these could be used to provide even more efficient energy transfers from the ultrasonic transducer through to the process medium being manufactured.

This research provides some basic theory and understanding of how nonlinear systems can be made more efficient. It has also initiated an identification of the nonlinear characteristics of some ultrasonic components, and other factors that will influence the nonlinearity. The practical goal has been to try to get the response of the blade (i.e. at the far end of the chain from the transducer) to be linear, irrespective of the fact that the transducer, or the interconnecting components such as joints and bar-horn, are all nonlinear. This is tackled by means of exploiting the alternately nonlinear characteristics of soft, hard, soft, hard, etc, effects that the serially linked transducer, joint, bar-horn, joint, and blade may provide.

Engineers and scientists are encouraged to use this new approach with prior understanding of the nonlinearity of the particular components to be coupled. More research could stem from here in understanding how

different variables (e.g. geometries, materials, wavelengths, etc) will contribute to a component's nonlinear characteristics. By obtaining a good basic understanding of each individual component, an ideal and robust overall linear system can ultimately be configured, and hence more reliable and efficient industrial systems can be designed. From here, one could intend to move onto fully representative *actual models of the ultrasonic system as initiated* from thinking about this simplistic theoretical vehicle, now that the experiments have borne out the theoretical proposal that this approach to the control of nonlinear behaviour of such a system is possible.

CHAPTER 9

RECOMMENDATIONS FOR FURTHER WORK

This thesis provides an enhanced understanding of the influence of nonlinearities in the design of high power ultrasonic cutting systems. Some further areas of research have been identified as a result of this work, and these could be used to emphasise the novel method of nonlinear response modification.

9.1 Experimental Work which is Directly Related to the Theoretical Results

The main result of this research is an experimental verification of the proposal that nonlinear modifications can be achieved in an industrial application of the ultrasonic cutting system, as well as the proposal of phenomenological models which allow an in-depth investigation into the principal theoretical mechanisms which underpin the main effects. These models are phenomenologically relevant to the problem in that they reduce it down to the basic essentials in order that it can be explored with a minimum of extraneous conditions and additional complicating effects. On the understanding that the theoretical models examined in this thesis are vehicles for the phenomena, rather than literal physically based models of the ultrasonic cutting system, it is suggested that further experimental work

relating specifically to the phenomenological models would also be of considerable interest and value. On this basis a partially completed sequence of experimental work of this nature is summarised here, with suggestions for completion and further developments.

Figure 9-1 shows two masses fitted onto a linear slide system and comprising the fundamentals of a two degree-of-freedom system. This system also consists of a hardening spring that is fitted between m_1 and the support structure. The two masses are connected together by means of a softening spring which is made up of an elastomeric material. Mass m_1 is directly excited by a shaker via a push rod. The stiffness characteristics of the hardening spring (see Figure 9-1(b)) are variable, by means of a specially designed spring based on a small beam, clamped at its upper end and with the lower end running in between rollers within a bracket on m_1. The stiffness can be easily adjusted by changing the length, or thickness of the beam, or even its initial deflection position. The softening spring is made up of natural elastomeric rubber bonded to an M6 screw fastener at each end. Natural rubber was selected because of its inherent nonlinear softening stiffness characteristics. Appendix F.1 discusses how the nonlinear characteristics of the softening spring were obtained experimentally.

A preliminary system set-up was tested in the laboratory with some initially encouraging results. Dissipation levels were generally found to be rather high, with damping ratios for each degree-of-freedom in the region of 0.35. It was subsequently observed that these high levels emanated from the friction within the linear bearing. Higher excitation levels, by means of a

more substantial shaker, and a higher quality linear bearing, will be implemented in the next version of this experimental rig.

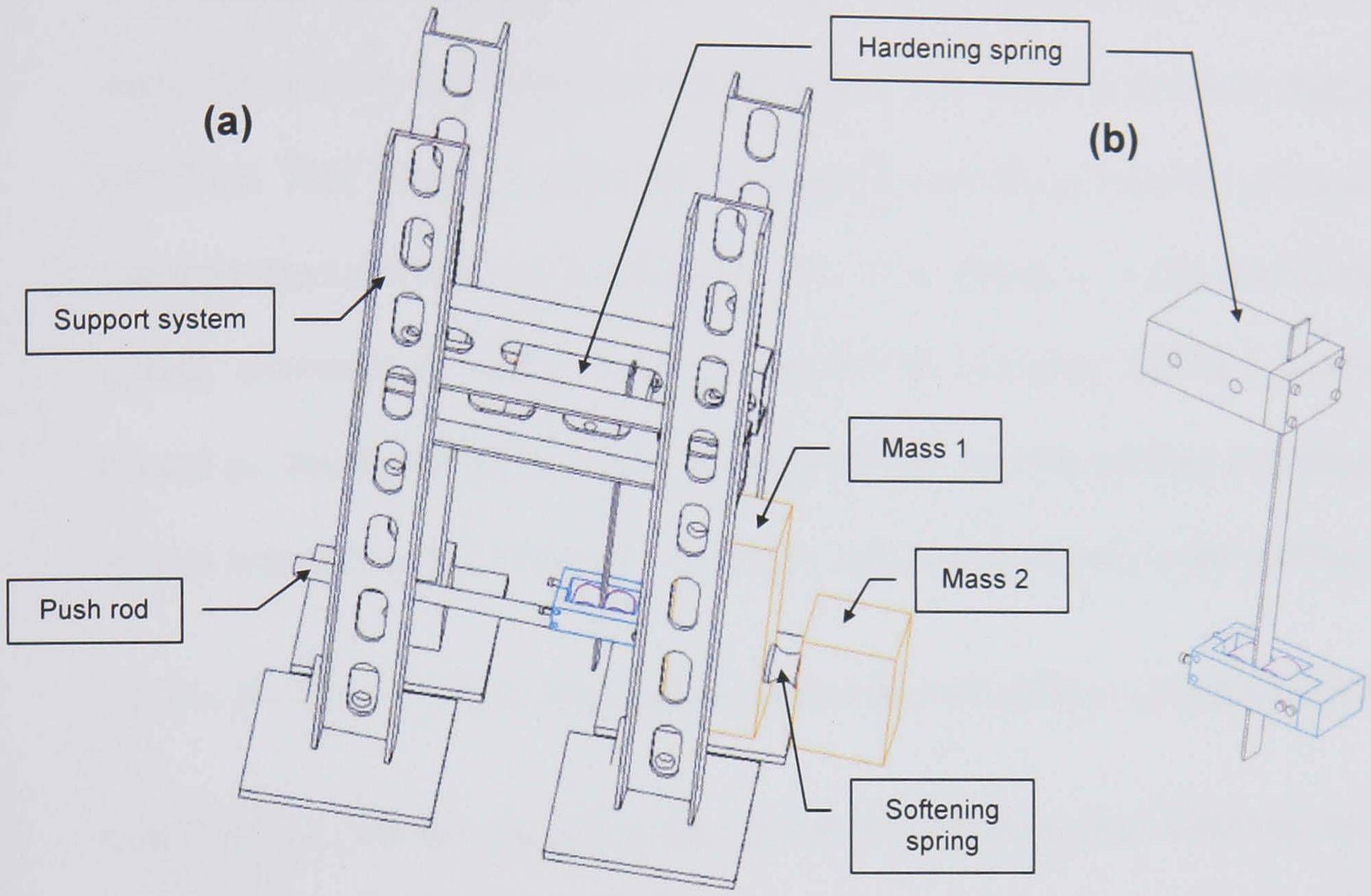

Figure 9-1: Modelling of stiffness-coupled system; (a) CAD drawing of set-up; (b) Hardening spring sub-assembly; (c) Complete experimental set-up

9.2 Pendulum System (Inertia Coupling)

The elastomeric spring and mass m_2 were replaced in an alternative experimental rig by means of a pendulum, forming the second degree-of-freedom. This alternative system was set up by attaching this pendulum to the translating mass m_1 (see Figure 9-2). The spring h, is still the hardening spring, whereas the softening characteristic is achieved with the pendulum, based on the fact that for large deflections (i.e. nonlinearities) the Maclaurin series expansion for $Sin\,\theta$ gives rise to cubic and higher order terms, thus, $Sin\,\theta \approx \theta - \frac{\theta^3}{3!} + \cdots$. This alternative experimental system posesses dynamic coupling (i.e. via the mass/inertia terms) in contrast to the stiffness coupling in the previous model.

The pendulum in Figure 9-2(b) comprises several short sections in order to facilitate an easy variation of the sub-system's natural softening characteristics via the pendulum length. Some limited explorations of this alternative experimental configuration are attributable to Tan (2002).

Appendix F.2 gives the derivation of the equations of motion for the pendulum system for three different cases; a harmonic force applied to the mass m_1; a harmonic force applied at the free end of the pendulum; and a combination of both of the two forces. The motivation for exploring this other system was to attempt to show that the nonlinear modification theory could be feasible within a range of different physical systems in order to show the same kind of effects. On this basis, a wider physical observation of the phenomenon implies a little more generality in application.

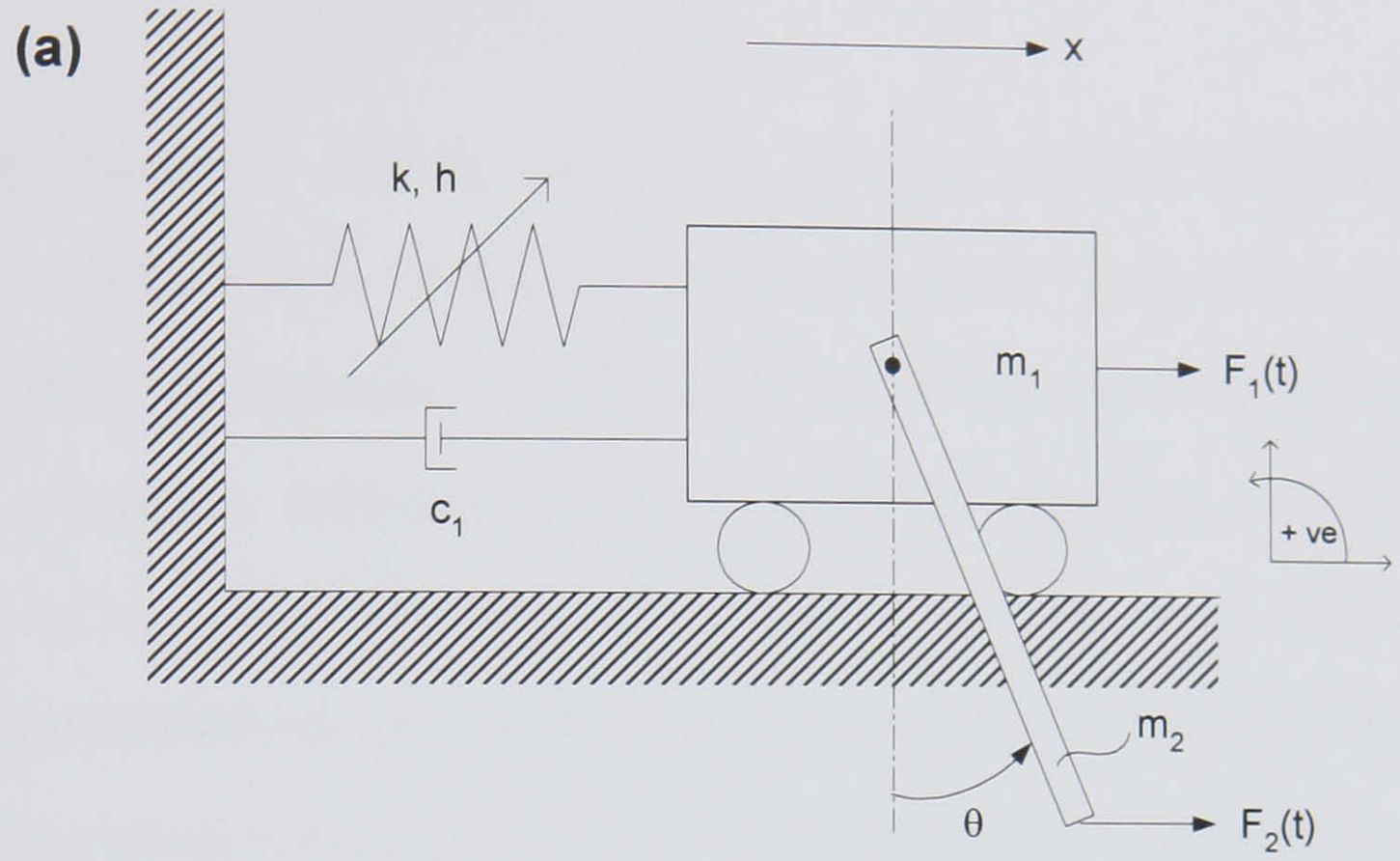

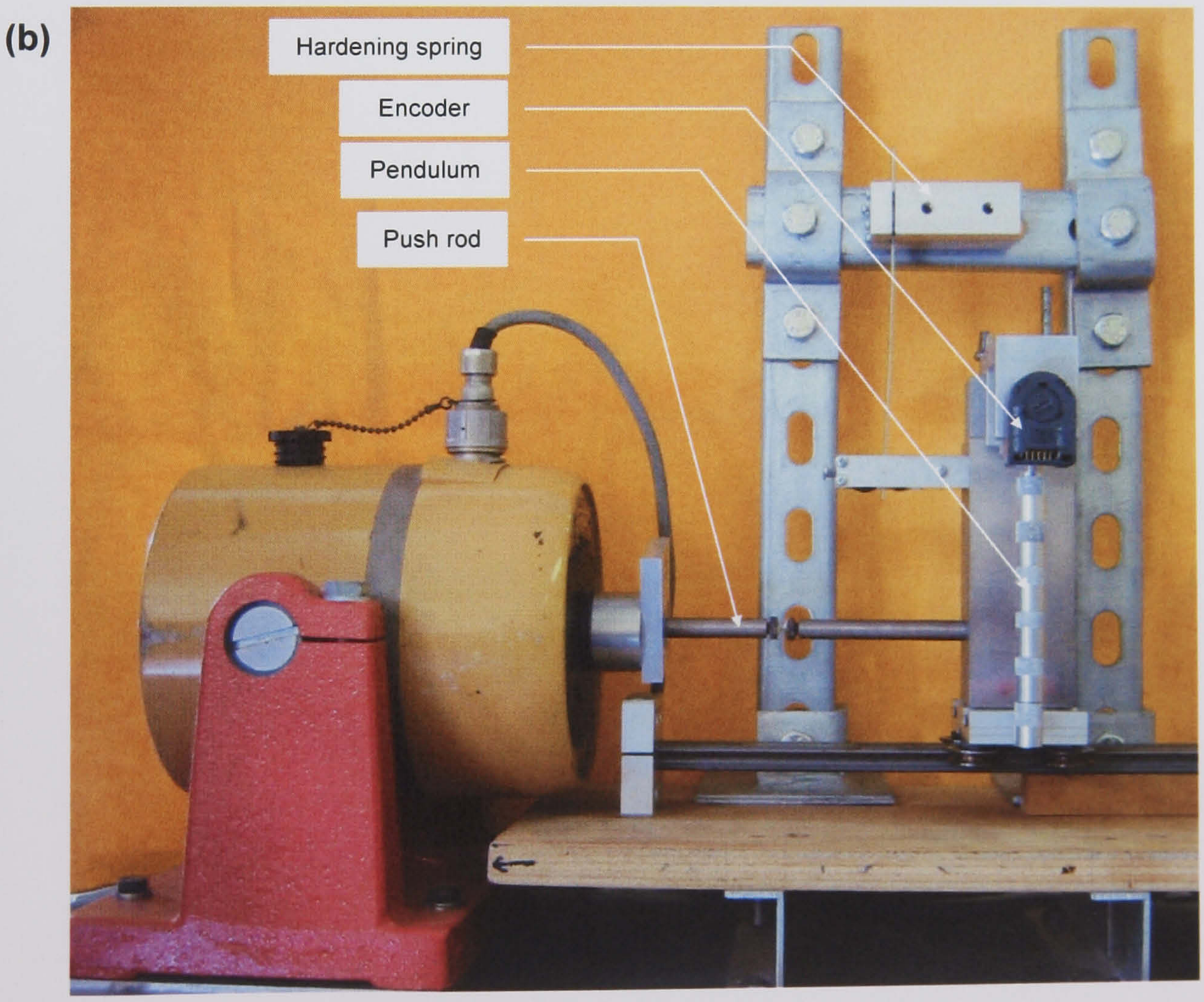

Figure 9-2: Modelling of inertia-coupled system;
(a) Schematic diagram; (b) Complete experimental set-up

9.3 Identification of Cubic Nonlinearities ('Degree of Nonlinearities') from Coupled Components

Further research should be done on the precise identification of the nonlinearities within individual components in these two systems. The nonlinear characteristics of the pertinent component will be dependent on mass, material, stiffness, damping, and wavelength. From thereon, the theory of nonlinear response modification could be more effectively applied having established a wider, and therefore better knowledge of the relevant nonlinear characteristics for practical, demonstrable, systems.

REFERENCES

1. ABDEL-ROHMAN M. and NAYFEH A. H. (1987), *ASCE Journal of Engineering Mechanics* **113**, 335-348. Active control of nonlinear oscillations in bridges.

2. AGRAWAL A. K. and YANG J. N. (1995), *National Center for Earthquake Engineering Research, Technical Report NCEER-95-0019*. Optimal polynomial control for linear and nonlinear structures.

3. AGRAWAL A. K., YANG J. N. and WU J. C. (1998), *International Journal of Non-Linear Mechanics* **33**(5), 829-841. Non-linear control strategies for Duffing systems.

See[1] Yang J. N. (1994b).

4. ASFAR K. R. (1992), *International Journal of Non-Linear Mechanics* **27**(6), 947-954. Effect of non-linearities in elastomeric material dampers on torsional vibration control. doi:10.1016/0020-7462(92)90047-B

5. AURELLE N., GUYOMAR D., RICHARD C., GONNARD P. and EYRAUD L. (1996), *Ultrasonics* **34**, 187-191. Nonlinear behavior of an ultrasonic transducer. doi:10.1016/0041-624X(95)00077-G

6. BOLOTIN V. V., GRISHKO A. A., KOUNADIS A. N., GANTES C. and ROBERTS J. B. (1998), *Nonlinear Dynamics* **15**(1), 63-81. Influence of initial conditions on the postcritical behavior of a nonlinear aeroelastic system.

[1] Cross-reference to other publications co-authored by the corresponding author.

7. BOYACI H. and PAKDEMIRLI M. (1997), *Journal of Sound and Vibration* **204**(4), 595-607. A comparison of different versions of the method of multiple scales for partial differential equations.

8. BRERETON G. J. and BRUNO B. A. (1994), *Journal of Sound and Vibration* **173**(5), 683-698. Particle removal by focused ultrasound. doi:10.1006/jsvi.1994.1253

9. CARDONI A. and LUCAS M. (2002), *Ultrasonics* **40**, 365-369. Enhanced vibration performance of ultrasonic block horns. doi:10.1016/S0041-624X(02)00123-3

   See Lucas M. (2001).

10. CARTMELL M. P. (1990), *Introduction to Linear, Parametric and Nonlinear Vibrations*. Chapman and Hall: London.

11. CARTMELL M. P., ZIEGLER S. W., KHANIN R. and FOREHAND D. I. M. (2003), *In press, Transactions of the American Society of Engineers Applied Mechanics Reviews*. Multiple scales analyses of the dynamics of weakly nonlinear mechanical systems.

    See Khanin R. (1999, 2001), Khanin R. *et al.* (2000) and Warmiński J. A. *et al.* (2003).

12. CHAKRABORTY G., MALLIK A. K. and HATWAL H. (1998), *Journal of Sound and Vibration* **210**(1), 19-36. Normal modes and near-resonance response of beams with non-linear effects.

13. CHAKRABORTY T. and RAND R. H. (1988), *International Journal of Non-Linear Mechanics* **23**, 369-376. The transition from phase locking to drift in a system of two weakly coupled Van der Pol oscillators.

14. CHEUNG Y. K. and IU V. P. (1988), *Engineering Computations* **5**, 134-140. An implicit implementation of harmonic balance method for nonlinear dynamics systems.

15. CHEUNG Y. K., CHEN S. H. and LAU S. L. (1991), *International Journal of Non-linear Mechanics* **26**, 367-378. A modified Lindstedt-Poincaré method for certain strongly non-linear oscillator.

16. CHIN W., OTT E., NUSSE H. E. and GREBOGI C. (1994), *Physical Review E* **50**(6), 4427-4444. Grazing bifurcations in impact oscillators.

17. CHOW P. L. and MAESTRELLO L. (2001), *International Journal of Non-Linear Mechanics* **36**, 709-718. Vibrational control of a non-linear elastic panel. doi:10.1016/S0020-7462(00)00038-X

18. CHUA L. O. (1992), *Archiv fur Elektronik und Ubertragungstechnik* **46**(4), 250-257. The genesis of Chua's circuit.

19. COLE J. D. and KEVORKIAN J. (1963), *Proceedings of International Symposium on Nonlinear Differential Equations and Nonlinear Mechanics*, 113-120. Uniformly valid asymptotic approximations for certain non-linear differential equations.

20. DITTO W. L., RAUSEO S. N. and SPANO M. L. (1990), *Physical Review Letters* **65**(26), 3211-3214. Experimental control of chaos. doi:10.1103/PhysRevLett.65.3211

21. DRESSLER U. and LAUTERBORN W. (1990), *Physical Review A* **41**(12), 6702-6715. Ruelle's rotation frequency for a symplectic chain of dissipative oscillators.

22. DUFFING G. (1918), *Erzwungene Schwingungen bei Veränderlicher Eigenfrequenz*, Vieweg: Braunschweig.

23. FERRI A. A. (1986), *Transactions of the ASME, Journal of Applied Mechanics* **53**, 455-457. On the equivalence of the incremental harmonic balance method and the harmonic balance Newton-Raphson method.

24. FRIEMAN E. A. (1963), *Journal of Mathematical Physics* **4**, 410-418. On a new method in the theory of irreversible processes.

25. FRISWELL M. I. and PENNY J. E. T. (1994), *Journal of Sound and Vibration* **169**(2), 261-269. The accuracy of jump frequencies in series solutions of the response of a Duffing oscillator. doi: 10.1006/jsvi.1994.1018

26. GEAR C. W. (1971), *Communications of the ACM* **14**(3), 176-179. The automatic integration of ordinary differential equations. doi:10.1145/362566.362571

27. GRAHAM G., PETZING J. N. and LUCAS M. (1999a), *Ultrasonics* **37**(2), 149-157. Modal analysis of ultrasonic block horns by ESPI. doi:10.1016/S0041-624X(98)00050-X

28. GRAHAM G., PETZING J. N. and LUCAS M. (1999b), *Ultrasonics* **37**(3), 231-238. Extracting modal parameters of ultrasonic bar horns from ESPI FRF data. doi:10.1016/S0041-624X(98)00051-1

See Lucas *et al.* (1996).

29. HARDY G. H. and WRIGHT E. M. (1979), *An Introduction to the Theory of Numbers, 5th ed.* Clarendon Press: Oxford (UK).

30. HARRIS J. and STEVENSON A. (1986), *Rubber Chemistry and Technology* **59**, 740-764. On the role of non-linearity in the dynamic behaviour of rubber components.

31. HARRIS J. A. (1987), *Rubber Chemistry and Technology* **60**, 870-887. Dynamic testing under non-sinusoidal conditions and the consequences of non-linearity on service performance.

32. HASSAN A. (1994a), *Journal of Sound and Vibration* **178**(1), 1-19. Use of transformations with the higher order method of multiple scales to determine the steady state periodic response of harmonically excited nonlinear oscillators, Part I: Transformation of derivative.

33. HASSAN A. (1994b), *Journal of Sound and Vibration* **178**(1), 21-40. Use of transformations with the higher order method of multiple scales to determine the steady state periodic response of harmonically excited nonlinear oscillators, Part II: Transformation of detuning.

34. HASSAN A. (1995), *Journal of Sound and Vibration* **184**(5), 907-928. A second comparison of two higher order perturbation schemes.

35. HE J. H. (1999), *Computer Methods in Applied Mechanics and Engineering* **178**, 257-262. Homotopy perturbation technique.

36. HE J. H. (2000), *International Journal of Non-Linear Mechanics* **35**, 37-43. A coupling method of homotopy technique and perturbation technique for non-linear problems.

37. HUBIGER B., DOEMER R., HENG H. and MARIENSSEN W. (1994), *International Journal of Bifurcation and Chaos in Applied Sciences and Engineering* **4**, 773-784. Approaching nonlinear dynamics by studying the motion of a pendulum, III: Predictability and chaotic motion.

38. HUGHES T. (1987), *The Finite Element Method – Linear Static and Dynamic Finite Element Analysis.* Prentice Hall, Inc.: Englewood Cliffs, N.J.

39. JORDAN D. W. and SMITH P. (1977), *Nonlinear Ordinary Differential Equations.* Oxford Applied Mathematics and Computing Science Series, Oxford University Press: Oxford (UK).

40. JERRELIND J. and STENSSON A. (2000), *Chaos, Solitons and Fractals* **11**(15), 2413-2428. Nonlinear dynamics of parts in engineering systems. doi:10.1016/S0960-0779(00)00016-3

41. JEZEQUEL L., SETIO H. D. and SETIO S. (1990), *Proceedings of the 8th IMAC Conference, 29 January – 1 February, Orlando Florida (USA)*, 334-340. Non-linear modal synthesis in frequency domain.

42. KAMAT M. P. (1988), *ASCE Journal of Aerospace Engineering.* **1**(1), 52-62. Active control of structures in nonlinear response.

43. KAPITANIAK T. (1993), *Physical Review E* **47**(5). R2975-R2978. Transition to hyperchaos in chaotically forced coupled oscillators.

44. KHANIN R. and CARTMELL M. P. (1999), *Mathematica in Education and Research* **8**(2), 19-26. Applying the perturbation method of multiple scales.

45. KHANIN R., CARTMELL M. P. and GILBERT A. (2000), *Computers and Structures* **76**(5), 565-575. A computerised implementation of the multiple scales perturbation method using *Mathematica*.

46. KHANIN R. and CARTMELL M. P. (2001), *Journal of Symbolic Computation* **31**(4), 461-473. Parallelization of perturbation analysis: Application to large-scale engineering problems. doi: 10.1006/jsco.1999.0434

See Cartmell *et al.* (2002) and Warmiński J. A. *et al.* (2003).

47. KOZLOWSKI J., PARLITZ U. and LAUTERBORN W. (1995), *Physical Review E* **51**(3), 1861-1867. Bifurcation analysis of two coupled periodically driven Duffing oscillators.

48. KUO S. M. and MORGAN D. R. (1996), *Active Noise Control Systems: Algorithms and DSP Implementations.* John Wiley and Sons: New York.

49. KUO S. M. and MORGAN D. R. (1999), *Proceedings of the IEEE* **87**(6), 943-973. Active noise control: A tutorial review.

50. LAU S. L. and CHEUNG Y. K. (1981), *Transactions of the ASME, Journal of Applied Mechanics* **48**, 959-964. Amplitude incremental variational principle for nonlinear vibration of elastic systems.

51. LAU S. L., CHEUNG Y. K. and WU S. Y. (1982), *Transactions of the ASME, Journal of Applied Mechanics* **49**, 849-853. A variable parameter incrementation method for dynamic instability of linear and nonlinear elastic systems.

52. LEE C. L. and LEE C. –T (1997), *Journal of Sound and Vibration* **202**(2), 284-287. A higher order method of multiple scales.

53. LEE W. K. and Park H. D. (1999), *International Journal of Non-Linear Mechanics* **34**, 749-757. Second-order approximation for chaotic responses of a harmonically excited spring-pendulum system.

54. LORENZ E. N. (1963), *Journal of Atmospheric Sciences* **20**(2), 130-141. Deterministic nonperiodic flow.

55. LUCAS M. and SMITH A. C. (1994), *Recent Advances in Experimental Mechanics - Proceedings of the 10th International Conference on Experimental Mechanics, 18 – 22 July, Lisbon (Portugal)*, 625-630. The design of large ultrasonic resonators.

56. LUCAS M., GRAHAM G. and SMITH A. C. (1996), *Ultrasonics* **34**, 205-211. Enhanced vibration control of an ultrasonic cutting process. doi:10.1016/0041-624X(95)00079-I

57. LUCAS M., PETZING J. N. and SMITH A. C. (1998), *Experimental Mechanics - Proceedings of the 11th International Conference on Experimental Mechanics, 24 – 28 August, Oxford (UK)*, 945-949. Experimental characterisation of nonlinear vibration in ultrasonic tools.

58. Lucas M., Petzing J. N., Cardoni A. and Smith, L. J. (2001), *Annals of the CIRP* **50**(1), 149-152. Design and Characterisation of Ultrasonic Cutting Tools.

See Cardoni A. (2002), Graham G. *et al.* (1999a, 1999b), Smith A. C. *et al.* (1996).

59. LUEG P. (1936), *U.S. Patent 2,043,416*, June 9. Process of silencing sound oscillations.

60. LUONGO A., REGA G. and VESTRONI F. (1986), *Journal of Applied Mechanics* **53**(3), 619-624. On nonlinear dynamics of planar shear indeformable beams.

61. LUONGO A. and PAOLONE A. (1999), *Nonlinear Dynamics* **19**, 133-156. On the reconstitution problem in the multiple time-scale method.

62. MACCARI A. (2003), *Journal of Sound and Vibration* **259**(4), 967-976. Multiple external excitations for two non-linearly coupled Van der Pol Oscillators.

63. MAESTRELLO L. (2001), *Journal of Sound and Vibration* **239**(4), 873-883. The influence of initial forcing on non-linear control. doi: 10.1006/jsvi.2000.3222

See Chow P. L. (2001).

64. MAJED R. and RAYNAUD J. L. (2003), *Journal of Sound and Vibration* **260**(5), 847-866. Analysis of a non-linear structure by considering two non-linear formulations. doi:10.1016/S0022-460X(02)00930-6

65. MALLIK A. K., KHER V., PURI M. and HATWAL H. (1999), *Journal of Sound and Vibration* **219**(2), 239-253. On the modelling of non-linear elastomeric vibration isolators. doi:10.1006/jsvi.1998.1883

See Chakraborty G. (1998), Ravindra B. (1995), Shekhar N. *et al.* (1998, 1999).

66. MASRI S. F., BEKEY G. A. and CAUGHEY T. K. (1981), *Transactions of the ASME, Journal of Applied Mechanics* **48**, 619-626. Optimum pulse control of flexible structures.

67. MASRI S. F., BEKEY G. A. and CAUGHEY T. K. (1982), *Transactions of the ASME, Journal of Applied Mechanics* **49**, 877-884. On-line control of nonlinear flexible structures.

68. MOON FRANCIS C. (1992), *Chaotic and Fractal Dynamics – An Introduction for Applied Scientists and Engineers*. John Wiley and Sons.

69. MOROZOV A. D. (1976), *Differential Equations* **12**, 164-174. A complete qualitative investigation of Duffing's equation.

70. MURDOCK J. A. (1999), *Perturbations: Theory and Methods.* SIAM: Philadelphia.

71. NAGARAJAIAH S. M., RILEY M. A. and REINHORN M. A. (1993), *ASCE Journal of Engineering Mechanics* **119**(11), 2317-2332. Hybrid control of sliding isolated bridges.

See Riley M. A. *et al.* (1993).

72. NAYFEH A. H. (1965a), *Journal of Mathematical Physics* **44**, 368-374. A perturbation method for treating nonlinear oscillation problems.

73. NAYFEH A. H. (1965b), *Physics of Fluids* **8**, 1896-1898. Nonlinear oscillations in a hot electron plasma.

74. NAYFEH A. H. (1968), *IEEE Trans. Circuit Theory* **15**(3), 192-200. Forced oscillations of the Van der Pol oscillator with delayed amplitude limiting.

75. NAYFEH A. H. (1973), *Perturbation Methods*. Wiley: New York.

76. NAYFEH A. H. and MOOK D. T. (1979), *Nonlinear Oscillations*. Wiley: New York.

77. NAYFEH A. H. and SANCHEZ N. E. (1989), *International Journal of Non-Linear Mechanics* **24**(6), 483-497. Bifurcations in a forced softening Duffing oscillator. doi:10.1016/0020-7462(89)90014-0

78. NAYFEH A. H. and BALACHANDRAN B. (1995), *Applied Nonlinear Dynamics: Analytical, Computational and Experimental Methods.* Wiley: New York.

79. NAYFEH A. H., CHIN C-M and PRATT J. (1997), *Journal of Manufacturing Science and Engineering* **119**, 485-493. Perturbation methods in nonlinear dynamics – Applications to machining dynamics.

See Abdel-Rohman M. (1987).

80. NERVES A. C., KRISHNAN R. and SINGH M. P. (1995), *Proceedings of 10th Engng Mech. Specialty Conf. ASCE Vol. 2, Boulder (Colorado)*, 1054-1057. Modeling, simulation and analysis of active control of structures with nonlinearity using neural networks.

81. NEWMARK N. M. (1959), *Journal of Engineering Mechanics Division ASCE* **85**(EM3), 67-94. A method of computation for structural dynamics.

82. NUSSE H. E. and YORKE J. A. (1994), *Dynamics: Numerical Explorations.* Springer-Verlag: New York.

83. NUSSE H. E., OTT E. and YORKE J. A. (1994), *Physical Review E* **49**(2), 1073-1076. Border-collision bifurcations: An explanation for observed bifurcation phenomena.

84. NUSSE H. E., OTT E. and YORKE J. A. (1995), *Physical Review Letters* **75**(13), 2482-2485. Saddle-node bifurcations on fractal basin boundaries.

85. NUSSE H. E. and YORKE J. A. (1998), *Dynamics: Numerical Explorations (2nd Edition).* Springer-Verlag: New York.

See Chin *et al.* (1994)

86. O'SULLIVAN J. A. and SAIN M. K. (1985), *Proceedings of American Control Conference*, 1600-1605. Nonlinear optimal control with tensors: Some computational issues.

87. OTT E., GREBOGI C. and YORKE J. A. (1990), *Physical Review Letters* **64**(11), 1196-1199. Controlling chaos. doi:10.1103/PhysRevLett.64.1196

See Chin *et al.* (1994).

88. PENNEY D. E. and EDWARDS C. H. (1999), *Differential Equations and Boundary Value Problems: Computing and Modeling (2nd Edition).* Prentice-Hall: New Jersey, pp194-195. Period doubling and chaos in mechanical systems.

89. PEZESHKI C. and DOWELL E. H. (1988), *Physica D* **32**, 194-209. On chaos and fractal behaviour in a generalized Duffing's system.

90. PIERRE C. and DOWELL E. H. (1985), *Transactions of the ASME, Journal of Applied Mechanics* **52**, 693-697. A study of dynamic instability of plates by an extended incremental harmonic balance method.

91. PIERRE C., FERRI A. A. and DOWELL E. H. (1985), *Transactions of the ASME, Journal of Applied Mechanics* **52**, 958-964. Multi-harmonic analysis of dry friction damped systems using an incremental harmonic balance method.

92. PRESS W. H., FLANNERY B. P., TEUKOLSKY S. A. and VETTERLING W. T. (1992), *Numerical Recipes in FOTRAN: The Art of Scientific Computing, 2nd Edition*. Cambridge University Press: England, pp. 740-744. Multistep, multivalue, and predictor-corrector Methods.

93. PYRAGAS K. and TAMAŠEVIČIUS A. (1993), *Physics Letters* **A180**, 99-102. Experimental control of chaos by delayed self-controlling feedback. doi:10.1016/0375-9601(93)90501-P

94. RAHMAN Z. and BURTON T. D. (1986), *Journal of Sound and Vibration* **110**(3), 363-380. Large amplitude primary and superharmonic resonances in the Duffing oscillator.

95. RAHMAN Z. and BURTON T. D. (1989), *Journal of Sound and Vibration* **133**(3), 369-379. On higher order methods of multiple scales in non-linear oscillators – Periodic steady state response.

96. RAJ S. P. and RAJASEKAR S. (1997), *Physical Review E* **55**(5), 6237-6240. Migration control in two coupled Duffing oscillators.

97. RAND R. H. and HOLMES P. J. (1980), *International Journal of Non-Linear Mechanics* **15**, 387-399. Bifurcation of periodic motions in two weakly coupled Van der Pol oscillators.

See Chakraborty T. (1988).

98. RAVINDRA B. and MALLIK A. K. (1995), *Journal of Sound and Vibration* **182**(3), 345-353. Chaotic response of a harmonically excited mass on an isolator with non-linear stiffness and damping characteristics. doi:10.1006/jsvi.1995.0203

99. REINHORN A. M., MANOLIS G. D. and WEN C. Y. (1987a), *ASCE Journal of Engineering Mechanics* **113**, 315-333. Active control of inelastic structures.

100. REINHORN A. M., SOONG T. T. and WEN C. Y. (1987b), *ASME Recent Advances in Design, Analysis, Testing and Qualification Methods, PVP* **127**, 413-419. Base-isolated structures with active control.

101. REINHORN A. M., SUBRAMANIAM R., NAGARAJAIAH S. M. and RILEY M. A. (1993), *Proceedings of International Workshop on Structural Control and Intelligent System, Honolulu (HI)*, 405-416. Study of hybrid systems for structural and non-structural systems.

See Nagarajaiah S. M. *et al.* (1993), Riley M. A. *et al.* (1993).

102. RILEY M. A., SUBRAMANIAM R., NAGARAJAIAH S. M. and REINHORN M. A. (1993), *Proceedings ATC-17-1 Seminar on Seismic Isolation, Passive Energy Dissipation and Active Control, San Francisco (CA)*, 799-810. Hybrid control for sliding based-isolated structures.

103. RÖSSLER O. E. (1976), *Physics Letters* **57A**(5), 397-398. An equation for continuous chaos. doi: 10.1016/0375-9601(76)90101-8

104. SANDERS J. A. and VERHULST F. (1985), *Averaging Methods in Nonlinear Dynamical Systems*. Applied Mathematical Sciences, Vol. 59, Springer-Verlag: New York.

105. SANDRI G. (1965), *Nuovo Cimento* **B36**, 67-93. A new method of expansion in mathematical physics.

106. SANDRI G. (1967), In *Nonlinear Partial Differential Equations: A Symposium on Methods of Solutions (Edited by Ames W. F.)*, Academic: New York, pp. 259-277. Uniformization of asymptotic expansions.

107. SATO S., SANO M. and SAWADA Y. (1983), *Physical Review A* **28**(3), 1654-1658. Universal scaling property in bifurcation structure of Duffing's and of generalized Duffing's equations.

108. SCHEFFCZYK C. PARLITZ U., KURZ T., KNOP W. and LAUTERBORN W. (1991), *Physical Review A* **43**(12), 6495-6502. Comparison of bifurcation structures of driven dissipative nonlinear oscillators.

109. SHEFER M. and BREAKWELL J. V. (1987), *Journal of Optimization Theory and Applications* **53**, 1-7. Estimation and control with cubic nonlinearities.

110. SHELLABEAR M. C. and TYRER J. R. (1989), *Stress and Vibrations – Proc. SPIE* **1084**, 252-261. Three-dimensional analysis of volume vibrations by electronic speckle pattern interferometry.

111. SHELLABEAR M. C. and TYRER J. R. (1991), *Optics and Lasers in Engineering* **15**, 43-56. Application of ESPI to three-dimensional vibration measurements.

112. SHEKHAR N. CHANDRA, HATWAL H. and MALLIK A. K. (1998), *Journal of Sound and Vibration* **214**(4), 589-603. Response of non-linear dissipative shock isolators. doi:10.1006/jsvi.1997.1468

113. SHEKHAR N. CHANDRA, HATWAL H. and MALLIK A. K. (1999), *Journal of Sound and Vibration* **227**(2), 293-307. Performance of non-linear isolators and absorbers to shock excitations. doi:10.1006/jsvi.1999.2346

114. SHING P. B., DIXON M., KERMICHE N., SU R. and FRANGOPOL D. M. (1995), *Proceedings of 10th Engng Mech. Specialty Conf. ASCE Vol. 2, Boulder (Colorado)*, 1235-1238. Design of hybrid control systems for building structures.

115. SINGER J., WANG Y-Z and BAU HAIM H. (1991), *Physical Review Letters* **66**(9), 1123-1125. Controlling a chaotic system.

116. SITTIG E. K., WARNER A. W. and COOK H. D. (1969), *Ultrasonics* **7**(2), 108-112. Bonded piezoelectric transducers for frequencies beyond 100MHz.

117. SMITH A. C., NURSE A., GRAHAM G. and LUCAS M. (1996), *Ultrasonics* **34**, 197-203. Ultrasonic cutting – A fracture mechanics model. doi:10.1016/0041-624X(95)00078-H

See Lucas (1994) and Lucas *et al.* (1996, 1998).

118. SOLIMAN M. S. (1997), *Journal of Sound and Vibration* **207**(3), 383-392. Non-linear vibrations of hardening systems: Chaotic dynamics and unpredictable jumps to and from resonance. doi:10.1006/jsvi.1997.1095

119. STROGATZ S. H. (1994), *Nonlinear Dynamics and Chaos (With Applications to Physics, Biology, Chemistry and Engineering)*. Addison-Wesley Publishing Company: Reading (MA).

120. STURROCK P. A. (1957), *Proc. Roy. Soc. London* **A242**, 277-299. Nonlinear effects in electron plasmas.

121. STURROCK P. A. (1963), *Stanford University Microwave Laboratory Rept.,* No. 1004. Nonlinear theory of electromagnetic waves in plasmas.

122. SUHARDJO J., SPENCER B. F. JR. and SAIN M. K. (1992), *International Journal of Non-Linear Mechanics* **27**(2), 157-172. Non-linear optimal control of Duffing system.

123. TAN B. C. (2002), *Experimental Testing of Nonlinearity in a Dynamically Coupled Oscillator*, University of Glasgow Final Year Project Report.

124. THOMPSON J. M. T. and STEWART H. B. (1986), *Nonlinear Dynamics and Chaos*. John Wiley and Sons.

125. THOMSEN J. J. (1997), *Vibrations and Stability – Order and Chaos*. McGraw-Hill: UK.

126. TOMLINSON G. R. and WORDEN K. (2000), *Nonlinearity in Structural Dynamics: Detection, Identification and Modelling*. The Institute of Physics: Philadelphia.

127. UEDA Y. (1979), *Journal of Statistical Physics* **20**(2), 181-196. Randomly transitional phenomena in the system governed by Duffing's equation.

128. UEDA Y. (1980a), in *New Approaches to Nonlinear Problems in Dynamics* (P. J. Holmes, editor). Philadelphia: SIAM, 311-322. Steady motions exhibited by Duffing's equation: A picture book of regular and chaotic motions.

129. UEDA Y. (1980b), *Annals New York Academy Sciences* **357**, 422-434. Explosion of strange attractors exhibited by Duffing's equation.

130. UMBERGER D. K., GREBOGI C, OTT E. and AFEYAN B. (1989), *Physical Review A* **39**(9), 4835-4842. Spatiotemporal dynamics in a dispersively coupled chain of nonlinear oscillators.

131. VAN DER POL B. (1927a), *Philosophical Magazine* **7**, 65-80. Forced oscillations in a system with nonlinear resistance.

132. VAN DER POL B. and VAN DER MARK J. (1927b), *Nature* **120**(3019), 363-364. Frequency demultiplication.

133. WARMIŃSKI J. A. (2001), *Drgania Regularne | Chaotyczne*. Politechnika Lubelska, Lubin (Poland) – in Polish.

134. WARMIŃSKI J. A., LITAK G., CARTMELL M. P., KHANIN R. and WIERCIGROCH M. (2003), *Journal of Sound and Vibration* **259**(4), 917-933. Approximate analytical solutions for primary chatter in the non-linear metal cutting model. doi:10.1006/jsvi.2002.5129

135. WILSON E. L. and CLOUGH R. W. (1962), *Proceedings, Symposium on the Use of Computers in Civil Engineering, Laboratorio Nacional de Engenharia Civil, 1 – 5 October, Lisbon (Portugal)*, 45.1 – 45.14. Dynamic response by step-by-step matrix analysis.

136. WILSON E. L., FARHOOMAND I. and BATHE K. J. (1973), *Earthquake Engineering and Structural Dynamics,* **1**, 241-252. Nonlinear dynamic analysis of complex structures.

137. WOAFO P., FOTSIN H. B. and CHEDJOU J. C. (1998), *Physica Scripta* **57**, 195-200. Dynamics of two nonlinearly coupled oscillators.

138. WOLFRAM S. (1996), *The Mathematica Book, 3rd Edition.* Wolfram Media and Cambridge University Press.

139. YANG J. N., LI Z., WU J. C. and HSU I. R. (1994a), *ASCE Journal of Engineering Mechanics* **16**(6), 437-444. Dynamic linearization for sliding isolated building.

140. YANG J. N., LI Z. and VONGCHAVALITKUL S. (1994b), *ASCE Journal of Engineering Mechanics* **120**(2), 266-283. A generalization of optimal control theory: linear and nonlinear control.

141. YANG J. N., WU J. C., AGRAWAL A. K. and LI Z. (1994c), *National Center for Earthquake Engineering Research, Technical Report NCEER-94-0017.* Sliding mode control of seismic-excited linear and nonlinear civil engineering structures.

See Agrawal A. K. (1995, 1998).

PUBLICATIONS

Journal Papers :

1) **Lim F. C. N.**, Cartmell M. P., Cardoni A. and Lucas M., "A Preliminary Investigation into Optimising the Response of Vibrating Systems used for Ultrasonic Cutting", *accepted by the Journal of Sound and Vibration – Dec 2002.*

2) Cardoni A., Lucas M., Cartmell M. P. and **Lim F. C. N.**, "A Novel Multiple Blade Ultrasonic Cutting Device", *accepted by Ultrasonics International '03*, July 2003, Granada (Spain).

3) Lucas M., Cardoni A., **Lim F. C. N.** and Cartmell M. P., "Effects of Modal Interactions on Vibration Performance in Ultrasonic Cutting", *accepted by CIRP Annual Congress (Annals of CIRP)*, August 2003, Montreal (Canada).

Conference Publications :

4) Cardoni A., **Lim F. C. N.**, Lucas M. and Cartmell M. P., "Characterising Modal Interactions in an Ultrasonic Cutting System", *Proceedings of the 3rd EAA European Congress on Acoustics (Forum Acusticum 2002)*, 16 – 20 September 2002, Sevilla (Spain). – Invited Paper

5) Lucas M., Cardoni A., Cartmell M. P. and **Lim F.**, "Experimental and Computational Modelling of Vibration Performance of Ultrasonic Tools for Manufacturing Applications", *32nd Ultrasonics Industries Association Symposium*, 21 – 23 October 2002, New York (USA).

6) Cartmell M. P., **Lim F. C. N.**, Cardoni A. and Lucas M., "Optimisation of the Vibrational Response of Ultrasonic Cutting Systems", *accepted by Proceedings of the Institute of Mathematics and its Application, Bifurcations: The Use and Control of Chaos*, 28 – 30 July 2003, Southampton (UK).

7) Lucas M., Cardoni A., Cartmell M. P. and **Lim F. C. N.**, "Controlling the Effects of Modal Interactions in Ultrasonic Cutting Devices", *accepted by World Congress on Ultrasonics*, September 2003, Paris (France). – Invited Paper

8) Cardoni A., Lucas M., Cartmell M. P. and **Lim F. C. N.**, "Nonlinear and Parametric Vibrations in Ultrasonic Cutting Systems", *accepted by Proceedings of the 5th International Conference on Modern Practice in Stress and Vibration Analysis - Institute of Physics, Stress and Vibration Group*, 09 – 11 September 2003, Glasgow (UK).

GLOSSARY

A

anharmonic: not harmonic.

antinode: a position in a standing wave pattern of maximum amplitude of vibration.

arbitrary value: one to which any value can be assigned at pleasure.

asymptotic: approaching a value or curve arbitrarily closely (i.e., as some sort of limit is taken). A curve A which is asymptotic to given curve C is called the asymptote of C. Hardy and Wright (1979, p. 7) use the symbol $\asymp$ to denote that one quantity is asymptotic to another. If $f \asymp \phi$, then Hardy and Wright say that f and ϕ are of the same order of magnitude.

attractor: a set of points or a subspace in phase space toward which a time history approaches after transients die out. For example, equilibrium points or fixed points in maps, limit cycles, or a toroidal surface for quasiperiodic motions are all classical dynamical attractors.

attractor, chaotic: when the attractor is sensitive to initial data. It contains a chaotic trajectory (a trajectory with a positive Lyapunov exponent). Generally may have very complicated structure, except for one dimensional maps. – emphasizing complicated dynamics.

attractor, strange: introduced by Ruelle and Takens (1971), was defined to mean an attractor with a very complicated geometric structure. – emphasizing complicated geometry. Primarily, it is the same as *chaotic attractor*.

autonomous: the independent variable time, t does not appear explicitly in the equation and only as a differential dt, the system is called *autonomous*.

autoparametric system: system that has an internal coupling involving at least two modes, where one is a forced response which parametrically excites the other. From a mathematical point of view, this coupling comes about due to non-linear coupling terms in the equations of motion.

B

basin of attraction: a set of initial conditions in phase space which leads to a particular long-time motion or attractor. Usually this set of points is connected and forms a continuous subspace in phase space. However, the boundary between different basins of attraction may or may not be smooth.

bifurcation: a qualitative change in dynamics upon a small variation in the parameters of a system.
bifurcation, Hopf: The emergence of a limit cycle oscillation from an equilibrium state as some system parameter is varied. Named after a mathematician who gave precise conditions for its existence in a dynamical system.
bifurcation theory: a methodology for studying how solutions of a nonlinear problem and their stability change as the parameters varies.
bifurcation value (critical value): the values of parameters at which the qualitative or topological nature of motion changes.

C

chaotic: denotes a type of motion that is sensitive to changes in initial conditions. A motion for which trajectories starting from slightly different initial conditions diverge exponentially. A motion with positive Lyapunov exponent.

circle map: this is a map or difference equation that maps points on a circle onto the original circle. In the theory of two coupled oscillators, some motions in phase space can be viewed as motion on a toroidal surface. A Poincare section that intersects the smaller diameter of the torus constitutes a circle map.

compliance: the degree to which a system is displaced or compressed per unit of applied force: the reciprocal of stiffness.

D

damping, C: any method of dissipating vibration energy within a vibrating system.

damping ratio, ζ: the ratio of the actual damping in a system to the critical damping, at a resonant frequency; $\zeta = C/C_c$.

degree-of-freedom: the number of degrees of freedom in a problem, distribution, etc., is the number of parameters which may be independently varied.

deterministic: refers to a dynamic system whose equations of motion, parameters and initial conditions are known and are not stochastic or random. However, deterministic systems may be motions that appear random.

differential equation:

ordinary differential equation: expressed in terms of ordinary derivatives of the dependent variable x with respect to the independent variable t.

duffing's equation: a second-order differential equation with a cubic nonlinearity and harmonic forcing $\ddot{x} + c\dot{x} + bx + ax^3 = f_0 \, Cos \, \omega t$. Named after G. Duffing (circa 1918).

E

equilibrium point: in a continuous dynamical system, a point in phase space toward which a solution may approach as transients decay $(t \to \infty)$. In mechanical systems, this usually means a state of zero acceleration and velocity. For maps, equilibrium points may come in a finite set where the system visits each point in a sequential manner as the map or difference equation is iterated. (Also called a *fixed point*.)

excitation:

external-excitation:

parametric-excitation: the external excitation acts through a parameter of a system (e.g. stiffness, damping parameter)

self-excitation:

F

fixed point: see *equilibrium point*.

fractal: a geometric property of a set of points in an n-dimensional space having the quality of self-similarity at different length scales and having a noninteger fractal dimension less than n.

fractal dimension: a quantitative property of a set of points in an n-dimensional space which measures the extent to which the points fill a subspace as the number of points becomes very large.

H

heteroclinic orbit: an orbit in a map that occurs when stable and unstable orbits from different saddle points intersect.

homoclinic orbit: an orbit in a map that occurs when stable and unstable manifolds of a saddle point intersect.

homogeneous: each term contains x or one of its derivatives.

Hopf bifurcation: see *bifurcation, Hopf.*

hyperchaos: a dynamic system where the phase space is stretched in two or more directions (i.e., two or more positive Lyapunov exponents).

I

intermittency: a type of chaotic motion in which long time intervals of regular, periodic, or stationary dynamical motion are followed by short bursts of random-like motion. The time interval between bursts is not fixed but is unpredictable.

invariant: not varying, constant.

J

jump phenomenon: an abrupt change in the amplitude and phase of the steady-state response due to a small change in the excitation.

L

limit cycle: A periodic motion that arises from a self-excited or autonomous system.

linear: there are no non-linear terms in x or its derivatives.

Lorenz equations: A set of three first order autonomous differential equations that exhibit chaotic solutions. The equations were derived and studied by E. N. Lorenz in 1963 as a model for

atmospheric convection. This set of equations is one of the principal paradigms for chaotic dynamics.

Lyapunov dimension: sometimes called the Kaplan-Yorke conjecture/dimension. Lyapunov dimension of an attractor is defined to be $k+\left(\lambda_1+\lambda_2+\cdots+\lambda_k\right)/\lambda_{k+1}$ where k is the maximum value of I for which $\lambda_1+\cdots+\lambda_i\rangle 0$

Lyapunov exponent: number that measure the exponential attraction or separation in time of two adjacent trajectories in phase space with different initial conditions. A positive Lyapunov exponent indicates a chaotic motion in a dynamical system with bounded trajectories. Named after the dynamicist Lyapunov (1857 – 1918) (in some books spelled Liapunov). The Lyapunov exponent (λ) is defined by taking the natural log of the Lyapunov number, as follows,

$$\lambda=\lim_{\substack{t\to\infty\\ |\Delta x_0|\to 0}}\frac{1}{t}\ln\frac{\left|\Delta x\left(X_0,t\right)\right|}{\left|\Delta x_0\right|}$$

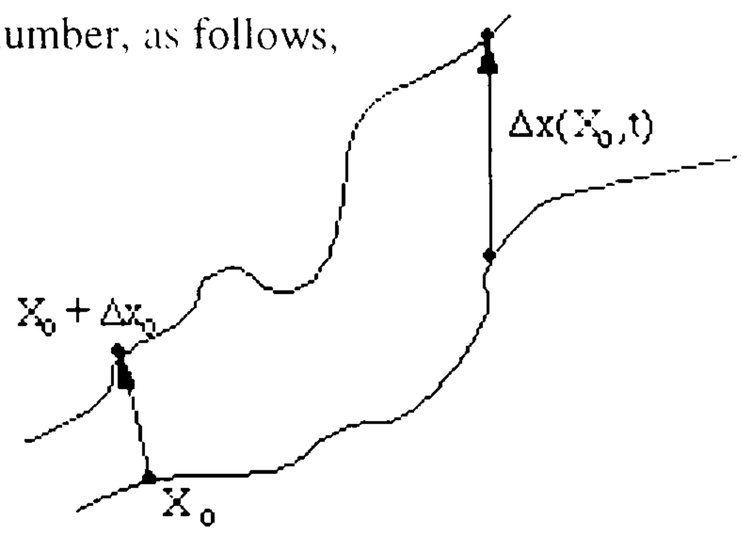

Lyapunov number: the measure (the ratio) of how fast two nearby points move apart after the first n iterations.

M

manifold: a subspace of phase space in which solutions with initial conditions in the manifold stay in the manifold or subspace, under the action of the differential or difference equations.

map, mapping: a mathematical rule that takes a collection of points in some n-dimensional space and maps them into another set of points. When this rule is iterated, a map is similar to a set of difference equations.

N

noise: in experiments, noise usually denotes the small random background disturbance of either mechanical, thermal, or electrical origin.

node: a position in a standing wave pattern of minimum amplitude of vibration.

nonlinear: a property of an input-output system or mathematical operation for which the output is not linearly proportional to the input.

O

ordinary differential equation: see *differential equation*

P

period doubling: refers to a sequence of periodic vibrations in which the period doubles as some parameter is varied. In the classic model, these frequency halving bifurcations occur at small and smaller intervals of the control parameter. Beyond a critical accumulation parameter, chaotic vibrations occur.

phase:

phase plane: usually plotted as velocity vs displacement graph. Time is implicit.

phase space: in mechanics, phase space is an abstract mathematical space whose coordinates are generalized coordinates and generalized momentum. In dynamical systems, governed by a set of first order evolution equations, the coordinates are the state variables or components of the state vector.

phase trajectory: the solution curve in a phase plane – always in a clockwise direction and crosses x- axis perpendicularly. (also known as *orbit* or *integral curve*)

Poincaré map (section): the sequence of points in phase space generated by the penetration of a continuous evolution trajectory through a generalized surface or plane in the space. For a periodically forced, second-order nonlinear oscillator, a Poincaré map can be obtained by stroboscopically observing the position and velocity at a particular phase of the forcing function (H. Poincaré, 1854-1912).

Q

quasiperiodic: a vibration motion consisting of two or more incommensurate (i.e. not proportional) frequencies. When the difference between driving and free oscillation frequencies is large. (a.k.a. *almost periodic*). They are not periodic and they may be mistaken for chaotic solutions, which they are not.

quenching: process of increasing the amplitude of excitation until the free-oscillation term decays. (Nayfeh, pg 17)

R

resonance:

external resonance: a system which has the external frequency in the neighbourhood of one of the linear natural frequencies.

S

saddle points: in the geometric theory of ordinary differential equations, an equilibrium point with real eigenvalues with at least one positive and one negative eigenvalue.

semitrivial solution: a secondary system is coupled to the primary system in a nonlinear way (i.e. autoparametric systems), but such that the secondary system can be at rest while the primary system is vibrating.

stochastic process: often refers to a type of chaotic motion found in conservative or non dissipative dynamical systems.

strange attractor: refers to the attracting set in phase space on which chaotic orbits move. An attractor that is not an equilibrium point nor a limit cycle, nor a quasiperiodic attractor. An attractor in phase space with fractal dimension.

T

transient chaos: a term describing motion that looks chaotic during a finite time: that is, it appears to move on the strange attractor, but eventually settles into a periodic or quasiperiodic motion.

V

Van der Pol equation: A second order differential equation with linear restoring for and non linear damping which exhibits a limit cycle (named after B. Van der Pol, circa 1927)

Sources:

http://www.dictionary.com/

http://mathworld.wolfram.com/topics/Terminology.html

CONTENT OF APPENDICES

APPENDIX A

DERIVATION OF EIGENVALUES (I.E. UNDAMPED LINEAR NATURAL FREQUENCIES) AND EIGENVECTORS (I.E. MODES) OF SYSTEM

A.1 Eigenvalues

This section derives the undamped linear natural frequencies (i.e. eigenvalues) of the system.

2 equations that defined the unforced, undamped and linear system:

$$m_1 \ddot{x}_1 + (k_1 + k_2)x_1 - k_2 x_2 = 0 \qquad \textbf{(A.1-1)}$$

$$m_2 \ddot{x}_2 - k_2 x_1 + k_2 x_2 = 0 \qquad \textbf{(A.1-2)}$$

To find natural frequencies, assume the motion of each mass to be harmonic.

Let :

$$x_1 = A_1 \, Sin \, \omega_e t \quad or \quad A_1 e^{i\omega_e t}$$

$$x_2 = A_2 \, Sin \, \omega_e t \quad or \quad A_2 e^{i\omega_e t}$$

where A_1 and A_2 are amplitudes and ω_e is the frequency in rad/s

Differentiating w.r.t. time

$$\dot{x}_1 = A_1 \omega_e \, Cos \, \omega_e t \qquad \dot{x}_2 = A_2 \omega_e \, Cos \, \omega_e t$$

$$\ddot{x}_1 = -A_1 \omega_e^2 \, Sin \, \omega_e t \qquad \ddot{x}_2 = -A_2 \omega_e^2 \, Sin \, \omega_e t$$

$$= -\omega_e^2 x_1 \qquad = -\omega_e^2 x_2$$

Substituting the above into Equation (A.1-1) and (A.1-2):

$$-m_1 A_1 \omega_e^{\,2} Sin\,\omega_e t + (k_1 + k_2) A_1 Sin\,\omega_e t - k_2 A_2 Sin\,\omega_e t = 0 \qquad \textbf{(A.1-3)}$$

$$-m_2 A_2 \omega_e^{\,2} Sin\,\omega_e t - k_2 A_1 Sin\,\omega_e t + k_2 A_2 Sin\,\omega_e t = 0 \qquad \textbf{(A.1-4)}$$

Dividing throughout by $Sin\,\omega_e t$:

$$(k_1 + k_2 - m_1 \omega_e^{\,2}) A_1 - k_2 A_2 = 0 \qquad \textbf{(A.1-5)}$$

$$-k_2 A_1 + (k_2 - m_2 \omega_e^{\,2}) A_2 = 0 \qquad \textbf{(A.1-6)}$$

For $A_1 \neq 0$ and $A_2 \neq 0$

Let the determinant of the above equations be zero

$$\begin{vmatrix} k_1 + k_2 - m_1 \omega_e^{\,2} & -k_2 \\ -k_2 & k_2 - m_2 \omega_e^{\,2} \end{vmatrix} = 0$$

$$(k_1 + k_2 - m_1 \omega_e^{\,2})(k_2 - m_2 \omega_e^{\,2}) - k_2^{\,2} = 0$$

$$k_1 k_2 - k_1 m_2 \omega_e^{\,2} + k_2^{\,2} - k_2 m_2 \omega_e^{\,2} - k_2 m_1 \omega_e^{\,2} + m_1 m_2 \omega_e^{\,4} - k_2^{\,2} = 0$$

$$m_1 m_2 \omega_e^{\,4} - (k_1 m_2 + k_2 m_2 + k_2 m_1) \omega_e^{\,2} + k_1 k_2 = 0$$

Let $\lambda = \omega_e^{\,2}$

$$m_1 m_2 \lambda^2 - (k_1 m_2 + k_2 m_2 + k_2 m_1) \lambda + k_1 k_2 = 0$$

$$\lambda^2 - \left(\frac{k_1}{m_1} + \frac{k_2}{m_1} + \frac{k_2}{m_2} \right) \lambda + \frac{k_1 k_2}{m_1 m_2} = 0$$

Let $\alpha_1 = \frac{k_1}{m_1}$, $\alpha_2 = \frac{k_2}{m_1}$ *and* $\alpha_3 = \frac{k_2}{m_2}$

$$\lambda^2 - (\alpha_1 + \alpha_2 + \alpha_3)\lambda + \alpha_1 \alpha_3 = 0$$

$$\lambda = \frac{(\alpha_1 + \alpha_2 + \alpha_3) \pm \sqrt{(\alpha_1 + \alpha_2 + \alpha_3)^2 - 4\alpha_1 \alpha_3}}{2}$$

$$\omega_e^2 = \frac{(\alpha_1 + \alpha_2 + \alpha_3) \pm \sqrt{\alpha_1^2 + \alpha_2^2 + \alpha_3^2 + 2\alpha_1 \alpha_2 + 2\alpha_2 \alpha_3 - 2\alpha_1 \alpha_3}}{2}$$

$$\therefore \quad \omega_{e1}^2 = \frac{(\alpha_1 + \alpha_2 + \alpha_3) - \sqrt{\alpha_1^2 + \alpha_2^2 + \alpha_3^2 + 2(\alpha_1 \alpha_2 + \alpha_2 \alpha_3 - \alpha_1 \alpha_3)}}{2}$$

$$\omega_{e2}^2 = \frac{(\alpha_1 + \alpha_2 + \alpha_3) + \sqrt{\alpha_1^2 + \alpha_2^2 + \alpha_3^2 + 2(\alpha_1 \alpha_2 + \alpha_2 \alpha_3 - \alpha_1 \alpha_3)}}{2}$$

Therefore, the natural frequencies of the system are:

$$\omega_{e1}^2 = \frac{1}{2}\left[\alpha_1 + \alpha_2 + \alpha_3 - \sqrt{\alpha_1^2 + 2\alpha_1(\alpha_2 - \alpha_3) + (\alpha_2 + \alpha_3)^2}\right] \qquad \textbf{(A.1-7)}$$

$$\omega_{e2}^2 = \frac{1}{2}\left[\alpha_1 + \alpha_2 + \alpha_3 + \sqrt{\alpha_1^2 + 2\alpha_1(\alpha_2 - \alpha_3) + (\alpha_2 + \alpha_3)^2}\right] \qquad \textbf{(A.1-8)}$$

A.2 Eigenvectors

From equations (A.1-5) and (A.1-6), two expressions for the ratio of the amplitudes are found:

$$\frac{A_1}{A_2} = \frac{k_2}{k_1 + k_2 - m_1 \omega_e^2} = \frac{k_2 - m_2 \omega_e^2}{k_2} \qquad \textbf{(A.2-1)}$$

Substitution of the natural frequencies in either of the above equations leads to the ratio of amplitudes.

For ω_{e1}^2, the amplitude ratio corresponding to the first natural frequency is:

$$\left(\frac{A_1}{A_2}\right)^{(1)} = \frac{k_2}{k_1 + k_2 - m_1 \omega_{e1}^2} \qquad \textbf{(A.2-2)}$$

For ω_{e2}^2, the amplitude ratio corresponding to the second natural frequency is:

$$\left(\frac{A_1}{A_2}\right)^{(2)} = \frac{k_2}{k_1 + k_2 - m_1 \omega_{e2}^2} \qquad \textbf{(A.2-3)}$$

APPENDIX B

VALIDATION OF EQUATIONS FOR HARMONIC SOLUTIONS

B.1 Validation of Equation (3.2-34)

From equation (3.2-34):

$$x_{10} = A_1(T_1)\, e^{i\omega_1 T_0} + \overline{A}_1(T_1)\, e^{-i\omega_1 T_0} \qquad \textbf{(3.2-34)}$$

From equation (3.2-26):

$$D_0^2 x_{10} + \gamma_1 x_{10} = 0 \qquad \textbf{(3.2-26)}$$

$$\begin{aligned} \therefore \quad D_0^2 x_{10} &= D_0^2 \left[A_1(T_1)\, e^{i\omega_1 T_0} + \overline{A}_1(T_1)\, e^{-i\omega_1 T_0} \right] \\ &= D_0 \left[i\omega_1 A_1(T_1)\, e^{i\omega_1 T_0} - i\omega_1 \overline{A}_1(T_1)\, e^{-i\omega_1 T_0} \right] \\ &= i^2 \omega_1^2 A_1(T_1)\, e^{i\omega_1 T_0} + i^2 \omega_1^2 \overline{A}_1(T_1)\, e^{-i\omega_1 T_0} \\ &= -\omega_1^2 A_1(T_1)\, e^{i\omega_1 T_0} - \omega_1^2 \overline{A}_1(T_1)\, e^{-i\omega_1 T_0} \end{aligned}$$

Substitute $D_0^2 x_{10}$ into (3.2-26):

$$-\omega_1^2 A_1(T_1)\, e^{i\omega_1 T_0} - \omega_1^2 \overline{A}_1(T_1)\, e^{-i\omega_1 T_0} + \omega_1^2 \left[A_1(T_1)\, e^{i\omega_1 T_0} + \overline{A}_1(T_1)\, e^{-i\omega_1 T_0} \right] = 0 \qquad \textbf{(B.1-1)}$$

L.H.S. = R.H.S.

B.2 Validation of Equation (3.2-35)

From equation (3.2-35):

$$x_{20} = A_2(T_1)\,e^{i\omega_2 T_0} + \overline{A}_2(T_1)\,e^{-i\omega_2 T_0} + A_3(T_1)\,e^{i\omega_1 T_0} + \overline{A}_3(T_1)\,e^{-i\omega_1 T_0} \qquad \textbf{(3.2-35)}$$

From equation (3.2-27):

$$D_0^2 x_{20} + \gamma_3 x_{20} - \gamma_3 x_{10} = 0 \qquad \textbf{(3.2-27)}$$

$$\begin{aligned}
\therefore \quad D_o^2 x_{20} &= D_0^2\left[A_2(T_1)\,e^{i\omega_2 T_0} + \overline{A}_2(T_1)\,e^{-i\omega_2 T_0} + A_3(T_1)\,e^{i\omega_1 T_0} + \overline{A}_3(T_1)\,e^{-i\omega_1 T_0}\right] \\
&= D_0\left[i\omega_2 A_2(T_1)\,e^{i\omega_2 T_0} - i\omega_2 \overline{A}_2(T_1)\,e^{-i\omega_2 T_0} + i\omega_1 A_3(T_1)\,e^{i\omega_1 T_0} - i\omega_1 \overline{A}_3(T_1)\,e^{-i\omega_1 T_0}\right] \\
&= i^2\omega_2^2 A_2(T_1)\,e^{i\omega_2 T_0} + i^2\omega_2^2 \overline{A}_2(T_1)\,e^{-i\omega_2 T_0} + i^2\omega_1^2 A_3(T_1)\,e^{i\omega_1 T_0} + i^2\omega_1^2 \overline{A}_3(T_1)\,e^{-i\omega_1 T_0} \\
&= -\omega_2^2 A_2(T_1)\,e^{i\omega_2 T_0} - \omega_2^2 \overline{A}_2(T_1)\,e^{-i\omega_2 T_0} - \omega_1^2 A_3(T_1)\,e^{i\omega_1 T_0} - \omega_1^2 \overline{A}_3(T_1)\,e^{-i\omega_1 T_0}
\end{aligned}$$

Substitute $D_o^2 x_{20}$ into (3.2-27):

$$D_0^2 x_{20} + \omega_2^2 x_{20} - \omega_2^2 x_{10} = 0$$

$$\begin{aligned}
&\left[-\omega_2^2 A_2(T_1)\,e^{i\omega_2 T_0} - \omega_2^2 \overline{A}_2(T_1)\,e^{-i\omega_2 T_0} - \omega_1^2 A_3(T_1)\,e^{i\omega_1 T_0} - \omega_1^2 \overline{A}_3(T_1)\,e^{-i\omega_1 T_0}\right] \\
&+\omega_2^2\left[A_2(T_1)\,e^{i\omega_2 T_0} + \overline{A}_2(T_1)\,e^{-i\omega_2 T_0} + A_3(T_1)\,e^{i\omega_1 T_0} + \overline{A}_3(T_1)\,e^{-i\omega_1 T_0}\right] \\
&-\omega_2^2\left[A_1(T_1)\,e^{i\omega_1 T_0} + \overline{A}_1(T_1)\,e^{-i\omega_1 T_0}\right] = 0
\end{aligned}$$

$$\begin{aligned}
&-\omega_1^2 A_3(T_1)\,e^{i\omega_1 T_0} - \omega_1^2 \overline{A}_3(T_1)\,e^{-i\omega_1 T_0} + \omega_2^2 A_3(T_1)\,e^{i\omega_1 T_0} + \omega_2^2 \overline{A}_3(T_1)\,e^{-i\omega_1 T_0} \\
&-\omega_2^2 A_1(T_1)\,e^{i\omega_1 T_0} - \omega_2^2 \overline{A}_1(T_1)\,e^{-i\omega_1 T_0} = 0
\end{aligned} \qquad \textbf{(B.2-1)}$$

Taking the conjugates of (B.2-1):

$$\begin{aligned}
-\omega_1^2 A_3(T_1)\,e^{i\omega_1 T_0} + \omega_2^2 A_3(T_1)\,e^{i\omega_1 T_0} - \omega_2^2 A_1(T_1)\,e^{i\omega_1 T_0} &= 0 \\
A_3(T_1)\left(\omega_2^2 - \omega_1^2\right) &= \omega_2^2 A_1(T_1) \\
A_3(T_1) &= \frac{\omega_2^2}{\omega_2^2 - \omega_1^2} A_1(T_1) \\
A_3(T_1) &= \Gamma A_1(T_1) \qquad \textbf{(B.2-2)}
\end{aligned}$$

where $$\Gamma = \frac{\omega_2^2}{\omega_2^2 - \omega_1^2} \qquad \textbf{(B.2-3)}$$

Likewise, taking the complex conjugates of (B.2-1):

$$
\begin{aligned}
-\omega_1^2 \overline{A}_3(T_1)\, e^{-i\omega_1 T_0} + \omega_2^2 \overline{A}_3(T_1)\, e^{-i\omega_1 T_0} - \omega_2^2 \overline{A}_1(T_1)\, e^{-i\omega_1 T_0} &= 0 \\
\overline{A}_3(T_1)\left(\omega_2^2 - \omega_1^2\right) &= \omega_2^2 \overline{A}_1(T_1) \\
\overline{A}_3(T_1) &= \frac{\omega_2^2}{\omega_2^2 - \omega_1^2}\, \overline{A}_1(T_1) \\
\overline{A}_3(T_1) &= \Gamma \overline{A}_1(T_1) \qquad \textbf{(B.2-4)}
\end{aligned}
$$

APPENDIX C

MATHEMATICA EVALUATIONS

C.1 Deriving the 'Always' Secular Terms for x_{11}

In[1]:=
$$x_{10} = A_1[T_1]\, e^{i\times\omega_1\times T_0} + \overline{A_1[T_1]}\, e^{-i\times\omega_1\times T_0};$$
$$x_{20} = A_2[T_1]\, e^{i\times\omega_2\times T_0} + \overline{A_2[T_1]}\, e^{-i\times\omega_2\times T_0} + A_3[T_1]\, e^{i\times\omega_1\times T_0} + \overline{A_3[T_1]}\, e^{-i\times\omega_1\times T_0};$$

In[3]:= `D[x10, T0]`

Out[3]=
$$-i\, e^{-i\,T_0\,\omega_1}\,\overline{A_1[T_1]}\,\omega_1 + i\, e^{i\,T_0\,\omega_1}\,\omega_1\,A_1[T_1]$$

In[4]:= `D[D[x10, T0], T1]`

Out[4]=
$$i\, e^{i\,T_0\,\omega_1}\,\omega_1\,A_1'[T_1] - i\, e^{-i\,T_0\,\omega_1}\,\omega_1\,\text{OverBar}'[A_1[T_1]]\,A_1'[T_1]$$

In[5]:= `D[x20, T0]`

Out[5]=
$$-i\, e^{-i\,T_0\,\omega_1}\,\overline{A_3[T_1]}\,\omega_1 - i\, e^{-i\,T_0\,\omega_2}\,\overline{A_2[T_1]}\,\omega_2 + i\, e^{i\,T_0\,\omega_2}\,\omega_2\,A_2[T_1] + i\, e^{i\,T_0\,\omega_1}\,\omega_1\,A_3[T_1]$$

In[6]:= `TrigToExp[F~ Cos[Ω t]]`

Out[6]=
$$\frac{1}{2}\, e^{-i\,t\,\Omega}\,\tilde{F} + \frac{1}{2}\, e^{i\,t\,\Omega}\,\tilde{F}$$

The above equation converts $\tilde{F}$ Cos Ω t into polar forms :

$$\tilde{F}\ \text{Cos}\ \Omega\ t = \frac{1}{2}\,\tilde{F}\, e^{i\,\Omega\,t} + \frac{1}{2}\,\tilde{F}\, e^{-i\,\Omega\,t}$$

From equation (3.3 - 19), $t \equiv T_0$

Let Right - Hand Side of equation (3.3 - 30) = RHS1

Substitute In[1] to In[6] into RHS1 :

In[7]:=
$$RHS1 = \frac{1}{2}\,\tilde{F}\, e^{i\,\Omega\,T_0} + \frac{1}{2}\,\tilde{F}\, e^{-i\,\Omega\,T_0} - 2\,D[D[x_{10}, T_0], T_1] - 2\,\tilde{\xi}_1\,D[x_{10}, T_0] - 2\,\tilde{\xi}_2\,D[x_{10}, T_0] + 2\,\tilde{\xi}_2\,D[x_{20}, T_0] - \tilde{\gamma}_2\,(x_{10}) + \tilde{\gamma}_2\,(x_{20}) - \tilde{\eta}_1 \times {x_{10}}^3 - \tilde{\eta}_2\,({x_{20}}^3 + 3\times {x_{10}}^2\times x_{20} - 3\times x_{10}\times {x_{20}}^2 - {x_{10}}^3)$$

```
Out[7]= 1/2 E^(-I Ω T0) F̃ + 1/2 E^(I Ω T0) F̃ - γ̃2 (E^(-I T0 ω1) Conjugate[A1[T1]] + E^(I T0 ω1) A1[T1]) -
 η̃1 (E^(-I T0 ω1) Conjugate[A1[T1]] + E^(I T0 ω1) A1[T1])^3 -
 2 ξ̃1 (-I E^(-I T0 ω1) Conjugate[A1[T1]] ω1 + I E^(I T0 ω1) ω1 A1[T1]) -
 2 ξ̃2 (-I E^(-I T0 ω1) Conjugate[A1[T1]] ω1 + I E^(I T0 ω1) ω1 A1[T1]) +
 γ̃2 (E^(-I T0 ω2) Conjugate[A2[T1]] + E^(-I T0 ω1) Conjugate[A3[T1]] + E^(I T0 ω2) A2[T1] + E^(I T0 ω1) A3[T1]) +
 2 ξ̃2 (-I E^(-I T0 ω1) Conjugate[A3[T1]] ω1 - I E^(-I T0 ω2) Conjugate[A2[T1]] ω2 + I E^(I T0 ω2) ω2 A2[T1] +
    I E^(I T0 ω1) ω1 A3[T1]) - η̃2 (-(E^(-I T0 ω1) Conjugate[A1[T1]] + E^(I T0 ω1) A1[T1])^3 +
    3 (E^(-I T0 ω1) Conjugate[A1[T1]] + E^(I T0 ω1) A1[T1])^2
     (E^(-I T0 ω2) Conjugate[A2[T1]] + E^(-I T0 ω1) Conjugate[A3[T1]] + E^(I T0 ω2) A2[T1] + E^(I T0 ω1) A3[T1]) -
    3 (E^(-I T0 ω1) Conjugate[A1[T1]] + E^(I T0 ω1) A1[T1])
     (E^(-I T0 ω2) Conjugate[A2[T1]] + E^(-I T0 ω1) Conjugate[A3[T1]] + E^(I T0 ω2) A2[T1] + E^(I T0 ω1) A3[T1])^2 +
    (E^(-I T0 ω2) Conjugate[A2[T1]] + E^(-I T0 ω1) Conjugate[A3[T1]] + E^(I T0 ω2) A2[T1] + E^(I T0 ω1) A3[T1])^3) -
 2 (I E^(I T0 ω1) ω1 A1'[T1] - I E^(-I T0 ω1) ω1 OverBar'[A1[T1]] A1'[T1])
```

```
In[8]:= RHS1 = ExpandAll[RHS1]
```

```
Out[8]= 1/2 E^(-I Ω T0) F̃ + 1/2 E^(I Ω T0) F̃ - E^(-I T0 ω1) Conjugate[A1[T1]] γ̃2 + E^(-I T0 ω2) Conjugate[A2[T1]] γ̃2 +
 E^(-I T0 ω1) Conjugate[A3[T1]] γ̃2 + 2 I E^(-I T0 ω1) Conjugate[A1[T1]] ω1 ξ̃1 + 2 I E^(-I T0 ω1) Conjugate[A1[T1]] ω1 ξ̃2 -
 2 I E^(-I T0 ω1) Conjugate[A3[T1]] ω1 ξ̃2 - 2 I E^(-I T0 ω2) Conjugate[A2[T1]] ω2 ξ̃2 - E^(-3 I T0 ω1) Conjugate[A1[T1]]^3 η̃1 +
 E^(-3 I T0 ω1) Conjugate[A1[T1]]^3 η̃2 - 3 E^(-2 I T0 ω1-I T0 ω2) Conjugate[A1[T1]]^2 Conjugate[A2[T1]] η̃2 +
 3 E^(-I T0 ω1-2 I T0 ω2) Conjugate[A1[T1]] Conjugate[A2[T1]]^2 η̃2 -
 E^(-3 I T0 ω2) Conjugate[A2[T1]]^3 η̃2 - 3 E^(-3 I T0 ω1) Conjugate[A1[T1]]^2 Conjugate[A3[T1]] η̃2 +
 6 E^(-2 I T0 ω1-I T0 ω2) Conjugate[A1[T1]] Conjugate[A2[T1]] Conjugate[A3[T1]] η̃2 -
 3 E^(-I T0 ω1-2 I T0 ω2) Conjugate[A2[T1]]^2 Conjugate[A3[T1]] η̃2 + 3 E^(-3 I T0 ω1) Conjugate[A1[T1]] Conjugate[A3[T1]]^2 η̃2 -
 3 E^(-2 I T0 ω1-I T0 ω2) Conjugate[A2[T1]] Conjugate[A3[T1]]^2 η̃2 - E^(-3 I T0 ω1) Conjugate[A3[T1]]^3 η̃2 -
 E^(I T0 ω1) γ̃2 A1[T1] - 2 I E^(I T0 ω1) ω1 ξ̃1 A1[T1] - 2 I E^(I T0 ω1) ω1 ξ̃2 A1[T1] -
 3 E^(-I T0 ω1) Conjugate[A1[T1]]^2 η̃1 A1[T1] + 3 E^(-I T0 ω1) Conjugate[A1[T1]]^2 η̃2 A1[T1] -
 6 E^(-I T0 ω2) Conjugate[A1[T1]] Conjugate[A2[T1]] η̃2 A1[T1] + 3 E^(I T0 ω1-2 I T0 ω2) Conjugate[A2[T1]]^2 η̃2 A1[T1] -
 6 E^(-I T0 ω1) Conjugate[A1[T1]] Conjugate[A3[T1]] η̃2 A1[T1] + 6 E^(-I T0 ω2) Conjugate[A2[T1]] Conjugate[A3[T1]] η̃2 A1[T1] +
 3 E^(-I T0 ω1) Conjugate[A3[T1]]^2 η̃2 A1[T1] - 3 E^(I T0 ω1) Conjugate[A1[T1]] η̃1 A1[T1]^2 +
 3 E^(I T0 ω1) Conjugate[A1[T1]] η̃2 A1[T1]^2 - 3 E^(2 I T0 ω1-I T0 ω2) Conjugate[A2[T1]] η̃2 A1[T1]^2 -
 3 E^(I T0 ω1) Conjugate[A3[T1]] η̃2 A1[T1]^2 - E^(3 I T0 ω1) η̃1 A1[T1]^3 +
 E^(3 I T0 ω1) η̃2 A1[T1]^3 + E^(I T0 ω2) γ̃2 A2[T1] + 2 I E^(I T0 ω2) ω2 ξ̃2 A2[T1] -
 3 E^(-2 I T0 ω1+I T0 ω2) Conjugate[A1[T1]]^2 η̃2 A2[T1] + 6 E^(-I T0 ω1) Conjugate[A1[T1]] Conjugate[A2[T1]] η̃2 A2[T1] -
 3 E^(-I T0 ω2) Conjugate[A2[T1]]^2 η̃2 A2[T1] + 6 E^(-2 I T0 ω1+I T0 ω2) Conjugate[A1[T1]] Conjugate[A3[T1]] η̃2 A2[T1] -
 6 E^(-I T0 ω1) Conjugate[A2[T1]] Conjugate[A3[T1]] η̃2 A2[T1] - 3 E^(-2 I T0 ω1+I T0 ω2) Conjugate[A3[T1]]^2 η̃2 A2[T1] -
 6 E^(I T0 ω2) Conjugate[A1[T1]] η̃2 A1[T1] A2[T1] + 6 E^(I T0 ω1) Conjugate[A2[T1]] η̃2 A1[T1] A2[T1] +
 6 E^(I T0 ω2) Conjugate[A3[T1]] η̃2 A1[T1] A2[T1] - 3 E^(2 I T0 ω1+I T0 ω2) η̃2 A1[T1]^2 A2[T1] +
 3 E^(-I T0 ω1+2 I T0 ω2) Conjugate[A1[T1]] η̃2 A2[T1]^2 - 3 E^(I T0 ω2) Conjugate[A2[T1]] η̃2 A2[T1]^2 -
 3 E^(-I T0 ω1+2 I T0 ω2) Conjugate[A3[T1]] η̃2 A2[T1]^2 + 3 E^(I T0 ω1+2 I T0 ω2) η̃2 A1[T1] A2[T1]^2 -
 E^(3 I T0 ω2) η̃2 A2[T1]^3 + E^(I T0 ω1) γ̃2 A3[T1] +
 2 I E^(I T0 ω1) ω1 ξ̃2 A3[T1] - 3 E^(-I T0 ω1) Conjugate[A1[T1]]^2 η̃2 A3[T1] +
 6 E^(-I T0 ω2) Conjugate[A1[T1]] Conjugate[A2[T1]] η̃2 A3[T1] - 3 E^(I T0 ω1-2 I T0 ω2) Conjugate[A2[T1]]^2 η̃2 A3[T1] +
 6 E^(-I T0 ω1) Conjugate[A1[T1]] Conjugate[A3[T1]] η̃2 A3[T1] - 6 E^(-I T0 ω2) Conjugate[A2[T1]] Conjugate[A3[T1]] η̃2 A3[T1] -
 3 E^(-I T0 ω1) Conjugate[A3[T1]]^2 η̃2 A3[T1] - 6 E^(I T0 ω1) Conjugate[A1[T1]] η̃2 A1[T1] A3[T1] +
 6 E^(2 I T0 ω1-I T0 ω2) Conjugate[A2[T1]] η̃2 A1[T1] A3[T1] +
 6 E^(I T0 ω1) Conjugate[A3[T1]] η̃2 A1[T1] A3[T1] -
 3 E^(3 I T0 ω1) η̃2 A1[T1]^2 A3[T1] + 6 E^(I T0 ω2) Conjugate[A1[T1]] η̃2 A2[T1] A3[T1] -
 6 E^(I T0 ω1) Conjugate[A2[T1]] η̃2 A2[T1] A3[T1] - 6 E^(I T0 ω2) Conjugate[A3[T1]] η̃2 A2[T1] A3[T1] +
 6 E^(2 I T0 ω1+I T0 ω2) η̃2 A1[T1] A2[T1] A3[T1] -
 3 E^(I T0 ω1+2 I T0 ω2) η̃2 A2[T1]^2 A3[T1] +
 3 E^(I T0 ω1) Conjugate[A1[T1]] η̃2 A3[T1]^2 - 3 E^(2 I T0 ω1-I T0 ω2) Conjugate[A2[T1]] η̃2 A3[T1]^2 -
 3 E^(I T0 ω1) Conjugate[A3[T1]] η̃2 A3[T1]^2 + 3 E^(3 I T0 ω1) η̃2 A1[T1] A3[T1]^2 -
 3 E^(2 I T0 ω1+I T0 ω2) η̃2 A2[T1] A3[T1]^2 - E^(3 I T0 ω1) η̃2 A3[T1]^3 -
 2 I E^(I T0 ω1) ω1 A1'[T1] + 2 I E^(-I T0 ω1) ω1 OverBar'[A1[T1]] A1'[T1]
```

Extracting the ' Always ' Secular Terms of RHS1 from Out[8] :

In[9]:=
```
Coefficient[RHS1, e^(i×ω1×T0)]
```

Out[9]=
$$-\tilde{\gamma}_2 A_1[T_1] - 2 i \omega_1 \tilde{\zeta}_1 A_1[T_1] - 2 i \omega_1 \tilde{\zeta}_2 A_1[T_1] - 3 \overline{A_1[T_1]} \tilde{\eta}_1 A_1[T_1]^2 + 3 \overline{A_1[T_1]} \tilde{\eta}_2 A_1[T_1]^2 - 3 \overline{A_3[T_1]} \tilde{\eta}_2 A_1[T_1]^2 + 6 \overline{A_2[T_1]} \tilde{\eta}_2 A_1[T_1] A_2[T_1] + \tilde{\gamma}_2 A_3[T_1] + 2 i \omega_1 \tilde{\zeta}_2 A_3[T_1] - 6 \overline{A_1[T_1]} \tilde{\eta}_2 A_1[T_1] A_3[T_1] + 6 \overline{A_3[T_1]} \tilde{\eta}_2 A_1[T_1] A_3[T_1] - 6 \overline{A_2[T_1]} \tilde{\eta}_2 A_2[T_1] A_3[T_1] + 3 \overline{A_1[T_1]} \tilde{\eta}_2 A_3[T_1]^2 - 3 \overline{A_3[T_1]} \tilde{\eta}_2 A_3[T_1]^2 - 2 i \omega_1 A_1'[T_1]$$

Extracting the ' Always ' Complex Conjugate Secular Terms of RHS1 from Out[8] :

In[10]:=
```
Coefficient[RHS1, e^(-i×ω1×T0)]
```

Out[10]=
$$-\overline{A_1[T_1]} \tilde{\gamma}_2 + \overline{A_3[T_1]} \tilde{\gamma}_2 + 2 i \overline{A_1[T_1]} \omega_1 \tilde{\zeta}_1 + 2 i \overline{A_1[T_1]} \omega_1 \tilde{\zeta}_2 - 2 i \overline{A_3[T_1]} \omega_1 \tilde{\zeta}_2 - 3 \overline{A_1[T_1]}^2 \tilde{\eta}_1 A_1[T_1] + 3 \overline{A_1[T_1]}^2 \tilde{\eta}_2 A_1[T_1] - 6 \overline{A_1[T_1]}\ \overline{A_3[T_1]} \tilde{\eta}_2 A_1[T_1] + 3 \overline{A_3[T_1]}^2 \tilde{\eta}_2 A_1[T_1] + 6 \overline{A_1[T_1]}\ \overline{A_2[T_1]} \tilde{\eta}_2 A_2[T_1] - 6 \overline{A_2[T_1]}\ \overline{A_3[T_1]} \tilde{\eta}_2 A_2[T_1] - 3 \overline{A_1[T_1]}^2 \tilde{\eta}_2 A_3[T_1] + 6 \overline{A_1[T_1]}\ \overline{A_3[T_1]} \tilde{\eta}_2 A_3[T_1] - 3 \overline{A_3[T_1]}^2 \tilde{\eta}_2 A_3[T_1] + 2 i \omega_1 \text{OverBar}'[A_1[T_1]] A_1'[T_1]$$

Below are the ' Always ' Secular and ' Always ' Complex Conjugate Secular Terms for x_{11} . They are the re - statement of Out[9] and Out[10] respectively , except that the excitation terms (i.e. the 1^{st} terms) are added in here as they are left out previously by Mathematica.

■ **The 'Always' Secular Terms of x_{11}:**

In[11]:=
```
1/2 e^(i (Ω-ω1) T0) F̃ - γ̃2 A1[T1] - 2 i ω1 ξ̃1 A1[T1] - 2 i ω1 ξ̃2 A1[T1] -
 3 Conjugate[A1[T1]] η̃1 A1[T1]^2 + 3 Conjugate[A1[T1]] η̃2 A1[T1]^2 - 3 Conjugate[A3[T1]] η̃2 A1[T1]^2 +
 6 Conjugate[A2[T1]] η̃2 A1[T1] A2[T1] + γ̃2 A3[T1] + 2 i ω1 ξ̃2 A3[T1] -
 6 Conjugate[A1[T1]] η̃2 A1[T1] A3[T1] + 6 Conjugate[A3[T1]] η̃2 A1[T1] A3[T1] -
 6 Conjugate[A2[T1]] η̃2 A2[T1] A3[T1] + 3 Conjugate[A1[T1]] η̃2 A3[T1]^2 - 3 Conjugate[A3[T1]] η̃2 A3[T1]^2 -
 2 i ω1 A1'[T1];
```

■ **The 'Always' Complex Conjugate Secular Terms of x_{11}:**

In[12]:=
```
1/2 e^(-i (Ω-ω1) T0) F̃ - Conjugate[A1[T1]] γ̃2 + Conjugate[A3[T1]] γ̃2 + 2 i Conjugate[A1[T1]] ω1 ξ̃1 +
 2 i Conjugate[A1[T1]] ω1 ξ̃2 - 2 i Conjugate[A3[T1]] ω1 ξ̃2 - 3 Conjugate[A1[T1]]^2 η̃1 A1[T1] +
 3 Conjugate[A1[T1]]^2 η̃2 A1[T1] - 6 Conjugate[A1[T1]] Conjugate[A3[T1]] η̃2 A1[T1] + 3 Conjugate[A3[T1]]^2 η̃2 A1[T1] +
 6 Conjugate[A1[T1]] Conjugate[A2[T1]] η̃2 A2[T1] - 6 Conjugate[A2[T1]] Conjugate[A3[T1]] η̃2 A2[T1] -
 3 Conjugate[A1[T1]]^2 η̃2 A3[T1] + 6 Conjugate[A1[T1]] Conjugate[A3[T1]] η̃2 A3[T1] - 3 Conjugate[A3[T1]]^2 η̃2 A3[T1] +
 2 i ω1 OverBar'[A1[T1]] A1'[T1];
```

Dividing RHS1 by $e^{i\omega_1 T_0}$ *and then grouping them for alike coefficients for easier identification. This purpose is to identify other secular terms :*

```
In[13]:= Collect[ExpandAll[RHS1 / e^(i×ω1×T0)],
           {e^(i ω1 T0), e^(-i ω1 T0), e^(3 i ω1 T0), e^(-3 i ω1 T0), e^(i ω2 T0), e^(-i ω2 T0),
            e^(2 i ω2 T0), e^(3 i ω2 T0), e^(-3 i ω2 T0)}]
```

Out[13]=

$$
\begin{aligned}
&e^{-4 i T_0 \omega_1} \left(-\overline{A_1[T_1]}^3 \tilde{\eta}_1 + \overline{A_1[T_1]}^3 \tilde{\eta}_2 - 3 \overline{A_1[T_1]}^2 \overline{A_3[T_1]} \tilde{\eta}_2 + 3 \overline{A_1[T_1]} \overline{A_3[T_1]}^2 \tilde{\eta}_2 - \overline{A_3[T_1]}^3 \tilde{\eta}_2\right) - \\
&\tilde{\gamma}_2 A_1[T_1] - 2 i \omega_1 \tilde{\xi}_1 A_1[T_1] - 2 i \omega_1 \tilde{\xi}_2 A_1[T_1] - \\
&3 \overline{A_1[T_1]} \tilde{\eta}_1 A_1[T_1]^2 + 3 \overline{A_1[T_1]} \tilde{\eta}_2 A_1[T_1]^2 - \\
&3 \overline{A_3[T_1]} \tilde{\eta}_2 A_1[T_1]^2 + 6 \overline{A_2[T_1]} \tilde{\eta}_2 A_1[T_1] A_2[T_1] + \\
&e^{-3 i T_0 \omega_1} \left(e^{-i T_0 \omega_2} \left(-3 \overline{A_1[T_1]}^2 \overline{A_2[T_1]} \tilde{\eta}_2 + 6 \overline{A_1[T_1]} \overline{A_2[T_1]} \overline{A_3[T_1]} \tilde{\eta}_2 - 3 \overline{A_2[T_1]} \overline{A_3[T_1]}^2 \tilde{\eta}_2\right) + e^{i T_0 \omega_2} \left(-3 \overline{A_1[T_1]}^2 \tilde{\eta}_2 A_2[T_1] + 6 \overline{A_1[T_1]} \overline{A_3[T_1]} \tilde{\eta}_2 A_2[T_1] - 3 \overline{A_3[T_1]}^2 \tilde{\eta}_2 A_2[T_1]\right)\right) + \\
&\tilde{\gamma}_2 A_3[T_1] + 2 i \omega_1 \tilde{\xi}_2 A_3[T_1] - 6 \overline{A_1[T_1]} \tilde{\eta}_2 A_1[T_1] A_3[T_1] + \\
&6 \overline{A_3[T_1]} \tilde{\eta}_2 A_1[T_1] A_3[T_1] - \\
&6 \overline{A_2[T_1]} \tilde{\eta}_2 A_2[T_1] A_3[T_1] + \\
&3 \overline{A_1[T_1]} \tilde{\eta}_2 A_3[T_1]^2 - \\
&3 \overline{A_3[T_1]} \tilde{\eta}_2 A_3[T_1]^2 + \\
&e^{-2 i T_0 \omega_2} \left(3 \overline{A_2[T_1]}^2 \tilde{\eta}_2 A_1[T_1] - 3 \overline{A_2[T_1]}^2 \tilde{\eta}_2 A_3[T_1]\right) + \\
&e^{2 i T_0 \omega_2} \left(3 \tilde{\eta}_2 A_1[T_1] A_2[T_1]^2 - 3 \tilde{\eta}_2 A_2[T_1]^2 A_3[T_1]\right) + \\
&e^{2 i T_0 \omega_1} \left(-\tilde{\eta}_1 A_1[T_1]^3 + \tilde{\eta}_2 A_1[T_1]^3 - 3 \tilde{\eta}_2 A_1[T_1]^2 A_3[T_1] + 3 \tilde{\eta}_2 A_1[T_1] A_3[T_1]^2 - \tilde{\eta}_2 A_3[T_1]^3\right) + e^{-i T_0 \omega_1} \\
&\left\{\frac{1}{2} e^{-i \Omega T_0} \tilde{F} + \frac{1}{2} e^{i \Omega T_0} \tilde{F} - e^{-3 i T_0 \omega_2} \overline{A_2[T_1]}^3 \tilde{\eta}_2 - e^{3 i T_0 \omega_2} \tilde{\eta}_2 A_2[T_1]^3 + \right. \\
&e^{-i T_0 \omega_2} \left(\overline{A_2[T_1]} \tilde{\gamma}_2 - 2 i \overline{A_2[T_1]} \omega_2 \tilde{\xi}_2 - 6 \overline{A_1[T_1]} \overline{A_2[T_1]} \tilde{\eta}_2 A_1[T_1] + 6 \overline{A_2[T_1]} \overline{A_3[T_1]} \tilde{\eta}_2 A_1[T_1] - 3 \overline{A_2[T_1]}^2 \tilde{\eta}_2 A_2[T_1] + 6 \overline{A_1[T_1]} \overline{A_2[T_1]} \tilde{\eta}_2 A_3[T_1] - 6 \overline{A_2[T_1]} \overline{A_3[T_1]} \tilde{\eta}_2 A_3[T_1]\right) + \\
&e^{i T_0 \omega_2} \left(\tilde{\gamma}_2 A_2[T_1] + 2 i \omega_2 \tilde{\xi}_2 A_2[T_1] - 6 \overline{A_1[T_1]} \tilde{\eta}_2 A_1[T_1] A_2[T_1] + 6 \overline{A_3[T_1]} \tilde{\eta}_2 A_1[T_1] A_2[T_1] - 3 \overline{A_2[T_1]} \tilde{\eta}_2 A_2[T_1]^2 + 6 \overline{A_1[T_1]} \tilde{\eta}_2 A_2[T_1] A_3[T_1] - 6 \overline{A_3[T_1]} \tilde{\eta}_2 A_2[T_1] A_3[T_1]\right)\Big\} + \\
&e^{i T_0 \omega_1} \left(e^{-i T_0 \omega_2} \left(-3 \overline{A_2[T_1]} \tilde{\eta}_2 A_1[T_1]^2 + 6 \overline{A_2[T_1]} \tilde{\eta}_2 A_1[T_1] A_3[T_1] - 3 \overline{A_2[T_1]} \tilde{\eta}_2 A_3[T_1]^2\right) + e^{i T_0 \omega_2} \left(-3 \tilde{\eta}_2 A_1[T_1]^2 A_2[T_1] + 6 \tilde{\eta}_2 A_1[T_1] A_2[T_1] A_3[T_1] - 3 \tilde{\eta}_2 A_2[T_1] A_3[T_1]^2\right)\right) - \\
&2 i \omega_1 A_1'[T_1] + e^{-2 i T_0 \omega_1} \left(-\overline{A_1[T_1]} \tilde{\gamma}_2 + \overline{A_3[T_1]} \tilde{\gamma}_2 + 2 i \overline{A_1[T_1]} \omega_1 \tilde{\xi}_1 + 2 i \overline{A_1[T_1]} \omega_1 \tilde{\xi}_2 - 2 i \overline{A_3[T_1]} \omega_1 \tilde{\xi}_2 + \right. \\
&e^{-2 i T_0 \omega_2} \left(3 \overline{A_1[T_1]} \overline{A_2[T_1]}^2 \tilde{\eta}_2 - 3 \overline{A_2[T_1]}^2 \overline{A_3[T_1]} \tilde{\eta}_2\right) - \\
&3 \overline{A_1[T_1]}^2 \tilde{\eta}_1 A_1[T_1] + 3 \overline{A_1[T_1]}^2 \tilde{\eta}_2 A_1[T_1] - \\
&6 \overline{A_1[T_1]} \overline{A_3[T_1]} \tilde{\eta}_2 A_1[T_1] + 3 \overline{A_3[T_1]}^2 \tilde{\eta}_2 A_1[T_1] + \\
&6 \overline{A_1[T_1]} \overline{A_2[T_1]} \tilde{\eta}_2 A_2[T_1] - 6 \overline{A_2[T_1]} \overline{A_3[T_1]} \tilde{\eta}_2 A_2[T_1] + \\
&e^{2 i T_0 \omega_2} \left(3 \overline{A_1[T_1]} \tilde{\eta}_2 A_2[T_1]^2 - 3 \overline{A_3[T_1]} \tilde{\eta}_2 A_2[T_1]^2\right) - \\
&3 \overline{A_1[T_1]}^2 \tilde{\eta}_2 A_3[T_1] + 6 \overline{A_1[T_1]} \overline{A_3[T_1]} \tilde{\eta}_2 A_3[T_1] - \\
&3 \overline{A_3[T_1]}^2 \tilde{\eta}_2 A_3[T_1] + 2 i \omega_1 \text{OverBar}'[A_1[T_1]] A_1'[T_1]
\end{aligned}
$$

Similarly, for the complex conjugate,
dividing RHS1 by $e^{-i\omega_1 T_0}$ *and then grouping them for alike coefficients for easier identification. The purpose of solving for the complex conjugates is to double check that all the terms in the conjugates are alike with the complex conjugates ones - which it does.*

```
In[14]:= Collect[ExpandAll[RHS1 / e^(-i×ω1×T0)],
          {e^(i ω1 T0), e^(-i ω1 T0), e^(3 i ω1 T0), e^(-3 i ω1 T0), e^(i ω2 T0), e^(-i ω2 T0),
           e^(2 i ω2 T0), e^(3 i ω2 T0), e^(-3 i ω2 T0)}]
```

$$
\begin{aligned}
\text{Out[14]}= {} & -\overline{A_1[T_1]}\,\tilde{\gamma}_2 + \overline{A_3[T_1]}\,\tilde{\gamma}_2 + 2\,i\,\overline{A_1[T_1]}\,\omega_1\,\tilde{\zeta}_1 + 2\,i\,\overline{A_1[T_1]}\,\omega_1\,\tilde{\zeta}_2 - \\
& 2\,i\,\overline{A_3[T_1]}\,\omega_1\,\tilde{\zeta}_2 + e^{-2\,i\,T_0\,\omega_2}\,(3\,\overline{A_1[T_1]}\,\overline{A_2[T_1]}^2\,\tilde{\eta}_2 - 3\,\overline{A_2[T_1]}^2\,\overline{A_3[T_1]}\,\tilde{\eta}_2) + \\
& e^{-2\,i\,T_0\,\omega_1}\,(-\overline{A_1[T_1]}^3\,\tilde{\eta}_1 + \overline{A_1[T_1]}^3\,\tilde{\eta}_2 - 3\,\overline{A_1[T_1]}^2\,\overline{A_3[T_1]}\,\tilde{\eta}_2 + \\
& \quad 3\,\overline{A_1[T_1]}\,\overline{A_3[T_1]}^2\,\tilde{\eta}_2 - \overline{A_3[T_1]}^3\,\tilde{\eta}_2) - 3\,\overline{A_1[T_1]}^2\,\tilde{\eta}_1\,A_1[T_1] + \\
& 3\,\overline{A_1[T_1]}^2\,\tilde{\eta}_2\,A_1[T_1] - 6\,\overline{A_1[T_1]}\,\overline{A_3[T_1]}\,\tilde{\eta}_2\,A_1[T_1] + 3\,\overline{A_3[T_1]}^2\,\tilde{\eta}_2\,A_1[T_1] + \\
& 6\,\overline{A_1[T_1]}\,\overline{A_2[T_1]}\,\tilde{\eta}_2\,A_2[T_1] - 6\,\overline{A_2[T_1]}\,\overline{A_3[T_1]}\,\tilde{\eta}_2\,A_2[T_1] + \\
& e^{2\,i\,T_0\,\omega_2}\,(3\,\overline{A_1[T_1]}\,\tilde{\eta}_2\,A_2[T_1]^2 - 3\,\overline{A_3[T_1]}\,\tilde{\eta}_2\,A_2[T_1]^2) + \\
& e^{-i\,T_0\,\omega_1}\,(e^{-i\,T_0\,\omega_2}\,(-3\,\overline{A_1[T_1]}^2\,\overline{A_2[T_1]}\,\tilde{\eta}_2 + 6\,\overline{A_1[T_1]}\,\overline{A_2[T_1]}\,\overline{A_3[T_1]}\,\tilde{\eta}_2 - \\
& \quad 3\,\overline{A_2[T_1]}\,\overline{A_3[T_1]}^2\,\tilde{\eta}_2) + e^{i\,T_0\,\omega_2}\,(-3\,\overline{A_1[T_1]}^2\,\tilde{\eta}_2\,A_2[T_1] + \\
& \quad 6\,\overline{A_1[T_1]}\,\overline{A_3[T_1]}\,\tilde{\eta}_2\,A_2[T_1] - 3\,\overline{A_3[T_1]}^2\,\tilde{\eta}_2\,A_2[T_1])) - \\
& 3\,\overline{A_1[T_1]}^2\,\tilde{\eta}_2\,A_3[T_1] + 6\,\overline{A_1[T_1]}\,\overline{A_3[T_1]}\,\tilde{\eta}_2\,A_3[T_1] - \\
& 3\,\overline{A_3[T_1]}^2\,\tilde{\eta}_2\,A_3[T_1] + \\
& e^{4\,i\,T_0\,\omega_1}\,(-\tilde{\eta}_1\,A_1[T_1]^3 + \tilde{\eta}_2\,A_1[T_1]^3 - 3\,\tilde{\eta}_2\,A_1[T_1]^2\,A_3[T_1] + \\
& \quad 3\,\tilde{\eta}_2\,A_1[T_1]\,A_3[T_1]^2 - \tilde{\eta}_2\,A_3[T_1]^3) + e^{i\,T_0\,\omega_1} \\
& \left(\frac{1}{2}\,e^{-i\,\Omega\,T_0}\,\tilde{F} + \frac{1}{2}\,e^{i\,\Omega\,T_0}\,\tilde{F} - e^{-3\,i\,T_0\,\omega_2}\,\overline{A_2[T_1]}^3\,\tilde{\eta}_2 - e^{3\,i\,T_0\,\omega_2}\,\tilde{\eta}_2\,A_2[T_1]^3 + \right. \\
& \quad e^{-i\,T_0\,\omega_2}\,(\overline{A_2[T_1]}\,\tilde{\gamma}_2 - 2\,i\,\overline{A_2[T_1]}\,\omega_2\,\tilde{\zeta}_2 - 6\,\overline{A_1[T_1]}\,\overline{A_2[T_1]}\,\tilde{\eta}_2\,A_1[T_1] + \\
& \quad 6\,\overline{A_2[T_1]}\,\overline{A_3[T_1]}\,\tilde{\eta}_2\,A_1[T_1] - 3\,\overline{A_2[T_1]}^2\,\tilde{\eta}_2\,A_2[T_1] + \\
& \quad 6\,\overline{A_1[T_1]}\,\overline{A_2[T_1]}\,\tilde{\eta}_2\,A_3[T_1] - 6\,\overline{A_2[T_1]}\,\overline{A_3[T_1]}\,\tilde{\eta}_2\,A_3[T_1]) + \\
& \quad e^{i\,T_0\,\omega_2}\,(\tilde{\gamma}_2\,A_2[T_1] + 2\,i\,\omega_2\,\tilde{\zeta}_2\,A_2[T_1] - 6\,\overline{A_1[T_1]}\,\tilde{\eta}_2\,A_1[T_1]\,A_2[T_1] + \\
& \quad 6\,\overline{A_3[T_1]}\,\tilde{\eta}_2\,A_1[T_1]\,A_2[T_1] - 3\,\overline{A_2[T_1]}\,\tilde{\eta}_2\,A_2[T_1]^2 + \\
& \quad \left. 6\,\overline{A_1[T_1]}\,\tilde{\eta}_2\,A_2[T_1]\,A_3[T_1] - 6\,\overline{A_3[T_1]}\,\tilde{\eta}_2\,A_2[T_1]\,A_3[T_1])\right) + \\
& e^{3\,i\,T_0\,\omega_1}\,(e^{-i\,T_0\,\omega_2}\,(-3\,\overline{A_2[T_1]}\,\tilde{\eta}_2\,A_1[T_1]^2 + 6\,\overline{A_2[T_1]}\,\tilde{\eta}_2\,A_1[T_1]\,A_3[T_1] - \\
& \quad 3\,\overline{A_2[T_1]}\,\tilde{\eta}_2\,A_3[T_1]^2) + e^{i\,T_0\,\omega_2}\,(-3\,\tilde{\eta}_2\,A_1[T_1]^2\,A_2[T_1] + \\
& \quad 6\,\tilde{\eta}_2\,A_1[T_1]\,A_2[T_1]\,A_3[T_1] - 3\,\tilde{\eta}_2\,A_2[T_1]\,A_3[T_1]^2)) + \\
& 2\,i\,\omega_1\,\text{OverBar}'[A_1[T_1]]\,A_1'[T_1] + e^{2\,i\,T_0\,\omega_1} \\
& (-\tilde{\gamma}_2\,A_1[T_1] - 2\,i\,\omega_1\,\tilde{\zeta}_1\,A_1[T_1] - 2\,i\,\omega_1\,\tilde{\zeta}_2\,A_1[T_1] - \\
& \quad 3\,\overline{A_1[T_1]}\,\tilde{\eta}_1\,A_1[T_1]^2 + 3\,\overline{A_1[T_1]}\,\tilde{\eta}_2\,A_1[T_1]^2 - \\
& \quad 3\,\overline{A_3[T_1]}\,\tilde{\eta}_2\,A_1[T_1]^2 + 6\,\overline{A_2[T_1]}\,\tilde{\eta}_2\,A_1[T_1]\,A_2[T_1] + \\
& \quad \tilde{\gamma}_2\,A_3[T_1] + 2\,i\,\omega_1\,\tilde{\zeta}_2\,A_3[T_1] - 6\,\overline{A_1[T_1]}\,\tilde{\eta}_2\,A_1[T_1]\,A_3[T_1] + \\
& \quad 6\,\overline{A_3[T_1]}\,\tilde{\eta}_2\,A_1[T_1]\,A_3[T_1] - 6\,\overline{A_2[T_1]}\,\tilde{\eta}_2\,A_2[T_1]\,A_3[T_1] + \\
& \quad 3\,\overline{A_1[T_1]}\,\tilde{\eta}_2\,A_3[T_1]^2 - 3\,\overline{A_3[T_1]}\,\tilde{\eta}_2\,A_3[T_1]^2 + \\
& \quad e^{-2\,i\,T_0\,\omega_2}\,(3\,\overline{A_2[T_1]}^2\,\tilde{\eta}_2\,A_1[T_1] - 3\,\overline{A_2[T_1]}^2\,\tilde{\eta}_2\,A_3[T_1]) + \\
& \quad e^{2\,i\,T_0\,\omega_2}\,(3\,\tilde{\eta}_2\,A_1[T_1]\,A_2[T_1]^2 - 3\,\tilde{\eta}_2\,A_2[T_1]^2\,A_3[T_1]) - 2\,i\,\omega_1\,A_1'[T_1])
\end{aligned}
$$

C.2 Identifying the Internal Resonances of x_{11}

With reference from *In[1]* of Appendix C.2 on the next page, all the terms admit resonances of one sort or another; a full list of these is given in Table C-1 below, in which it may be seen that some appear in one or two of the first-order perturbation equations. Only resonances that show coupling between at least two modes are of practical interest.

Secular Terms	Possible Internal Resonance	Complex Conjugates	Possible Internal Resonance
$e^{i2\omega_2 T_0}$	N.A.	$e^{-i(2\omega_2+2\omega_1)T_0}$	$\omega_2 \approx -\omega_1$
$e^{i2\omega_1 T_0}$	N.A.	$e^{-i4\omega_1 T_0}$	N.A.
$e^{i(3\omega_2-\omega_1)T_0}$	$\boxed{\omega_2 \approx \frac{1}{3}\omega_1}$	$e^{-i(3\omega_2+\omega_1)T_0}$	$\omega_2 \approx -\frac{1}{3}\omega_1$
$e^{i(\omega_2-\omega_1)T_0}$	$\boxed{\omega_2 \approx \omega_1}$	$e^{-i(\omega_2+\omega_1)T_0}$	$\omega_2 \approx -\omega_1$
$e^{i(\omega_2-3\omega_1)T_0}$	$\boxed{\omega_2 \approx 3\omega_1}$	$e^{-i(\omega_2-\omega_1)T_0}$	$\omega_2 \approx \omega_1$
$e^{i(\omega_2+\omega_1)T_0}$	$\omega_2 \approx -\omega_1$	$e^{-i(\omega_2+3\omega_1)T_0}$	$\omega_2 \approx -3\omega_1$
$e^{i(2\omega_2-2\omega_1)T_0}$	$\boxed{\omega_2 \approx \omega_1}$	$e^{-i2\omega_2 T_0}$	N.A.

Table C-1: Possible internal resonances for 1st order perturbation equations (Case 1)

From the table above, the internal resonances of the system are contributed by the terms that are highlighted with a box, i.e. $\omega_2 \approx \frac{1}{3}\omega_1$, $\omega_2 \approx 3\omega_1$ and $\omega_2 \approx \omega_1$.

Multiplying $e^{\dot{\imath} T_0 \omega_1}$ back into Out[13] from Appendix C.1 and rearranging it:

In[1]:=

$$
\begin{aligned}
&\mathrm{RHS1} == \\
&e^{\dot{\imath} T_0 \omega_1} \Big(e^{2 \dot{\imath} T_0 \omega_2} \left(3 \tilde{\eta}_2 A_1[T_1] A_2[T_1]^2 - 3 \tilde{\eta}_2 A_2[T_1]^2 A_3[T_1]\right) + \\
&\quad e^{-\dot{\imath} T_0 (2\omega_2 + 2\omega_1)} \left(3 \overline{A_1[T_1]}\, \overline{A_2[T_1]}^2 \tilde{\eta}_2 - 3 \overline{A_2[T_1]}^2 \overline{A_3[T_1]}\, \tilde{\eta}_2\right) + \\
&\quad e^{2 \dot{\imath} T_0 \omega_1} \left(-\tilde{\eta}_1 A_1[T_1]^3 + \tilde{\eta}_2 A_1[T_1]^3 - 3 \tilde{\eta}_2 A_1[T_1]^2 A_3[T_1] + \right. \\
&\qquad \left. 3 \tilde{\eta}_2 A_1[T_1] A_3[T_1]^2 - \tilde{\eta}_2 A_3[T_1]^3\right) + \\
&\quad e^{-4 \dot{\imath} T_0 \omega_1} \left(-\overline{A_1[T_1]}^3 \tilde{\eta}_1 + \overline{A_1[T_1]}^3 \tilde{\eta}_2 - 3 \overline{A_1[T_1]}^2 \overline{A_3[T_1]}\, \tilde{\eta}_2 + \right. \\
&\qquad \left. 3 \overline{A_1[T_1]}\, \overline{A_3[T_1]}^2 \tilde{\eta}_2 - \overline{A_3[T_1]}^3 \tilde{\eta}_2\right) - e^{\dot{\imath} T_0 (3\omega_2 - \omega_1)} \tilde{\eta}_2 A_2[T_1]^3 - \\
&\quad e^{-\dot{\imath} T_0 (3\omega_2 + \omega_1)} \overline{A_2[T_1]}^3 \tilde{\eta}_2 + \\
&\quad e^{\dot{\imath} T_0 (\omega_2 - \omega_1)} \\
&\qquad \left(\tilde{\gamma}_2 A_2[T_1] + 2 \dot{\imath} \omega_2 \tilde{\xi}_2 A_2[T_1] - 6 \overline{A_1[T_1]} \tilde{\eta}_2 A_1[T_1] A_2[T_1] + \right. \\
&\qquad\quad 6 \overline{A_3[T_1]} \tilde{\eta}_2 A_1[T_1] A_2[T_1] - 3 \overline{A_2[T_1]} \tilde{\eta}_2 A_2[T_1]^2 + \\
&\qquad\quad \left. 6 \overline{A_1[T_1]} \tilde{\eta}_2 A_2[T_1] A_3[T_1] - 6 \overline{A_3[T_1]} \tilde{\eta}_2 A_2[T_1] A_3[T_1]\right) + \\
&\quad e^{-\dot{\imath} T_0 (\omega_2 + \omega_1)} \\
&\qquad \left(\overline{A_2[T_1]}\, \tilde{\gamma}_2 - 2 \dot{\imath} \overline{A_2[T_1]}\, \omega_2 \tilde{\xi}_2 - 6 \overline{A_1[T_1]}\, \overline{A_2[T_1]}\, \tilde{\eta}_2 A_1[T_1] + \right. \\
&\qquad\quad 6 \overline{A_2[T_1]}\, \overline{A_3[T_1]}\, \tilde{\eta}_2 A_1[T_1] - 3 \overline{A_2[T_1]}^2 \tilde{\eta}_2 A_2[T_1] + \\
&\qquad\quad \left. 6 \overline{A_1[T_1]}\, \overline{A_2[T_1]}\, \tilde{\eta}_2 A_3[T_1] - 6 \overline{A_2[T_1]}\, \overline{A_3[T_1]}\, \tilde{\eta}_2 A_3[T_1]\right) + \\
&\quad e^{\dot{\imath} T_0 (\omega_2 - 3\omega_1)} \\
&\qquad \left(-3 \overline{A_1[T_1]}^2 \tilde{\eta}_2 A_2[T_1] + 6 \overline{A_1[T_1]}\, \overline{A_3[T_1]}\, \tilde{\eta}_2 A_2[T_1] - \right. \\
&\qquad\quad \left. 3 \overline{A_3[T_1]}^2 \tilde{\eta}_2 A_2[T_1]\right) + \\
&\quad e^{-\dot{\imath} T_0 (\omega_2 - \omega_1)} \\
&\qquad \left(-3 \overline{A_2[T_1]}\, \tilde{\eta}_2 A_1[T_1]^2 + 6 \overline{A_2[T_1]}\, \tilde{\eta}_2 A_1[T_1] A_3[T_1] - \right. \\
&\qquad\quad \left. 3 \overline{A_2[T_1]}\, \tilde{\eta}_2 A_3[T_1]^2\right) + \\
&\quad e^{\dot{\imath} T_0 (\omega_2 + \omega_1)} \left(-3 \tilde{\eta}_2 A_1[T_1]^2 A_2[T_1] + 6 \tilde{\eta}_2 A_1[T_1] A_2[T_1] A_3[T_1] - \right. \\
&\qquad \left. 3 \tilde{\eta}_2 A_2[T_1] A_3[T_1]^2\right) + \\
&\quad e^{-\dot{\imath} T_0 (\omega_2 + 3\omega_1)} \\
&\qquad \left(-3 \overline{A_1[T_1]}^2 \overline{A_2[T_1]}\, \tilde{\eta}_2 + 6 \overline{A_1[T_1]}\, \overline{A_2[T_1]}\, \overline{A_3[T_1]}\, \tilde{\eta}_2 - \right. \\
&\qquad\quad \left. 3 \overline{A_2[T_1]}\, \overline{A_3[T_1]}^2 \tilde{\eta}_2\right) + \\
&\quad e^{\dot{\imath} T_0 (2\omega_2 - 2\omega_1)} \left(3 \overline{A_1[T_1]}\, \tilde{\eta}_2 A_2[T_1]^2 - 3 \overline{A_3[T_1]}\, \tilde{\eta}_2 A_2[T_1]^2\right) + \\
&\quad e^{-2 \dot{\imath} T_0 \omega_2} \left(3 \overline{A_2[T_1]}^2 \tilde{\eta}_2 A_1[T_1] - 3 \overline{A_2[T_1]}^2 \tilde{\eta}_2 A_3[T_1]\right) + \\
&\quad \frac{1}{2} e^{\dot{\imath} (\Omega - \omega_1) T_0} \tilde{F} - \tilde{\gamma}_2 A_1[T_1] - 2 \dot{\imath} \omega_1 \tilde{\xi}_1 A_1[T_1] - 2 \dot{\imath} \omega_1 \tilde{\xi}_2 A_1[T_1] - \\
&\quad 3 \overline{A_1[T_1]} \tilde{\eta}_1 A_1[T_1]^2 + 3 \overline{A_1[T_1]} \tilde{\eta}_2 A_1[T_1]^2 - 3 \overline{A_3[T_1]} \tilde{\eta}_2 A_1[T_1]^2 + \\
&\quad 6 \overline{A_2[T_1]} \tilde{\eta}_2 A_1[T_1] A_2[T_1] + \tilde{\gamma}_2 A_3[T_1] + 2 \dot{\imath} \omega_1 \tilde{\xi}_2 A_3[T_1] - \\
&\quad 6 \overline{A_1[T_1]} \tilde{\eta}_2 A_1[T_1] A_3[T_1] + 6 \overline{A_3[T_1]} \tilde{\eta}_2 A_1[T_1] A_3[T_1] - \\
&\quad 6 \overline{A_2[T_1]} \tilde{\eta}_2 A_2[T_1] A_3[T_1] + 3 \overline{A_1[T_1]} \tilde{\eta}_2 A_3[T_1]^2 - 3 \overline{A_3[T_1]} \tilde{\eta}_2 A_3[T_1]^2 - \\
&\quad 2 \dot{\imath} \omega_1 A_1'[T_1] + \frac{1}{2} e^{-\dot{\imath} (\Omega + \omega_1) T_0} \tilde{F} + \\
&\quad e^{-2 \dot{\imath} T_0 \omega_1} \left(-\overline{A_1[T_1]}\, \tilde{\gamma}_2 + \overline{A_3[T_1]}\, \tilde{\gamma}_2 + 2 \dot{\imath} \overline{A_1[T_1]}\, \omega_1 \tilde{\xi}_1 + \right. \\
&\qquad 2 \dot{\imath} \overline{A_1[T_1]}\, \omega_1 \tilde{\xi}_2 - 2 \dot{\imath} \overline{A_3[T_1]}\, \omega_1 \tilde{\xi}_2 - 3 \overline{A_1[T_1]}^2 \tilde{\eta}_1 A_1[T_1] + \\
&\qquad 3 \overline{A_1[T_1]}^2 \tilde{\eta}_2 A_1[T_1] - 6 \overline{A_1[T_1]}\, \overline{A_3[T_1]}\, \tilde{\eta}_2 A_1[T_1] + \\
&\qquad 3 \overline{A_3[T_1]}^2 \tilde{\eta}_2 A_1[T_1] + 6 \overline{A_1[T_1]}\, \overline{A_2[T_1]}\, \tilde{\eta}_2 A_2[T_1] - \\
&\qquad 6 \overline{A_2[T_1]}\, \overline{A_3[T_1]}\, \tilde{\eta}_2 A_2[T_1] - 3 \overline{A_1[T_1]}^2 \tilde{\eta}_2 A_3[T_1] + \\
&\qquad 6 \overline{A_1[T_1]}\, \overline{A_3[T_1]}\, \tilde{\eta}_2 A_3[T_1] - 3 \overline{A_3[T_1]}^2 \tilde{\eta}_2 A_3[T_1] + \\
&\qquad \left. 2 \dot{\imath} \omega_1 \mathrm{OverBar}'[A_1[T_1]] A_1'[T_1]\right);
\end{aligned}
$$

: 'Always' Secular Terms

Italics: Complex Conjugates of the Preceding Terms

C.3 Case 1 (Superharmonic Resonance): Solving for x_{11}

Non-secular terms of RHS1, after removing the secular and complex conjugate terms in (3.3-43)

```
In[1]:= RHS1 ==
  e^(i T0 ω1) (e^(2 i T0 ω2) (3 η̃2 A1[T1] A2[T1]^2 - 3 η̃2 A2[T1]^2 A3[T1]) +
    e^(-i T0 (2 ω2+2 ω1)) (3 Conjugate[A1[T1]] Conjugate[A2[T1]]^2 η̃2 - 3 Conjugate[A2[T1]]^2 Conjugate[A3[T1]] η̃2) +
    e^(2 i T0 ω1) (-η̃1 A1[T1]^3 + η̃2 A1[T1]^3 - 3 η̃2 A1[T1]^2 A3[T1] +
      3 η̃2 A1[T1] A3[T1]^2 - η̃2 A3[T1]^3) +
    e^(-4 i T0 ω1) (-Conjugate[A1[T1]]^3 η̃1 + Conjugate[A1[T1]]^3 η̃2 - 3 Conjugate[A1[T1]]^2 Conjugate[A3[T1]] η̃2 +
      3 Conjugate[A1[T1]] Conjugate[A3[T1]]^2 η̃2 - Conjugate[A3[T1]]^3 η̃2) +
    e^(i T0 (ω2-ω1))
     (Ỹ2 A2[T1] + 2 i ω2 ξ̃2 A2[T1] - 6 Conjugate[A1[T1]] η̃2 A1[T1] A2[T1] +
      6 Conjugate[A3[T1]] η̃2 A1[T1] A2[T1] - 3 Conjugate[A2[T1]] η̃2 A2[T1]^2 +
      6 Conjugate[A1[T1]] η̃2 A2[T1] A3[T1] - 6 Conjugate[A3[T1]] η̃2 A2[T1] A3[T1]) +
    e^(-i T0 (ω2+ω1))
     (Conjugate[A2[T1]] Ỹ2 - 2 i Conjugate[A2[T1]] ω2 ξ̃2 - 6 Conjugate[A1[T1]] Conjugate[A2[T1]] η̃2 A1[T1] +
      6 Conjugate[A2[T1]] Conjugate[A3[T1]] η̃2 A1[T1] - 3 Conjugate[A2[T1]]^2 η̃2 A2[T1] +
      6 Conjugate[A1[T1]] Conjugate[A2[T1]] η̃2 A3[T1] - 6 Conjugate[A2[T1]] Conjugate[A3[T1]] η̃2 A3[T1]) +
    e^(i T0 (ω2-3 ω1))
     (-3 Conjugate[A1[T1]]^2 η̃2 A2[T1] + 6 Conjugate[A1[T1]] Conjugate[A3[T1]] η̃2 A2[T1] -
      3 Conjugate[A3[T1]]^2 η̃2 A2[T1]) +
    e^(-i T0 (ω2-ω1))
     (-3 Conjugate[A2[T1]] η̃2 A1[T1]^2 + 6 Conjugate[A2[T1]] η̃2 A1[T1] A3[T1] -
      3 Conjugate[A2[T1]] η̃2 A3[T1]^2) +
    e^(i T0 (ω2+ω1)) (-3 η̃2 A1[T1]^2 A2[T1] + 6 η̃2 A1[T1] A2[T1] A3[T1] -
      3 η̃2 A2[T1] A3[T1]^2) +
    e^(-i T0 (ω2+3 ω1))
     (-3 Conjugate[A1[T1]]^2 Conjugate[A2[T1]] η̃2 + 6 Conjugate[A1[T1]] Conjugate[A2[T1]] Conjugate[A3[T1]] η̃2 -
      3 Conjugate[A2[T1]] Conjugate[A3[T1]]^2 η̃2) +
    e^(i T0 (2 ω2-2 ω1)) (3 Conjugate[A1[T1]] η̃2 A2[T1]^2 - 3 Conjugate[A3[T1]] η̃2 A2[T1]^2) +
    e^(-2 i T0 ω2) (3 Conjugate[A2[T1]]^2 η̃2 A1[T1] - 3 Conjugate[A2[T1]]^2 η̃2 A3[T1]));
```

Multiply out the term $e^{i T_0 \omega_1}$ in In[1]:

In[2]:=
```
RHS1 == e^(i T0 (2 ω2+ω1)) (3 η̃2 A1[T1] A2[T1]^2 - 3 η̃2 A2[T1]^2 A3[T1]) +
  e^(-i T0 (2 ω2+ω1)) (3 Conjugate[A1[T1]] Conjugate[A2[T1]]^2 η̃2 - 3 Conjugate[A2[T1]]^2 Conjugate[A3[T1]] η̃2) +
  e^(3 i T0 ω1) (-η̃1 A1[T1]^3 + η̃2 A1[T1]^3 - 3 η̃2 A1[T1]^2 A3[T1] +
    3 η̃2 A1[T1] A3[T1]^2 - η̃2 A3[T1]^3) +
  e^(-3 i T0 ω1) (-Conjugate[A1[T1]]^3 η̃1 + Conjugate[A1[T1]]^3 η̃2 - 3 Conjugate[A1[T1]]^2 Conjugate[A3[T1]] η̃2 +
    3 Conjugate[A1[T1]] Conjugate[A3[T1]]^2 η̃2 - Conjugate[A3[T1]]^3 η̃2) +
  e^(i T0 ω2) (γ̃2 A2[T1] + 2 i ω2 ξ̃2 A2[T1] - 6 Conjugate[A1[T1]] η̃2 A1[T1] A2[T1] +
    6 Conjugate[A3[T1]] η̃2 A1[T1] A2[T1] - 3 Conjugate[A2[T1]] η̃2 A2[T1]^2 +
    6 Conjugate[A1[T1]] η̃2 A2[T1] A3[T1] - 6 Conjugate[A3[T1]] η̃2 A2[T1] A3[T1]) +
  e^(-i T0 ω2) (Conjugate[A2[T1]] γ̃2 - 2 i Conjugate[A2[T1]] ω2 ξ̃2 - 6 Conjugate[A1[T1]] Conjugate[A2[T1]] η̃2 A1[T1] +
    6 Conjugate[A2[T1]] Conjugate[A3[T1]] η̃2 A1[T1] - 3 Conjugate[A2[T1]]^2 η̃2 A2[T1] +
    6 Conjugate[A1[T1]] Conjugate[A2[T1]] η̃2 A3[T1] - 6 Conjugate[A2[T1]] Conjugate[A3[T1]] η̃2 A3[T1]) +
  e^(i T0 (ω2-2 ω1))
   (-3 Conjugate[A1[T1]]^2 η̃2 A2[T1] + 6 Conjugate[A1[T1]] Conjugate[A3[T1]] η̃2 A2[T1] -
    3 Conjugate[A3[T1]]^2 η̃2 A2[T1]) +
  e^(-i T0 (ω2-2 ω1))
   (-3 Conjugate[A2[T1]] η̃2 A1[T1]^2 + 6 Conjugate[A2[T1]] η̃2 A1[T1] A3[T1] -
    3 Conjugate[A2[T1]] η̃2 A3[T1]^2) +
  e^(i T0 (ω2+2 ω1))
   (-3 η̃2 A1[T1]^2 A2[T1] + 6 η̃2 A1[T1] A2[T1] A3[T1] -
    3 η̃2 A2[T1] A3[T1]^2) +
  e^(-i T0 (ω2+2 ω1))
   (-3 Conjugate[A1[T1]]^2 Conjugate[A2[T1]] η̃2 + 6 Conjugate[A1[T1]] Conjugate[A2[T1]] Conjugate[A3[T1]] η̃2 -
    3 Conjugate[A2[T1]] Conjugate[A3[T1]]^2 η̃2) +
  e^(i T0 (2 ω2-ω1)) (3 Conjugate[A1[T1]] η̃2 A2[T1]^2 - 3 Conjugate[A3[T1]] η̃2 A2[T1]^2) +
  e^(-i T0 (2 ω2-ω1)) (3 Conjugate[A2[T1]]^2 η̃2 A1[T1] - 3 Conjugate[A2[T1]]^2 η̃2 A3[T1]);
```

Assume trial solution for x_{11} (Note: E and I are not used here as they are Mathematica's reserved letters.):

In[3]:=
```
x11 = B e^(i T0 (2 ω2+ω1)) + C e^(-i T0 (2 ω2+ω1)) + D e^(3 i T0 ω1) + F e^(-3 i T0 ω1) +
  G e^(i T0 ω2) + H e^(-i T0 ω2) + J e^(i T0 (ω2-2 ω1)) + K e^(-i T0 (ω2-2 ω1)) +
  L e^(i T0 (ω2+2 ω1)) + M e^(-i T0 (ω2+2 ω1)) + N e^(i T0 (2 ω2-ω1)) + O e^(-i T0 (2 ω2-ω1));
```

Differentiate In[3] by 2 times:

In[4]:=
```
D[x11, {T0, 2}]
```

Out[4]=
```
-9 D e^(3 i T0 ω1) ω1^2 - 9 e^(-3 i T0 ω1) F ω1^2 - e^(i T0 ω2) G ω2^2 - e^(-i T0 ω2) H ω2^2 -
  e^(i T0 (-2 ω1+ω2)) J (-2 ω1 + ω2)^2 - e^(-i T0 (-2 ω1+ω2)) K (-2 ω1 + ω2)^2 -
  e^(i T0 (2 ω1+ω2)) L (2 ω1 + ω2)^2 - e^(-i T0 (2 ω1+ω2)) M (2 ω1 + ω2)^2 -
  e^(i T0 (-ω1+2 ω2)) N (-ω1 + 2 ω2)^2 - e^(-i T0 (-ω1+2 ω2)) O (-ω1 + 2 ω2)^2 -
  C e^(-i T0 (ω1+2 ω2)) (ω1 + 2 ω2)^2 - B e^(i T0 (ω1+2 ω2)) (ω1 + 2 ω2)^2
```

From L.H.S. of equation (3.3-30):

In[5]:=
```
D[x11, {T0, 2}] + ω1^2 x11
```

Out[5]=
```
-9 D E^(3 i T0 ω1) ω1^2 - 9 E^(-3 i T0 ω1) F ω1^2 +
 (D E^(3 i T0 ω1) + C E^(-i T0 (ω1+2 ω2)) + B E^(i T0 (ω1+2 ω2)) + E^(-3 i T0 ω1) F + E^(i T0 ω2) G +
    E^(-i T0 ω2) H + E^(i T0 (-2 ω1+ω2)) J + E^(-i T0 (-2 ω1+ω2)) K + E^(i T0 (2 ω1+ω2)) L +
    E^(-i T0 (2 ω1+ω2)) M + E^(i T0 (-ω1+2 ω2)) N + E^(-i T0 (-ω1+2 ω2)) O) ω1^2 -
 E^(i T0 ω2) G ω2^2 - E^(-i T0 ω2) H ω2^2 - E^(i T0 (-2 ω1+ω2)) J (-2 ω1 + ω2)^2 -
 E^(-i T0 (-2 ω1+ω2)) K (-2 ω1 + ω2)^2 -
 E^(i T0 (2 ω1+ω2)) L (2 ω1 + ω2)^2 - E^(-i T0 (2 ω1+ω2)) M (2 ω1 + ω2)^2 -
 E^(i T0 (-ω1+2 ω2)) N (-ω1 + 2 ω2)^2 - E^(-i T0 (-ω1+2 ω2)) O (-ω1 + 2 ω2)^2 -
 C E^(-i T0 (ω1+2 ω2)) (ω1 + 2 ω2)^2 - B E^(i T0 (ω1+2 ω2)) (ω1 + 2 ω2)^2
```

Simplifying Out[5] above:

In[6]:=
```
B E^(i T0 (ω1+2 ω2)) (ω1^2 - (ω1 + 2 ω2)^2) + C E^(-i T0 (ω1+2 ω2)) (ω1^2 - (ω1 + 2 ω2)^2) -
 8 D E^(3 i T0 ω1) ω1^2 - 8 E^(-3 i T0 ω1) F ω1^2 + E^(i T0 ω2) G (ω1^2 - ω2^2) +
 E^(-i T0 ω2) H (ω1^2 - ω2^2) + E^(i T0 (-2 ω1+ω2)) J (ω1^2 - (-2 ω1 + ω2)^2) +
 E^(-i T0 (-2 ω1+ω2)) K (ω1^2 - (-2 ω1 + ω2)^2) + E^(i T0 (2 ω1+ω2)) L (ω1^2 - (2 ω1 + ω2)^2) +
 E^(-i T0 (2 ω1+ω2)) M (ω1^2 - (2 ω1 + ω2)^2) + E^(i T0 (-ω1+2 ω2)) N (ω1^2 - (-ω1 + 2 ω2)^2) +
 E^(-i T0 (-ω1+2 ω2)) O (ω1^2 - (-ω1 + 2 ω2)^2);
```

Referring to In[2], solution to x_{11} can be derived:

In[7]:=
```
B == 1/(ω1^2 - (ω1 + 2 ω2)^2) (3 η̃2 A1[T1] A2[T1]^2 - 3 η̃2 A2[T1]^2 A3[T1]);

C == 1/(ω1^2 - (ω1 + 2 ω2)^2) (3 Conjugate[A1[T1]] Conjugate[A2[T1]]^2 η̃2 - 3 Conjugate[A2[T1]]^2 Conjugate[A3[T1]] η̃2);

D ==
 -1/(8 ω1^2) (-η̃1 A1[T1]^3 + η̃2 A1[T1]^3 - 3 η̃2 A1[T1]^2 A3[T1] +
    3 η̃2 A1[T1] A3[T1]^2 - η̃2 A3[T1]^3);

F ==
 -1/(8 ω1^2) (-Conjugate[A1[T1]]^3 η̃1 + Conjugate[A1[T1]]^3 η̃2 - 3 Conjugate[A1[T1]]^2 Conjugate[A3[T1]] η̃2 +
    3 Conjugate[A1[T1]] Conjugate[A3[T1]]^2 η̃2 - Conjugate[A3[T1]]^3 η̃2);

G ==
 1/(ω1^2 - ω2^2) (γ̃2 A2[T1] + 2 i ω2 ξ̃2 A2[T1] - 6 Conjugate[A1[T1]] η̃2 A1[T1] A2[T1] +
    6 Conjugate[A3[T1]] η̃2 A1[T1] A2[T1] - 3 Conjugate[A2[T1]] η̃2 A2[T1]^2 +
    6 Conjugate[A1[T1]] η̃2 A2[T1] A3[T1] - 6 Conjugate[A3[T1]] η̃2 A2[T1] A3[T1]);

H ==
 1/(ω1^2 - ω2^2)
  (Conjugate[A2[T1]] γ̃2 - 2 i Conjugate[A2[T1]] ω2 ξ̃2 - 6 Conjugate[A1[T1]] Conjugate[A2[T1]] η̃2 A1[T1] +
    6 Conjugate[A2[T1]] Conjugate[A3[T1]] η̃2 A1[T1] - 3 Conjugate[A2[T1]]^2 η̃2 A2[T1] +
    6 Conjugate[A1[T1]] Conjugate[A2[T1]] η̃2 A3[T1] - 6 Conjugate[A2[T1]] Conjugate[A3[T1]] η̃2 A3[T1]);

J == 1/(ω1^2 - (-2 ω1 + ω2)^2)
  (-3 Conjugate[A1[T1]]^2 η̃2 A2[T1] + 6 Conjugate[A1[T1]] Conjugate[A3[T1]] η̃2 A2[T1] -
    3 Conjugate[A3[T1]]^2 η̃2 A2[T1]);
```

$$K == \frac{1}{\omega_1^2 - (-2\omega_1 + \omega_2)^2}$$
$$(-3\,\overline{A_2[T_1]}\,\tilde{\eta}_2\,A_1[T_1]^2 + 6\,\overline{A_2[T_1]}\,\tilde{\eta}_2\,A_1[T_1]\,A_3[T_1] -$$
$$3\,\overline{A_2[T_1]}\,\tilde{\eta}_2\,A_3[T_1]^2);$$

$$L == \frac{1}{\omega_1^2 - (2\omega_1 + \omega_2)^2}$$
$$(-3\,\tilde{\eta}_2\,A_1[T_1]^2\,A_2[T_1] + 6\,\tilde{\eta}_2\,A_1[T_1]\,A_2[T_1]\,A_3[T_1] -$$
$$3\,\tilde{\eta}_2\,A_2[T_1]\,A_3[T_1]^2);$$

$$M == \frac{1}{\omega_1^2 - (2\omega_1 + \omega_2)^2}$$
$$(-3\,\overline{A_1[T_1]}^2\,\overline{A_2[T_1]}\,\tilde{\eta}_2 + 6\,\overline{A_1[T_1]}\,\overline{A_2[T_1]}\,\overline{A_3[T_1]}\,\tilde{\eta}_2 -$$
$$3\,\overline{A_2[T_1]}\,\overline{A_3[T_1]}^2\,\tilde{\eta}_2);$$

$$N == \frac{1}{\omega_1^2 - (-\omega_1 + 2\omega_2)^2}\,(3\,\overline{A_1[T_1]}\,\tilde{\eta}_2\,A_2[T_1]^2 - 3\,\overline{A_3[T_1]}\,\tilde{\eta}_2\,A_2[T_1]^2);$$

$$O == \frac{1}{\omega_1^2 - (-\omega_1 + 2\omega_2)^2}\,(3\,\overline{A_2[T_1]}^2\,\tilde{\eta}_2\,A_1[T_1] - 3\,\overline{A_2[T_1]}^2\,\tilde{\eta}_2\,A_3[T_1]);$$

Substitute In[7] - In[18] into In[3], solution to x_{11} is derived as:

In[19]:=

$$x_{11} =$$
$$e^{i T_0 (2\omega_2+\omega_1)}\left(\frac{1}{\omega_1^2 - (\omega_1 + 2\omega_2)^2}\,(3\,\tilde{\eta}_2\,A_1[T_1]\,A_2[T_1]^2 - 3\,\tilde{\eta}_2\,A_2[T_1]^2\,A_3[T_1])\right) +$$
$$e^{-i T_0 (2\omega_2+\omega_1)}\left(\frac{1}{\omega_1^2 - (\omega_1 + 2\omega_2)^2}\,(3\,\overline{A_1[T_1]}\,\overline{A_2[T_1]}^2\,\tilde{\eta}_2 - 3\,\overline{A_2[T_1]}^2\,\overline{A_3[T_1]}\,\tilde{\eta}_2)\right) -$$
$$e^{3 i T_0 \omega_1}\left(\frac{1}{8\omega_1^2}\,(-\tilde{\eta}_1\,A_1[T_1]^3 + \tilde{\eta}_2\,A_1[T_1]^3 - 3\,\tilde{\eta}_2\,A_1[T_1]^2\,A_3[T_1] +\right.$$
$$\left. 3\,\tilde{\eta}_2\,A_1[T_1]\,A_3[T_1]^2 - \tilde{\eta}_2\,A_3[T_1]^3)\right) -$$
$$e^{-3 i T_0 \omega_1}\left(\frac{1}{8\omega_1^2}\,(-\overline{A_1[T_1]}^3\,\tilde{\eta}_1 + \overline{A_1[T_1]}^3\,\tilde{\eta}_2 - 3\,\overline{A_1[T_1]}^2\,\overline{A_3[T_1]}\,\tilde{\eta}_2 +\right.$$
$$\left. 3\,\overline{A_1[T_1]}\,\overline{A_3[T_1]}^2\,\tilde{\eta}_2 - \overline{A_3[T_1]}^3\,\tilde{\eta}_2)\right) +$$
$$e^{i T_0 \omega_2}\left(\frac{1}{\omega_1^2 - \omega_2^2}\,(\tilde{\gamma}_2\,A_2[T_1] + 2\,i\,\omega_2\,\tilde{\xi}_2\,A_2[T_1] - 6\,\overline{A_1[T_1]}\,\tilde{\eta}_2\,A_1[T_1]\,A_2[T_1] +\right.$$
$$6\,\overline{A_3[T_1]}\,\tilde{\eta}_2\,A_1[T_1]\,A_2[T_1] - 3\,\overline{A_2[T_1]}\,\tilde{\eta}_2\,A_2[T_1]^2 +$$
$$\left. 6\,\overline{A_1[T_1]}\,\tilde{\eta}_2\,A_2[T_1]\,A_3[T_1] - 6\,\overline{A_3[T_1]}\,\tilde{\eta}_2\,A_2[T_1]\,A_3[T_1])\right) +$$
$$e^{-i T_0 \omega_2}\left(\frac{1}{\omega_1^2 - \omega_2^2}\,(\overline{A_2[T_1]}\,\tilde{\gamma}_2 - 2\,i\,\overline{A_2[T_1]}\,\omega_2\,\tilde{\xi}_2 - 6\,\overline{A_1[T_1]}\,\overline{A_2[T_1]}\,\tilde{\eta}_2\,A_1[T_1] +\right.$$
$$6\,\overline{A_2[T_1]}\,\overline{A_3[T_1]}\,\tilde{\eta}_2\,A_1[T_1] - 3\,\overline{A_2[T_1]}^2\,\tilde{\eta}_2\,A_2[T_1] +$$
$$\left. 6\,\overline{A_1[T_1]}\,\overline{A_2[T_1]}\,\tilde{\eta}_2\,A_3[T_1] - 6\,\overline{A_2[T_1]}\,\overline{A_3[T_1]}\,\tilde{\eta}_2\,A_3[T_1])\right) +$$

$$e^{\dot{n}\,T_0\,(\omega_2-2\,\omega_1)}\left(\frac{1}{\omega_1^2-(-2\,\omega_1+\omega_2)^2}\left(-3\,\overline{A_1[T_1]}^2\,\tilde{\eta}_2\,A_2[T_1]+6\,\overline{A_1[T_1]}\,\overline{A_3[T_1]}\,\tilde{\eta}_2\,A_2[T_1]-3\,\overline{A_3[T_1]}^2\,\tilde{\eta}_2\,A_2[T_1]\right)\right)+$$

$$e^{-\dot{n}\,T_0\,(\omega_2-2\,\omega_1)}\left(\frac{1}{\omega_1^2-(-2\,\omega_1+\omega_2)^2}\left(-3\,\overline{A_2[T_1]}\,\tilde{\eta}_2\,A_1[T_1]^2+6\,\overline{A_2[T_1]}\,\tilde{\eta}_2\,A_1[T_1]\,A_3[T_1]-3\,\overline{A_2[T_1]}\,\tilde{\eta}_2\,A_3[T_1]^2\right)\right)+$$

$$e^{\dot{n}\,T_0\,(\omega_2+2\,\omega_1)}\left(\frac{1}{\omega_1^2-(2\,\omega_1+\omega_2)^2}\left(-3\,\tilde{\eta}_2\,A_1[T_1]^2\,A_2[T_1]+6\,\tilde{\eta}_2\,A_1[T_1]\,A_2[T_1]\,A_3[T_1]-3\,\tilde{\eta}_2\,A_2[T_1]\,A_3[T_1]^2\right)\right)+$$

$$e^{-\dot{n}\,T_0\,(\omega_2+2\,\omega_1)}\left(\frac{1}{\omega_1^2-(2\,\omega_1+\omega_2)^2}\left(-3\,\overline{A_1[T_1]}^2\,\overline{A_2[T_1]}\,\tilde{\eta}_2+6\,\overline{A_1[T_1]}\,\overline{A_2[T_1]}\,\overline{A_3[T_1]}\,\tilde{\eta}_2-3\,\overline{A_2[T_1]}\,\overline{A_3[T_1]}^2\,\tilde{\eta}_2\right)\right)+$$

$$e^{\dot{n}\,T_0\,(2\,\omega_2-\omega_1)}\left(\frac{1}{\omega_1^2-(-\omega_1+2\,\omega_2)^2}\left(3\,\overline{A_1[T_1]}\,\tilde{\eta}_2\,A_2[T_1]^2-3\,\overline{A_3[T_1]}\,\tilde{\eta}_2\,A_2[T_1]^2\right)\right)+$$

$$e^{-\dot{n}\,T_0\,(2\,\omega_2-\omega_1)}\left(\frac{1}{\omega_1^2-(-\omega_1+2\,\omega_2)^2}\left(3\,\overline{A_2[T_1]}^2\,\tilde{\eta}_2\,A_1[T_1]-3\,\overline{A_2[T_1]}^2\,\tilde{\eta}_2\,A_3[T_1]\right)\right);$$

■ Counter – Checking the Solution to x_{11} :

(START of Checking .....)

In[20]:=
```
D[x11, {T0, 2}] + ω1^2 x11;
```

Divide Out[20] by In[2], gives a solution of 1 which proves that x_{11} is correctly derived:

In[21]:=
```
FullSimplify[
  (%) / (e^(n̂ T0 (2 ω2+ω1)) (3 η̃2 A1[T1] A2[T1]^2 - 3 η̃2 A2[T1]^2 A3[T1]) +
    e^(-n̂ T0 (2 ω2+ω1)) (3 Conjugate[A1[T1]] Conjugate[A2[T1]]^2 η̃2 - 3 Conjugate[A2[T1]]^2 Conjugate[A3[T1]] η̃2) +
    e^(3 n̂ T0 ω1) (-η̃1 A1[T1]^3 + η̃2 A1[T1]^3 - 3 η̃2 A1[T1]^2 A3[T1] +
      3 η̃2 A1[T1] A3[T1]^2 - η̃2 A3[T1]^3) +
    e^(-3 n̂ T0 ω1) (-Conjugate[A1[T1]]^3 η̃1 + Conjugate[A1[T1]]^3 η̃2 - 3 Conjugate[A1[T1]]^2 Conjugate[A3[T1]] η̃2 +
      3 Conjugate[A1[T1]] Conjugate[A3[T1]]^2 η̃2 - Conjugate[A3[T1]]^3 η̃2) +
    e^(n̂ T0 ω2) (γ̃2 A2[T1] + 2 n̂ ω2 ξ̃2 A2[T1] - 6 Conjugate[A1[T1]] η̃2 A1[T1] A2[T1] +
      6 Conjugate[A3[T1]] η̃2 A1[T1] A2[T1] - 3 Conjugate[A2[T1]] η̃2 A2[T1]^2 +
      6 Conjugate[A1[T1]] η̃2 A2[T1] A3[T1] - 6 Conjugate[A3[T1]] η̃2 A2[T1] A3[T1]) +
    e^(-n̂ T0 ω2) (Conjugate[A2[T1]] γ̃2 - 2 n̂ Conjugate[A2[T1]] ω2 ξ̃2 - 6 Conjugate[A1[T1]] Conjugate[A2[T1]] η̃2 A1[T1] +
      6 Conjugate[A2[T1]] Conjugate[A3[T1]] η̃2 A1[T1] - 3 Conjugate[A2[T1]]^2 η̃2 A2[T1] +
      6 Conjugate[A1[T1]] Conjugate[A2[T1]] η̃2 A3[T1] - 6 Conjugate[A2[T1]] Conjugate[A3[T1]] η̃2 A3[T1]) +
```

```
e^(i n T0 (ω2 - 2 ω1))
  (-3 Conjugate[A1[T1]]^2 η2 A2[T1] + 6 Conjugate[A1[T1]] Conjugate[A3[T1]] η2 A2[T1] -
     3 Conjugate[A3[T1]]^2 η2 A2[T1]) +
e^(-i n T0 (ω2 - 2 ω1))
  (-3 Conjugate[A2[T1]] η2 A1[T1]^2 + 6 Conjugate[A2[T1]] η2 A1[T1] A3[T1] -
     3 Conjugate[A2[T1]] η2 A3[T1]^2) +
e^(i n T0 (ω2 + 2 ω1))
  (-3 η2 A1[T1]^2 A2[T1] + 6 η2 A1[T1] A2[T1] A3[T1] -
     3 η2 A2[T1] A3[T1]^2) +
e^(-i n T0 (ω2 + 2 ω1))
  (-3 Conjugate[A1[T1]]^2 Conjugate[A2[T1]] η2 + 6 Conjugate[A1[T1]] Conjugate[A2[T1]] Conjugate[A3[T1]] η2 -
     3 Conjugate[A2[T1]] Conjugate[A3[T1]]^2 η2) +
e^(i n T0 (2 ω2 - ω1)) (3 Conjugate[A1[T1]] η2 A2[T1]^2 - 3 Conjugate[A3[T1]] η2 A2[T1]^2) +
e^(-i n T0 (2 ω2 - ω1)) (3 Conjugate[A2[T1]]^2 η2 A1[T1] - 3 Conjugate[A2[T1]]^2 η2 A3[T1]))]
```

Out[21]= 1

(..... END of Checking)

C.4 Deriving the 'Always' Secular Terms for x_{21}

From equation (3.3 - 34) & (3.3 - 35) :

```
In[1]:= x10 = A1[T1] e^(i×ω1×T0) + Conjugate[A1[T1]] e^(-i×ω1×T0);
        x20 = A2[T1] e^(i×ω2×T0) + Conjugate[A2[T1]] e^(-i×ω2×T0) + A3[T1] e^(i×ω1×T0) +
          Conjugate[A3[T1]] e^(-i×ω1×T0);

In[3]:= D[x10, T0]

Out[3]= -i e^(-i T0 ω1) Conjugate[A1[T1]] ω1 + i e^(i T0 ω1) ω1 A1[T1]

In[4]:= D[x20, T0]

Out[4]= -i e^(-i T0 ω1) Conjugate[A3[T1]] ω1 - i e^(-i T0 ω2) Conjugate[A2[T1]] ω2 +
         i e^(i T0 ω2) ω2 A2[T1] + i e^(i T0 ω1) ω1 A3[T1]

In[5]:= D[D[x20, T0], T1]

Out[5]= i e^(i T0 ω2) ω2 A2'[T1] - i e^(-i T0 ω2) ω2 OverBar'[A2[T1]] A2'[T1] +
         i e^(i T0 ω1) ω1 A3'[T1] - i e^(-i T0 ω1) ω1 OverBar'[A3[T1]] A3'[T1]
```

From equation In[19] of Appendix C.3 :

```
In[6]:= x11 =
          e^(i T0 (2 ω2+ω1))
            (1/(ω1^2 - (ω1 + 2 ω2)^2) (3 η2~ A1[T1] A2[T1]^2 - 3 η2~ A2[T1]^2 A3[T1])) +
          e^(-i T0 (2 ω2+ω1))
            (1/(ω1^2 - (ω1 + 2 ω2)^2) (3 Conjugate[A1[T1]] Conjugate[A2[T1]]^2 η2~ -
              3 Conjugate[A2[T1]]^2 Conjugate[A3[T1]] η2~)) -
          e^(3 i T0 ω1)
            (1/(8 ω1^2) (-η1~ A1[T1]^3 + η2~ A1[T1]^3 - 3 η2~ A1[T1]^2 A3[T1] +
              3 η2~ A1[T1] A3[T1]^2 - η2~ A3[T1]^3)) -
          e^(-3 i T0 ω1)
            (1/(8 ω1^2) (-Conjugate[A1[T1]]^3 η1~ + Conjugate[A1[T1]]^3 η2~ -
              3 Conjugate[A1[T1]]^2 Conjugate[A3[T1]] η2~ +
              3 Conjugate[A1[T1]] Conjugate[A3[T1]]^2 η2~ - Conjugate[A3[T1]]^3 η2~)) +
          e^(i T0 ω2)
            (1/(ω1^2 - ω2^2) (γ2~ A2[T1] + 2 i ω2 ξ2~ A2[T1] - 6 Conjugate[A1[T1]] η2~ A1[T1] A2[T1] +
              6 Conjugate[A3[T1]] η2~ A1[T1] A2[T1] - 3 Conjugate[A2[T1]] η2~ A2[T1]^2 +
              6 Conjugate[A1[T1]] η2~ A2[T1] A3[T1] - 6 Conjugate[A3[T1]] η2~ A2[T1] A3[T1])) +
          e^(-i T0 ω2)
            (1/(ω1^2 - ω2^2) (Conjugate[A2[T1]] γ2~ - 2 i Conjugate[A2[T1]] ω2 ξ2~ -
              6 Conjugate[A1[T1]] Conjugate[A2[T1]] η2~ A1[T1] +
              6 Conjugate[A2[T1]] Conjugate[A3[T1]] η2~ A1[T1] - 3 Conjugate[A2[T1]]^2 η2~ A2[T1] +
              6 Conjugate[A1[T1]] Conjugate[A2[T1]] η2~ A3[T1] - 6 Conjugate[A2[T1]] Conjugate[A3[T1]] η2~ A3[T1])) +
```

$$e^{i n T_0 (\omega_2 - 2\omega_1)} \left(\frac{1}{\omega_1^2 - (-2\omega_1 + \omega_2)^2} \left(-3 \overline{A_1[T_1]}^2 \tilde{\eta}_2 A_2[T_1] + 6 \overline{A_1[T_1]}\, \overline{A_3[T_1]}\, \tilde{\eta}_2 A_2[T_1] - 3 \overline{A_3[T_1]}^2 \tilde{\eta}_2 A_2[T_1] \right) \right) +$$

$$e^{-i n T_0 (\omega_2 - 2\omega_1)} \left(\frac{1}{\omega_1^2 - (-2\omega_1 + \omega_2)^2} \left(-3 \overline{A_2[T_1]}\, \tilde{\eta}_2 A_1[T_1]^2 + 6 \overline{A_2[T_1]}\, \tilde{\eta}_2 A_1[T_1] A_3[T_1] - 3 \overline{A_2[T_1]}\, \tilde{\eta}_2 A_3[T_1]^2 \right) \right) +$$

$$e^{i n T_0 (\omega_2 + 2\omega_1)} \left(\frac{1}{\omega_1^2 - (2\omega_1 + \omega_2)^2} \left(-3 \tilde{\eta}_2 A_1[T_1]^2 A_2[T_1] + 6 \tilde{\eta}_2 A_1[T_1] A_2[T_1] A_3[T_1] - 3 \tilde{\eta}_2 A_2[T_1] A_3[T_1]^2 \right) \right) +$$

$$e^{-i n T_0 (\omega_2 + 2\omega_1)} \left(\frac{1}{\omega_1^2 - (2\omega_1 + \omega_2)^2} \left(-3 \overline{A_1[T_1]}^2 \overline{A_2[T_1]}\, \tilde{\eta}_2 + 6 \overline{A_1[T_1]}\, \overline{A_2[T_1]}\, \overline{A_3[T_1]}\, \tilde{\eta}_2 - 3 \overline{A_2[T_1]}\, \overline{A_3[T_1]}^2 \tilde{\eta}_2 \right) \right) +$$

$$e^{i n T_0 (2\omega_2 - \omega_1)} \left(\frac{1}{\omega_1^2 - (-\omega_1 + 2\omega_2)^2} \left(3 \overline{A_1[T_1]}\, \tilde{\eta}_2 A_2[T_1]^2 - 3 \overline{A_3[T_1]}\, \tilde{\eta}_2 A_2[T_1]^2 \right) \right) +$$

$$e^{-i n T_0 (2\omega_2 - \omega_1)} \left(\frac{1}{\omega_1^2 - (-\omega_1 + 2\omega_2)^2} \left(3 \overline{A_2[T_1]}^2 \tilde{\eta}_2 A_1[T_1] - 3 \overline{A_2[T_1]}^2 \tilde{\eta}_2 A_3[T_1] \right) \right);$$

Let Right - Hand Side of equation (3.3 - 31) = RHS2

Substitute In[1] to In[6] into RHS2 :

In[7]:=
```
RHS2 = 2 ξ̃3 D[x10, T0] - 2 ξ̃3 D[x20, T0] - 2 D[D[x20, T0], T1] +
       ω2^2 × x11 + η̃3 (x20^3 + 3 × x10^2 × x20 - 3 × x10 × x20^2 - x10^3)
```

Out[7]=

$$\begin{aligned}
&2\tilde{\xi}_3 \left(-i e^{-i n T_0 \omega_1} \overline{A_1[T_1]}\, \omega_1 + i e^{i n T_0 \omega_1} \omega_1 A_1[T_1] \right) - \\
&2\tilde{\xi}_3 \left(-i e^{-i n T_0 \omega_1} \overline{A_3[T_1]}\, \omega_1 - i e^{-i n T_0 \omega_2} \overline{A_2[T_1]}\, \omega_2 + i e^{i n T_0 \omega_2} \omega_2 A_2[T_1] + \right. \\
&\quad \left. i e^{i n T_0 \omega_1} \omega_1 A_3[T_1] \right) + \tilde{\eta}_3 \left(-\left(e^{-i n T_0 \omega_1} \overline{A_1[T_1]} + e^{i n T_0 \omega_1} A_1[T_1] \right)^3 + \right. \\
&3 \left(e^{-i n T_0 \omega_1} \overline{A_1[T_1]} + e^{i n T_0 \omega_1} A_1[T_1] \right)^2 \\
&\quad \left(e^{-i n T_0 \omega_2} \overline{A_2[T_1]} + e^{-i n T_0 \omega_1} \overline{A_3[T_1]} + e^{i n T_0 \omega_2} A_2[T_1] + e^{i n T_0 \omega_1} A_3[T_1] \right) - \\
&3 \left(e^{-i n T_0 \omega_1} \overline{A_1[T_1]} + e^{i n T_0 \omega_1} A_1[T_1] \right) \\
&\quad \left(e^{-i n T_0 \omega_2} \overline{A_2[T_1]} + e^{-i n T_0 \omega_1} \overline{A_3[T_1]} + e^{i n T_0 \omega_2} A_2[T_1] + e^{i n T_0 \omega_1} A_3[T_1] \right)^2 + \\
&\left. \left(e^{-i n T_0 \omega_2} \overline{A_2[T_1]} + e^{-i n T_0 \omega_1} \overline{A_3[T_1]} + e^{i n T_0 \omega_2} A_2[T_1] + e^{i n T_0 \omega_1} A_3[T_1] \right)^3 \right) + \\
&\omega_2^2 \left(\frac{e^{-i n T_0 (\omega_1 + 2\omega_2)} \left(3 \overline{A_1[T_1]}\, \overline{A_2[T_1]}^2 \tilde{\eta}_2 - 3 \overline{A_2[T_1]}^2 \overline{A_3[T_1]}\, \tilde{\eta}_2 \right)}{\omega_1^2 - (\omega_1 + 2\omega_2)^2} + \right. \\
&\frac{1}{\omega_1^2 - (2\omega_1 + \omega_2)^2} \left(e^{-i n T_0 (2\omega_1 + \omega_2)} \left(-3 \overline{A_1[T_1]}^2 \overline{A_2[T_1]}\, \tilde{\eta}_2 + \right. \right. \\
&\quad \left. \left. 6 \overline{A_1[T_1]}\, \overline{A_2[T_1]}\, \overline{A_3[T_1]}\, \tilde{\eta}_2 - 3 \overline{A_2[T_1]}\, \overline{A_3[T_1]}^2 \tilde{\eta}_2 \right) \right) - \frac{1}{8\omega_1^2} \\
&\left(e^{-3 i n T_0 \omega_1} \left(-\overline{A_1[T_1]}^3 \tilde{\eta}_1 + \overline{A_1[T_1]}^3 \tilde{\eta}_2 - 3 \overline{A_1[T_1]}^2 \overline{A_3[T_1]}\, \tilde{\eta}_2 + \right. \right. \\
&\quad \left. \left. 3 \overline{A_1[T_1]}\, \overline{A_3[T_1]}^2 \tilde{\eta}_2 - \overline{A_3[T_1]}^3 \tilde{\eta}_2 \right) \right) +
\end{aligned}$$

$$\frac{1}{\omega_1^2 - (-2\,\omega_1 + \omega_2)^2}\,(e^{i\,T_0\,(-2\,\omega_1+\omega_2)}\,(-3\,\overline{A_1[T_1]}^2\,\tilde{\eta}_2\,A_2[T_1] + 6\,\overline{A_1[T_1]}\,\overline{A_3[T_1]}\,\tilde{\eta}_2\,A_2[T_1] - 3\,\overline{A_3[T_1]}^2\,\tilde{\eta}_2\,A_2[T_1])) +$$

$$\frac{e^{i\,T_0\,(-\omega_1+2\,\omega_2)}\,(3\,\overline{A_1[T_1]}\,\tilde{\eta}_2\,A_2[T_1]^2 - 3\,\overline{A_3[T_1]}\,\tilde{\eta}_2\,A_2[T_1]^2)}{\omega_1^2 - (-\omega_1 + 2\,\omega_2)^2} +$$

$$\frac{e^{-i\,T_0\,(-\omega_1+2\,\omega_2)}\,(3\,\overline{A_2[T_1]}^2\,\tilde{\eta}_2\,A_1[T_1] - 3\,\overline{A_2[T_1]}^2\,\tilde{\eta}_2\,A_3[T_1])}{\omega_1^2 - (-\omega_1 + 2\,\omega_2)^2} + \frac{1}{\omega_1^2 - \omega_2^2}$$

$$(e^{-i\,T_0\,\omega_2}\,(\overline{A_2[T_1]}\,\tilde{\gamma}_2 - 2\,i\,\overline{A_2[T_1]}\,\omega_2\,\tilde{\zeta}_2 - 6\,\overline{A_1[T_1]}\,\overline{A_2[T_1]}\,\tilde{\eta}_2\,A_1[T_1] + 6\,\overline{A_2[T_1]}\,\overline{A_3[T_1]}\,\tilde{\eta}_2\,A_1[T_1] - 3\,\overline{A_2[T_1]}^2\,\tilde{\eta}_2\,A_2[T_1] +$$

$$6\,\overline{A_1[T_1]}\,\overline{A_2[T_1]}\,\tilde{\eta}_2\,A_3[T_1] - 6\,\overline{A_2[T_1]}\,\overline{A_3[T_1]}\,\tilde{\eta}_2\,A_3[T_1])) + \frac{1}{\omega_1^2 - \omega_2^2}$$

$$(e^{i\,T_0\,\omega_2}\,(\tilde{\gamma}_2\,A_2[T_1] + 2\,i\,\omega_2\,\tilde{\zeta}_2\,A_2[T_1] - 6\,\overline{A_1[T_1]}\,\tilde{\eta}_2\,A_1[T_1]\,A_2[T_1] + 6\,\overline{A_3[T_1]}\,\tilde{\eta}_2\,A_1[T_1]\,A_2[T_1] - 3\,\overline{A_2[T_1]}\,\tilde{\eta}_2\,A_2[T_1]^2 +$$

$$6\,\overline{A_1[T_1]}\,\tilde{\eta}_2\,A_2[T_1]\,A_3[T_1] - 6\,\overline{A_3[T_1]}\,\tilde{\eta}_2\,A_2[T_1]\,A_3[T_1])) +$$

$$\frac{e^{i\,T_0\,(\omega_1+2\,\omega_2)}\,(3\,\tilde{\eta}_2\,A_1[T_1]\,A_2[T_1]^2 - 3\,\tilde{\eta}_2\,A_2[T_1]^2\,A_3[T_1])}{\omega_1^2 - (\omega_1 + 2\,\omega_2)^2} +$$

$$\frac{1}{\omega_1^2 - (-2\,\omega_1 + \omega_2)^2}\,(e^{-i\,T_0\,(-2\,\omega_1+\omega_2)}\,(-3\,\overline{A_2[T_1]}\,\tilde{\eta}_2\,A_1[T_1]^2 + 6\,\overline{A_2[T_1]}\,\tilde{\eta}_2\,A_1[T_1]\,A_3[T_1] - 3\,\overline{A_2[T_1]}\,\tilde{\eta}_2\,A_3[T_1]^2)) +$$

$$\frac{1}{\omega_1^2 - (2\,\omega_1 + \omega_2)^2}\,(e^{i\,T_0\,(2\,\omega_1+\omega_2)}\,(-3\,\tilde{\eta}_2\,A_1[T_1]^2\,A_2[T_1] + 6\,\tilde{\eta}_2\,A_1[T_1]\,A_2[T_1]\,A_3[T_1] - 3\,\tilde{\eta}_2\,A_2[T_1]\,A_3[T_1]^2)) - \frac{1}{8\,\omega_1^2}$$

$$(e^{3\,i\,T_0\,\omega_1}\,(-\tilde{\eta}_1\,A_1[T_1]^3 + \tilde{\eta}_2\,A_1[T_1]^3 - 3\,\tilde{\eta}_2\,A_1[T_1]^2\,A_3[T_1] + 3\,\tilde{\eta}_2\,A_1[T_1]\,A_3[T_1]^2 - \tilde{\eta}_2\,A_3[T_1]^3))\Big) -$$

$$2\,(i\,e^{i\,T_0\,\omega_2}\,\omega_2\,A_2'[T_1] - i\,e^{-i\,T_0\,\omega_2}\,\omega_2\,\text{OverBar}'[A_2[T_1]]\,A_2'[T_1] + i\,e^{i\,T_0\,\omega_1}\,\omega_1\,A_3'[T_1] - i\,e^{-i\,T_0\,\omega_1}\,\omega_1\,\text{OverBar}'[A_3[T_1]]\,A_3'[T_1])$$

In[8]:= **RHS2 = ExpandAll[RHS2]**

Out[8]=

$$\frac{\overline{A_2[T_1]}\,\omega_2^2\,\tilde{\gamma}_2}{e^{i\,T_0\,\omega_2}\,\omega_1^2 - e^{i\,T_0\,\omega_2}\,\omega_2^2} - \frac{2\,i\,\overline{A_2[T_1]}\,\omega_2^3\,\tilde{\zeta}_2}{e^{i\,T_0\,\omega_2}\,\omega_1^2 - e^{i\,T_0\,\omega_2}\,\omega_2^2} -$$

$$2\,i\,e^{-i\,T_0\,\omega_1}\,\overline{A_1[T_1]}\,\omega_1\,\tilde{\zeta}_3 + 2\,i\,e^{-i\,T_0\,\omega_1}\,\overline{A_3[T_1]}\,\omega_1\,\tilde{\zeta}_3 +$$

$$2\,i\,e^{-i\,T_0\,\omega_2}\,\overline{A_2[T_1]}\,\omega_2\,\tilde{\zeta}_3 + \frac{e^{-3\,i\,T_0\,\omega_1}\,\overline{A_1[T_1]}^3\,\omega_2^2\,\tilde{\eta}_1}{8\,\omega_1^2} -$$

$$\frac{e^{-3\,i\,T_0\,\omega_1}\,\overline{A_1[T_1]}^3\,\omega_2^2\,\tilde{\eta}_2}{8\,\omega_1^2} + \frac{3\,e^{-3\,i\,T_0\,\omega_1}\,\overline{A_1[T_1]}^2\,\overline{A_3[T_1]}\,\omega_2^2\,\tilde{\eta}_2}{8\,\omega_1^2} -$$

$$\frac{3\,e^{-3\,i\,T_0\,\omega_1}\,\overline{A_1[T_1]}\,\overline{A_3[T_1]}^2\,\omega_2^2\,\tilde{\eta}_2}{8\,\omega_1^2} + \frac{e^{-3\,i\,T_0\,\omega_1}\,\overline{A_3[T_1]}^3\,\omega_2^2\,\tilde{\eta}_2}{8\,\omega_1^2} -$$

$$\frac{3\,\overline{A_1[T_1]}^2\,\overline{A_2[T_1]}\,\omega_2^2\,\tilde{\eta}_2}{-3\,e^{2\,i\,T_0\,\omega_1+i\,T_0\,\omega_2}\,\omega_1^2 - 4\,e^{2\,i\,T_0\,\omega_1+i\,T_0\,\omega_2}\,\omega_1\,\omega_2 - e^{2\,i\,T_0\,\omega_1+i\,T_0\,\omega_2}\,\omega_2^2} +$$

$$\frac{6\,\overline{A_1[T_1]}\,\overline{A_2[T_1]}\,\overline{A_3[T_1]}\,\omega_2^2\,\tilde{\eta}_2}{-3\,e^{2\,i\,T_0\,\omega_1+i\,T_0\,\omega_2}\,\omega_1^2 - 4\,e^{2\,i\,T_0\,\omega_1+i\,T_0\,\omega_2}\,\omega_1\,\omega_2 - e^{2\,i\,T_0\,\omega_1+i\,T_0\,\omega_2}\,\omega_2^2} -$$

$$\frac{3\,\overline{A_2[T_1]}\,\overline{A_3[T_1]}^2\,\omega_2^2\,\tilde{\eta}_2}{-3\,e^{2\,i\,T_0\,\omega_1+i\,T_0\,\omega_2}\,\omega_1^2 - 4\,e^{2\,i\,T_0\,\omega_1+i\,T_0\,\omega_2}\,\omega_1\,\omega_2 - e^{2\,i\,T_0\,\omega_1+i\,T_0\,\omega_2}\,\omega_2^2} +$$

$$\frac{3\,\overline{A_1[T_1]}\,\overline{A_2[T_1]}^2\,\omega_2^2\,\tilde{\eta}_2}{-4\,e^{i\,T_0\,\omega_1+2\,i\,T_0\,\omega_2}\,\omega_1\,\omega_2 - 4\,e^{i\,T_0\,\omega_1+2\,i\,T_0\,\omega_2}\,\omega_2^2} -$$

$$\frac{3\,\overline{A_2[T_1]}^2\,\overline{A_3[T_1]}\,\omega_2^2\,\tilde{\eta}_2}{-4\,e^{i\,T_0\,\omega_1+2\,i\,T_0\,\omega_2}\,\omega_1\,\omega_2 - 4\,e^{i\,T_0\,\omega_1+2\,i\,T_0\,\omega_2}\,\omega_2^2} -$$

$$e^{-3\,i\,T_0\,\omega_1}\,\overline{A_1[T_1]}^3\,\tilde{\eta}_3 + 3\,e^{-2\,i\,T_0\,\omega_1-i\,T_0\,\omega_2}\,\overline{A_1[T_1]}^2\,\overline{A_2[T_1]}\,\tilde{\eta}_3 -$$

$$3\,e^{-i\,T_0\,\omega_1-2\,i\,T_0\,\omega_2}\,\overline{A_1[T_1]}\,\overline{A_2[T_1]}^2\,\tilde{\eta}_3 +$$

$$e^{-3 i T_0 \omega_2} \overline{A_2[T_1]}^3 \tilde{\eta}_3 + 3 e^{-3 i T_0 \omega_1} \overline{A_1[T_1]}^2 \overline{A_3[T_1]} \tilde{\eta}_3 -$$
$$6 e^{-2 i T_0 \omega_1 - i T_0 \omega_2} \overline{A_1[T_1]}\, \overline{A_2[T_1]}\, \overline{A_3[T_1]} \tilde{\eta}_3 +$$
$$3 e^{-i T_0 \omega_1 - 2 i T_0 \omega_2} \overline{A_2[T_1]}^2 \overline{A_3[T_1]} \tilde{\eta}_3 -$$
$$3 e^{-3 i T_0 \omega_1} \overline{A_1[T_1]}\, \overline{A_3[T_1]}^2 \tilde{\eta}_3 + 3 e^{-2 i T_0 \omega_1 - i T_0 \omega_2} \overline{A_2[T_1]}\, \overline{A_3[T_1]}^2 \tilde{\eta}_3 +$$
$$e^{-3 i T_0 \omega_1} \overline{A_3[T_1]}^3 \tilde{\eta}_3 + 2 i e^{i T_0 \omega_1} \omega_1 \tilde{\zeta}_3 A_1[T_1] -$$
$$\frac{6 \overline{A_1[T_1]}\, \overline{A_2[T_1]}\, \omega_2^2 \tilde{\eta}_2 A_1[T_1]}{e^{i T_0 \omega_2} \omega_1^2 - e^{i T_0 \omega_2} \omega_2^2} + \frac{6 \overline{A_2[T_1]}\, \overline{A_3[T_1]}\, \omega_2^2 \tilde{\eta}_2 A_1[T_1]}{e^{i T_0 \omega_2} \omega_1^2 - e^{i T_0 \omega_2} \omega_2^2} +$$
$$\frac{3 \overline{A_2[T_1]}^2 \omega_2^2 \tilde{\eta}_2 A_1[T_1]}{4 e^{-i T_0 \omega_1 + 2 i T_0 \omega_2} \omega_1 \omega_2 - 4 e^{-i T_0 \omega_1 + 2 i T_0 \omega_2} \omega_2^2} -$$
$$3 e^{-i T_0 \omega_1} \overline{A_1[T_1]}^2 \tilde{\eta}_3 A_1[T_1] + 6 e^{-i T_0 \omega_2} \overline{A_1[T_1]}\, \overline{A_2[T_1]}\, \tilde{\eta}_3 A_1[T_1] -$$
$$3 e^{i T_0 \omega_1 - 2 i T_0 \omega_2} \overline{A_2[T_1]}^2 \tilde{\eta}_3 A_1[T_1] + 6 e^{-i T_0 \omega_1} \overline{A_1[T_1]}\, \overline{A_3[T_1]}\, \tilde{\eta}_3 A_1[T_1] -$$
$$6 e^{-i T_0 \omega_2} \overline{A_2[T_1]}\, \overline{A_3[T_1]}\, \tilde{\eta}_3 A_1[T_1] - 3 e^{-i T_0 \omega_1} \overline{A_3[T_1]}^2 \tilde{\eta}_3 A_1[T_1] -$$
$$\frac{3 \overline{A_2[T_1]}\, \omega_2^2 \tilde{\eta}_2 A_1[T_1]^2}{-3 e^{-2 i T_0 \omega_1 + i T_0 \omega_2} \omega_1^2 + 4 e^{-2 i T_0 \omega_1 + i T_0 \omega_2} \omega_1 \omega_2 - e^{-2 i T_0 \omega_1 + i T_0 \omega_2} \omega_2^2} -$$
$$3 e^{i T_0 \omega_1} \overline{A_1[T_1]}\, \tilde{\eta}_3 A_1[T_1]^2 + 3 e^{2 i T_0 \omega_1 - i T_0 \omega_2} \overline{A_2[T_1]}\, \tilde{\eta}_3 A_1[T_1]^2 +$$
$$3 e^{i T_0 \omega_1} \overline{A_3[T_1]}\, \tilde{\eta}_3 A_1[T_1]^2 + \frac{e^{3 i T_0 \omega_1} \omega_2^2 \tilde{\eta}_1 A_1[T_1]^3}{8 \omega_1^2} -$$
$$\frac{e^{3 i T_0 \omega_1} \omega_2^2 \tilde{\eta}_2 A_1[T_1]^3}{8 \omega_1^2} - e^{3 i T_0 \omega_1} \tilde{\eta}_3 A_1[T_1]^3 +$$
$$\frac{e^{i T_0 \omega_2} \omega_2^2 \tilde{\gamma}_2 A_2[T_1]}{\omega_1^2 - \omega_2^2} + \frac{2 i e^{i T_0 \omega_2} \omega_2^3 \tilde{\zeta}_2 A_2[T_1]}{\omega_1^2 - \omega_2^2} -$$
$$2 i e^{i T_0 \omega_2} \omega_2 \tilde{\zeta}_3 A_2[T_1] - \frac{3 e^{-2 i T_0 \omega_1 + i T_0 \omega_2} \overline{A_1[T_1]}^2 \omega_2^2 \tilde{\eta}_2 A_2[T_1]}{-3 \omega_1^2 + 4 \omega_1 \omega_2 - \omega_2^2} +$$
$$\frac{6 e^{-2 i T_0 \omega_1 + i T_0 \omega_2} \overline{A_1[T_1]}\, \overline{A_3[T_1]}\, \omega_2^2 \tilde{\eta}_2 A_2[T_1]}{-3 \omega_1^2 + 4 \omega_1 \omega_2 - \omega_2^2} -$$
$$\frac{3 e^{-2 i T_0 \omega_1 + i T_0 \omega_2} \overline{A_3[T_1]}^2 \omega_2^2 \tilde{\eta}_2 A_2[T_1]}{-3 \omega_1^2 + 4 \omega_1 \omega_2 - \omega_2^2} - \frac{3 \overline{A_2[T_1]}^2 \omega_2^2 \tilde{\eta}_2 A_2[T_1]}{e^{i T_0 \omega_2} \omega_1^2 - e^{i T_0 \omega_2} \omega_2^2} +$$
$$3 e^{-2 i T_0 \omega_1 + i T_0 \omega_2} \overline{A_1[T_1]}^2 \tilde{\eta}_3 A_2[T_1] - 6 e^{-i T_0 \omega_1} \overline{A_1[T_1]}\, \overline{A_2[T_1]}\, \tilde{\eta}_3 A_2[T_1] +$$
$$3 e^{-i T_0 \omega_2} \overline{A_2[T_1]}^2 \tilde{\eta}_3 A_2[T_1] - 6 e^{-2 i T_0 \omega_1 + i T_0 \omega_2} \overline{A_1[T_1]}\, \overline{A_3[T_1]}\, \tilde{\eta}_3 A_2[T_1] +$$
$$6 e^{-i T_0 \omega_1} \overline{A_2[T_1]}\, \overline{A_3[T_1]}\, \tilde{\eta}_3 A_2[T_1] + 3 e^{-2 i T_0 \omega_1 + i T_0 \omega_2} \overline{A_3[T_1]}^2 \tilde{\eta}_3 A_2[T_1] -$$
$$\frac{6 e^{i T_0 \omega_2} \overline{A_1[T_1]}\, \omega_2^2 \tilde{\eta}_2 A_1[T_1]\, A_2[T_1]}{\omega_1^2 - \omega_2^2} +$$
$$\frac{6 e^{i T_0 \omega_2} \overline{A_3[T_1]}\, \omega_2^2 \tilde{\eta}_2 A_1[T_1]\, A_2[T_1]}{\omega_1^2 - \omega_2^2} + 6 e^{i T_0 \omega_2} \overline{A_1[T_1]}\, \tilde{\eta}_3 A_1[T_1]\, A_2[T_1] -$$
$$6 e^{i T_0 \omega_1} \overline{A_2[T_1]}\, \tilde{\eta}_3 A_1[T_1]\, A_2[T_1] - 6 e^{i T_0 \omega_2} \overline{A_3[T_1]}\, \tilde{\eta}_3 A_1[T_1]\, A_2[T_1] -$$
$$\frac{3 e^{2 i T_0 \omega_1 + i T_0 \omega_2} \omega_2^2 \tilde{\eta}_2 A_1[T_1]^2 A_2[T_1]}{-3 \omega_1^2 - 4 \omega_1 \omega_2 - \omega_2^2} +$$
$$3 e^{2 i T_0 \omega_1 + i T_0 \omega_2} \tilde{\eta}_3 A_1[T_1]^2 A_2[T_1] +$$
$$\frac{3 e^{-i T_0 \omega_1 + 2 i T_0 \omega_2} \overline{A_1[T_1]}\, \omega_2^2 \tilde{\eta}_2 A_2[T_1]^2}{4 \omega_1 \omega_2 - 4 \omega_2^2} -$$
$$\frac{3 e^{-i T_0 \omega_1 + 2 i T_0 \omega_2} \overline{A_3[T_1]}\, \omega_2^2 \tilde{\eta}_2 A_2[T_1]^2}{4 \omega_1 \omega_2 - 4 \omega_2^2} -$$
$$\frac{3 e^{i T_0 \omega_2} \overline{A_2[T_1]}\, \omega_2^2 \tilde{\eta}_2 A_2[T_1]^2}{\omega_1^2 - \omega_2^2} - 3 e^{-i T_0 \omega_1 + 2 i T_0 \omega_2} \overline{A_1[T_1]}\, \tilde{\eta}_3 A_2[T_1]^2 +$$
$$3 e^{i T_0 \omega_2} \overline{A_2[T_1]}\, \tilde{\eta}_3 A_2[T_1]^2 + 3 e^{-i T_0 \omega_1 + 2 i T_0 \omega_2} \overline{A_3[T_1]}\, \tilde{\eta}_3 A_2[T_1]^2 +$$
$$\frac{3 e^{i T_0 \omega_1 + 2 i T_0 \omega_2} \omega_2^2 \tilde{\eta}_2 A_1[T_1]\, A_2[T_1]^2}{-4 \omega_1 \omega_2 - 4 \omega_2^2} -$$
$$3 e^{i T_0 \omega_1 + 2 i T_0 \omega_2} \tilde{\eta}_3 A_1[T_1]\, A_2[T_1]^2 +$$
$$e^{3 i T_0 \omega_2} \tilde{\eta}_3 A_2[T_1]^3 - 2 i e^{i T_0 \omega_1} \omega_1 \tilde{\zeta}_3 A_3[T_1] +$$
$$\frac{6 \overline{A_1[T_1]}\, \overline{A_2[T_1]}\, \omega_2^2 \tilde{\eta}_2 A_3[T_1]}{e^{i T_0 \omega_2} \omega_1^2 - e^{i T_0 \omega_2} \omega_2^2} - \frac{6 \overline{A_2[T_1]}\, \overline{A_3[T_1]}\, \omega_2^2 \tilde{\eta}_2 A_3[T_1]}{e^{i T_0 \omega_2} \omega_1^2 - e^{i T_0 \omega_2} \omega_2^2} -$$

$$\frac{3\,\overline{A_2[T_1]}^2\,\omega_2^2\,\tilde{\eta}_2\,A_3[T_1]}{4\,e^{-i\,T_0\,\omega_1+2\,i\,T_0\,\omega_2}\,\omega_1\,\omega_2-4\,e^{-i\,T_0\,\omega_1+2\,i\,T_0\,\omega_2}\,\omega_2^2}+$$

$$3\,e^{-i\,T_0\,\omega_1}\,\overline{A_1[T_1]}^2\,\tilde{\eta}_3\,A_3[T_1]-6\,e^{-i\,T_0\,\omega_2}\,\overline{A_1[T_1]}\,\overline{A_2[T_1]}\,\tilde{\eta}_3\,A_3[T_1]+$$

$$3\,e^{i\,T_0\,\omega_1-2\,i\,T_0\,\omega_2}\,\overline{A_2[T_1]}^2\,\tilde{\eta}_3\,A_3[T_1]-6\,e^{-i\,T_0\,\omega_1}\,\overline{A_1[T_1]}\,\overline{A_3[T_1]}\,\tilde{\eta}_3\,A_3[T_1]+$$

$$6\,e^{-i\,T_0\,\omega_2}\,\overline{A_2[T_1]}\,\overline{A_3[T_1]}\,\tilde{\eta}_3\,A_3[T_1]+3\,e^{-i\,T_0\,\omega_1}\,\overline{A_3[T_1]}^2\,\tilde{\eta}_3\,A_3[T_1]+$$

$$\frac{6\,\overline{A_2[T_1]}\,\omega_2^2\,\tilde{\eta}_2\,A_1[T_1]\,A_3[T_1]}{-3\,e^{-2\,i\,T_0\,\omega_1+i\,T_0\,\omega_2}\,\omega_1^2+4\,e^{-2\,i\,T_0\,\omega_1+i\,T_0\,\omega_2}\,\omega_1\,\omega_2-e^{-2\,i\,T_0\,\omega_1+i\,T_0\,\omega_2}\,\omega_2^2}+$$

$$6\,e^{i\,T_0\,\omega_1}\,\overline{A_1[T_1]}\,\tilde{\eta}_3\,A_1[T_1]\,A_3[T_1]-$$

$$6\,e^{2\,i\,T_0\,\omega_1-i\,T_0\,\omega_2}\,\overline{A_2[T_1]}\,\tilde{\eta}_3\,A_1[T_1]\,A_3[T_1]-$$

$$6\,e^{i\,T_0\,\omega_1}\,\overline{A_3[T_1]}\,\tilde{\eta}_3\,A_1[T_1]\,A_3[T_1]+\frac{3\,e^{3\,i\,T_0\,\omega_1}\,\omega_2^2\,\tilde{\eta}_2\,A_1[T_1]^2\,A_3[T_1]}{8\,\omega_1^2}+$$

$$3\,e^{3\,i\,T_0\,\omega_1}\,\tilde{\eta}_3\,A_1[T_1]^2\,A_3[T_1]+\frac{6\,e^{i\,T_0\,\omega_2}\,\overline{A_1[T_1]}\,\omega_2^2\,\tilde{\eta}_2\,A_2[T_1]\,A_3[T_1]}{\omega_1^2-\omega_2^2}-$$

$$\frac{6\,e^{i\,T_0\,\omega_2}\,\overline{A_3[T_1]}\,\omega_2^2\,\tilde{\eta}_2\,A_2[T_1]\,A_3[T_1]}{\omega_1^2-\omega_2^2}-6\,e^{i\,T_0\,\omega_2}\,\overline{A_1[T_1]}\,\tilde{\eta}_3\,A_2[T_1]\,A_3[T_1]+$$

$$6\,e^{i\,T_0\,\omega_1}\,\overline{A_2[T_1]}\,\tilde{\eta}_3\,A_2[T_1]\,A_3[T_1]+6\,e^{i\,T_0\,\omega_2}\,\overline{A_3[T_1]}\,\tilde{\eta}_3\,A_2[T_1]\,A_3[T_1]+$$

$$\frac{6\,e^{2\,i\,T_0\,\omega_1+i\,T_0\,\omega_2}\,\omega_2^2\,\tilde{\eta}_2\,A_1[T_1]\,A_2[T_1]\,A_3[T_1]}{-3\,\omega_1^2-4\,\omega_1\,\omega_2-\omega_2^2}-$$

$$6\,e^{2\,i\,T_0\,\omega_1+i\,T_0\,\omega_2}\,\tilde{\eta}_3\,A_1[T_1]\,A_2[T_1]\,A_3[T_1]-$$

$$\frac{3\,e^{i\,T_0\,\omega_1+2\,i\,T_0\,\omega_2}\,\omega_2^2\,\tilde{\eta}_2\,A_2[T_1]^2\,A_3[T_1]}{-4\,\omega_1\,\omega_2-4\,\omega_2^2}+$$

$$3\,e^{i\,T_0\,\omega_1+2\,i\,T_0\,\omega_2}\,\tilde{\eta}_3\,A_2[T_1]^2\,A_3[T_1]-$$

$$\frac{3\,\overline{A_2[T_1]}\,\omega_2^2\,\tilde{\eta}_2\,A_3[T_1]^2}{-3\,e^{-2\,i\,T_0\,\omega_1+i\,T_0\,\omega_2}\,\omega_1^2+4\,e^{-2\,i\,T_0\,\omega_1+i\,T_0\,\omega_2}\,\omega_1\,\omega_2-e^{-2\,i\,T_0\,\omega_1+i\,T_0\,\omega_2}\,\omega_2^2}-$$

$$3\,e^{i\,T_0\,\omega_1}\,\overline{A_1[T_1]}\,\tilde{\eta}_3\,A_3[T_1]^2+3\,e^{2\,i\,T_0\,\omega_1-i\,T_0\,\omega_2}\,\overline{A_2[T_1]}\,\tilde{\eta}_3\,A_3[T_1]^2+$$

$$3\,e^{i\,T_0\,\omega_1}\,\overline{A_3[T_1]}\,\tilde{\eta}_3\,A_3[T_1]^2-\frac{3\,e^{3\,i\,T_0\,\omega_1}\,\omega_2^2\,\tilde{\eta}_2\,A_1[T_1]\,A_3[T_1]^2}{8\,\omega_1^2}-$$

$$3\,e^{3\,i\,T_0\,\omega_1}\,\tilde{\eta}_3\,A_1[T_1]\,A_3[T_1]^2-\frac{3\,e^{2\,i\,T_0\,\omega_1+i\,T_0\,\omega_2}\,\omega_2^2\,\tilde{\eta}_2\,A_2[T_1]\,A_3[T_1]^2}{-3\,\omega_1^2-4\,\omega_1\,\omega_2-\omega_2^2}+$$

$$3\,e^{2\,i\,T_0\,\omega_1+i\,T_0\,\omega_2}\,\tilde{\eta}_3\,A_2[T_1]\,A_3[T_1]^2+\frac{e^{3\,i\,T_0\,\omega_1}\,\omega_2^2\,\tilde{\eta}_2\,A_3[T_1]^3}{8\,\omega_1^2}+$$

$$e^{3\,i\,T_0\,\omega_1}\,\tilde{\eta}_3\,A_3[T_1]^3-2\,i\,e^{i\,T_0\,\omega_2}\,\omega_2\,A_2'[T_1]+$$

$$2\,i\,e^{-i\,T_0\,\omega_2}\,\omega_2\,\text{OverBar}'[A_2[T_1]]\,A_2'[T_1]-$$

$$2\,i\,e^{i\,T_0\,\omega_1}\,\omega_1\,A_3'[T_1]+2\,i\,e^{-i\,T_0\,\omega_1}\,\omega_1\,\text{OverBar}'[A_3[T_1]]\,A_3'[T_1]$$

Extracting the 'Always' Secular Terms of RHS2 from Out[8] :

In[9]:= **Coefficient[RHS2, $e^{i\times\omega_2\times T_0}$]**

Out[9]=

$$\frac{\omega_2^2\,\tilde{\gamma}_2\,A_2[T_1]}{\omega_1^2-\omega_2^2}+\frac{2\,i\,\omega_2^3\,\tilde{\xi}_2\,A_2[T_1]}{\omega_1^2-\omega_2^2}-2\,i\,\omega_2\,\tilde{\xi}_3\,A_2[T_1]-$$

$$\frac{6\,\overline{A_1[T_1]}\,\omega_2^2\,\tilde{\eta}_2\,A_1[T_1]\,A_2[T_1]}{\omega_1^2-\omega_2^2}+\frac{6\,\overline{A_3[T_1]}\,\omega_2^2\,\tilde{\eta}_2\,A_1[T_1]\,A_2[T_1]}{\omega_1^2-\omega_2^2}+$$

$$6\,\overline{A_1[T_1]}\,\tilde{\eta}_3\,A_1[T_1]\,A_2[T_1]-6\,\overline{A_3[T_1]}\,\tilde{\eta}_3\,A_1[T_1]\,A_2[T_1]-$$

$$\frac{3\,\overline{A_2[T_1]}\,\omega_2^2\,\tilde{\eta}_2\,A_2[T_1]^2}{\omega_1^2-\omega_2^2}+3\,\overline{A_2[T_1]}\,\tilde{\eta}_3\,A_2[T_1]^2+$$

$$\frac{6\,\overline{A_1[T_1]}\,\omega_2^2\,\tilde{\eta}_2\,A_2[T_1]\,A_3[T_1]}{\omega_1^2-\omega_2^2}-\frac{6\,\overline{A_3[T_1]}\,\omega_2^2\,\tilde{\eta}_2\,A_2[T_1]\,A_3[T_1]}{\omega_1^2-\omega_2^2}-$$

$$6\,\overline{A_1[T_1]}\,\tilde{\eta}_3\,A_2[T_1]\,A_3[T_1]+6\,\overline{A_3[T_1]}\,\tilde{\eta}_3\,A_2[T_1]\,A_3[T_1]-2\,i\,\omega_2\,A_2'[T_1]$$

Extracting the ' Always ' Complex
Conjugate Secular Terms (C.C.S.T.) of RHS2 from Out[8] :

In[10]:=
```
Coefficient[RHS2, e^(-i*ω2*T0)]
```

Out[10]=
$$2\,i\,\overline{A_2[T_1]}\,\omega_2\,\tilde{\xi}_3 + 6\,\overline{A_1[T_1]}\,\overline{A_2[T_1]}\,\tilde{\eta}_3\,A_1[T_1] - 6\,\overline{A_2[T_1]}\,\overline{A_3[T_1]}\,\tilde{\eta}_3\,A_1[T_1] + 3\,\overline{A_2[T_1]}^2\,\tilde{\eta}_3\,A_2[T_1] - 6\,\overline{A_1[T_1]}\,\overline{A_2[T_1]}\,\tilde{\eta}_3\,A_3[T_1] + 6\,\overline{A_2[T_1]}\,\overline{A_3[T_1]}\,\tilde{\eta}_3\,A_3[T_1] + 2\,i\,\omega_2\,\text{OverBar}'[A_2[T_1]]\,A_2'[T_1]$$

Due to some terms missing from the Mathematica extraction of the C.C.S.T.,
below is the corrected C.C.S.T. :

In[11]:=
$$2\,i\,\overline{A_2[T_1]}\,\omega_2\,\tilde{\xi}_3 + 6\,\overline{A_1[T_1]}\,\overline{A_2[T_1]}\,\tilde{\eta}_3\,A_1[T_1] - 6\,\overline{A_2[T_1]}\,\overline{A_3[T_1]}\,\tilde{\eta}_3\,A_1[T_1] + 3\,\overline{A_2[T_1]}^2\,\tilde{\eta}_3\,A_2[T_1] - 6\,\overline{A_1[T_1]}\,\overline{A_2[T_1]}\,\tilde{\eta}_3\,A_3[T_1] + 6\,\overline{A_2[T_1]}\,\overline{A_3[T_1]}\,\tilde{\eta}_3\,A_3[T_1] + 2\,i\,\omega_2\,\text{OverBar}'[A_2[T_1]]\,A_2'[T_1] + \frac{\overline{A_2[T_1]}\,\omega_2^2\,\tilde{\gamma}_2}{\omega_1^2-\omega_2^2} - \frac{2\,i\,\overline{A_2[T_1]}\,\omega_2^3\,\tilde{\xi}_2}{\omega_1^2-\omega_2^2} - \frac{6\,\overline{A_1[T_1]}\,\overline{A_2[T_1]}\,\omega_2^2\,\tilde{\eta}_2\,A_1[T_1]}{\omega_1^2-\omega_2^2} + \frac{6\,\overline{A_2[T_1]}\,\overline{A_3[T_1]}\,\omega_2^2\,\tilde{\eta}_2\,A_1[T_1]}{\omega_1^2-\omega_2^2} - \frac{3\,\overline{A_2[T_1]}^2\,\omega_2^2\,\tilde{\eta}_2\,A_2[T_1]}{\omega_1^2-\omega_2^2} + \frac{6\,\overline{A_1[T_1]}\,\overline{A_2[T_1]}\,\omega_2^2\,\tilde{\eta}_2\,A_3[T_1]}{\omega_1^2-\omega_2^2} - \frac{6\,\overline{A_2[T_1]}\,\overline{A_3[T_1]}\,\omega_2^2\,\tilde{\eta}_2\,A_3[T_1]}{\omega_1^2-\omega_2^2};$$

Below are the ' Always ' Secular and ' Always ' Complex Conjugate Secular Terms for x_{21}.
They are the re - statement of Out[9] and In[11] respectively.

■ **The 'Always' Secular Terms of x_{21} (Case 1):**

In[12]:=
$$\frac{\omega_2^2\,\tilde{\gamma}_2\,A_2[T_1]}{\omega_1^2-\omega_2^2} + \frac{2\,i\,\omega_2^3\,\tilde{\xi}_2\,A_2[T_1]}{\omega_1^2-\omega_2^2} - 2\,i\,\omega_2\,\tilde{\xi}_3\,A_2[T_1] - \frac{6\,\overline{A_1[T_1]}\,\omega_2^2\,\tilde{\eta}_2\,A_1[T_1]\,A_2[T_1]}{\omega_1^2-\omega_2^2} + \frac{6\,\overline{A_3[T_1]}\,\omega_2^2\,\tilde{\eta}_2\,A_1[T_1]\,A_2[T_1]}{\omega_1^2-\omega_2^2} + 6\,\overline{A_1[T_1]}\,\tilde{\eta}_3\,A_1[T_1]\,A_2[T_1] - 6\,\overline{A_3[T_1]}\,\tilde{\eta}_3\,A_1[T_1]\,A_2[T_1] - \frac{3\,\overline{A_2[T_1]}\,\omega_2^2\,\tilde{\eta}_2\,A_2[T_1]^2}{\omega_1^2-\omega_2^2} + 3\,\overline{A_2[T_1]}\,\tilde{\eta}_3\,A_2[T_1]^2 + \frac{6\,\overline{A_1[T_1]}\,\omega_2^2\,\tilde{\eta}_2\,A_2[T_1]\,A_3[T_1]}{\omega_1^2-\omega_2^2} - \frac{6\,\overline{A_3[T_1]}\,\omega_2^2\,\tilde{\eta}_2\,A_2[T_1]\,A_3[T_1]}{\omega_1^2-\omega_2^2} - 6\,\overline{A_1[T_1]}\,\tilde{\eta}_3\,A_2[T_1]\,A_3[T_1] + 6\,\overline{A_3[T_1]}\,\tilde{\eta}_3\,A_2[T_1]\,A_3[T_1] - 2\,i\,\omega_2\,A_2'[T_1];$$

■ The 'Always' Complex Conjugate Secular Terms of x_{21} (Case 1):

In[13]:=
```
2 i A2[T1] ω2 ξ3 + 6 A1[T1] A2[T1] η3 A1[T1] - 6 A2[T1] A3[T1] η3 A1[T1] +
 3 A2[T1]^2 η3 A2[T1] - 6 A1[T1] A2[T1] η3 A3[T1] +
 6 A2[T1] A3[T1] η3 A3[T1] + 2 i ω2 OverBar'[A2[T1]] A2'[T1] +
 A2[T1] ω2^2 γ2 / (ω1^2 - ω2^2) - 2 i A2[T1] ω2^3 ξ2 / (ω1^2 - ω2^2) - 6 A1[T1] A2[T1] ω2^2 η2 A1[T1] / (ω1^2 - ω2^2) +
 6 A2[T1] A3[T1] ω2^2 η2 A1[T1] / (ω1^2 - ω2^2) - 3 A2[T1]^2 ω2^2 η2 A2[T1] / (ω1^2 - ω2^2) +
 6 A1[T1] A2[T1] ω2^2 η2 A3[T1] / (ω1^2 - ω2^2) - 6 A2[T1] A3[T1] ω2^2 η2 A3[T1] / (ω1^2 - ω2^2);
```

Dividing RHS2 by $e^{i\omega_2 T_0}$ and then grouping them for alike coefficients for easier identification. This purpose is to identify other secular terms :

In[14]:=
```
Collect[ExpandAll[RHS2 / e^(i×ω2×T0)],
 {e^(-i ω2 T0 - 3 i ω1 T0), e^(-i ω2 T0 + 3 i ω1 T0), e^(-2 i ω2 T0 - 2 i ω1 T0),
  e^(-2 i ω2 T0 + 2 i ω1 T0), e^(-3 i ω2 T0 - i ω1 T0), e^(-3 i ω2 T0 + i ω1 T0),
  e^(-i ω2 T0 - i ω1 T0), e^(-i ω2 T0 + i ω1 T0), e^(i ω2 T0 + i ω1 T0), e^(i ω2 T0 - i ω1 T0)}]
```

Out[14]=
$$\frac{e^{-i T_0 \omega_2}\,\overline{A_2[T_1]}\,\omega_2^2\,\tilde{\gamma}_2}{e^{i T_0 \omega_2}\,\omega_1^2 - e^{i T_0 \omega_2}\,\omega_2^2} -$$

$$\frac{2\,i\,e^{-i T_0 \omega_2}\,\overline{A_2[T_1]}\,\omega_2^3\,\tilde{\zeta}_2}{e^{i T_0 \omega_2}\,\omega_1^2 - e^{i T_0 \omega_2}\,\omega_2^2} + 2\,i\,e^{-2 i T_0 \omega_2}\,\overline{A_2[T_1]}\,\omega_2\,\tilde{\xi}_3 -$$

$$\frac{3\,e^{-i T_0 \omega_2}\,\overline{A_1[T_1]}^2\,\overline{A_2[T_1]}\,\omega_2^2\,\tilde{\eta}_2}{-3\,e^{2 i T_0 \omega_1 + i T_0 \omega_2}\,\omega_1^2 - 4\,e^{2 i T_0 \omega_1 + i T_0 \omega_2}\,\omega_1\,\omega_2 - e^{2 i T_0 \omega_1 + i T_0 \omega_2}\,\omega_2^2} +$$

$$\frac{6\,e^{-i T_0 \omega_2}\,\overline{A_1[T_1]}\,\overline{A_2[T_1]}\,\overline{A_3[T_1]}\,\omega_2^2\,\tilde{\eta}_2}{-3\,e^{2 i T_0 \omega_1 + i T_0 \omega_2}\,\omega_1^2 - 4\,e^{2 i T_0 \omega_1 + i T_0 \omega_2}\,\omega_1\,\omega_2 - e^{2 i T_0 \omega_1 + i T_0 \omega_2}\,\omega_2^2} -$$

$$\frac{3\,e^{-i T_0 \omega_2}\,\overline{A_2[T_1]}\,\overline{A_3[T_1]}^2\,\omega_2^2\,\tilde{\eta}_2}{-3\,e^{2 i T_0 \omega_1 + i T_0 \omega_2}\,\omega_1^2 - 4\,e^{2 i T_0 \omega_1 + i T_0 \omega_2}\,\omega_1\,\omega_2 - e^{2 i T_0 \omega_1 + i T_0 \omega_2}\,\omega_2^2} +$$

$$\frac{3\,e^{-i T_0 \omega_2}\,\overline{A_1[T_1]}\,\overline{A_2[T_1]}^2\,\omega_2^2\,\tilde{\eta}_2}{-4\,e^{i T_0 \omega_1 + 2 i T_0 \omega_2}\,\omega_1\,\omega_2 - 4\,e^{i T_0 \omega_1 + 2 i T_0 \omega_2}\,\omega_2^2} -$$

$$\frac{3\,e^{-i T_0 \omega_2}\,\overline{A_2[T_1]}^2\,\overline{A_3[T_1]}\,\omega_2^2\,\tilde{\eta}_2}{-4\,e^{i T_0 \omega_1 + 2 i T_0 \omega_2}\,\omega_1\,\omega_2 - 4\,e^{i T_0 \omega_1 + 2 i T_0 \omega_2}\,\omega_2^2} + e^{-4 i T_0 \omega_2}\,\overline{A_2[T_1]}^3\,\tilde{\eta}_3 +$$

$$e^{-i T_0 \omega_1 - 3 i T_0 \omega_2}\,(-3\,\overline{A_1[T_1]}\,\overline{A_2[T_1]}^2\,\tilde{\eta}_3 + 3\,\overline{A_2[T_1]}^2\,\overline{A_3[T_1]}\,\tilde{\eta}_3) +$$

$$e^{-2 i T_0 \omega_1 - 2 i T_0 \omega_2}\,(3\,\overline{A_1[T_1]}^2\,\overline{A_2[T_1]}\,\tilde{\eta}_3 -$$

$$6\,\overline{A_1[T_1]}\,\overline{A_2[T_1]}\,\overline{A_3[T_1]}\,\tilde{\eta}_3 + 3\,\overline{A_2[T_1]}\,\overline{A_3[T_1]}^2\,\tilde{\eta}_3) +$$

$$e^{-3 i T_0 \omega_1 - i T_0 \omega_2}\left(\frac{\overline{A_1[T_1]}^3\,\omega_2^2\,\tilde{\eta}_1}{8\,\omega_1^2} - \frac{\overline{A_1[T_1]}^3\,\omega_2^2\,\tilde{\eta}_2}{8\,\omega_1^2} +\right.$$

$$\frac{3\,\overline{A_1[T_1]}^2\,\overline{A_3[T_1]}\,\omega_2^2\,\tilde{\eta}_2}{8\,\omega_1^2} - \frac{3\,\overline{A_1[T_1]}\,\overline{A_3[T_1]}^2\,\omega_2^2\,\tilde{\eta}_2}{8\,\omega_1^2} + \frac{\overline{A_3[T_1]}^3\,\omega_2^2\,\tilde{\eta}_2}{8\,\omega_1^2} -$$

$$\left.\overline{A_1[T_1]}^3\,\tilde{\eta}_3 + 3\,\overline{A_1[T_1]}^2\,\overline{A_3[T_1]}\,\tilde{\eta}_3 - 3\,\overline{A_1[T_1]}\,\overline{A_3[T_1]}^2\,\tilde{\eta}_3 + \overline{A_3[T_1]}^3\,\tilde{\eta}_3\right) -$$

$$\frac{6\,e^{-i T_0 \omega_2}\,\overline{A_1[T_1]}\,\overline{A_2[T_1]}\,\omega_2^2\,\tilde{\eta}_2\,A_1[T_1]}{e^{i T_0 \omega_2}\,\omega_1^2 - e^{i T_0 \omega_2}\,\omega_2^2} +$$

$$\frac{6\,e^{-i T_0 \omega_2}\,\overline{A_2[T_1]}\,\overline{A_3[T_1]}\,\omega_2^2\,\tilde{\eta}_2\,A_1[T_1]}{e^{i T_0 \omega_2}\,\omega_1^2 - e^{i T_0 \omega_2}\,\omega_2^2} +$$

$$\frac{3\,e^{-i T_0 \omega_2}\,\overline{A_2[T_1]}^2\,\omega_2^2\,\tilde{\eta}_2\,A_1[T_1]}{4\,e^{-i T_0 \omega_1 + 2 i T_0 \omega_2}\,\omega_1\,\omega_2 - 4\,e^{-i T_0 \omega_1 + 2 i T_0 \omega_2}\,\omega_2^2} +$$

$$6\,e^{-2\,i\,T_0\,\omega_2}\,\overline{A_1[T_1]}\,\overline{A_2[T_1]}\,\tilde{\eta}_3\,A_1[T_1] -$$
$$6\,e^{-2\,i\,T_0\,\omega_2}\,\overline{A_2[T_1]}\,\overline{A_3[T_1]}\,\tilde{\eta}_3\,A_1[T_1] -$$
$$\frac{3\,e^{-i\,T_0\,\omega_2}\,\overline{A_2[T_1]}\,\omega_2^2\,\tilde{\eta}_2\,A_1[T_1]^2}{-3\,e^{-2\,i\,T_0\,\omega_1+i\,T_0\,\omega_2}\,\omega_1^2+4\,e^{-2\,i\,T_0\,\omega_1+i\,T_0\,\omega_2}\,\omega_1\,\omega_2-e^{-2\,i\,T_0\,\omega_1+i\,T_0\,\omega_2}\,\omega_2^2} +$$
$$\frac{\omega_2^2\,\tilde{\gamma}_2\,A_2[T_1]}{\omega_1^2-\omega_2^2} + \frac{2\,i\,\omega_2^3\,\tilde{\zeta}_2\,A_2[T_1]}{\omega_1^2-\omega_2^2} - 2\,i\,\omega_2\,\tilde{\zeta}_3\,A_2[T_1] -$$
$$\frac{3\,\overline{A_1[T_1]}^2\,\omega_2^2\,\tilde{\eta}_2\,A_2[T_1]}{-3\,e^{2\,i\,T_0\,\omega_1}\,\omega_1^2+4\,e^{2\,i\,T_0\,\omega_1}\,\omega_1\,\omega_2-e^{2\,i\,T_0\,\omega_1}\,\omega_2^2} +$$
$$\frac{6\,\overline{A_1[T_1]}\,\overline{A_3[T_1]}\,\omega_2^2\,\tilde{\eta}_2\,A_2[T_1]}{-3\,e^{2\,i\,T_0\,\omega_1}\,\omega_1^2+4\,e^{2\,i\,T_0\,\omega_1}\,\omega_1\,\omega_2-e^{2\,i\,T_0\,\omega_1}\,\omega_2^2} -$$
$$\frac{3\,\overline{A_3[T_1]}^2\,\omega_2^2\,\tilde{\eta}_2\,A_2[T_1]}{-3\,e^{2\,i\,T_0\,\omega_1}\,\omega_1^2+4\,e^{2\,i\,T_0\,\omega_1}\,\omega_1\,\omega_2-e^{2\,i\,T_0\,\omega_1}\,\omega_2^2} -$$
$$\frac{3\,e^{-i\,T_0\,\omega_2}\,\overline{A_2[T_1]}^2\,\omega_2^2\,\tilde{\eta}_2\,A_2[T_1]}{e^{i\,T_0\,\omega_2}\,\omega_1^2-e^{i\,T_0\,\omega_2}\,\omega_2^2} + 3\,e^{-2\,i\,T_0\,\omega_1}\,\overline{A_1[T_1]}^2\,\tilde{\eta}_3\,A_2[T_1] +$$
$$3\,e^{-2\,i\,T_0\,\omega_2}\,\overline{A_2[T_1]}^2\,\tilde{\eta}_3\,A_2[T_1] - 6\,e^{-2\,i\,T_0\,\omega_1}\,\overline{A_1[T_1]}\,\overline{A_3[T_1]}\,\tilde{\eta}_3\,A_2[T_1] +$$
$$3\,e^{-2\,i\,T_0\,\omega_1}\,\overline{A_3[T_1]}^2\,\tilde{\eta}_3\,A_2[T_1] - \frac{6\,\overline{A_1[T_1]}\,\omega_2^2\,\tilde{\eta}_2\,A_1[T_1]\,A_2[T_1]}{\omega_1^2-\omega_2^2} +$$
$$\frac{6\,\overline{A_3[T_1]}\,\omega_2^2\,\tilde{\eta}_2\,A_1[T_1]\,A_2[T_1]}{\omega_1^2-\omega_2^2} + 6\,\overline{A_1[T_1]}\,\tilde{\eta}_3\,A_1[T_1]\,A_2[T_1] -$$
$$6\,\overline{A_3[T_1]}\,\tilde{\eta}_3\,A_1[T_1]\,A_2[T_1] - \frac{3\,e^{2\,i\,T_0\,\omega_1}\,\omega_2^2\,\tilde{\eta}_2\,A_1[T_1]^2\,A_2[T_1]}{-3\,\omega_1^2-4\,\omega_1\,\omega_2-\omega_2^2} +$$
$$3\,e^{2\,i\,T_0\,\omega_1}\,\tilde{\eta}_3\,A_1[T_1]^2\,A_2[T_1] - \frac{3\,\overline{A_2[T_1]}\,\omega_2^2\,\tilde{\eta}_2\,A_2[T_1]^2}{\omega_1^2-\omega_2^2} +$$
$$\frac{3\,e^{i\,T_0\,\omega_2}\,\overline{A_1[T_1]}\,\omega_2^2\,\tilde{\eta}_2\,A_2[T_1]^2}{4\,e^{i\,T_0\,\omega_1}\,\omega_1\,\omega_2-4\,e^{i\,T_0\,\omega_1}\,\omega_2^2} - \frac{3\,e^{i\,T_0\,\omega_2}\,\overline{A_3[T_1]}\,\omega_2^2\,\tilde{\eta}_2\,A_2[T_1]^2}{4\,e^{i\,T_0\,\omega_1}\,\omega_1\,\omega_2-4\,e^{i\,T_0\,\omega_1}\,\omega_2^2} +$$
$$3\,\overline{A_2[T_1]}\,\tilde{\eta}_3\,A_2[T_1]^2 + e^{2\,i\,T_0\,\omega_2}\,\tilde{\eta}_3\,A_2[T_1]^3 +$$
$$e^{-i\,T_0\,\omega_1+i\,T_0\,\omega_2}\,(-3\,\overline{A_1[T_1]}\,\tilde{\eta}_3\,A_2[T_1]^2+3\,\overline{A_3[T_1]}\,\tilde{\eta}_3\,A_2[T_1]^2) +$$
$$\frac{6\,e^{-i\,T_0\,\omega_2}\,\overline{A_1[T_1]}\,\overline{A_2[T_1]}\,\omega_2^2\,\tilde{\eta}_2\,A_3[T_1]}{e^{i\,T_0\,\omega_2}\,\omega_1^2-e^{i\,T_0\,\omega_2}\,\omega_2^2} -$$
$$\frac{6\,e^{-i\,T_0\,\omega_2}\,\overline{A_2[T_1]}\,\overline{A_3[T_1]}\,\omega_2^2\,\tilde{\eta}_2\,A_3[T_1]}{e^{i\,T_0\,\omega_2}\,\omega_1^2-e^{i\,T_0\,\omega_2}\,\omega_2^2} -$$
$$\frac{3\,e^{-i\,T_0\,\omega_2}\,\overline{A_2[T_1]}^2\,\omega_2^2\,\tilde{\eta}_2\,A_3[T_1]}{4\,e^{-i\,T_0\,\omega_1+2\,i\,T_0\,\omega_2}\,\omega_1\,\omega_2-4\,e^{-i\,T_0\,\omega_1+2\,i\,T_0\,\omega_2}\,\omega_2^2} -$$
$$6\,e^{-2\,i\,T_0\,\omega_2}\,\overline{A_1[T_1]}\,\overline{A_2[T_1]}\,\tilde{\eta}_3\,A_3[T_1] +$$
$$6\,e^{-2\,i\,T_0\,\omega_2}\,\overline{A_2[T_1]}\,\overline{A_3[T_1]}\,\tilde{\eta}_3\,A_3[T_1] +$$
$$\frac{6\,e^{-i\,T_0\,\omega_2}\,\overline{A_2[T_1]}\,\omega_2^2\,\tilde{\eta}_2\,A_1[T_1]\,A_3[T_1]}{-3\,e^{-2\,i\,T_0\,\omega_1+i\,T_0\,\omega_2}\,\omega_1^2+4\,e^{-2\,i\,T_0\,\omega_1+i\,T_0\,\omega_2}\,\omega_1\,\omega_2-e^{-2\,i\,T_0\,\omega_1+i\,T_0\,\omega_2}\,\omega_2^2} +$$
$$\frac{6\,\overline{A_1[T_1]}\,\omega_2^2\,\tilde{\eta}_2\,A_2[T_1]\,A_3[T_1]}{\omega_1^2-\omega_2^2} - \frac{6\,\overline{A_3[T_1]}\,\omega_2^2\,\tilde{\eta}_2\,A_2[T_1]\,A_3[T_1]}{\omega_1^2-\omega_2^2} -$$
$$6\,\overline{A_1[T_1]}\,\tilde{\eta}_3\,A_2[T_1]\,A_3[T_1] + 6\,\overline{A_3[T_1]}\,\tilde{\eta}_3\,A_2[T_1]\,A_3[T_1] +$$
$$\frac{6\,e^{2\,i\,T_0\,\omega_1}\,\omega_2^2\,\tilde{\eta}_2\,A_1[T_1]\,A_2[T_1]\,A_3[T_1]}{-3\,\omega_1^2-4\,\omega_1\,\omega_2-\omega_2^2} -$$
$$6\,e^{2\,i\,T_0\,\omega_1}\,\tilde{\eta}_3\,A_1[T_1]\,A_2[T_1]\,A_3[T_1] -$$
$$\frac{3\,e^{-i\,T_0\,\omega_2}\,\overline{A_2[T_1]}\,\omega_2^2\,\tilde{\eta}_2\,A_3[T_1]^2}{-3\,e^{-2\,i\,T_0\,\omega_1+i\,T_0\,\omega_2}\,\omega_1^2+4\,e^{-2\,i\,T_0\,\omega_1+i\,T_0\,\omega_2}\,\omega_1\,\omega_2-e^{-2\,i\,T_0\,\omega_1+i\,T_0\,\omega_2}\,\omega_2^2} -$$
$$\frac{3\,e^{2\,i\,T_0\,\omega_1}\,\omega_2^2\,\tilde{\eta}_2\,A_2[T_1]\,A_3[T_1]^2}{-3\,\omega_1^2-4\,\omega_1\,\omega_2-\omega_2^2} + 3\,e^{2\,i\,T_0\,\omega_1}\,\tilde{\eta}_3\,A_2[T_1]\,A_3[T_1]^2 +$$
$$e^{i\,T_0\,\omega_1-3\,i\,T_0\,\omega_2}\,(-3\,\overline{A_2[T_1]}^2\,\tilde{\eta}_3\,A_1[T_1]+3\,\overline{A_2[T_1]}^2\,\tilde{\eta}_3\,A_3[T_1]) +$$

$$e^{i T_0 \omega_1 + i T_0 \omega_2} \left(\frac{3 \omega_2^2 \tilde{\eta}_2 A_1[T_1] A_2[T_1]^2}{-4 \omega_1 \omega_2 - 4 \omega_2^2} - 3 \tilde{\eta}_3 A_1[T_1] A_2[T_1]^2 - \right.$$
$$\left. \frac{3 \omega_2^2 \tilde{\eta}_2 A_2[T_1]^2 A_3[T_1]}{-4 \omega_1 \omega_2 - 4 \omega_2^2} + 3 \tilde{\eta}_3 A_2[T_1]^2 A_3[T_1] \right) +$$
$$e^{2 i T_0 \omega_1 - 2 i T_0 \omega_2} (3 \overline{A_2[T_1]} \tilde{\eta}_3 A_1[T_1]^2 - 6 \overline{A_2[T_1]} \tilde{\eta}_3 A_1[T_1] A_3[T_1] +$$
$$3 \overline{A_2[T_1]} \tilde{\eta}_3 A_3[T_1]^2) + e^{3 i T_0 \omega_1 - i T_0 \omega_2}$$
$$\left(\frac{\omega_2^2 \tilde{\eta}_1 A_1[T_1]^3}{8 \omega_1^2} - \frac{\omega_2^2 \tilde{\eta}_2 A_1[T_1]^3}{8 \omega_1^2} - \tilde{\eta}_3 A_1[T_1]^3 + \frac{3 \omega_2^2 \tilde{\eta}_2 A_1[T_1]^2 A_3[T_1]}{8 \omega_1^2} + \right.$$
$$3 \tilde{\eta}_3 A_1[T_1]^2 A_3[T_1] - \frac{3 \omega_2^2 \tilde{\eta}_2 A_1[T_1] A_3[T_1]^2}{8 \omega_1^2} -$$
$$\left. 3 \tilde{\eta}_3 A_1[T_1] A_3[T_1]^2 + \frac{\omega_2^2 \tilde{\eta}_2 A_3[T_1]^3}{8 \omega_1^2} + \tilde{\eta}_3 A_3[T_1]^3 \right) - 2 i \omega_2 A_2'[T_1] +$$
$$2 i e^{-2 i T_0 \omega_2} \omega_2 \text{ OverBar}'[A_2[T_1]] A_2'[T_1] + e^{i T_0 \omega_1 - i T_0 \omega_2}$$
$$(2 i \omega_1 \tilde{\zeta}_3 A_1[T_1] - 3 \overline{A_1[T_1]} \tilde{\eta}_3 A_1[T_1]^2 + 3 \overline{A_3[T_1]} \tilde{\eta}_3 A_1[T_1]^2 -$$
$$6 \overline{A_2[T_1]} \tilde{\eta}_3 A_1[T_1] A_2[T_1] - 2 i \omega_1 \tilde{\zeta}_3 A_3[T_1] + 6 \overline{A_1[T_1]} \tilde{\eta}_3 A_1[T_1]$$
$$A_3[T_1] - 6 \overline{A_3[T_1]} \tilde{\eta}_3 A_1[T_1] A_3[T_1] + 6 \overline{A_2[T_1]} \tilde{\eta}_3 A_2[T_1] A_3[T_1] -$$
$$3 \overline{A_1[T_1]} \tilde{\eta}_3 A_3[T_1]^2 + 3 \overline{A_3[T_1]} \tilde{\eta}_3 A_3[T_1]^2 - 2 i \omega_1 A_3'[T_1]) +$$
$$e^{-i T_0 \omega_1 - i T_0 \omega_2} (-2 i \overline{A_1[T_1]} \omega_1 \tilde{\zeta}_3 + 2 i \overline{A_3[T_1]} \omega_1 \tilde{\zeta}_3 - 3 \overline{A_1[T_1]}^2$$
$$\tilde{\eta}_3 A_1[T_1] + 6 \overline{A_1[T_1]} \overline{A_3[T_1]} \tilde{\eta}_3 A_1[T_1] - 3 \overline{A_3[T_1]}^2 \tilde{\eta}_3 A_1[T_1] -$$
$$6 \overline{A_1[T_1]} \overline{A_2[T_1]} \tilde{\eta}_3 A_2[T_1] + 6 \overline{A_2[T_1]} \overline{A_3[T_1]} \tilde{\eta}_3 A_2[T_1] +$$
$$3 \overline{A_1[T_1]}^2 \tilde{\eta}_3 A_3[T_1] - 6 \overline{A_1[T_1]} \overline{A_3[T_1]} \tilde{\eta}_3 A_3[T_1] +$$
$$3 \overline{A_3[T_1]}^2 \tilde{\eta}_3 A_3[T_1] + 2 i \omega_1 \text{ OverBar}'[A_3[T_1]] A_3'[T_1])$$

Similarly, for the complex conjugate, dividing RHS2 by $e^{-i \omega_2 T_0}$ and then grouping them for alike coefficients for easier identification. The purpose of solving for the complex conjugates is to double check that all the terms in the conjugates are alike with the complex conjugates ones - which it does.

In[15]:=
```
Collect[ExpandAll[RHS2 / e^(-i*ω2*T0)],
 {e^(i ω2 T0 - 3 i ω1 T0), e^(i ω2 T0 - 3 i ω1 T0), e^(i ω2 T0 + 3 i ω1 T0), e^(-i ω2 T0 - i ω1 T0),
  e^(-i ω2 T0 + i ω1 T0), e^(i ω2 T0 - i ω1 T0), e^(i ω2 T0 + i ω1 T0), e^(2 i ω2 T0 - 2 i ω1 T0),
  e^(2 i ω2 T0 + 2 i ω1 T0), e^(3 i ω2 T0 - i ω1 T0), e^(3 i ω2 T0 + i ω1 T0)}]
```

Out[15]=
$$\frac{e^{i T_0 \omega_2} \overline{A_2[T_1]} \omega_2^2 \tilde{\gamma}_2}{e^{i T_0 \omega_2} \omega_1^2 - e^{i T_0 \omega_2} \omega_2^2} - \frac{2 i e^{i T_0 \omega_2} \overline{A_2[T_1]} \omega_2^3 \tilde{\zeta}_2}{e^{i T_0 \omega_2} \omega_1^2 - e^{i T_0 \omega_2} \omega_2^2} + 2 i \overline{A_2[T_1]} \omega_2 \tilde{\zeta}_3 -$$
$$\frac{3 e^{i T_0 \omega_2} \overline{A_1[T_1]}^2 \overline{A_2[T_1]} \omega_2^2 \tilde{\eta}_2}{-3 e^{2 i T_0 \omega_1 + i T_0 \omega_2} \omega_1^2 - 4 e^{2 i T_0 \omega_1 + i T_0 \omega_2} \omega_1 \omega_2 - e^{2 i T_0 \omega_1 + i T_0 \omega_2} \omega_2^2} +$$
$$\frac{6 e^{i T_0 \omega_2} \overline{A_1[T_1]} \overline{A_2[T_1]} \overline{A_3[T_1]} \omega_2^2 \tilde{\eta}_2}{-3 e^{2 i T_0 \omega_1 + i T_0 \omega_2} \omega_1^2 - 4 e^{2 i T_0 \omega_1 + i T_0 \omega_2} \omega_1 \omega_2 - e^{2 i T_0 \omega_1 + i T_0 \omega_2} \omega_2^2} -$$
$$\frac{3 e^{i T_0 \omega_2} \overline{A_2[T_1]} \overline{A_3[T_1]}^2 \omega_2^2 \tilde{\eta}_2}{-3 e^{2 i T_0 \omega_1 + i T_0 \omega_2} \omega_1^2 - 4 e^{2 i T_0 \omega_1 + i T_0 \omega_2} \omega_1 \omega_2 - e^{2 i T_0 \omega_1 + i T_0 \omega_2} \omega_2^2} +$$
$$\frac{3 e^{i T_0 \omega_2} \overline{A_1[T_1]} \overline{A_2[T_1]}^2 \omega_2^2 \tilde{\eta}_2}{-4 e^{i T_0 \omega_1 + 2 i T_0 \omega_2} \omega_1 \omega_2 - 4 e^{i T_0 \omega_1 + 2 i T_0 \omega_2} \omega_2^2} -$$
$$\frac{3 e^{i T_0 \omega_2} \overline{A_2[T_1]}^2 \overline{A_3[T_1]} \omega_2^2 \tilde{\eta}_2}{-4 e^{i T_0 \omega_1 + 2 i T_0 \omega_2} \omega_1 \omega_2 - 4 e^{i T_0 \omega_1 + 2 i T_0 \omega_2} \omega_2^2} +$$
$$3 e^{-2 i T_0 \omega_1} \overline{A_1[T_1]}^2 \overline{A_2[T_1]} \tilde{\eta}_3 + e^{-2 i T_0 \omega_2} \overline{A_2[T_1]}^3 \tilde{\eta}_3 -$$
$$6 e^{-2 i T_0 \omega_1} \overline{A_1[T_1]} \overline{A_2[T_1]} \overline{A_3[T_1]} \tilde{\eta}_3 + 3 e^{-2 i T_0 \omega_1} \overline{A_2[T_1]} \overline{A_3[T_1]}^2 \tilde{\eta}_3 +$$
$$e^{-i T_0 \omega_1 - i T_0 \omega_2} (-3 \overline{A_1[T_1]} \overline{A_2[T_1]}^2 \tilde{\eta}_3 + 3 \overline{A_2[T_1]}^2 \overline{A_3[T_1]} \tilde{\eta}_3) +$$
$$e^{-3 i T_0 \omega_1 + i T_0 \omega_2} \left(\frac{\overline{A_1[T_1]}^3 \omega_2^2 \tilde{\eta}_1}{8 \omega_1^2} - \frac{\overline{A_1[T_1]}^3 \omega_2^2 \tilde{\eta}_2}{8 \omega_1^2} + \right.$$

$$\frac{3\,\overline{A_1[T_1]}^2\,\overline{A_3[T_1]}\,\omega_2^2\,\tilde{\eta}_2}{8\,\omega_1^2} - \frac{3\,\overline{A_1[T_1]}\,\overline{A_3[T_1]}^2\,\omega_2^2\,\tilde{\eta}_2}{8\,\omega_1^2} + \frac{\overline{A_3[T_1]}^3\,\omega_2^2\,\tilde{\eta}_2}{8\,\omega_1^2} -$$

$$\overline{A_1[T_1]}^3\,\tilde{\eta}_3 + 3\,\overline{A_1[T_1]}^2\,\overline{A_3[T_1]}\,\tilde{\eta}_3 - 3\,\overline{A_1[T_1]}\,\overline{A_3[T_1]}^2\,\tilde{\eta}_3 + \overline{A_3[T_1]}^3\,\tilde{\eta}_3\Big\} -$$

$$\frac{6\,e^{i\,T_0\,\omega_2}\,\overline{A_1[T_1]}\,\overline{A_2[T_1]}\,\omega_2^2\,\tilde{\eta}_2\,A_1[T_1]}{e^{i\,T_0\,\omega_2}\,\omega_1^2 - e^{i\,T_0\,\omega_2}\,\omega_2^2} +$$

$$\frac{6\,e^{i\,T_0\,\omega_2}\,\overline{A_2[T_1]}\,\overline{A_3[T_1]}\,\omega_2^2\,\tilde{\eta}_2\,A_1[T_1]}{e^{i\,T_0\,\omega_2}\,\omega_1^2 - e^{i\,T_0\,\omega_2}\,\omega_2^2} +$$

$$\frac{3\,e^{i\,T_0\,\omega_2}\,\overline{A_2[T_1]}^2\,\omega_2^2\,\tilde{\eta}_2\,A_1[T_1]}{4\,e^{-i\,T_0\,\omega_1+2\,i\,T_0\,\omega_2}\,\omega_1\,\omega_2 - 4\,e^{-i\,T_0\,\omega_1+2\,i\,T_0\,\omega_2}\,\omega_2^2} +$$

$$6\,\overline{A_1[T_1]}\,\overline{A_2[T_1]}\,\tilde{\eta}_3\,A_1[T_1] - 6\,\overline{A_2[T_1]}\,\overline{A_3[T_1]}\,\tilde{\eta}_3\,A_1[T_1] -$$

$$\frac{3\,e^{i\,T_0\,\omega_2}\,\overline{A_2[T_1]}\,\omega_2^2\,\tilde{\eta}_2\,A_1[T_1]^2}{-3\,e^{-2\,i\,T_0\,\omega_1+i\,T_0\,\omega_2}\,\omega_1^2 + 4\,e^{-2\,i\,T_0\,\omega_1+i\,T_0\,\omega_2}\,\omega_1\,\omega_2 - e^{-2\,i\,T_0\,\omega_1+i\,T_0\,\omega_2}\,\omega_2^2} +$$

$$3\,e^{2\,i\,T_0\,\omega_1}\,\overline{A_2[T_1]}\,\tilde{\eta}_3\,A_1[T_1]^2 + \frac{e^{2\,i\,T_0\,\omega_2}\,\omega_2^2\,\tilde{\gamma}_2\,A_2[T_1]}{\omega_1^2 - \omega_2^2} +$$

$$\frac{2\,i\,e^{2\,i\,T_0\,\omega_2}\,\omega_2^3\,\tilde{\xi}_2\,A_2[T_1]}{\omega_1^2 - \omega_2^2} - 2\,i\,e^{2\,i\,T_0\,\omega_2}\,\omega_2\,\tilde{\xi}_3\,A_2[T_1] -$$

$$\frac{3\,e^{2\,i\,T_0\,\omega_2}\,\overline{A_1[T_1]}^2\,\omega_2^2\,\tilde{\eta}_2\,A_2[T_1]}{-3\,e^{2\,i\,T_0\,\omega_1}\,\omega_1^2 + 4\,e^{2\,i\,T_0\,\omega_1}\,\omega_1\,\omega_2 - e^{2\,i\,T_0\,\omega_1}\,\omega_2^2} +$$

$$\frac{6\,e^{2\,i\,T_0\,\omega_2}\,\overline{A_1[T_1]}\,\overline{A_3[T_1]}\,\omega_2^2\,\tilde{\eta}_2\,A_2[T_1]}{-3\,e^{2\,i\,T_0\,\omega_1}\,\omega_1^2 + 4\,e^{2\,i\,T_0\,\omega_1}\,\omega_1\,\omega_2 - e^{2\,i\,T_0\,\omega_1}\,\omega_2^2} -$$

$$\frac{3\,e^{2\,i\,T_0\,\omega_2}\,\overline{A_3[T_1]}^2\,\omega_2^2\,\tilde{\eta}_2\,A_2[T_1]}{-3\,e^{2\,i\,T_0\,\omega_1}\,\omega_1^2 + 4\,e^{2\,i\,T_0\,\omega_1}\,\omega_1\,\omega_2 - e^{2\,i\,T_0\,\omega_1}\,\omega_2^2} -$$

$$\frac{3\,e^{i\,T_0\,\omega_2}\,\overline{A_2[T_1]}^2\,\omega_2^2\,\tilde{\eta}_2\,A_2[T_1]}{e^{i\,T_0\,\omega_2}\,\omega_1^2 - e^{i\,T_0\,\omega_2}\,\omega_2^2} + 3\,\overline{A_2[T_1]}^2\,\tilde{\eta}_3\,A_2[T_1] -$$

$$\frac{6\,e^{2\,i\,T_0\,\omega_2}\,\overline{A_1[T_1]}\,\omega_2^2\,\tilde{\eta}_2\,A_1[T_1]\,A_2[T_1]}{\omega_1^2 - \omega_2^2} +$$

$$\frac{6\,e^{2\,i\,T_0\,\omega_2}\,\overline{A_3[T_1]}\,\omega_2^2\,\tilde{\eta}_2\,A_1[T_1]\,A_2[T_1]}{\omega_1^2 - \omega_2^2} +$$

$$6\,e^{2\,i\,T_0\,\omega_2}\,\overline{A_1[T_1]}\,\tilde{\eta}_3\,A_1[T_1]\,A_2[T_1] - 6\,e^{2\,i\,T_0\,\omega_2}\,\overline{A_3[T_1]}\,\tilde{\eta}_3\,A_1[T_1]\,A_2[T_1] -$$

$$\frac{3\,e^{2\,i\,T_0\,\omega_2}\,\overline{A_2[T_1]}\,\omega_2^2\,\tilde{\eta}_2\,A_2[T_1]^2}{\omega_1^2 - \omega_2^2} + \frac{3\,e^{3\,i\,T_0\,\omega_2}\,\overline{A_1[T_1]}\,\omega_2^2\,\tilde{\eta}_2\,A_2[T_1]^2}{4\,e^{i\,T_0\,\omega_1}\,\omega_1\,\omega_2 - 4\,e^{i\,T_0\,\omega_1}\,\omega_2^2} -$$

$$\frac{3\,e^{3\,i\,T_0\,\omega_2}\,\overline{A_3[T_1]}\,\omega_2^2\,\tilde{\eta}_2\,A_2[T_1]^2}{4\,e^{i\,T_0\,\omega_1}\,\omega_1\,\omega_2 - 4\,e^{i\,T_0\,\omega_1}\,\omega_2^2} + 3\,e^{2\,i\,T_0\,\omega_2}\,\overline{A_2[T_1]}\,\tilde{\eta}_3\,A_2[T_1]^2 +$$

$$e^{4\,i\,T_0\,\omega_2}\,\tilde{\eta}_3\,A_2[T_1]^3 + e^{-2\,i\,T_0\,\omega_1+2\,i\,T_0\,\omega_2}\,\left(3\,\overline{A_1[T_1]}^2\,\tilde{\eta}_3\,A_2[T_1] - 6\,\overline{A_1[T_1]}\,\overline{A_3[T_1]}\,\tilde{\eta}_3\,A_2[T_1] + 3\,\overline{A_3[T_1]}^2\,\tilde{\eta}_3\,A_2[T_1]\right) +$$

$$e^{-i\,T_0\,\omega_1+3\,i\,T_0\,\omega_2}\,\left(-3\,\overline{A_1[T_1]}\,\tilde{\eta}_3\,A_2[T_1]^2 + 3\,\overline{A_3[T_1]}\,\tilde{\eta}_3\,A_2[T_1]^2\right) +$$

$$\frac{6\,e^{i\,T_0\,\omega_2}\,\overline{A_1[T_1]}\,\overline{A_2[T_1]}\,\omega_2^2\,\tilde{\eta}_2\,A_3[T_1]}{e^{i\,T_0\,\omega_2}\,\omega_1^2 - e^{i\,T_0\,\omega_2}\,\omega_2^2} -$$

$$\frac{6\,e^{i\,T_0\,\omega_2}\,\overline{A_2[T_1]}\,\overline{A_3[T_1]}\,\omega_2^2\,\tilde{\eta}_2\,A_3[T_1]}{e^{i\,T_0\,\omega_2}\,\omega_1^2 - e^{i\,T_0\,\omega_2}\,\omega_2^2} -$$

$$\frac{3\,e^{i\,T_0\,\omega_2}\,\overline{A_2[T_1]}^2\,\omega_2^2\,\tilde{\eta}_2\,A_3[T_1]}{4\,e^{-i\,T_0\,\omega_1+2\,i\,T_0\,\omega_2}\,\omega_1\,\omega_2 - 4\,e^{-i\,T_0\,\omega_1+2\,i\,T_0\,\omega_2}\,\omega_2^2} -$$

$$6\,\overline{A_1[T_1]}\,\overline{A_2[T_1]}\,\tilde{\eta}_3\,A_3[T_1] + 6\,\overline{A_2[T_1]}\,\overline{A_3[T_1]}\,\tilde{\eta}_3\,A_3[T_1] +$$

$$\frac{6\,e^{i\,T_0\,\omega_2}\,\overline{A_2[T_1]}\,\omega_2^2\,\tilde{\eta}_2\,A_1[T_1]\,A_3[T_1]}{-3\,e^{-2\,i\,T_0\,\omega_1+i\,T_0\,\omega_2}\,\omega_1^2 + 4\,e^{-2\,i\,T_0\,\omega_1+i\,T_0\,\omega_2}\,\omega_1\,\omega_2 - e^{-2\,i\,T_0\,\omega_1+i\,T_0\,\omega_2}\,\omega_2^2} -$$

$$6\,e^{2\,i\,T_0\,\omega_1}\,\overline{A_2[T_1]}\,\tilde{\eta}_3\,A_1[T_1]\,A_3[T_1] +$$

$$\frac{6\,e^{2\,i\,T_0\,\omega_2}\,\overline{A_1[T_1]}\,\omega_2^2\,\tilde{\eta}_2\,A_2[T_1]\,A_3[T_1]}{\omega_1^2 - \omega_2^2} -$$

$$\frac{6\,e^{2\,i\,T_0\,\omega_2}\,\overline{A_3[T_1]}\,\omega_2^2\,\tilde{\eta}_2\,A_2[T_1]\,A_3[T_1]}{\omega_1^2-\omega_2^2}-$$

$$\frac{\begin{aligned}&6\,e^{2\,i\,T_0\,\omega_2}\,\overline{A_1[T_1]}\,\tilde{\eta}_3\,A_2[T_1]\,A_3[T_1]+6\,e^{2\,i\,T_0\,\omega_2}\,\overline{A_3[T_1]}\,\tilde{\eta}_3\,A_2[T_1]\,A_3[T_1]-\\&3\,e^{i\,T_0\,\omega_2}\,\overline{A_2[T_1]}\,\omega_2^2\,\tilde{\eta}_2\,A_3[T_1]^2\end{aligned}}{-3\,e^{-2\,i\,T_0\,\omega_1+i\,T_0\,\omega_2}\,\omega_1^2+4\,e^{-2\,i\,T_0\,\omega_1+i\,T_0\,\omega_2}\,\omega_1\,\omega_2-e^{-2\,i\,T_0\,\omega_1+i\,T_0\,\omega_2}\,\omega_2^2}+$$

$$3\,e^{2\,i\,T_0\,\omega_1}\,\overline{A_2[T_1]}\,\tilde{\eta}_3\,A_3[T_1]^2+$$

$$e^{i\,T_0\,\omega_1-i\,T_0\,\omega_2}\,\left(-3\,\overline{A_2[T_1]}^2\,\tilde{\eta}_3\,A_1[T_1]+3\,\overline{A_2[T_1]}^2\,\tilde{\eta}_3\,A_3[T_1]\right)+$$

$$e^{i\,T_0\,\omega_1+3\,i\,T_0\,\omega_2}\left\{\frac{3\,\omega_2^2\,\tilde{\eta}_2\,A_1[T_1]\,A_2[T_1]^2}{-4\,\omega_1\,\omega_2-4\,\omega_2^2}-3\,\tilde{\eta}_3\,A_1[T_1]\,A_2[T_1]^2-\right.$$

$$\left.\frac{3\,\omega_2^2\,\tilde{\eta}_2\,A_2[T_1]^2\,A_3[T_1]}{-4\,\omega_1\,\omega_2-4\,\omega_2^2}+3\,\tilde{\eta}_3\,A_2[T_1]^2\,A_3[T_1]\right\}+$$

$$e^{2\,i\,T_0\,\omega_1+2\,i\,T_0\,\omega_2}\left\{-\frac{3\,\omega_2^2\,\tilde{\eta}_2\,A_1[T_1]^2\,A_2[T_1]}{-3\,\omega_1^2-4\,\omega_1\,\omega_2-\omega_2^2}+3\,\tilde{\eta}_3\,A_1[T_1]^2\,A_2[T_1]+\right.$$

$$\frac{6\,\omega_2^2\,\tilde{\eta}_2\,A_1[T_1]\,A_2[T_1]\,A_3[T_1]}{-3\,\omega_1^2-4\,\omega_1\,\omega_2-\omega_2^2}-6\,\tilde{\eta}_3\,A_1[T_1]\,A_2[T_1]\,A_3[T_1]-$$

$$\left.\frac{3\,\omega_2^2\,\tilde{\eta}_2\,A_2[T_1]\,A_3[T_1]^2}{-3\,\omega_1^2-4\,\omega_1\,\omega_2-\omega_2^2}+3\,\tilde{\eta}_3\,A_2[T_1]\,A_3[T_1]^2\right\}+e^{3\,i\,T_0\,\omega_1+i\,T_0\,\omega_2}$$

$$\left\{\frac{\omega_2^2\,\tilde{\eta}_1\,A_1[T_1]^3}{8\,\omega_1^2}-\frac{\omega_2^2\,\tilde{\eta}_2\,A_1[T_1]^3}{8\,\omega_1^2}-\tilde{\eta}_3\,A_1[T_1]^3+\frac{3\,\omega_2^2\,\tilde{\eta}_2\,A_1[T_1]^2\,A_3[T_1]}{8\,\omega_1^2}+\right.$$

$$3\,\tilde{\eta}_3\,A_1[T_1]^2\,A_3[T_1]-\frac{3\,\omega_2^2\,\tilde{\eta}_2\,A_1[T_1]\,A_3[T_1]^2}{8\,\omega_1^2}-$$

$$\left.3\,\tilde{\eta}_3\,A_1[T_1]\,A_3[T_1]^2+\frac{\omega_2^2\,\tilde{\eta}_2\,A_3[T_1]^3}{8\,\omega_1^2}+\tilde{\eta}_3\,A_3[T_1]^3\right\}-$$

$$2\,i\,e^{2\,i\,T_0\,\omega_2}\,\omega_2\,A_2'[T_1]+2\,i\,\omega_2\,\text{OverBar}'[A_2[T_1]]\,A_2'[T_1]+e^{i\,T_0\,\omega_1+i\,T_0\,\omega_2}$$

$$\begin{aligned}&(2\,i\,\omega_1\,\tilde{\zeta}_3\,A_1[T_1]-3\,\overline{A_1[T_1]}\,\tilde{\eta}_3\,A_1[T_1]^2+3\,\overline{A_3[T_1]}\,\tilde{\eta}_3\,A_1[T_1]^2-\\&6\,\overline{A_2[T_1]}\,\tilde{\eta}_3\,A_1[T_1]\,A_2[T_1]-2\,i\,\omega_1\,\tilde{\zeta}_3\,A_3[T_1]+6\,\overline{A_1[T_1]}\,\tilde{\eta}_3\,A_1[T_1]\\&A_3[T_1]-6\,\overline{A_3[T_1]}\,\tilde{\eta}_3\,A_1[T_1]\,A_3[T_1]+6\,\overline{A_2[T_1]}\,\tilde{\eta}_3\,A_2[T_1]\,A_3[T_1]-\\&3\,\overline{A_1[T_1]}\,\tilde{\eta}_3\,A_3[T_1]^2+3\,\overline{A_3[T_1]}\,\tilde{\eta}_3\,A_3[T_1]^2-2\,i\,\omega_1\,A_3'[T_1])+\\&e^{-i\,T_0\,\omega_1+i\,T_0\,\omega_2}\,(-2\,i\,\overline{A_1[T_1]}\,\omega_1\,\tilde{\zeta}_3+2\,i\,\overline{A_3[T_1]}\,\omega_1\,\tilde{\zeta}_3-3\,\overline{A_1[T_1]}^2\\&\tilde{\eta}_3\,A_1[T_1]+6\,\overline{A_1[T_1]}\,\overline{A_3[T_1]}\,\tilde{\eta}_3\,A_1[T_1]-3\,\overline{A_3[T_1]}^2\,\tilde{\eta}_3\,A_1[T_1]-\\&6\,\overline{A_1[T_1]}\,\overline{A_2[T_1]}\,\tilde{\eta}_3\,A_2[T_1]+6\,\overline{A_2[T_1]}\,\overline{A_3[T_1]}\,\tilde{\eta}_3\,A_2[T_1]+\\&3\,\overline{A_1[T_1]}^2\,\tilde{\eta}_3\,A_3[T_1]-6\,\overline{A_1[T_1]}\,\overline{A_3[T_1]}\,\tilde{\eta}_3\,A_3[T_1]+\\&3\,\overline{A_3[T_1]}^2\,\tilde{\eta}_3\,A_3[T_1]+2\,i\,\omega_1\,\text{OverBar}'[A_3[T_1]]\,A_3'[T_1])\end{aligned}$$

C.5 Identifying the Internal Resonances of x_{21}

Similar to Appendix C.2, Table C-2 below gives a full list of resonances from *In[1]* of Appendix C.5 on the next page. And only resonances that show coupling between at least two modes are relevant.

Secular Terms	Possible Internal Resonance	Complex Conjugates	Possible Internal Resonance
$e^{i2\omega_2 T_0}$	N.A.	$e^{-i4\omega_2 T_0}$	N.A.
$e^{i(\omega_1+\omega_2)T_0}$	$\omega_2 \approx -\omega_1$	$e^{-i(\omega_1+3\omega_2)T_0}$	$\omega_2 \approx -\frac{1}{3}\omega_1$
$e^{i2\omega_1 T_0}$	N.A.	$e^{-i(2\omega_1+2\omega_2)T_0}$	$\omega_2 \approx -\omega_1$
$e^{i(3\omega_1-\omega_2)T_0}$	$\boxed{\omega_2 \approx 3\omega_1}$	$e^{-i(3\omega_1+\omega_2)T_0}$	$\omega_2 \approx -3\omega_1$
$e^{i(\omega_1-3\omega_2)T_0}$	$\boxed{\omega_2 \approx \frac{1}{3}\omega_1}$	$e^{-i(\omega_1-\omega_2)T_0}$	$\omega_2 \approx \omega_1$
$e^{i(2\omega_1-2\omega_2)T_0}$	$\boxed{\omega_2 \approx \omega_1}$	$e^{-i2\omega_1 T_0}$	N.A.
$e^{i(\omega_1-\omega_2)T_0}$	$\boxed{\omega_2 \approx \omega_1}$	$e^{-i(\omega_1+\omega_2)T_0}$	$\omega_2 \approx -\omega_1$

Table C-2: Possible internal resonances for 2nd order perturbation equations (Case 1)

From the table above, the internal resonances of the system are contributed by the terms that are highlighted with a box, i.e. $\omega_2 \approx \frac{1}{3}\omega_1$, $\omega_2 \approx 3\omega_1$ and $\omega_2 \approx \omega_1$.

Multiplying $e^{\dot{\imath} T_0 \omega_2}$ back into Out[14] from Appendix C.4 and rearranging it:

In[1]:= RHS2 ==

$$
\begin{aligned}
&e^{\dot{\imath} T_0 \omega_2} \left(e^{2\,\dot{\imath} T_0 \omega_2}\, \tilde{\eta}_3\, A_2[T_1]^3 + e^{-4\,\dot{\imath} T_0 \omega_2}\, \overline{A_2[T_1]}^3\, \tilde{\eta}_3 + \right. \\
&\quad e^{\dot{\imath} T_0 \omega_1 + \dot{\imath} T_0 \omega_2} \\
&\qquad \left(\frac{3\,\omega_2^2\,\tilde{\eta}_2\, A_1[T_1]\, A_2[T_1]^2}{-4\,\omega_1\,\omega_2 - 4\,\omega_2^2} - 3\,\tilde{\eta}_3\, A_1[T_1]\, A_2[T_1]^2 - \right. \\
&\qquad\quad \left. \frac{3\,\omega_2^2\,\tilde{\eta}_2\, A_2[T_1]^2\, A_3[T_1]}{-4\,\omega_1\,\omega_2 - 4\,\omega_2^2} + 3\,\tilde{\eta}_3\, A_2[T_1]^2\, A_3[T_1] \right) + \\
&e^{-\dot{\imath} T_0 \omega_1 - 3\,\dot{\imath} T_0 \omega_2} \\
&\qquad \left(\frac{3\,\overline{A_1[T_1]}\,\overline{A_2[T_1]}^2\,\omega_2^2\,\tilde{\eta}_2}{-4\,\omega_1\,\omega_2 - 4\,\omega_2^2} - 3\,\overline{A_1[T_1]}\,\overline{A_2[T_1]}^2\,\tilde{\eta}_3 - \right. \\
&\qquad\quad \left. \frac{3\,\overline{A_2[T_1]}^2\,\overline{A_3[T_1]}\,\omega_2^2\,\tilde{\eta}_2}{-4\,\omega_1\,\omega_2 - 4\,\omega_2^2} + 3\,\overline{A_2[T_1]}^2\,\overline{A_3[T_1]}\,\tilde{\eta}_3 \right) + \\
&e^{2\,\dot{\imath} T_0 \omega_1} \left(\frac{6\,\omega_2^2\,\tilde{\eta}_2\, A_1[T_1]\, A_2[T_1]\, A_3[T_1]}{-3\,\omega_1^2 - 4\,\omega_1\,\omega_2 - \omega_2^2} - 6\,\tilde{\eta}_3\, A_1[T_1]\, A_2[T_1]\, A_3[T_1] - \right. \\
&\qquad \frac{3\,\omega_2^2\,\tilde{\eta}_2\, A_2[T_1]\, A_3[T_1]^2}{-3\,\omega_1^2 - 4\,\omega_1\,\omega_2 - \omega_2^2} + 3\,\tilde{\eta}_3\, A_2[T_1]\, A_3[T_1]^2 - \\
&\qquad \left. \frac{3\,\omega_2^2\,\tilde{\eta}_2\, A_1[T_1]^2\, A_2[T_1]}{-3\,\omega_1^2 - 4\,\omega_1\,\omega_2 - \omega_2^2} + 3\,\tilde{\eta}_3\, A_1[T_1]^2\, A_2[T_1] \right) + \\
&e^{-2\,\dot{\imath} T_0 \omega_1 - 2\,\dot{\imath} T_0 \omega_2} \\
&\qquad \left(\frac{6\,\overline{A_1[T_1]}\,\overline{A_2[T_1]}\,\overline{A_3[T_1]}\,\omega_2^2\,\tilde{\eta}_2}{-3\,\omega_1^2 - 4\,\omega_1\,\omega_2 - \omega_2^2} - 6\,\overline{A_1[T_1]}\,\overline{A_2[T_1]}\,\overline{A_3[T_1]}\,\tilde{\eta}_3 - \right. \\
&\qquad \frac{3\,\overline{A_2[T_1]}\,\overline{A_3[T_1]}^2\,\omega_2^2\,\tilde{\eta}_2}{-3\,\omega_1^2 - 4\,\omega_1\,\omega_2 - \omega_2^2} + 3\,\overline{A_2[T_1]}\,\overline{A_3[T_1]}^2\,\tilde{\eta}_3 - \\
&\qquad \left. \frac{3\,\overline{A_1[T_1]}^2\,\overline{A_2[T_1]}\,\omega_2^2\,\tilde{\eta}_2}{-3\,\omega_1^2 - 4\,\omega_1\,\omega_2 - \omega_2^2} + 3\,\overline{A_1[T_1]}^2\,\overline{A_2[T_1]}\,\tilde{\eta}_3 \right) + \\
&e^{3\,\dot{\imath} T_0 \omega_1 - \dot{\imath} T_0 \omega_2} \\
&\qquad \left(\frac{\omega_2^2\,\tilde{\eta}_1\, A_1[T_1]^3}{8\,\omega_1^2} - \frac{\omega_2^2\,\tilde{\eta}_2\, A_1[T_1]^3}{8\,\omega_1^2} - \tilde{\eta}_3\, A_1[T_1]^3 + \right. \\
&\qquad\quad \frac{3\,\omega_2^2\,\tilde{\eta}_2\, A_1[T_1]^2\, A_3[T_1]}{8\,\omega_1^2} + 3\,\tilde{\eta}_3\, A_1[T_1]^2\, A_3[T_1] - \\
&\qquad\quad \frac{3\,\omega_2^2\,\tilde{\eta}_2\, A_1[T_1]\, A_3[T_1]^2}{8\,\omega_1^2} - 3\,\tilde{\eta}_3\, A_1[T_1]\, A_3[T_1]^2 + \frac{\omega_2^2\,\tilde{\eta}_2\, A_3[T_1]^3}{8\,\omega_1^2} + \\
&\qquad\quad \left. \tilde{\eta}_3\, A_3[T_1]^3 \right) + \\
&e^{-3\,\dot{\imath} T_0 \omega_1 - \dot{\imath} T_0 \omega_2} \\
&\qquad \left(\frac{\overline{A_1[T_1]}^3\,\omega_2^2\,\tilde{\eta}_1}{8\,\omega_1^2} - \frac{\overline{A_1[T_1]}^3\,\omega_2^2\,\tilde{\eta}_2}{8\,\omega_1^2} - \overline{A_1[T_1]}^3\,\tilde{\eta}_3 + \right. \\
&\qquad\quad \frac{3\,\overline{A_1[T_1]}^2\,\overline{A_3[T_1]}\,\omega_2^2\,\tilde{\eta}_2}{8\,\omega_1^2} + 3\,\overline{A_1[T_1]}^2\,\overline{A_3[T_1]}\,\tilde{\eta}_3 - \\
&\qquad\quad \frac{3\,\overline{A_1[T_1]}\,\overline{A_3[T_1]}^2\,\omega_2^2\,\tilde{\eta}_2}{8\,\omega_1^2} - 3\,\overline{A_1[T_1]}\,\overline{A_3[T_1]}^2\,\tilde{\eta}_3 + \frac{\overline{A_3[T_1]}^3\,\omega_2^2\,\tilde{\eta}_2}{8\,\omega_1^2} + \\
&\qquad\quad \left. \overline{A_3[T_1]}^3\,\tilde{\eta}_3 \right) +
\end{aligned}
$$

$$e^{i n T_0 \omega_1 - 3 i n T_0 \omega_2}$$

$$\left(-3\,\overline{A_2[T_1]}^2\,\tilde{\eta}_3\,A_1[T_1] + 3\,\overline{A_2[T_1]}^2\,\tilde{\eta}_3\,A_3[T_1] + \frac{3\,\overline{A_2[T_1]}^2\,\omega_2^2\,\tilde{\eta}_2\,A_1[T_1]}{4\,\omega_1\,\omega_2 - 4\,\omega_2^2} - \frac{3\,\overline{A_2[T_1]}^2\,\omega_2^2\,\tilde{\eta}_2\,A_3[T_1]}{4\,\omega_1\,\omega_2 - 4\,\omega_2^2}\right) +$$

$$e^{-i n T_0 \omega_1 + i n T_0 \omega_2}$$

$$\left(-3\,\overline{A_1[T_1]}\,\tilde{\eta}_3\,A_2[T_1]^2 + 3\,\overline{A_3[T_1]}\,\tilde{\eta}_3\,A_2[T_1]^2 + \frac{3\,\overline{A_1[T_1]}\,\omega_2^2\,\tilde{\eta}_2\,A_2[T_1]^2}{4\,\omega_1\,\omega_2 - 4\,\omega_2^2} - \frac{3\,\overline{A_3[T_1]}\,\omega_2^2\,\tilde{\eta}_2\,A_2[T_1]^2}{4\,\omega_1\,\omega_2 - 4\,\omega_2^2}\right) +$$

$$e^{2 i n T_0 \omega_1 - 2 i n T_0 \omega_2}$$

$$\left(3\,\overline{A_2[T_1]}\,\tilde{\eta}_3\,A_1[T_1]^2 - 6\,\overline{A_2[T_1]}\,\tilde{\eta}_3\,A_1[T_1]\,A_3[T_1] + 3\,\overline{A_2[T_1]}\,\tilde{\eta}_3\,A_3[T_1]^2 - \frac{3\,\overline{A_2[T_1]}\,\omega_2^2\,\tilde{\eta}_2\,A_1[T_1]^2}{-3\,\omega_1^2 + 4\,\omega_1\,\omega_2 - \omega_2^2} + \frac{6\,\overline{A_2[T_1]}\,\omega_2^2\,\tilde{\eta}_2\,A_1[T_1]\,A_3[T_1]}{-3\,\omega_1^2 + 4\,\omega_1\,\omega_2 - \omega_2^2} - \frac{3\,\overline{A_2[T_1]}\,\omega_2^2\,\tilde{\eta}_2\,A_3[T_1]^2}{-3\,\omega_1^2 + 4\,\omega_1\,\omega_2 - \omega_2^2}\right) +$$

$$e^{-2 i n T_0 \omega_1}\left(3\,\overline{A_1[T_1]}^2\,\tilde{\eta}_3\,A_2[T_1] - 6\,\overline{A_1[T_1]}\,\overline{A_3[T_1]}\,\tilde{\eta}_3\,A_2[T_1] + 3\,\overline{A_3[T_1]}^2\,\tilde{\eta}_3\,A_2[T_1] - \frac{3\,\overline{A_1[T_1]}^2\,\omega_2^2\,\tilde{\eta}_2\,A_2[T_1]}{-3\,\omega_1^2 + 4\,\omega_1\,\omega_2 - \omega_2^2} + \frac{6\,\overline{A_1[T_1]}\,\overline{A_3[T_1]}\,\omega_2^2\,\tilde{\eta}_2\,A_2[T_1]}{-3\,\omega_1^2 + 4\,\omega_1\,\omega_2 - \omega_2^2} - \frac{3\,\overline{A_3[T_1]}^2\,\omega_2^2\,\tilde{\eta}_2\,A_2[T_1]}{-3\,\omega_1^2 + 4\,\omega_1\,\omega_2 - \omega_2^2}\right) +$$

$$e^{i n T_0 \omega_1 - i n T_0 \omega_2}$$

$$\begin{aligned}&(2\,i n\,\omega_1\,\tilde{\xi}_3\,A_1[T_1] - 3\,\overline{A_1[T_1]}\,\tilde{\eta}_3\,A_1[T_1]^2 + 3\,\overline{A_3[T_1]}\,\tilde{\eta}_3\,A_1[T_1]^2 - \\ &\quad 6\,\overline{A_2[T_1]}\,\tilde{\eta}_3\,A_1[T_1]\,A_2[T_1] - 2\,i n\,\omega_1\,\tilde{\xi}_3\,A_3[T_1] + \\ &\quad 6\,\overline{A_1[T_1]}\,\tilde{\eta}_3\,A_1[T_1]\,A_3[T_1] - 6\,\overline{A_3[T_1]}\,\tilde{\eta}_3\,A_1[T_1]\,A_3[T_1] + \\ &\quad 6\,\overline{A_2[T_1]}\,\tilde{\eta}_3\,A_2[T_1]\,A_3[T_1] - 3\,\overline{A_1[T_1]}\,\tilde{\eta}_3\,A_3[T_1]^2 + \\ &\quad 3\,\overline{A_3[T_1]}\,\tilde{\eta}_3\,A_3[T_1]^2 - 2\,i n\,\omega_1\,A_3'[T_1])\,+\end{aligned}$$

$$e^{-i n T_0 \omega_1 - i n T_0 \omega_2}$$

$$\begin{aligned}&(-2\,i n\,\overline{A_1[T_1]}\,\omega_1\,\tilde{\xi}_3 - 3\,\overline{A_1[T_1]}^2\,\tilde{\eta}_3\,A_1[T_1] + 3\,\overline{A_1[T_1]}^2\,\tilde{\eta}_3\,A_3[T_1] - \\ &\quad 6\,\overline{A_1[T_1]}\,\overline{A_2[T_1]}\,\tilde{\eta}_3\,A_2[T_1] + 2\,i n\,\overline{A_3[T_1]}\,\omega_1\,\tilde{\xi}_3 + \\ &\quad 6\,\overline{A_1[T_1]}\,\overline{A_3[T_1]}\,\tilde{\eta}_3\,A_1[T_1] - 6\,\overline{A_1[T_1]}\,\overline{A_3[T_1]}\,\tilde{\eta}_3\,A_3[T_1] + \\ &\quad 6\,\overline{A_2[T_1]}\,\overline{A_3[T_1]}\,\tilde{\eta}_3\,A_2[T_1] - 3\,\overline{A_3[T_1]}^2\,\tilde{\eta}_3\,A_1[T_1] + \\ &\quad 3\,\overline{A_3[T_1]}^2\,\tilde{\eta}_3\,A_3[T_1] + 2\,i n\,\omega_1\,\mathit{OverBar}'[A_3[T_1]]\,A_3'[T_1])\,+\end{aligned}$$

$$\begin{aligned}&\frac{\omega_2^2\,\tilde{\gamma}_2\,A_2[T_1]}{\omega_1^2 - \omega_2^2} + \frac{2\,i n\,\omega_2^3\,\tilde{\xi}_2\,A_2[T_1]}{\omega_1^2 - \omega_2^2} - 2\,i n\,\omega_2\,\tilde{\xi}_3\,A_2[T_1] - \\ &\frac{6\,\overline{A_1[T_1]}\,\omega_2^2\,\tilde{\eta}_2\,A_1[T_1]\,A_2[T_1]}{\omega_1^2 - \omega_2^2} + \frac{6\,\overline{A_3[T_1]}\,\omega_2^2\,\tilde{\eta}_2\,A_1[T_1]\,A_2[T_1]}{\omega_1^2 - \omega_2^2} + \\ &6\,\overline{A_1[T_1]}\,\tilde{\eta}_3\,A_1[T_1]\,A_2[T_1] - 6\,\overline{A_3[T_1]}\,\tilde{\eta}_3\,A_1[T_1]\,A_2[T_1] - \\ &\frac{3\,\overline{A_2[T_1]}\,\omega_2^2\,\tilde{\eta}_2\,A_2[T_1]^2}{\omega_1^2 - \omega_2^2} + 3\,\overline{A_2[T_1]}\,\tilde{\eta}_3\,A_2[T_1]^2 + \\ &\frac{6\,\overline{A_1[T_1]}\,\omega_2^2\,\tilde{\eta}_2\,A_2[T_1]\,A_3[T_1]}{\omega_1^2 - \omega_2^2} - \frac{6\,\overline{A_3[T_1]}\,\omega_2^2\,\tilde{\eta}_2\,A_2[T_1]\,A_3[T_1]}{\omega_1^2 - \omega_2^2} - \\ &6\,\overline{A_1[T_1]}\,\tilde{\eta}_3\,A_2[T_1]\,A_3[T_1] + 6\,\overline{A_3[T_1]}\,\tilde{\eta}_3\,A_2[T_1]\,A_3[T_1] - \\ &2\,i n\,\omega_2\,A_2'[T_1] + \frac{e^{-i n T_0 \omega_2}\,\overline{A_2[T_1]}\,\omega_2^2\,\tilde{\gamma}_2}{e^{i n T_0 \omega_2}\,\omega_1^2 - e^{i n T_0 \omega_2}\,\omega_2^2} - \frac{2\,i n\,e^{-i n T_0 \omega_2}\,\overline{A_2[T_1]}\,\omega_2^3\,\tilde{\xi}_2}{e^{i n T_0 \omega_2}\,\omega_1^2 - e^{i n T_0 \omega_2}\,\omega_2^2} - \\ &\frac{6\,e^{-i n T_0 \omega_2}\,\overline{A_1[T_1]}\,\overline{A_2[T_1]}\,\omega_2^2\,\tilde{\eta}_2\,A_1[T_1]}{e^{i n T_0 \omega_2}\,\omega_1^2 - e^{i n T_0 \omega_2}\,\omega_2^2} +\end{aligned}$$

$$\frac{6\,e^{-\dot{n}T_0\omega_2}\,\overline{A_2[T_1]}\,\overline{A_3[T_1]}\,\omega_2^2\,\tilde{\eta}_2\,A_1[T_1]}{e^{\dot{n}T_0\omega_2}\,\omega_1^2 - e^{\dot{n}T_0\omega_2}\,\omega_2^2} -$$

$$\frac{3\,e^{-\dot{n}T_0\omega_2}\,\overline{A_2[T_1]}^2\,\omega_2^2\,\tilde{\eta}_2\,A_2[T_1]}{e^{\dot{n}T_0\omega_2}\,\omega_1^2 - e^{\dot{n}T_0\omega_2}\,\omega_2^2} +$$

$$\frac{6\,e^{-\dot{n}T_0\omega_2}\,\overline{A_1[T_1]}\,\overline{A_2[T_1]}\,\omega_2^2\,\tilde{\eta}_2\,A_3[T_1]}{e^{\dot{n}T_0\omega_2}\,\omega_1^2 - e^{\dot{n}T_0\omega_2}\,\omega_2^2} -$$

$$\frac{6\,e^{-\dot{n}T_0\omega_2}\,\overline{A_2[T_1]}\,\overline{A_3[T_1]}\,\omega_2^2\,\tilde{\eta}_2\,A_3[T_1]}{e^{\dot{n}T_0\omega_2}\,\omega_1^2 - e^{\dot{n}T_0\omega_2}\,\omega_2^2} + 2\,\dot{n}\,e^{-2\dot{n}T_0\omega_2}\,\overline{A_2[T_1]}\,\omega_2\,\tilde{\xi}_3 +$$

$$6\,e^{-2\dot{n}T_0\omega_2}\,\overline{A_1[T_1]}\,\overline{A_2[T_1]}\,\tilde{\eta}_3\,A_1[T_1] -$$

$$6\,e^{-2\dot{n}T_0\omega_2}\,\overline{A_2[T_1]}\,\overline{A_3[T_1]}\,\tilde{\eta}_3\,A_1[T_1] + 3\,e^{-2\dot{n}T_0\omega_2}\,\overline{A_2[T_1]}^2\,\tilde{\eta}_3\,A_2[T_1] -$$

$$6\,e^{-2\dot{n}T_0\omega_2}\,\overline{A_1[T_1]}\,\overline{A_2[T_1]}\,\tilde{\eta}_3\,A_3[T_1] +$$

$$6\,e^{-2\dot{n}T_0\omega_2}\,\overline{A_2[T_1]}\,\overline{A_3[T_1]}\,\tilde{\eta}_3\,A_3[T_1] +$$

$$2\,\dot{n}\,e^{-2\dot{n}T_0\omega_2}\,\omega_2\,\mathrm{OverBar}'[A_2[T_1]]\,A_2'[T_1]\Big);$$

: *'Always' Secular Terms*

Italics: Complex Conjugates of the Preceding Terms

C.6 Derivation of Modulation Equations

From equation (3.3 - 49), the polar expressions are :

In[1]:=
$$A_1[T_1] = \frac{a_1[T_1]}{2} \times e^{i \times \beta_1[T_1]};$$
$$\overline{A_1[T_1]} = \frac{a_1[T_1]}{2} \times e^{-i \times \beta_1[T_1]};$$
$$A_2[T_1] = \frac{a_2[T_1]}{2} \times e^{i \times \beta_2[T_1]};$$
$$\overline{A_2[T_1]} = \frac{a_2[T_1]}{2} \times e^{-i \times \beta_2[T_1]};$$

From equation (3.3-36) :

In[5]:=
$$A_3[T_1] = \Gamma\left(\frac{a_1[T_1]}{2} \times e^{i \times \beta_1[T_1]}\right);$$
$$\overline{A_3[T_1]} = \Gamma\left(\frac{a_1[T_1]}{2} \times e^{-i \times \beta_1[T_1]}\right);$$

Derivative of $A_1[T_1]$:

In[7]:=
$$A_1'[T_1] = \frac{1}{2} e^{i \beta_1[T_1]} a_1'[T_1] + \frac{1}{2} i e^{i \beta_1[T_1]} a_1[T_1] \beta_1'[T_1];$$

The secular terms of x_{11} from equation (3.3-44) :

In[8]:=
$$ST1 == -e^{i T_0 (3\omega_2 - \omega_1)} \tilde{\eta}_2 A_2[T_1]^3 + \frac{1}{2} e^{i (\Omega - \omega_1) T_0} \tilde{F} - \tilde{\gamma}_2 A_1[T_1] - 2 i \omega_1 \tilde{\xi}_1 A_1[T_1] - 2 i \omega_1 \tilde{\xi}_2 A_1[T_1] - 3 \overline{A_1[T_1]} \tilde{\eta}_1 A_1[T_1]^2 + 3 \overline{A_1[T_1]} \tilde{\eta}_2 A_1[T_1]^2 - 3 \overline{A_3[T_1]} \tilde{\eta}_2 A_1[T_1]^2 + 6 \overline{A_2[T_1]} \tilde{\eta}_2 A_1[T_1] A_2[T_1] + \tilde{\gamma}_2 A_3[T_1] + 2 i \omega_1 \tilde{\xi}_2 A_3[T_1] - 6 \overline{A_1[T_1]} \tilde{\eta}_2 A_1[T_1] A_3[T_1] + 6 \overline{A_3[T_1]} \tilde{\eta}_2 A_1[T_1] A_3[T_1] - 6 \overline{A_2[T_1]} \tilde{\eta}_2 A_2[T_1] A_3[T_1] + 3 \overline{A_1[T_1]} \tilde{\eta}_2 A_3[T_1]^2 - 3 \overline{A_3[T_1]} \tilde{\eta}_2 A_3[T_1]^2 - 2 i \omega_1 A_1'[T_1];$$

From equation (3.3-39) :

In[9]:=
$$\varepsilon \nu_1 == \Omega - \omega_1;$$

From equation (3.3-40) :

In[10]:=
$$\varepsilon \sigma_1 == \omega_2 - \frac{1}{3} \omega_1;$$

And because $\varepsilon T_0 \equiv T_1$:

In[11]:=
$$\varepsilon \nu_1 T_0 == \nu_1 T_1;$$

In[12]:=
$$\varepsilon \sigma_1 T_0 == \sigma_1 T_1;$$

Therefore, equation In[8] becomes:

```
In[13]:= ST1 = -e^(i×3×σ1×T1) η̃2 A2[T1]^3 + 1/2 e^(i×ν×T1) F̃ - γ̃2 A1[T1] - 2 i ω1 ξ̃1 A1[T1] -
          2 i ω1 ξ̃2 A1[T1] - 3 Conjugate[A1[T1]] η̃1 A1[T1]^2 + 3 Conjugate[A1[T1]] η̃2 A1[T1]^2 -
          3 Conjugate[A3[T1]] η̃2 A1[T1]^2 + 6 Conjugate[A2[T1]] η̃2 A1[T1] A2[T1] + γ̃2 A3[T1] +
          2 i ω1 ξ̃2 A3[T1] - 6 Conjugate[A1[T1]] η̃2 A1[T1] A3[T1] + 6 Conjugate[A3[T1]] η̃2 A1[T1] A3[T1] -
          6 Conjugate[A2[T1]] η̃2 A2[T1] A3[T1] + 3 Conjugate[A1[T1]] η̃2 A3[T1]^2 - 3 Conjugate[A3[T1]] η̃2 A3[T1]^2 -
          2 i ω1 A1'[T1]
```

Substituting polar expressions In[1] to In[7] into In[13]:

$$
\begin{aligned}
\text{Out[13]}= \;& \frac{1}{2} e^{i\nu T_1} \tilde{F} - \frac{1}{2} e^{i\beta_1[T_1]} \tilde{\gamma}_2 a_1[T_1] + \frac{1}{2} e^{i\beta_1[T_1]} \Gamma \tilde{\gamma}_2 a_1[T_1] - \\
& i e^{i\beta_1[T_1]} \omega_1 \tilde{\xi}_1 a_1[T_1] - i e^{i\beta_1[T_1]} \omega_1 \tilde{\xi}_2 a_1[T_1] + \\
& i e^{i\beta_1[T_1]} \Gamma \omega_1 \tilde{\xi}_2 a_1[T_1] - \frac{3}{8} e^{i\beta_1[T_1]} \tilde{\eta}_1 a_1[T_1]^3 + \frac{3}{8} e^{i\beta_1[T_1]} \tilde{\eta}_2 a_1[T_1]^3 - \\
& \frac{9}{8} e^{i\beta_1[T_1]} \Gamma \tilde{\eta}_2 a_1[T_1]^3 + \frac{9}{8} e^{i\beta_1[T_1]} \Gamma^2 \tilde{\eta}_2 a_1[T_1]^3 - \\
& \frac{3}{8} e^{i\beta_1[T_1]} \Gamma^3 \tilde{\eta}_2 a_1[T_1]^3 + \frac{3}{4} e^{i\beta_1[T_1]} \tilde{\eta}_2 a_1[T_1] a_2[T_1]^2 - \\
& \frac{3}{4} e^{i\beta_1[T_1]} \Gamma \tilde{\eta}_2 a_1[T_1] a_2[T_1]^2 - \frac{1}{8} e^{3 i T_1 \sigma_1 + 3 i \beta_2[T_1]} \tilde{\eta}_2 a_2[T_1]^3 - \\
& 2 i \omega_1 \left(\frac{1}{2} e^{i\beta_1[T_1]} a_1'[T_1] + \frac{1}{2} i e^{i\beta_1[T_1]} a_1[T_1] \beta_1'[T_1] \right)
\end{aligned}
$$

Dividing throughout by $e^{i\times\beta_1[T_1]}$:

```
In[14]:= ExpandAll[ST1 / e^(i×β1[T1])]
```

$$
\begin{aligned}
\text{Out[14]}= \;& \frac{1}{2} e^{i\nu T_1 - i\beta_1[T_1]} \tilde{F} - \frac{1}{2} \tilde{\gamma}_2 a_1[T_1] + \frac{1}{2} \Gamma \tilde{\gamma}_2 a_1[T_1] - \\
& i \omega_1 \tilde{\xi}_1 a_1[T_1] - i \omega_1 \tilde{\xi}_2 a_1[T_1] + i \Gamma \omega_1 \tilde{\xi}_2 a_1[T_1] - \frac{3}{8} \tilde{\eta}_1 a_1[T_1]^3 + \\
& \frac{3}{8} \tilde{\eta}_2 a_1[T_1]^3 - \frac{9}{8} \Gamma \tilde{\eta}_2 a_1[T_1]^3 + \frac{9}{8} \Gamma^2 \tilde{\eta}_2 a_1[T_1]^3 - \\
& \frac{3}{8} \Gamma^3 \tilde{\eta}_2 a_1[T_1]^3 + \frac{3}{4} \tilde{\eta}_2 a_1[T_1] a_2[T_1]^2 - \frac{3}{4} \Gamma \tilde{\eta}_2 a_1[T_1] a_2[T_1]^2 - \\
& \frac{1}{8} e^{3 i T_1 \sigma_1 - i\beta_1[T_1] + 3 i \beta_2[T_1]} \tilde{\eta}_2 a_2[T_1]^3 - i \omega_1 a_1'[T_1] + \omega_1 a_1[T_1] \beta_1'[T_1]
\end{aligned}
$$

Let

```
In[15]:= Λ1 == ν1 T1 - β1[T1];
```

```
In[16]:= Φ1 == 3 σ1 T1 - β1[T1] + 3 β2[T1];
```

Substitute above into Out[14] and convert them into trigonometrical forms

In[17]:=
```
ExpToTrig[1/2 e^(i*Λ1) F~ - 1/8 e^(i*Ξ1) η~2 a2[T1]^3 - 1/2 γ~2 a1[T1] +
  1/2 Γ γ~2 a1[T1] - i ω1 ξ~1 a1[T1] - i ω1 ξ~2 a1[T1] + i Γ ω1 ξ~2 a1[T1] -
  3/8 η~1 a1[T1]^3 + 3/8 η~2 a1[T1]^3 - 9/8 Γ η~2 a1[T1]^3 + 9/8 Γ^2 η~2 a1[T1]^3 -
  3/8 Γ^3 η~2 a1[T1]^3 + 3/4 η~2 a1[T1] a2[T1]^2 - 3/4 Γ η~2 a1[T1] a2[T1]^2 -
  i ω1 a1'[T1] + ω1 a1[T1] β1'[T1]]
```

Out[17]=
$$\frac{1}{2}\cos[\Lambda_1]\,\tilde{F} + \frac{1}{2} i \tilde{F} \sin[\Lambda_1] - \frac{1}{2}\tilde{\gamma}_2 a_1[T_1] + \frac{1}{2}\Gamma\tilde{\gamma}_2 a_1[T_1] - i\omega_1\tilde{\xi}_1 a_1[T_1] - i\omega_1\tilde{\xi}_2 a_1[T_1] + i\Gamma\omega_1\tilde{\xi}_2 a_1[T_1] - \frac{3}{8}\tilde{\eta}_1 a_1[T_1]^3 + \frac{3}{8}\tilde{\eta}_2 a_1[T_1]^3 - \frac{9}{8}\Gamma\tilde{\eta}_2 a_1[T_1]^3 + \frac{9}{8}\Gamma^2\tilde{\eta}_2 a_1[T_1]^3 - \frac{3}{8}\Gamma^3\tilde{\eta}_2 a_1[T_1]^3 + \frac{3}{4}\tilde{\eta}_2 a_1[T_1] a_2[T_1]^2 - \frac{3}{4}\Gamma\tilde{\eta}_2 a_1[T_1] a_2[T_1]^2 - \frac{1}{8}\cos[\Phi_1]\tilde{\eta}_2 a_2[T_1]^3 - \frac{1}{8} i \sin[\Phi_1]\tilde{\eta}_2 a_2[T_1]^3 - i\omega_1 a_1'[T_1] + \omega_1 a_1[T_1]\beta_1'[T_1]$$

Separating them into real and imaginary components:

■ Real:

In[18]:=
```
1/2 Cos[Λ1] F~ - 1/2 γ~2 a1[T1] + 1/2 Γ γ~2 a1[T1] - 3/8 η~1 a1[T1]^3 +
  3/8 η~2 a1[T1]^3 - 9/8 Γ η~2 a1[T1]^3 + 9/8 Γ^2 η~2 a1[T1]^3 - 3/8 Γ^3 η~2 a1[T1]^3 +
  3/4 η~2 a1[T1] a2[T1]^2 - 3/4 Γ η~2 a1[T1] a2[T1]^2 - 1/8 Cos[Φ1] η~2 a2[T1]^3 +
  ω1 a1[T1] β1'[T1] == 0;
```

■ Imaginary:

In[19]:=
```
1/2 F~ Sin[Λ1] - ω1 ξ~1 a1[T1] - ω1 ξ~2 a1[T1] + Γ ω1 ξ~2 a1[T1] -
  1/8 Sin[Φ1] η~2 a2[T1]^3 - ω1 a1'[T1] == 0;
```

Derivative of $A_2[T_1]$:

In[20]:=
$$A_2'[T_1] = \frac{1}{2} e^{i\beta_2[T_1]} a_2'[T_1] + \frac{1}{2} i e^{i\beta_2[T_1]} a_2[T_1] \beta_2'[T_1];$$

The secular terms of x_{21} from equation (3.3-48) :

In[21]:=
$$ST2 == e^{i T_0 \omega_1 - 3 i T_0 \omega_2} \left(-3 \overline{A_2[T_1]}^2 \tilde{\eta}_3 A_1[T_1] + 3 \overline{A_2[T_1]}^2 \tilde{\eta}_3 A_3[T_1] + \frac{3 \overline{A_2[T_1]}^2 \omega_2^2 \tilde{\eta}_2 A_1[T_1]}{4\omega_1\omega_2 - 4\omega_2^2} - \frac{3 \overline{A_2[T_1]}^2 \omega_2^2 \tilde{\eta}_2 A_3[T_1]}{4\omega_1\omega_2 - 4\omega_2^2} \right) + \frac{\omega_2^2 \tilde{\gamma}_2 A_2[T_1]}{\omega_1^2 - \omega_2^2} + \frac{2 i \omega_2^3 \tilde{\xi}_2 A_2[T_1]}{\omega_1^2 - \omega_2^2} - 2 i \omega_2 \tilde{\xi}_3 A_2[T_1] - \frac{6 \overline{A_1[T_1]} \omega_2^2 \tilde{\eta}_2 A_1[T_1] A_2[T_1]}{\omega_1^2 - \omega_2^2} + \frac{6 \overline{A_3[T_1]} \omega_2^2 \tilde{\eta}_2 A_1[T_1] A_2[T_1]}{\omega_1^2 - \omega_2^2} + 6 \overline{A_1[T_1]} \tilde{\eta}_3 A_1[T_1] A_2[T_1] - 6 \overline{A_3[T_1]} \tilde{\eta}_3 A_1[T_1] A_2[T_1] - \frac{3 \overline{A_2[T_1]} \omega_2^2 \tilde{\eta}_2 A_2[T_1]^2}{\omega_1^2 - \omega_2^2} + 3 \overline{A_2[T_1]} \tilde{\eta}_3 A_2[T_1]^2 + \frac{6 \overline{A_1[T_1]} \omega_2^2 \tilde{\eta}_2 A_2[T_1] A_3[T_1]}{\omega_1^2 - \omega_2^2} - \frac{6 \overline{A_3[T_1]} \omega_2^2 \tilde{\eta}_2 A_2[T_1] A_3[T_1]}{\omega_1^2 - \omega_2^2} - 6 \overline{A_1[T_1]} \tilde{\eta}_3 A_2[T_1] A_3[T_1] + 6 \overline{A_3[T_1]} \tilde{\eta}_3 A_2[T_1] A_3[T_1] - 2 i \omega_2 A_2'[T_1];$$

Substituting equation In[10] & In[12], equation In[21] becomes:

In[22]:=
$$ST2 = e^{-i\times 3\times\sigma_1\times T_1} \left(-3 \overline{A_2[T_1]}^2 \tilde{\eta}_3 A_1[T_1] + 3 \overline{A_2[T_1]}^2 \tilde{\eta}_3 A_3[T_1] + \frac{3 \overline{A_2[T_1]}^2 \omega_2^2 \tilde{\eta}_2 A_1[T_1]}{4\omega_1\omega_2 - 4\omega_2^2} - \frac{3 \overline{A_2[T_1]}^2 \omega_2^2 \tilde{\eta}_2 A_3[T_1]}{4\omega_1\omega_2 - 4\omega_2^2} \right) + \frac{\omega_2^2 \tilde{\gamma}_2 A_2[T_1]}{\omega_1^2 - \omega_2^2} + \frac{2 i \omega_2^3 \tilde{\xi}_2 A_2[T_1]}{\omega_1^2 - \omega_2^2} - 2 i \omega_2 \tilde{\xi}_3 A_2[T_1] - \frac{6 \overline{A_1[T_1]} \omega_2^2 \tilde{\eta}_2 A_1[T_1] A_2[T_1]}{\omega_1^2 - \omega_2^2} + \frac{6 \overline{A_3[T_1]} \omega_2^2 \tilde{\eta}_2 A_1[T_1] A_2[T_1]}{\omega_1^2 - \omega_2^2} + 6 \overline{A_1[T_1]} \tilde{\eta}_3 A_1[T_1] A_2[T_1] - 6 \overline{A_3[T_1]} \tilde{\eta}_3 A_1[T_1] A_2[T_1] - \frac{3 \overline{A_2[T_1]} \omega_2^2 \tilde{\eta}_2 A_2[T_1]^2}{\omega_1^2 - \omega_2^2} + 3 \overline{A_2[T_1]} \tilde{\eta}_3 A_2[T_1]^2 + \frac{6 \overline{A_1[T_1]} \omega_2^2 \tilde{\eta}_2 A_2[T_1] A_3[T_1]}{\omega_1^2 - \omega_2^2} - \frac{6 \overline{A_3[T_1]} \omega_2^2 \tilde{\eta}_2 A_2[T_1] A_3[T_1]}{\omega_1^2 - \omega_2^2} - 6 \overline{A_1[T_1]} \tilde{\eta}_3 A_2[T_1] A_3[T_1] + 6 \overline{A_3[T_1]} \tilde{\eta}_3 A_2[T_1] A_3[T_1] - 2 i \omega_2 A_2'[T_1]$$

Substituting polar expressions In[1] to In[6] & In[20] into In[22]:

$$\text{Out[22]=}\ \frac{e^{i\beta_2[T_1]}\omega_2^2\tilde{\gamma}_2 a_2[T_1]}{2(\omega_1^2-\omega_2^2)}+\frac{i e^{i\beta_2[T_1]}\omega_2^3\tilde{\zeta}_2 a_2[T_1]}{\omega_1^2-\omega_2^2}-i e^{i\beta_2[T_1]}\omega_2\tilde{\zeta}_3 a_2[T_1]-$$
$$\frac{3 e^{i\beta_2[T_1]}\omega_2^2\tilde{\eta}_2 a_1[T_1]^2 a_2[T_1]}{4(\omega_1^2-\omega_2^2)}+\frac{3 e^{i\beta_2[T_1]}\Gamma\omega_2^2\tilde{\eta}_2 a_1[T_1]^2 a_2[T_1]}{2(\omega_1^2-\omega_2^2)}-$$
$$\frac{3 e^{i\beta_2[T_1]}\Gamma^2\omega_2^2\tilde{\eta}_2 a_1[T_1]^2 a_2[T_1]}{4(\omega_1^2-\omega_2^2)}+\frac{3}{4}e^{i\beta_2[T_1]}\tilde{\eta}_3 a_1[T_1]^2 a_2[T_1]-$$
$$\frac{3}{2}e^{i\beta_2[T_1]}\Gamma\tilde{\eta}_3 a_1[T_1]^2 a_2[T_1]+\frac{3}{4}e^{i\beta_2[T_1]}\Gamma^2\tilde{\eta}_3 a_1[T_1]^2 a_2[T_1]-$$
$$\frac{3 e^{i\beta_2[T_1]}\omega_2^2\tilde{\eta}_2 a_2[T_1]^3}{8(\omega_1^2-\omega_2^2)}+\frac{3}{8}e^{i\beta_2[T_1]}\tilde{\eta}_3 a_2[T_1]^3+$$
$$e^{-3 i T_1\sigma_1}\left(\frac{3 e^{i\beta_1[T_1]-2 i\beta_2[T_1]}\omega_2^2\tilde{\eta}_2 a_1[T_1] a_2[T_1]^2}{8(4\omega_1\omega_2-4\omega_2^2)}-\right.$$
$$\frac{3 e^{i\beta_1[T_1]-2 i\beta_2[T_1]}\Gamma\omega_2^2\tilde{\eta}_2 a_1[T_1] a_2[T_1]^2}{8(4\omega_1\omega_2-4\omega_2^2)}-\frac{3}{8}e^{i\beta_1[T_1]-2 i\beta_2[T_1]}$$
$$\left.\tilde{\eta}_3 a_1[T_1] a_2[T_1]^2+\frac{3}{8}e^{i\beta_1[T_1]-2 i\beta_2[T_1]}\Gamma\tilde{\eta}_3 a_1[T_1] a_2[T_1]^2\right)-$$
$$2 i\omega_2\left(\frac{1}{2}e^{i\beta_2[T_1]}a_2'[T_1]+\frac{1}{2}i e^{i\beta_2[T_1]}a_2[T_1]\beta_2'[T_1]\right)$$

Dividing throughout by $e^{i\times\beta_2[T_1]}$:

```
In[23]:= ExpandAll[ST2 / e^(i×β2[T1])]
```

$$\text{Out[23]=}\ \frac{\omega_2^2\tilde{\gamma}_2 a_2[T_1]}{2\omega_1^2-2\omega_2^2}+\frac{i\omega_2^3\tilde{\zeta}_2 a_2[T_1]}{\omega_1^2-\omega_2^2}-i\omega_2\tilde{\zeta}_3 a_2[T_1]-\frac{3\omega_2^2\tilde{\eta}_2 a_1[T_1]^2 a_2[T_1]}{4\omega_1^2-4\omega_2^2}-$$
$$\frac{3\Gamma^2\omega_2^2\tilde{\eta}_2 a_1[T_1]^2 a_2[T_1]}{4\omega_1^2-4\omega_2^2}+\frac{3\Gamma\omega_2^2\tilde{\eta}_2 a_1[T_1]^2 a_2[T_1]}{2\omega_1^2-2\omega_2^2}+$$
$$\frac{3}{4}\tilde{\eta}_3 a_1[T_1]^2 a_2[T_1]-\frac{3}{2}\Gamma\tilde{\eta}_3 a_1[T_1]^2 a_2[T_1]+\frac{3}{4}\Gamma^2\tilde{\eta}_3 a_1[T_1]^2 a_2[T_1]+$$
$$\frac{3 e^{-3 i T_1\sigma_1+i\beta_1[T_1]-i\beta_2[T_1]}\omega_2^2\tilde{\eta}_2 a_1[T_1] a_2[T_1]^2}{32 e^{2 i\beta_2[T_1]}\omega_1\omega_2-32 e^{2 i\beta_2[T_1]}\omega_2^2}-$$
$$\frac{3 e^{-3 i T_1\sigma_1+i\beta_1[T_1]-i\beta_2[T_1]}\Gamma\omega_2^2\tilde{\eta}_2 a_1[T_1] a_2[T_1]^2}{32 e^{2 i\beta_2[T_1]}\omega_1\omega_2-32 e^{2 i\beta_2[T_1]}\omega_2^2}-$$
$$\frac{3}{8}e^{-3 i T_1\sigma_1+i\beta_1[T_1]-3 i\beta_2[T_1]}\tilde{\eta}_3 a_1[T_1] a_2[T_1]^2+$$
$$\frac{3}{8}e^{-3 i T_1\sigma_1+i\beta_1[T_1]-3 i\beta_2[T_1]}\Gamma\tilde{\eta}_3 a_1[T_1] a_2[T_1]^2-$$
$$\frac{3\omega_2^2\tilde{\eta}_2 a_2[T_1]^3}{8\omega_1^2-8\omega_2^2}+\frac{3}{8}\tilde{\eta}_3 a_2[T_1]^3-i\omega_2 a_2'[T_1]+\omega_2 a_2[T_1]\beta_2'[T_1]$$

Factorising it:

In[24]:= **Collect[%, {e^{-3 i T1 σ1+i β1[T1]-3 i β2[T1]}}]**

Out[24]=
$$\frac{\omega_2^2\,\tilde{\gamma}_2\,a_2[T_1]}{2\,\omega_1^2-2\,\omega_2^2}+\frac{i\,\omega_2^3\,\tilde{\xi}_2\,a_2[T_1]}{\omega_1^2-\omega_2^2}-i\,\omega_2\,\tilde{\xi}_3\,a_2[T_1]-\frac{3\,\omega_2^2\,\tilde{\eta}_2\,a_1[T_1]^2\,a_2[T_1]}{4\,\omega_1^2-4\,\omega_2^2}-$$
$$\frac{3\,\Gamma^2\,\omega_2^2\,\tilde{\eta}_2\,a_1[T_1]^2\,a_2[T_1]}{4\,\omega_1^2-4\,\omega_2^2}+\frac{3\,\Gamma\,\omega_2^2\,\tilde{\eta}_2\,a_1[T_1]^2\,a_2[T_1]}{2\,\omega_1^2-2\,\omega_2^2}+$$
$$\frac{3}{4}\,\tilde{\eta}_3\,a_1[T_1]^2\,a_2[T_1]-\frac{3}{2}\,\Gamma\,\tilde{\eta}_3\,a_1[T_1]^2\,a_2[T_1]+\frac{3}{4}\,\Gamma^2\,\tilde{\eta}_3\,a_1[T_1]^2\,a_2[T_1]+$$
$$\frac{3\,e^{-3\,i\,T_1\,\sigma_1+i\,\beta_1[T_1]-i\,\beta_2[T_1]}\,\omega_2^2\,\tilde{\eta}_2\,a_1[T_1]\,a_2[T_1]^2}{32\,e^{2\,i\,\beta_2[T_1]}\,\omega_1\,\omega_2-32\,e^{2\,i\,\beta_2[T_1]}\,\omega_2^2}-$$
$$\frac{3\,e^{-3\,i\,T_1\,\sigma_1+i\,\beta_1[T_1]-i\,\beta_2[T_1]}\,\Gamma\,\omega_2^2\,\tilde{\eta}_2\,a_1[T_1]\,a_2[T_1]^2}{32\,e^{2\,i\,\beta_2[T_1]}\,\omega_1\,\omega_2-32\,e^{2\,i\,\beta_2[T_1]}\,\omega_2^2}-$$
$$\frac{3\,\omega_2^2\,\tilde{\eta}_2\,a_2[T_1]^3}{8\,\omega_1^2-8\,\omega_2^2}+\frac{3}{8}\,\tilde{\eta}_3\,a_2[T_1]^3+e^{-3\,i\,T_1\,\sigma_1+i\,\beta_1[T_1]-3\,i\,\beta_2[T_1]}$$
$$\left(-\frac{3}{8}\,\tilde{\eta}_3\,a_1[T_1]\,a_2[T_1]^2+\frac{3}{8}\,\Gamma\,\tilde{\eta}_3\,a_1[T_1]\,a_2[T_1]^2\right)-$$
$$i\,\omega_2\,a_2'[T_1]+\omega_2\,a_2[T_1]\,\beta_2'[T_1]$$

Substitute In[16] into Out[24] and convert them into trigonometrical forms

In[25]:= **ExpToTrig[**
$$e^{-i\times\Phi_1}\left(-\frac{3}{8}\,\tilde{\eta}_3\,a_1[T_1]\,a_2[T_1]^2+\frac{3}{8}\,\Gamma\,\tilde{\eta}_3\,a_1[T_1]\,a_2[T_1]^2+\right.$$
$$\left.\frac{3\,\omega_2^2\,\tilde{\eta}_2\,a_1[T_1]\,a_2[T_1]^2}{32\,\omega_1\,\omega_2-32\,\omega_2^2}-\frac{3\,\Gamma\,\omega_2^2\,\tilde{\eta}_2\,a_1[T_1]\,a_2[T_1]^2}{32\,\omega_1\,\omega_2-32\,\omega_2^2}\right)+$$
$$\frac{\omega_2^2\,\tilde{\gamma}_2\,a_2[T_1]}{2\,\omega_1^2-2\,\omega_2^2}+\frac{i\,\omega_2^3\,\tilde{\xi}_2\,a_2[T_1]}{\omega_1^2-\omega_2^2}-i\,\omega_2\,\tilde{\xi}_3\,a_2[T_1]-$$
$$\frac{3\,\omega_2^2\,\tilde{\eta}_2\,a_1[T_1]^2\,a_2[T_1]}{4\,\omega_1^2-4\,\omega_2^2}-\frac{3\,\Gamma^2\,\omega_2^2\,\tilde{\eta}_2\,a_1[T_1]^2\,a_2[T_1]}{4\,\omega_1^2-4\,\omega_2^2}+$$
$$\frac{3\,\Gamma\,\omega_2^2\,\tilde{\eta}_2\,a_1[T_1]^2\,a_2[T_1]}{2\,\omega_1^2-2\,\omega_2^2}+\frac{3}{4}\,\tilde{\eta}_3\,a_1[T_1]^2\,a_2[T_1]-$$
$$\frac{3}{2}\,\Gamma\,\tilde{\eta}_3\,a_1[T_1]^2\,a_2[T_1]+\frac{3}{4}\,\Gamma^2\,\tilde{\eta}_3\,a_1[T_1]^2\,a_2[T_1]-\frac{3\,\omega_2^2\,\tilde{\eta}_2\,a_2[T_1]^3}{8\,\omega_1^2-8\,\omega_2^2}+$$
$$\frac{3}{8}\,\tilde{\eta}_3\,a_2[T_1]^3-i\,\omega_2\,a_2'[T_1]+\omega_2\,a_2[T_1]\,\beta_2'[T_1]\,\Big]$$

Out[25]=
$$\frac{\omega_2^2\,\tilde{\gamma}_2\,a_2[T_1]}{2\,\omega_1^2-2\,\omega_2^2}+\frac{i\,\omega_2^3\,\tilde{\xi}_2\,a_2[T_1]}{\omega_1^2-\omega_2^2}-i\,\omega_2\,\tilde{\xi}_3\,a_2[T_1]-\frac{3\,\omega_2^2\,\tilde{\eta}_2\,a_1[T_1]^2\,a_2[T_1]}{4\,\omega_1^2-4\,\omega_2^2}-$$
$$\frac{3\,\Gamma^2\,\omega_2^2\,\tilde{\eta}_2\,a_1[T_1]^2\,a_2[T_1]}{4\,\omega_1^2-4\,\omega_2^2}+\frac{3\,\Gamma\,\omega_2^2\,\tilde{\eta}_2\,a_1[T_1]^2\,a_2[T_1]}{2\,\omega_1^2-2\,\omega_2^2}+$$
$$\frac{3}{4}\,\tilde{\eta}_3\,a_1[T_1]^2\,a_2[T_1]-\frac{3}{2}\,\Gamma\,\tilde{\eta}_3\,a_1[T_1]^2\,a_2[T_1]+\frac{3}{4}\,\Gamma^2\,\tilde{\eta}_3\,a_1[T_1]^2\,a_2[T_1]+$$
$$\frac{3\,\text{Cos}[\Phi_1]\,\omega_2^2\,\tilde{\eta}_2\,a_1[T_1]\,a_2[T_1]^2}{32\,\omega_1\,\omega_2-32\,\omega_2^2}-\frac{3\,\Gamma\,\text{Cos}[\Phi_1]\,\omega_2^2\,\tilde{\eta}_2\,a_1[T_1]\,a_2[T_1]^2}{32\,\omega_1\,\omega_2-32\,\omega_2^2}-$$
$$\frac{3\,i\,\text{Sin}[\Phi_1]\,\omega_2^2\,\tilde{\eta}_2\,a_1[T_1]\,a_2[T_1]^2}{32\,\omega_1\,\omega_2-32\,\omega_2^2}+\frac{3\,i\,\Gamma\,\text{Sin}[\Phi_1]\,\omega_2^2\,\tilde{\eta}_2\,a_1[T_1]\,a_2[T_1]^2}{32\,\omega_1\,\omega_2-32\,\omega_2^2}-$$
$$\frac{3}{8}\,\text{Cos}[\Phi_1]\,\tilde{\eta}_3\,a_1[T_1]\,a_2[T_1]^2+\frac{3}{8}\,\Gamma\,\text{Cos}[\Phi_1]\,\tilde{\eta}_3\,a_1[T_1]\,a_2[T_1]^2+$$
$$\frac{3}{8}\,i\,\text{Sin}[\Phi_1]\,\tilde{\eta}_3\,a_1[T_1]\,a_2[T_1]^2-\frac{3}{8}\,i\,\Gamma\,\text{Sin}[\Phi_1]\,\tilde{\eta}_3\,a_1[T_1]\,a_2[T_1]^2-$$
$$\frac{3\,\omega_2^2\,\tilde{\eta}_2\,a_2[T_1]^3}{8\,\omega_1^2-8\,\omega_2^2}+\frac{3}{8}\,\tilde{\eta}_3\,a_2[T_1]^3-i\,\omega_2\,a_2'[T_1]+\omega_2\,a_2[T_1]\,\beta_2'[T_1]$$

Separating them into real and imaginary components:

■ **Real:**

```
In[26]:= ω2^2 γ̃2 a2[T1] / (2 ω1^2 - 2 ω2^2) - 3 ω2^2 η̃2 a1[T1]^2 a2[T1] / (4 ω1^2 - 4 ω2^2) - 3 Γ^2 ω2^2 η̃2 a1[T1]^2 a2[T1] / (4 ω1^2 - 4 ω2^2) +
  3 Γ ω2^2 η̃2 a1[T1]^2 a2[T1] / (2 ω1^2 - 2 ω2^2) + 3/4 η̃3 a1[T1]^2 a2[T1] - 3/2 Γ η̃3 a1[T1]^2 a2[T1] +
  3/4 Γ^2 η̃3 a1[T1]^2 a2[T1] + 3 Cos[Φ1] ω2^2 η̃2 a1[T1] a2[T1]^2 / (32 ω1 ω2 - 32 ω2^2) -
  3 Γ Cos[Φ1] ω2^2 η̃2 a1[T1] a2[T1]^2 / (32 ω1 ω2 - 32 ω2^2) - 3/8 Cos[Φ1] η̃3 a1[T1] a2[T1]^2 +
  3/8 Γ Cos[Φ1] η̃3 a1[T1] a2[T1]^2 - 3 ω2^2 η̃2 a2[T1]^3 / (8 ω1^2 - 8 ω2^2) + 3/8 η̃3 a2[T1]^3 +
  ω2 a2[T1] β2'[T1] == 0;
```

■ **Imaginary:**

```
In[27]:= ω2^3 ζ̃2 a2[T1] / (ω1^2 - ω2^2) - ω2 ζ̃3 a2[T1] - 3 Sin[Φ1] ω2^2 η̃2 a1[T1] a2[T1]^2 / (32 ω1 ω2 - 32 ω2^2) +
  3 Γ Sin[Φ1] ω2^2 η̃2 a1[T1] a2[T1]^2 / (32 ω1 ω2 - 32 ω2^2) + 3/8 Sin[Φ1] η̃3 a1[T1] a2[T1]^2 -
  3/8 Γ Sin[Φ1] η̃3 a1[T1] a2[T1]^2 - ω2 a2'[T1] == 0;
```

C.7 Derivation of Solvability Equations

The 4 Modulation Equations for Case 1 are as follows:

In[1]:=
$$\frac{1}{2}\,\text{Cos}[\Lambda_1]\,\tilde{F} - \frac{1}{2}\,\tilde{\gamma}_2\,a_1[T_1] + \frac{1}{2}\,\Gamma\,\tilde{\gamma}_2\,a_1[T_1] - \frac{3}{8}\,\tilde{\eta}_1\,a_1[T_1]^3 + \frac{3}{8}\,\tilde{\eta}_2\,a_1[T_1]^3 - \frac{9}{8}\,\Gamma\,\tilde{\eta}_2\,a_1[T_1]^3 + \frac{9}{8}\,\Gamma^2\,\tilde{\eta}_2\,a_1[T_1]^3 - \frac{3}{8}\,\Gamma^3\,\tilde{\eta}_2\,a_1[T_1]^3 + \frac{3}{4}\,\tilde{\eta}_2\,a_1[T_1]\,a_2[T_1]^2 - \frac{3}{4}\,\Gamma\,\tilde{\eta}_2\,a_1[T_1]\,a_2[T_1]^2 - \frac{1}{8}\,\text{Cos}[\Phi_1]\,\tilde{\eta}_2\,a_2[T_1]^3 + \omega_1\,a_1[T_1]\,\beta_1'[T_1] == 0;$$

In[2]:=
$$\frac{1}{2}\,\tilde{F}\,\text{Sin}[\Lambda_1] - \omega_1\,\tilde{\xi}_1\,a_1[T_1] - \omega_1\,\tilde{\xi}_2\,a_1[T_1] + \Gamma\,\omega_1\,\tilde{\xi}_2\,a_1[T_1] - \frac{1}{8}\,\text{Sin}[\Phi_1]\,\tilde{\eta}_2\,a_2[T_1]^3 - \omega_1\,a_1'[T_1] == 0;$$

In[3]:=
$$\frac{\omega_2^2\,\tilde{\gamma}_2\,a_2[T_1]}{2\,\omega_1^2 - 2\,\omega_2^2} - \frac{3\,\omega_2^2\,\tilde{\eta}_2\,a_1[T_1]^2\,a_2[T_1]}{4\,\omega_1^2 - 4\,\omega_2^2} - \frac{3\,\Gamma^2\,\omega_2^2\,\tilde{\eta}_2\,a_1[T_1]^2\,a_2[T_1]}{4\,\omega_1^2 - 4\,\omega_2^2} + \frac{3\,\Gamma\,\omega_2^2\,\tilde{\eta}_2\,a_1[T_1]^2\,a_2[T_1]}{2\,\omega_1^2 - 2\,\omega_2^2} + \frac{3}{4}\,\tilde{\eta}_3\,a_1[T_1]^2\,a_2[T_1] - \frac{3}{2}\,\Gamma\,\tilde{\eta}_3\,a_1[T_1]^2\,a_2[T_1] + \frac{3}{4}\,\Gamma^2\,\tilde{\eta}_3\,a_1[T_1]^2\,a_2[T_1] + \frac{3\,\text{Cos}[\Phi_1]\,\omega_2^2\,\tilde{\eta}_2\,a_1[T_1]\,a_2[T_1]^2}{32\,\omega_1\,\omega_2 - 32\,\omega_2^2} - \frac{3\,\Gamma\,\text{Cos}[\Phi_1]\,\omega_2^2\,\tilde{\eta}_2\,a_1[T_1]\,a_2[T_1]^2}{32\,\omega_1\,\omega_2 - 32\,\omega_2^2} - \frac{3}{8}\,\text{Cos}[\Phi_1]\,\tilde{\eta}_3\,a_1[T_1]\,a_2[T_1]^2 + \frac{3}{8}\,\Gamma\,\text{Cos}[\Phi_1]\,\tilde{\eta}_3\,a_1[T_1]\,a_2[T_1]^2 - \frac{3\,\omega_2^2\,\tilde{\eta}_2\,a_2[T_1]^3}{8\,\omega_1^2 - 8\,\omega_2^2} + \frac{3}{8}\,\tilde{\eta}_3\,a_2[T_1]^3 + \omega_2\,a_2[T_1]\,\beta_2'[T_1] == 0;$$

In[4]:=
$$\frac{\omega_2^3\,\tilde{\xi}_2\,a_2[T_1]}{\omega_1^2 - \omega_2^2} - \omega_2\,\tilde{\xi}_3\,a_2[T_1] - \frac{3\,\text{Sin}[\Phi_1]\,\omega_2^2\,\tilde{\eta}_2\,a_1[T_1]\,a_2[T_1]^2}{32\,\omega_1\,\omega_2 - 32\,\omega_2^2} + \frac{3\,\Gamma\,\text{Sin}[\Phi_1]\,\omega_2^2\,\tilde{\eta}_2\,a_1[T_1]\,a_2[T_1]^2}{32\,\omega_1\,\omega_2 - 32\,\omega_2^2} + \frac{3}{8}\,\text{Sin}[\Phi_1]\,\tilde{\eta}_3\,a_1[T_1]\,a_2[T_1]^2 - \frac{3}{8}\,\Gamma\,\text{Sin}[\Phi_1]\,\tilde{\eta}_3\,a_1[T_1]\,a_2[T_1]^2 - \omega_2\,a_2'[T_1] == 0;$$

For steady - state, the condition is required whereby :

In[5]:= $a_1'[T_1] == a_2'[T_1] = \Lambda_1' == \Phi_1' \approx 0;$

From In[15] of Appendix C.6:

$\Lambda_1 == \nu_1\,T_1 - \beta_1[T_1];$

$\Lambda_1' == \nu_1 - \beta_1'[T_1];$

$\nu\ \Lambda_1' \approx 0,\quad \Lambda$

In[6]:= $\beta_1'[T_1] == \nu_1;$

From In[16] of Appendix C.6:

$$\Phi_1 == 3\,\sigma_1\,T_1 - \beta_1[T_1] + 3\,\beta_2[T_1];$$

$$\Phi_1' == 3\,\sigma_1 - \beta_1'[T_1] + 3\,\beta_2'[T_1];$$

$$\text{v}\ \ \Phi_1' \approx 0, \quad \text{a}$$

$$\beta_2'[T_1] == \frac{1}{3}\,\beta_1'[T_1] - \sigma_1;$$

In[7]:=
$$\beta_2'[T_1] == \frac{1}{3}\,\nu_1 - \sigma_1;$$

Subst. In[5] to In[7] into In[1] to In[4] & Bringing Trig. Terms to LHS:

In[8]:=
$$\frac{1}{2}\,\text{Cos}[\Lambda_1]\,\tilde{F} == \frac{1}{8}\,\text{Cos}[\Phi_1]\,\tilde{\eta}_2\,a_2[T_1]^3 + \frac{1}{2}\,\tilde{\gamma}_2\,a_1[T_1] - \frac{1}{2}\,\Gamma\,\tilde{\gamma}_2\,a_1[T_1] + \frac{3}{8}\,\tilde{\eta}_1\,a_1[T_1]^3 - \frac{3}{8}\,\tilde{\eta}_2\,a_1[T_1]^3 + \frac{9}{8}\,\Gamma\,\tilde{\eta}_2\,a_1[T_1]^3 - \frac{9}{8}\,\Gamma^2\,\tilde{\eta}_2\,a_1[T_1]^3 + \frac{3}{8}\,\Gamma^3\,\tilde{\eta}_2\,a_1[T_1]^3 - \frac{3}{4}\,\tilde{\eta}_2\,a_1[T_1]\,a_2[T_1]^2 + \frac{3}{4}\,\Gamma\,\tilde{\eta}_2\,a_1[T_1]\,a_2[T_1]^2 - \omega_1\,a_1[T_1] \times \nu_1;$$

In[9]:=
$$\frac{1}{2}\,\tilde{F}\,\text{Sin}[\Lambda_1] == \frac{1}{8}\,\text{Sin}[\Phi_1]\,\tilde{\eta}_2\,a_2[T_1]^3 + \omega_1\,\tilde{\xi}_1\,a_1[T_1] + \omega_1\,\tilde{\xi}_2\,a_1[T_1] - \Gamma\,\omega_1\,\tilde{\xi}_2\,a_1[T_1];$$

In[10]:=
$$\text{Cos}[\Phi_1]\left(\frac{3\,\omega_2^2\,\tilde{\eta}_2\,a_1[T_1]\,a_2[T_1]^2}{32\,\omega_1\,\omega_2 - 32\,\omega_2^2} - \frac{3\,\Gamma\,\omega_2^2\,\tilde{\eta}_2\,a_1[T_1]\,a_2[T_1]^2}{32\,\omega_1\,\omega_2 - 32\,\omega_2^2} - \frac{3}{8}\,\tilde{\eta}_3\,a_1[T_1]\,a_2[T_1]^2 + \frac{3}{8}\,\Gamma\,\tilde{\eta}_3\,a_1[T_1]\,a_2[T_1]^2\right) == -\frac{\omega_2^2\,\tilde{\gamma}_2\,a_2[T_1]}{2\,\omega_1^2 - 2\,\omega_2^2} + \frac{3\,\omega_2^2\,\tilde{\eta}_2\,a_1[T_1]^2\,a_2[T_1]}{4\,\omega_1^2 - 4\,\omega_2^2} + \frac{3\,\Gamma^2\,\omega_2^2\,\tilde{\eta}_2\,a_1[T_1]^2\,a_2[T_1]}{4\,\omega_1^2 - 4\,\omega_2^2} - \frac{3\,\Gamma\,\omega_2^2\,\tilde{\eta}_2\,a_1[T_1]^2\,a_2[T_1]}{2\,\omega_1^2 - 2\,\omega_2^2} - \frac{3}{4}\,\tilde{\eta}_3\,a_1[T_1]^2\,a_2[T_1] + \frac{3}{2}\,\Gamma\,\tilde{\eta}_3\,a_1[T_1]^2\,a_2[T_1] - \frac{3}{4}\,\Gamma^2\,\tilde{\eta}_3\,a_1[T_1]^2\,a_2[T_1] + \frac{3\,\omega_2^2\,\tilde{\eta}_2\,a_2[T_1]^3}{8\,\omega_1^2 - 8\,\omega_2^2} - \frac{3}{8}\,\tilde{\eta}_3\,a_2[T_1]^3 - \omega_2\,a_2[T_1] \times \left(\frac{1}{3}\,\nu_1 - \sigma_1\right);$$

In[11]:=
$$\text{Sin}[\Phi_1]\left(\frac{3\,\omega_2^2\,\tilde{\eta}_2\,a_1[T_1]\,a_2[T_1]^2}{32\,\omega_1\,\omega_2 - 32\,\omega_2^2} - \frac{3\,\Gamma\,\omega_2^2\,\tilde{\eta}_2\,a_1[T_1]\,a_2[T_1]^2}{32\,\omega_1\,\omega_2 - 32\,\omega_2^2} - \frac{3}{8}\,\tilde{\eta}_3\,a_1[T_1]\,a_2[T_1]^2 + \frac{3}{8}\,\Gamma\,\tilde{\eta}_3\,a_1[T_1]\,a_2[T_1]^2\right) == \frac{\omega_2^3\,\tilde{\xi}_2\,a_2[T_1]}{\omega_1^2 - \omega_2^2} - \omega_2\,\tilde{\xi}_3\,a_2[T_1];$$

From In[10] and In[11]:

In[12]:=
$$\text{Cos}[\Phi_1] == 1 \Big/ \left(\frac{3\,\omega_2^2\,\tilde{\eta}_2\,a_1[T_1]\,a_2[T_1]^2}{32\,\omega_1\,\omega_2 - 32\,\omega_2^2} - \frac{3\,\Gamma\,\omega_2^2\,\tilde{\eta}_2\,a_1[T_1]\,a_2[T_1]^2}{32\,\omega_1\,\omega_2 - 32\,\omega_2^2} - \frac{3}{8}\,\tilde{\eta}_3\,a_1[T_1]\,a_2[T_1]^2 + \frac{3}{8}\,\Gamma\,\tilde{\eta}_3\,a_1[T_1]\,a_2[T_1]^2 \right)$$
$$\left(-\frac{\omega_2^2\,\tilde{\gamma}_2\,a_2[T_1]}{2\,\omega_1^2 - 2\,\omega_2^2} + \frac{3\,\omega_2^2\,\tilde{\eta}_2\,a_1[T_1]^2\,a_2[T_1]}{4\,\omega_1^2 - 4\,\omega_2^2} + \frac{3\,\Gamma^2\,\omega_2^2\,\tilde{\eta}_2\,a_1[T_1]^2\,a_2[T_1]}{4\,\omega_1^2 - 4\,\omega_2^2} - \frac{3\,\Gamma\,\omega_2^2\,\tilde{\eta}_2\,a_1[T_1]^2\,a_2[T_1]}{2\,\omega_1^2 - 2\,\omega_2^2} - \frac{3}{4}\,\tilde{\eta}_3\,a_1[T_1]^2\,a_2[T_1] + \frac{3}{2}\,\Gamma\,\tilde{\eta}_3\,a_1[T_1]^2\,a_2[T_1] - \frac{3}{4}\,\Gamma^2\,\tilde{\eta}_3\,a_1[T_1]^2\,a_2[T_1] + \frac{3\,\omega_2^2\,\tilde{\eta}_2\,a_2[T_1]^3}{8\,\omega_1^2 - 8\,\omega_2^2} - \frac{3}{8}\,\tilde{\eta}_3\,a_2[T_1]^3 - \omega_2\,a_2[T_1] \times \left(\frac{1}{3}\,\nu_1 - \sigma_1 \right) \right);$$

In[13]:=
$$\text{Sin}[\Phi_1] == \left(\frac{\omega_2^3\,\tilde{\xi}_2\,a_2[T_1]}{\omega_1^2 - \omega_2^2} - \omega_2\,\tilde{\xi}_3\,a_2[T_1] \right) \Big/ \left(\frac{3\,\omega_2^2\,\tilde{\eta}_2\,a_1[T_1]\,a_2[T_1]^2}{32\,\omega_1\,\omega_2 - 32\,\omega_2^2} - \frac{3\,\Gamma\,\omega_2^2\,\tilde{\eta}_2\,a_1[T_1]\,a_2[T_1]^2}{32\,\omega_1\,\omega_2 - 32\,\omega_2^2} - \frac{3}{8}\,\tilde{\eta}_3\,a_1[T_1]\,a_2[T_1]^2 + \frac{3}{8}\,\Gamma\,\tilde{\eta}_3\,a_1[T_1]\,a_2[T_1]^2 \right);$$

Squaring In[8] and In[9] and Adding them:

In[14]:=
```
FullSimplify[((1/2) Cos[Λ1] F̃)^2 + ((1/2) F̃ Sin[Λ1])^2 ==
 ((1/8) η̃2 a2[T1]^3
  (1/(((3 ω2^2 η̃2 a1[T1] a2[T1]^2)/(32 ω1 ω2 - 32 ω2^2) - (3 Γ ω2^2 η̃2 a1[T1] a2[T1]^2)/(32 ω1 ω2 - 32 ω2^2) -
     (3/8) η̃3 a1[T1] a2[T1]^2 + (3/8) Γ η̃3 a1[T1] a2[T1]^2)
   (-(ω2^2 γ̃2 a2[T1])/(2 ω1^2 - 2 ω2^2) + (3 ω2^2 η̃2 a1[T1]^2 a2[T1])/(4 ω1^2 - 4 ω2^2) +
    (3 Γ^2 ω2^2 η̃2 a1[T1]^2 a2[T1])/(4 ω1^2 - 4 ω2^2) - (3 Γ ω2^2 η̃2 a1[T1]^2 a2[T1])/(2 ω1^2 - 2 ω2^2) -
    (3/4) η̃3 a1[T1]^2 a2[T1] + (3/2) Γ η̃3 a1[T1]^2 a2[T1] -
    (3/4) Γ^2 η̃3 a1[T1]^2 a2[T1] + (3 ω2^2 η̃2 a2[T1]^3)/(8 ω1^2 - 8 ω2^2) - (3/8) η̃3 a2[T1]^3 -
    ω2 a2[T1] × ((1/3) ν1 - σ1))) + (1/2) γ̃2 a1[T1] - (1/2) Γ γ̃2 a1[T1] +
  (3/8) η̃1 a1[T1]^3 - (3/8) η̃2 a1[T1]^3 + (9/8) Γ η̃2 a1[T1]^3 - (9/8) Γ^2 η̃2 a1[T1]^3 +
  (3/8) Γ^3 η̃2 a1[T1]^3 - (3/4) η̃2 a1[T1] a2[T1]^2 + (3/4) Γ η̃2 a1[T1] a2[T1]^2 -
  ω1 a1[T1] × ν1)^2 +
 ((1/8) η̃2 a2[T1]^3 (((ω2^3 ξ̃2 a2[T1])/(ω1^2 - ω2^2) - ω2 ξ̃3 a2[T1])/
    (((3 ω2^2 η̃2 a1[T1] a2[T1]^2)/(32 ω1 ω2 - 32 ω2^2) - (3 Γ ω2^2 η̃2 a1[T1] a2[T1]^2)/(32 ω1 ω2 - 32 ω2^2) -
       (3/8) η̃3 a1[T1] a2[T1]^2 + (3/8) Γ η̃3 a1[T1] a2[T1]^2)) +
  ω1 ξ̃1 a1[T1] + ω1 ξ̃2 a1[T1] - Γ ω1 ξ̃2 a1[T1])^2]
```

Out[14]=
$$\frac{\tilde{F}^2}{4} == \Bigg\{\omega_1 \left(\tilde{\xi}_1 - (-1+\Gamma)\,\tilde{\xi}_2\right) a_1[T_1] - \frac{4\,\omega_2\left(-\omega_1^2\,\tilde{\xi}_3 + \omega_2^2\left(\tilde{\xi}_2+\tilde{\xi}_3\right)\right)\tilde{\eta}_2\,a_2[T_1]^2}{3\,(-1+\Gamma)\,(\omega_1+\omega_2)\,\left(\omega_2\,\tilde{\eta}_2 + 4\,(-\omega_1+\omega_2)\,\tilde{\eta}_3\right)\,a_1[T_1]}\Bigg\}^2 +$$
$$\Big(9\,(-1+\Gamma)\,(\omega_1+\omega_2)\,\left(4\,\omega_1\,\tilde{\eta}_3 - \omega_2\,(\tilde{\eta}_2+4\,\tilde{\eta}_3)\right)\,a_1[T_1]^2$$
$$\left(8\,\nu_1\,\omega_1 + 4\,(-1+\Gamma)\,\tilde{\gamma}_2 - 3\,\left(\tilde{\eta}_1 + (-1+\Gamma)^3\,\tilde{\eta}_2\right)\,a_1[T_1]^2\right) +$$
$$2\,\tilde{\eta}_2\,\left(8\,\omega_2\,\left(2\,(\nu_1 - 3\,\sigma_1)\,(\omega_1^2-\omega_2^2) + 3\,\omega_2\,\tilde{\gamma}_2\right) -$$
$$9\,(-1+\Gamma)^2\,\left(\omega_2\,(-3\,\omega_1+\omega_2)\,\tilde{\eta}_2 + 8\,(\omega_1^2-\omega_2^2)\,\tilde{\eta}_3\right)\,a_1[T_1]^2\Big)$$
$$a_2[T_1]^2 - 36\,\tilde{\eta}_2\,\left(-\omega_1^2\,\tilde{\eta}_3 + \omega_2^2\,\left(\tilde{\eta}_2+\tilde{\eta}_3\right)\right)\,a_2[T_1]^4\Big)^2 \Big/$$
$$\left(5184\,(-1+\Gamma)^2\,(\omega_1+\omega_2)^2\,\left(\omega_2\,\tilde{\eta}_2 + 4\,(-\omega_1+\omega_2)\,\tilde{\eta}_3\right)^2\,a_1[T_1]^2\right)$$

Squaring In[12] and In[13] and Adding them:

In[15]:=
```
FullSimplify[(Cos[Φ1])^2 + (Sin[Φ1])^2 ==
 (1/((3 ω2^2 η̃2 a1[T1] a2[T1]^2)/(32 ω1 ω2 - 32 ω2^2) - (3 Γ ω2^2 η̃2 a1[T1] a2[T1]^2)/(32 ω1 ω2 - 32 ω2^2) -
     3/8 η̃3 a1[T1] a2[T1]^2 + 3/8 Γ η̃3 a1[T1] a2[T1]^2))
  (-(ω2^2 γ̃2 a2[T1])/(2 ω1^2 - 2 ω2^2) + (3 ω2^2 η̃2 a1[T1]^2 a2[T1])/(4 ω1^2 - 4 ω2^2) +
   (3 Γ^2 ω2^2 η̃2 a1[T1]^2 a2[T1])/(4 ω1^2 - 4 ω2^2) - (3 Γ ω2^2 η̃2 a1[T1]^2 a2[T1])/(2 ω1^2 - 2 ω2^2) -
   3/4 η̃3 a1[T1]^2 a2[T1] + 3/2 Γ η̃3 a1[T1]^2 a2[T1] -
   3/4 Γ^2 η̃3 a1[T1]^2 a2[T1] + (3 ω2^2 η̃2 a2[T1]^3)/(8 ω1^2 - 8 ω2^2) - 3/8 η̃3 a2[T1]^3 -
   ω2 a2[T1] × (1/3 ν1 - σ1))^2 +
 (((ω2^3 ξ̃2 a2[T1])/(ω1^2 - ω2^2) - ω2 ξ̃3 a2[T1]) /
   (3 ω2^2 η̃2 a1[T1] a2[T1]^2)/(32 ω1 ω2 - 32 ω2^2) - (3 Γ ω2^2 η̃2 a1[T1] a2[T1]^2)/(32 ω1 ω2 - 32 ω2^2) -
   3/8 η̃3 a1[T1] a2[T1]^2 + 3/8 Γ η̃3 a1[T1] a2[T1]^2))^2]
```

Out[15]=
```
(16 (ω1 - ω2)^2 (576 ω2^2 ((ω2^2 ξ̃2)/(-ω1^2 + ω2^2) + ξ̃3)^2 +
   1/(ω1^2 - ω2^2)^2 ((4 ω2 (2 (ν1 - 3 σ1) (-ω1^2 + ω2^2) - 3 ω2 γ̃2) +
       18 (-1 + Γ)^2 (-ω1^2 η̃3 + ω2^2 (η̃2 + η̃3)) a1[T1]^2 +
       9 (-ω1^2 η̃3 + ω2^2 (η̃2 + η̃3)) a2[T1]^2)^2)) /
 (81 (-1 + Γ)^2 (ω2 η̃2 + 4 (-ω1 + ω2) η̃3)^2 a1[T1]^2 a2[T1]^2) ==
1
```

Therefore, the 2 'solvability' equations are:

```
In[16]:= F̃^2/4 ==
  (ω1 (ξ̃1 - (-1 + Γ) ξ̃2) a1[T1] -
     4 ω2 (-ω1^2 ξ̃3 + ω2^2 (ξ̃2 + ξ̃3)) η̃2 a2[T1]^2 /
      (3 (-1 + Γ) (ω1 + ω2) (ω2 η̃2 + 4 (-ω1 + ω2) η̃3) a1[T1]))^2 +
  (9 (-1 + Γ) (ω1 + ω2) (4 ω1 η̃3 - ω2 (η̃2 + 4 η̃3)) a1[T1]^2
     (8 ν1 ω1 + 4 (-1 + Γ) γ̃2 - 3 (η̃1 + (-1 + Γ)^3 η̃2) a1[T1]^2) +
    2 η̃2 (8 ω2 (2 (ν1 - 3 σ1) (ω1^2 - ω2^2) + 3 ω2 γ̃2) -
       9 (-1 + Γ)^2 (ω2 (-3 ω1 + ω2) η̃2 + 8 (ω1^2 - ω2^2) η̃3) a1[T1]^2)
     a2[T1]^2 - 36 η̃2 (-ω1^2 η̃3 + ω2^2 (η̃2 + η̃3)) a2[T1]^4)^2 /
  (5184 (-1 + Γ)^2 (ω1 + ω2)^2 (ω2 η̃2 + 4 (-ω1 + ω2) η̃3)^2 a1[T1]^2);

In[17]:= (16 (ω1 - ω2)^2
    (576 ω2^2 (ω2^2 ξ̃2 / (-ω1^2 + ω2^2) + ξ̃3)^2 +
      1/(ω1^2 - ω2^2)^2
       ((4 ω2 (2 (ν1 - 3 σ1) (-ω1^2 + ω2^2) - 3 ω2 γ̃2) +
          18 (-1 + Γ)^2 (-ω1^2 η̃3 + ω2^2 (η̃2 + η̃3)) a1[T1]^2 +
          9 (-ω1^2 η̃3 + ω2^2 (η̃2 + η̃3)) a2[T1]^2)^2)) /
  (81 (-1 + Γ)^2 (ω2 η̃2 + 4 (-ω1 + ω2) η̃3)^2 a1[T1]^2 a2[T1]^2) == 1;
```

Multiplying ε throughout the equations allows a return to the originally defined parameters in the equations of motion:

```
In[18]:= ε F̃^2/4 ==
  (ω1 (ε ξ̃1 - (-1 + Γ) ε ξ̃2) a1[T1] -
     4 ω2 (-ω1^2 ε ξ̃3 + ω2^2 (ε ξ̃2 + ε ξ̃3)) ε η̃2 a2[T1]^2 /
      (3 (-1 + Γ) (ω1 + ω2) (ω2 ε η̃2 + 4 (-ω1 + ω2) ε η̃3) a1[T1]))^2 +
  (9 (-1 + Γ) (ω1 + ω2) (4 ω1 ε η̃3 - ω2 (ε η̃2 + 4 ε η̃3)) a1[T1]^2
     (8 ε ν1 ω1 + 4 (-1 + Γ) ε γ̃2 - 3 (ε η̃1 + (-1 + Γ)^3 ε η̃2) a1[T1]^2) +
    2 ε η̃2 (8 ω2 (2 (ε ν1 - 3 ε σ1) (ω1^2 - ω2^2) + 3 ω2 ε γ̃2) -
       9 (-1 + Γ)^2 (ω2 (-3 ω1 + ω2) ε η̃2 + 8 (ω1^2 - ω2^2) ε η̃3) a1[T1]^2)
     a2[T1]^2 - 36 ε η̃2 (-ω1^2 ε η̃3 + ω2^2 (ε η̃2 + ε η̃3)) a2[T1]^4)^2 /
  (5184 (-1 + Γ)^2 (ω1 + ω2)^2 (ω2 ε η̃2 + 4 (-ω1 + ω2) ε η̃3)^2 a1[T1]^2);
```

In[19]:=
$$\left(16\,(\omega_1-\omega_2)^2\left(576\,\omega_2^2\left(\frac{\omega_2^2\,\epsilon\,\tilde{\xi}_2}{-\omega_1^2+\omega_2^2}+\epsilon\,\tilde{\xi}_3\right)^2+\frac{1}{(\omega_1^2-\omega_2^2)^2}\left((4\,\omega_2\,(2\,(\epsilon\nu_1-3\,\epsilon\sigma_1)\,(-\omega_1^2+\omega_2^2)-3\,\omega_2\,\epsilon\,\tilde{\gamma}_2)+18\,(-1+\Gamma)^2\,(-\omega_1^2\,\epsilon\,\tilde{\eta}_3+\omega_2^2\,(\epsilon\,\tilde{\eta}_2+\epsilon\,\tilde{\eta}_3))\,a_1[T_1]^2+9\,(-\omega_1^2\,\epsilon\,\tilde{\eta}_3+\omega_2^2\,(\epsilon\,\tilde{\eta}_2+\epsilon\,\tilde{\eta}_3))\,a_2[T_1]^2)^2\right)\right)\right)\Big/\left(81\,(-1+\Gamma)^2\,(\omega_2\,\epsilon\,\tilde{\eta}_2+4\,(-\omega_1+\omega_2)\,\epsilon\,\tilde{\eta}_3)^2\,a_1[T_1]^2\,a_2[T_1]^2\right)==1;$$

Rearranging and Simplying In[18] and In[19] above:

In[20]:=
$$1296\,\epsilon\,\tilde{F}^2\,((-1+\Gamma)^2\,(\omega_1+\omega_2)^2\,(\omega_2\,\epsilon\,\tilde{\eta}_2+4\,(-\omega_1+\omega_2)\,\epsilon\,\tilde{\eta}_3)^2\,a_1[T_1]^2)==\left(\omega_1\,(\epsilon\,\tilde{\xi}_1-(-1+\Gamma)\,\epsilon\,\tilde{\xi}_2)\,a_1[T_1]-\frac{4\,\omega_2\,(-\omega_1^2\,\epsilon\,\tilde{\xi}_3+\omega_2^2\,(\epsilon\,\tilde{\xi}_2+\epsilon\,\tilde{\xi}_3))\,\epsilon\,\tilde{\eta}_2\,a_2[T_1]^2}{3\,(-1+\Gamma)\,(\omega_1+\omega_2)\,(\omega_2\,\epsilon\,\tilde{\eta}_2+4\,(-\omega_1+\omega_2)\,\epsilon\,\tilde{\eta}_3)\,a_1[T_1]}\right)^2+(9\,(-1+\Gamma)\,(\omega_1+\omega_2)\,(4\,\omega_1\,\epsilon\,\tilde{\eta}_3-\omega_2\,(\epsilon\,\tilde{\eta}_2+4\,\epsilon\,\tilde{\eta}_3))\,a_1[T_1]^2(8\,\epsilon\nu_1\,\omega_1+4\,(-1+\Gamma)\,\epsilon\,\tilde{\gamma}_2-3\,(\epsilon\,\tilde{\eta}_1+(-1+\Gamma)^3\,\epsilon\,\tilde{\eta}_2)\,a_1[T_1]^2)+2\,\epsilon\,\tilde{\eta}_2\,(8\,\omega_2\,(2\,(\epsilon\nu_1-3\,\epsilon\,\sigma_1)\,(\omega_1^2-\omega_2^2)+3\,\omega_2\,\epsilon\,\tilde{\gamma}_2)-9\,(-1+\Gamma)^2\,(\omega_2\,(-3\,\omega_1+\omega_2)\,\epsilon\,\tilde{\eta}_2+8\,(\omega_1^2-\omega_2^2)\,\epsilon\,\tilde{\eta}_3)\,a_1[T_1]^2)\,a_2[T_1]^2-36\,\epsilon\,\tilde{\eta}_2\,(-\omega_1^2\,\epsilon\,\tilde{\eta}_3+\omega_2^2\,(\epsilon\,\tilde{\eta}_2+\epsilon\,\tilde{\eta}_3))\,a_2[T_1]^4)^2;$$

In[21]:=
$$(\omega_1-\omega_2)^2\left(576\,\omega_2^2\left(\frac{\omega_2^2\,\epsilon\,\tilde{\xi}_2}{-\omega_1^2+\omega_2^2}+\epsilon\,\tilde{\xi}_3\right)^2+\frac{1}{(\omega_1^2-\omega_2^2)^2}\left(4\,\omega_2\,(2\,(\epsilon\nu_1-3\,\epsilon\sigma_1)\,(-\omega_1^2+\omega_2^2)-3\,\omega_2\,\epsilon\,\tilde{\gamma}_2)+9\,(\omega_2^2\,(\epsilon\,\tilde{\eta}_2+\epsilon\,\tilde{\eta}_3)-\epsilon\,\omega_1^2\,\tilde{\eta}_3)(2\,(-1+\Gamma)^2\,a_1[T_1]^2+a_2[T_1]^2)\right)^2\right)==\frac{81}{16}\,(-1+\Gamma)^2\,(\omega_2\,\epsilon\,\tilde{\eta}_2+4\,(-\omega_1+\omega_2)\,\epsilon\,\tilde{\eta}_3)^2\,a_1[T_1]^2\,a_2[T_1]^2;$$

APPENDIX D

NUMERICAL INTEGRATION

D.1 Program Code for Numerical Integration

On the next page, the code that numerically integrates the governing equations of motion of equations (3.3-1) and (3.3-2) can be found. It is written in *Mathematica* and this code is for an upward frequency sweep.

```
Timing[
 (* Setting variables to zero *)
 Clear[result1, result2, a1, a2, Ω, Ωstep, i, ans, maxiter, start, tz, x1vel, x1dis, x2vel, x2dis];


 (* Defining values of constants - Large start & tz values to ensure steady-state *)
 m1 = 2; m2 = 1.125; c1 = c2 = 0.05; k1 = 847776; k2 = 52986; h1 = 1200 x 10^6; h2 = 100 x 10^6; F0 = 10; Ω = 205;
 Ωstep = 0.2; maxiter = 51; start = 2000; tz = 2010;

 (* Defining Arrays *)
 result1 = Array[a1, {maxiter, 2}];
 result2 = Array[a2, {maxiter, 2}];

 (* Function to extract the highest peak from the graph *)
 HighestPeak[gr_] :=
  Reverse[
 Last[Sort[ReplaceList[Join @@ Cases[gr, Line[pts_] :> pts, Infinity],
 {___, {x1_, y1_}, {x2_, y2_}, {x3_, y3_}, ___} /;
 y1 < y2 && y2 > y3 -> {y2, x2}]]]];

  (* Defining initial boundary conditions *)
 x1vel = 0; x1dis = 0; x2vel = 0; x2dis = 0;

 (* Loop to numerically integrate the equations *)
 For[i = 1, i ≤ maxiter, i++,
  Clear[ans, x, t, gr1, gr2];
  Case1 =
   NDSolve[{x1''[t] + (c1 + c2)/m1 x1'[t] - c2/m1 x2'[t] + (k1 + k2)/m1 x1[t] - k2/m1 x2[t] + h1/m1 x1[t]^3 + h2/m1 (x2[t] - x1[t])^3 == F0/m1 Cos[Ω x t],
     x2''[t] + c2/m2 x2'[t] - c2/m2 x1'[t] + k2/m2 x2[t] - k2/m2 x1[t] - h2/m2 (x2[t] - x1[t])^3 == 0, x1'[0] == x1vel, x1[0] == x1dis,
     x2'[0] == x2vel, x2[0] == x2dis}, {x1, x2}, {t, start, tz}, MaxSteps → Infinity, Method → RungeKutta,
    WorkingPrecision → 16, PrecisionGoal → ∞];

  (* Storing results into the array *)
  gr1 = Plot[Evaluate[x1[t] /. Case1], {t, start, tz}, DisplayFunction → Identity];
  a1[i, 1] = Ω;
  a1[i, 2] = HighestPeak[gr1][[2]];

  gr2 = Plot[Evaluate[x2[t] /. Case1], {t, start, tz}, DisplayFunction → Identity];
  a2[i, 1] = Ω;
  a2[i, 2] = HighestPeak[gr2][[2]];

  (* Assigning last velocity & displacement to be used for next calculation loop *)
  x1vel = Evaluate[x1'[tz] /. Case1][[1]];
  x1dis = Evaluate[x1[tz] /. Case1][[1]];
  x2vel = Evaluate[x2'[tz] /. Case1][[1]];
  x2dis = Evaluate[x2[tz] /. Case1][[1]];

  Ω = Ω + Ωstep;
 ]]

(* Storing data into harddisk *)
SetDirectory["c:\mdata"];
Export["a1_h2=100-Z1.dat", result1, "CSV"];
Export["a2_h2=100-Z1.dat", result2, "CSV"];

(* Displays numerical results *)
result1
result2

(* Displays graphical results - Without Lines *)
ListPlot[result1, Frame → True, FrameTicks → Automatic, GridLines → None,
  FrameLabel → {"Frequency, Ω [rad/s]" , x1 [metres]} ];
ListPlot[result2, Frame → True, FrameTicks → Automatic, GridLines → None,
  FrameLabel → {"Frequency, Ω [rad/s]" , x2 [metres]} ];

(* Displays graphical results - With Lines *)
ListPlot[result1, PlotJoined → True, Frame → True, FrameTicks → Automatic, GridLines → None,
  FrameLabel → {"Frequency, Ω [rad/s]" , x1 [metres]} ];
ListPlot[result2, PlotJoined → True, Frame → True, FrameTicks → Automatic, GridLines → None,
  FrameLabel → {"Frequency, Ω [rad/s]" , x2 [metres]} ];
```

D.2 Definition of the Program Code

The different sections of the code (in Appendix D.1) are defined here in details:

- Initially it is necessary to clear all the variables to zero before running the program.

- All the constants such as the masses, damping coefficients, linear and cubic stiffnesses, and excitation force are defined next. Other constants that are also defined are the start value for the excitation frequency (Ω), frequency step size (Ωstep), number of iterations (maxiter), integration start time (start), and end time (tz). The integration start time is defined with a large value to ensure that the system is in steady-state.

- In a nonlinear frequency-response analysis it is common to do a sweep up and down over a range of frequencies. This results in an implied unstable region of the system defined by an enclosure of the upward and downward jumps. To achieve the downward frequency sweep the frequency step-size is required to be negative.

- Two arrays are defined for storing the results of the amplitudes x_1 and x_2 in an appropriate format.

- *(*Function to extract the highest peak from the graph*)*

  This function *HighestPeak[gr_]* is used to automatically extract the highest peak value of the graph plotted between the integration start time and end time. This value is used as the assumed steady-state value for plotting a point in the frequency-response graph.

- Next all the initial response values are set to zero.

- *(*Loop to numerically integrate the solutions*)*

  This section uses the powerful *NDSolve[ ]* function within *Mathematica* to integrate numerically the two equations of motion. The method used is as specifically stated in the code: Method → RungeKutta . The integration is repeated for a total of *maxiter* number of times. *NDSolve[ ]* can potentially use a wide variety of other integration methodologies such as the Adams method, Gear method, and Gel'fand-Lokutsiyevskii chasing method.

- *(* Storing results into the array *)*

  The highest peak value of the result from the numerical integration is extracted and stored into an array with its respective frequency.

- *(*Assigining last velocity & displacement to be used for next calculation loop*)*

  This is an important sub-section because at each frequency step the previous displacement and velocity are assigned as the next initialised response values, in order to construct a frequency domain.

- Following on from this the two arrays are subsequently stored to the hard disk in 'CSV' (Comma-Separated Values) format for extraction of data to *MS Excel* for more detailed plotting of graphs. The contents of the two arrays are displayed and the response displacements for x_1 and x_2 are plotted as individual frequency domain points, after which inter-point interpolation is carried out by means of the internal *Mathematica* operation, $\text{PlotJoined} \rightarrow \text{True}$.

APPENDIX E

DYNAMICS 2 COMMANDS

E.1 General

* : to get help with commands
(e.g. *MM – help with main menu)

. : pauses the program after plotting one dot.
<space bar> returns the program to normal

& : Cycle through the most important menus

<Enter> : Fetch previous menu

<Esc> : current routine terminates or fetches parent menu of current menu

<space bar> : removes menu and continues plotting

<Tab> : prints the speed (in dots per second) and a selection of parameter values.

dynamics : Starts the program

MM : Main menu

C : clear screen & core memory

R : refresh screen

E.2 Colour

<F7> : decrease colour number by 1

<F8> : increase colour number by 1

<F9> : choose colour number

CT · displays colour table

E.3 Change Parameters:

PM : Parameter Menu

<+> : increase PRM (e.g. RHO) by the amount PS
(i.e. Parameter Step)

<-> : decrease PRM by the amount PS

<Home> or <Shift 3> : halve PS

<PgUp> or <Shift 4> : double PS

E.4 Crosses

<End> or <Shift 1> : halve step size for small cross

<PgDn> or <Shift 2> : double step size for small cross

K : big temporary cross shows y as trajectory is plotted

KK : draw permanent cross at y

KKK : permanent cross at each point as trajectory is plotted

KK1 : draw permanent cross at y1

KKS : set size of permanent cross

E.5 Display

BXM : Box Menu

B : draws a box around the screen

B1 : draws a box with tic marks - *use **while** the pic is plotted*

B2 : draws a box with double tic marks - *to get BIFR scale*

B20 : draws a box with double tic marks but no numbers

ROT : rotates picture 90 deg. clockwise

FLIPH : flips picture horizontally

FLIPV : flips picture vertically

XAX, YAX : draws the x-axis & y-axis respectively

XAX1, YAX1 : draws the x-axis & y-axis respectively with 1 tic mark

XAX2, YAX2 : draws the x-axis & y-axis respectively with 2 tic marks

XS : change X-axis scale (i.e. **XS**<Enter> **-2 2**<Enter>)

YS : change Y-axis scale

E.6 Plotting

I : initialize y using y1

II : initialize and iterate

CON : connects consecutive dots

PT : toggle 'Plot Time' to have time on the horizontal axis

T : plots the trajectory

E.7 Storing

TD : to disk

FD : from disk

AFD : add from disk – adds the old picture onto the screen

E.8 Window Parameters

OW

OW1, OW2 ..OW4

<F1> : upper left

<F2> : upper right

<F3> : lower left

<F4> : lower right

<F10> : whole screen

E.9 Lyapunov Commands

L : sets number of Lyapunov exponents $(0 \le L \le 2)$ to be computed.

LL : prints the current values of the Lyapunov exponents, numbers and dimension on the screen.

E.10 Bifurcation Commands

BIFM : Bifurcation Diagram Menu

BIFD : sets the number of dots to be plotted (per horizontal line).

BIFI : re-initialise y for each parameter

BIFP : toggle the printing of parameter values.

BIFPI : sets the number of pre-iterates.

BIFR : specifying range of the bifurcation parameter (e.g. RHO).

BIFS : plots bifurcation diagram on screen.

BIFV : for higher quality picture
(recommend 720 horizontal lines per page, screen has 480 l/pg. Space between each horizontal line plotted => higher = closer)

PRM : parameter to be varied

E.11 Procedures

Finding a Fixed Point:

1) **II** <Enter>
2) Use arrow keys to move the small cross to be together with the big cross.
3) **YV**<Enter>
4) Fixed point is displayed

Computation of Lyapunov Dimension and Exponents:

1) Set the number of Lyapunov exponents to be computed (command **L**)

2) Plot trajectory (command **T**, or **SST**, or **BST** etc)

Optional:

- Set Text Level to be 2 to speed up computation (command **T2**).
- Use "List Lyapunov exponents and numbers" command **LL** to get current estimates of the Lyapunov exponents and Lyapunov numbers.

Plotting of Lyapunov Exponents versus Time

1) Set the number of Lyapunov exponents to be computed (command **L**)
2) Set the horizontal axis for the time scale (command **XS**)
3) Set the vertical axis for the range of Lyapunov exponents (command **YS**)
4) Set the number of exponents to be computed (command **L**)
5) Turn the toggle **PT** on (command **PT**)
6) Start a process like **T** or **SST**.

Computation of Bifurcation Diagram:

1) Set the X Scale (command **XS**)
2) Set the PaRaMeter to be varied (command **PRM**)
3) Set the BIFurcation Range (command **BIFR**)
4) Set the number of BIFurcation Pre-Iterates (command **BIFPI**)
5) Set the number of BIFurcation Dots (command **BIFD**)
6) Set the number of BIFurcation Values (command **BIFV**)
7) Set the number of BIFurcations Initializations (command **BIFI**);

   If BIFI > 1, then set vectors ya and yb appropriately.
8) Plot the BIFurcation diagram (on the screen) (commands **BIFS**, **BIF**).

Plotting of Lyapunov Exponent Bifurcation Diagram:

1) Set the number of Lyapunov exponents to be computed (command **L**)
2) Set the horizontal axis for the range of the Lyapunov exponents (command **XS**)
3) Set the PaRaMeter to be varied (command **PRM**)
4) Set the vertical axis for the range of the parameter to be varied (command **BIFR**)
5) Set the number of parameter values (command **BIFV**)
6) Set the length of the transient time interval (command **BIFPI**)
7) Set the length of the time interval for the approximate Lyapunov exponents to be plotted (command **BIFD**)
8) Set the Screen Diameter to a higher value (command **SD**)
9) Optional : Connect the consecutive dots (command **CON**)
10) Plot the Lyapunov exponents (command **BIFS** or **BIF**)

E.12 Adding OWN Differential Equation:

Documentation window

The Documentation window provides text that will appear whenever the Main Menu or Parameter Menu is called.

Vector field window

The differential equations to be added are written in the Vector field window. Refering to Figure 5-1,

Line 5: The period is defined as 2*pi/phi.

Line 6: Definition of time

Line 7: Assigning x' to u

Line 8: Assigning y' to v

Line 9-11: The two differential equations of equations (3.3-1) and (3.3-2) are defined here in this window as !EOM1 and !EOM2

Initialisation window

This window is to define and initialise all the variables and the step sized used by the differential equation solver .

Line 12: All the initial response values of the system is set to zero here. (i.e. time, displacement and velocity)

Line 13: Defining the coordinates to be plotted

The program makes a list in alphabetical order of the variables that are defined and assigns to them to y[0], y[1], y[2], ... For example, in the code of Figure 5-1, y[0]=s; y[1]=t; y[2]=x'; y[3]=y'; y[4]=x; y[5]=y. Therefore, XCO:=4 YCO:=2 is defining the x- and y-axis as x and x' respectively.

Line 14: Defining the scale of both the x- and y-axis.

Line 15: Defining the stiffness variables, k where,

$c1=k_1/m_1$; $c2=k_2/m_1$; $c3=k_2/m_2$;

Line 16: Defining the damping variables, c where,

$c4=c_1/m_1$; $c5=c_2/m_1$; $c6=c_2/m_2$;

Line 17: Defining the nonlinear cubic variables, h where,

$c7=h_1/m_1$; $c8=h_2/m_1$; $c9=h_2/m_2$;

Line 18: Defining the force, F and frequency, Ω where,

$rho=F/m_1$; $phi=\Omega$

Line 19: SPC is Steps Per Cycle. This is to define the period of the forcing which is 2π/phi (also true in several cases).

Line 20: IPP is to set Iterates Per Plot. The process is iterated IPP times before each plot. If SPC is set to 2000, then setting IPP to 2000 will mean that one point is plotted for every cycle.

Modulo window

The use of the modulo window is optional. The equation(s) in this window are applied after each time step of the differential equation solver.

E.13 Tips on Using Dynamics 2

SPC : (Default = 30)

- Is the number of differential equation steps in one period of the forcing period.
- It must not be small!
- The larger the value, the more accurate the solution and less fuzzy.

IPP : (Default = 30)

- If IPP=1, then T plots every time step.
- If IPP=SPC, then T is a Poincaré return map, it plots one point per cycle.
- For Time and Phase Plots, set IPP=1.
- For Bifurcation and Lyapunov diagrams, set SPC=IPP.

BIFD : (Default =200)

- Sets the number of dots to be plotted per horizontal line.
- Higher resolution the better.

BIFV : (Default = 480)

- Controls the quality of the picture.
- Space between each horizontal line plotted => higher = closer.
- Recommends 720 horizontal lines per page, screen has 480 l/pg.

BIFPI : (Default = 60)

- For Lyapunov diagrams, BIFPI=10000.
- For Bifurcation diagrams, BIFPI=10000.

PI : (Default = 60)

- For Poincaré maps, Phase and Time Plots, set PI=0.

E.14 Comparison:

Example of Henon Map - Chapter 2

- Henon map is $(x, y) \Rightarrow (\rho - x^2 + c_1 y\ ,\ x)$

- Default values: $\rho = 2.12\ ,\ c_1 = -0.3\ ,\ x[0] = 0.0\ ,\ y[0] = 2.0$

- Comparison of Computationally & Manually:

Dot	*Dynamics 2* Program		Manually	
	x	y	x	y
#1	1.52	0	1.52	0
#2	-0.1904	1.52	-0.1904	1.52
#3	1.6277	-0.1904	1.6277	-0.1904
#4	-0.4724	1.6277	-0.4724	1.6277

APPENDIX F

FURTHER WORK

F.1 Obtaining the Characteristics of the Nonlinear Softening Spring

The characteristics of the nonlinear softening spring were obtained for use in the analytical and numerical computations. A compression test using a Lloyd Testing Machine was carried out on the nonlinear softening spring. The experimental curve was then curve fitted by means of the equation below (refer to Figure F-1):

$$y = -1200000000\,x^3 + 52986\,x \qquad \textbf{(F.1-1)}$$

Therefore, the stiffnesses of the spring can be extracted as being,

$$k_2 = 52.986\,\text{kN/m} \quad ; \quad h_2 = 1.2\times10^9 = 1.2\,\text{GN/m}^3$$

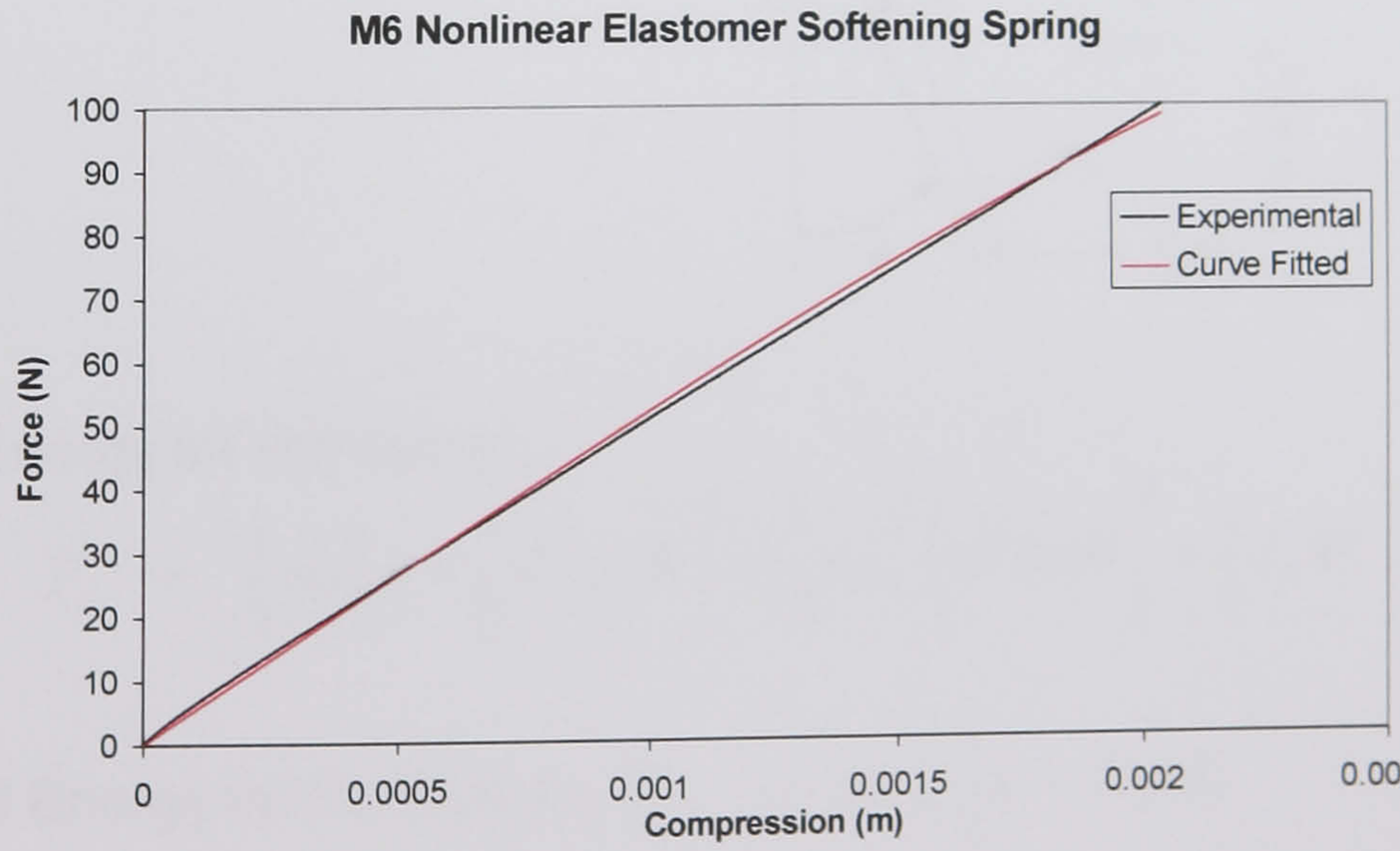

Figure F-1: Curve fitting the experimental curve of the nonlinear softening spring

F.2 Inertia Coupled System (Physical Coordinates)

For the Block:

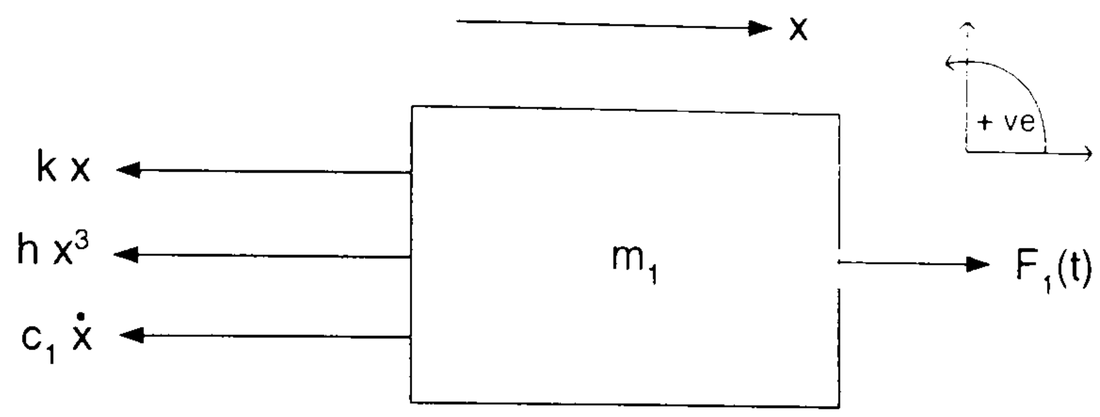

Kinetic Energy for Block, $T_b = \frac{1}{2} m_1 \dot{x}^2$ **(F.2-1)**

Potential Energy for Block, $U_b = \frac{1}{2} k x^2 + \frac{1}{4} h x^4$ **(F.2-2)**

For the Pendulum:

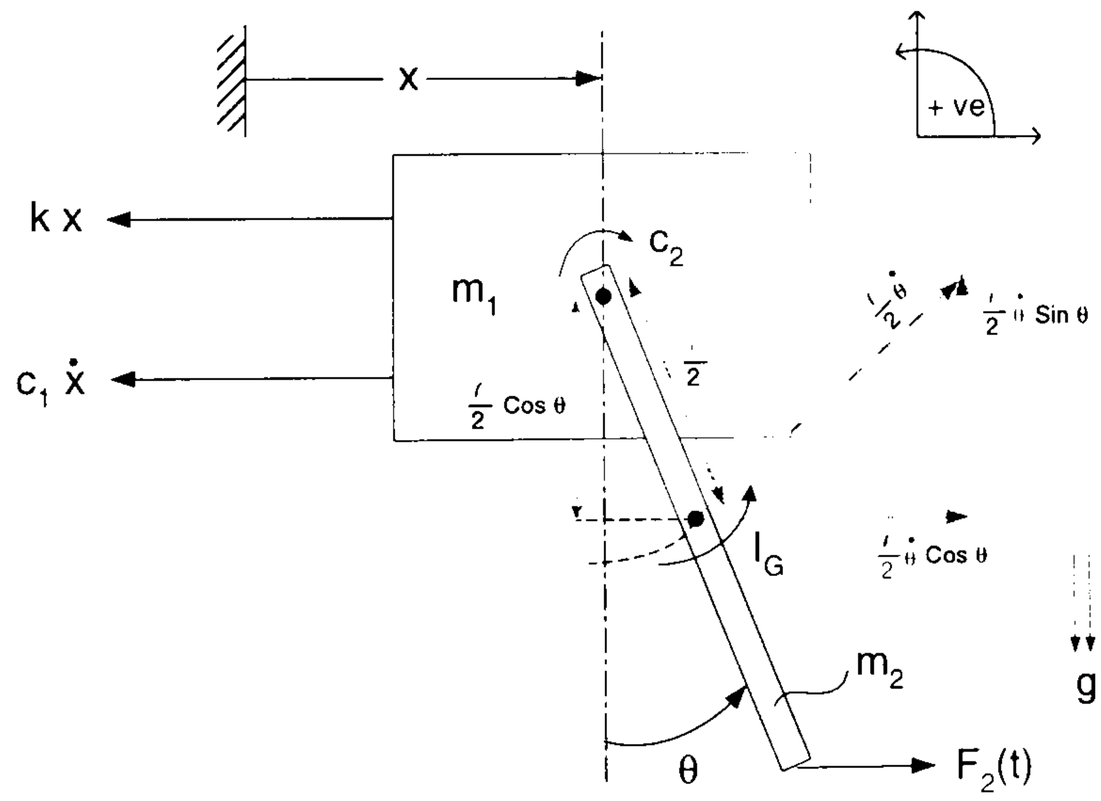

Kinetic Energy for Pendulum,

$$T_p = \frac{1}{2} m_2 \left(\dot{x} + \frac{l}{2} \dot{\theta}\, Cos\theta \right)^2 + \frac{1}{2} m_2 \left(\frac{l}{2} \dot{\theta}\, Sin\theta \right)^2 + \frac{1}{2} I_G \dot{\theta}^2 \qquad \textbf{(F.2-3)}$$

Potential Energy for Pendulum, $U_p = m_2\, g\, \frac{l}{2} (1 - Cos\theta)$ **(F.2-4)**

Kinetic energy for the whole system:

$$\begin{aligned} T &= T_b + T_p \\ &= \frac{1}{2} m_1 \dot{x}^2 + \frac{1}{2} m_2 \left(\dot{x} + \frac{l}{2} \dot{\theta}\, Cos\theta \right)^2 + \frac{1}{2} m_2 \left(\frac{l}{2} \dot{\theta}\, Sin\theta \right)^2 + \frac{1}{2} I_G \dot{\theta}^2 \\ &= \frac{1}{2} m_1 \dot{x}^2 + \frac{1}{2} m_2 \left[\dot{x}^2 + l\, \dot{x}\, \dot{\theta} Cos\theta + \frac{l^2}{4} \dot{\theta}^2 Cos^2\theta + \frac{l}{4} \dot{\theta}^2 Sin^2\theta \right] + \frac{1}{24} m_2 l^2 \dot{\theta}^2 \\ &= \frac{1}{2} m_1 \dot{x}^2 + \frac{1}{24} m_2 l^2 \dot{\theta}^2 + \frac{1}{2} m_2 \dot{x}^2 + \frac{1}{2} m_2\, l\, \dot{x}\, \dot{\theta} Cos\theta + \frac{1}{8} m_2 l^2 \dot{\theta}^2 Cos^2\theta + \frac{1}{8} m_2 l^2 \dot{\theta}^2 Sin^2\theta \\ &= \frac{1}{2} m_1 \dot{x}^2 + \frac{1}{24} m_2 l^2 \dot{\theta}^2 + \frac{1}{2} m_2 \dot{x}^2 + \frac{1}{2} m_2\, l\, \dot{x}\, \dot{\theta} Cos\theta + \frac{1}{8} m_2 l^2 \dot{\theta}^2 \\ &= \frac{1}{2} (m_1 + m_2) \dot{x}^2 + \frac{1}{6} m_2 l^2 \dot{\theta}^2 + \frac{1}{2} m_2\, l\, \dot{x}\, \dot{\theta} Cos\theta \end{aligned} \qquad \textbf{(F.2-5)}$$

Potential energy for the whole system:

$$\begin{aligned} U &= U_b + U_p \\ &= \frac{1}{2} k\, x^2 + \frac{1}{4} h\, x^4 + m_2\, g\, \frac{l}{2} (1 - Cos\theta) \end{aligned} \qquad \textbf{(F.2-6)}$$

$$\begin{aligned} L &= T - U \\ &= \frac{1}{2} (m_1 + m_2) \dot{x}^2 + \frac{1}{6} m_2 l^2 \dot{\theta}^2 + \frac{1}{2} m_2\, l\, \dot{x}\, \dot{\theta} Cos\theta - \frac{1}{2} k\, x^2 - \frac{1}{4} h\, x^4 - m_2\, g\, \frac{l}{2} (1 - Cos\theta) \\ &= \frac{1}{2} (m_1 + m_2) \dot{x}^2 + \frac{1}{6} m_2 l^2 \dot{\theta}^2 + \frac{1}{2} m_2\, l\, \dot{x}\, \dot{\theta} Cos\theta - \frac{1}{2} k\, x^2 - \frac{1}{4} h\, x^4 - m_2\, g\, \frac{l}{2} + m_2\, g\, \frac{l}{2} Cos\theta \end{aligned} \qquad \textbf{(F.2-7)}$$

The 2 equations of motion for the dynamically coupled system are conveniently set up using Lagrange's equations,

$$\frac{d}{dt} \left(\frac{\partial L}{\partial \dot{q}_i} \right) - \frac{\partial L}{\partial q_i} = Q_{bj.pj} \qquad \textbf{(F.2-8)}$$

where

$q_1 = x$; $q_2 = \theta$; $L = T - U$; $b : block$; $p : pendulum$ $j : 1, 2, 3\ (Cases\ of\ Excitation)$

For $q_1 = x$:

$$\frac{\partial L}{\partial \dot{x}} = (m_1 + m_2)\dot{x} + \frac{m_2 l}{2}\dot{\theta}\,Cos\theta$$

$$\frac{d}{dt}\left(\frac{\partial L}{\partial \dot{x}}\right) = (m_1 + m_2)\ddot{x} + \frac{m_2 l}{2}\ddot{\theta}\,Cos\theta - \frac{m_2 l}{2}\dot{\theta}^2\,Sin\theta$$

$$\frac{\partial L}{\partial x} = -k\,x - h\,x^3$$

Therefore, using equation (F.2-8):

$$\frac{d}{dt}\left(\frac{\partial L}{\partial \dot{x}}\right) - \frac{\partial L}{\partial x} = Q_{hj}$$

$$(m_1 + m_2)\ddot{x} + \frac{m_2 l\,\ddot{\theta}}{2}Cos\theta - \frac{m_2 l\,\dot{\theta}^2}{2}Sin\theta + k\,x + h\,x^3 = Q_{hj} \qquad \textbf{(F.2-9)}$$

For $q_2 = \theta$:

$$\frac{\partial L}{\partial \dot{\theta}} = \frac{m_2 l^2}{3}\dot{\theta} + \frac{m_2 l}{2}\dot{x}\,Cos\theta$$

$$\frac{d}{dt}\left(\frac{\partial L}{\partial \dot{\theta}}\right) = \frac{m_2 l^2}{3}\ddot{\theta} + \frac{m_2 l}{2}Cos\theta\,\ddot{x} - \frac{m_2 l}{2}Sin\theta\,\dot{\theta}\,\dot{x}$$

$$\frac{\partial L}{\partial \theta} = -\frac{m_2 l}{2}Sin\theta\,\dot{\theta}\,\dot{x} - \frac{m_2 g l}{2}Sin\theta$$

Therefore, using Equation (F.2-8):

$$\frac{d}{dt}\left(\frac{\partial L}{\partial \dot{\theta}}\right) - \frac{\partial L}{\partial \theta} = Q_{pj}$$

$$\frac{m_2 l^2}{3}\ddot{\theta} + \frac{m_2 l\,\ddot{x}}{2}Cos\theta - \frac{m_2 l}{2}Sin\theta\,\dot{\theta}\,\dot{x} + \frac{m_2 l}{2}Sin\theta\,\dot{\theta}\,\dot{x} + \frac{m_2 g l}{2}Sin\theta = Q_{pj}$$

$$\frac{m_2 l^2}{3}\ddot{\theta} + \frac{m_2 l\,\ddot{x}}{2}Cos\theta + \frac{m_2 g l}{2}Sin\theta = Q_{pj} \qquad \textbf{(F.2-10)}$$

Restating the 2 equations of motion (i.e. equations (F.2-9) & (F.2-10)):

$$(m_1 + m_2)\ddot{x} + \frac{m_2 l\,\ddot{\theta}}{2}Cos\theta - \frac{m_2 l\,\dot{\theta}^2}{2}Sin\theta + k\,x + h\,x^3 = Q_{hj}$$

$$\frac{m_2 l^2}{3}\ddot{\theta} + \frac{m_2 l\,\ddot{x}}{2}Cos\theta + \frac{m_2 g l}{2}Sin\theta = Q_{pj}$$

Generalised Forces for the System (3 Cases):

Case 1 : Single force applied at the mass m_1 only

Thus, $Q_{x1} = F_1(t)$

$Q_{\theta 1} = 0$

Case 2 : Single force applied at the free end of the pendulum only

(i) Thus, $Q_{x2} = F_2(t)$

(ii) Thus, $Q_{\theta 2} = F_2(t) l\, Cos\theta$

Case 3 : Forces applied at the free end of the pendulum and to the mass m_1

Because it's a combination of Case 1 & 2:

$$Q_{x3} = Q_{x1} + Q_{x2}$$
$$= F_1(t) + F_2(t)$$

$$Q_{\theta 3} = Q_{\theta 1} + Q_{\theta 2}$$
$$= F_2(t) l\, Cos\theta$$

Equations of Motions

Generalised Forces for Block,

Case 1 (Block only) : $Q_{b1} = F_1(t) - c_1 \dot{x}$

Case 2 (Pendulum only) : $Q_{b2} = F_2(t) - c_1 \dot{x}$

Case 3 (Block + Pendulum) : $Q_{b3} = F_1(t) + F_2(t) - c_1 \dot{x}$

Generalised Forces for Pendulum,

Case 2 (Block only) : $Q_{p1} = -c_2 l^2 \dot{\theta}$

Case 1 (Pendulum only) : $Q_{p2} = F_2(t) l Cos\theta - c_2 l^2 \dot{\theta}$

Case 3 (Block + Pendulum) : $Q_{p3} = F_2(t) l Cos\theta - c_2 l^2 \dot{\theta}$

Case 1 : Single force applied at the mass m_1 only

$$(m_1 + m_2)\ddot{x} + \frac{m_2 l \ddot{\theta}}{2} Cos\theta - \frac{m_2 l \dot{\theta}^2}{2} Sin\theta + k x + h x^3 = Q_{b1}$$

$$\boxed{(m_1 + m_2)\ddot{x} + \frac{m_2 l \ddot{\theta}}{2} Cos\theta + c_1 \dot{x} + k x + h x^3 - \frac{m_2 l \dot{\theta}^2}{2} Sin\theta = F_1(t)} \quad \textbf{(F.2-11)}$$

$$\frac{m_2 l^2}{3}\ddot{\theta} + \frac{m_2 l \ddot{x}}{2} Cos\theta + \frac{m_2 g l}{2} Sin\theta = Q_{p1}$$

$$\boxed{\frac{m_2 l^2}{3}\ddot{\theta} + \frac{m_2 l \ddot{x}}{2} Cos\theta + c_2 l^2 \dot{\theta} + \frac{m_2 g l}{2} Sin\theta = 0} \quad \textbf{(F.2-12)}$$

$$\therefore \quad \omega_1 = \sqrt{\frac{k}{m_1 + m_2}} \qquad and \qquad \omega_2 = \sqrt{\frac{3g}{2l}} \quad \textbf{(F.2-13)}$$

Case 2 : Single force applied at the free end of the pendulum only

$$(m_1 + m_2)\ddot{x} + \frac{m_2 l \ddot{\theta}}{2} Cos\theta - \frac{m_2 l \dot{\theta}^2}{2} Sin\theta + k x + h x^3 = Q_{p2}$$

$$\boxed{(m_1 + m_2)\ddot{x} + \frac{m_2 l \ddot{\theta}}{2} Cos\theta + c_1 \dot{x} + k x + h x^3 - \frac{m_2 l \dot{\theta}^2}{2} Sin\theta = F_2(t)} \quad \textbf{(F.2-14)}$$

$$\frac{m_2 l^2}{3}\ddot{\theta} + \frac{m_2 l\,\ddot{x}}{2}Cos\theta + \frac{m_2 gl}{2}Sin\theta \quad = \quad Q_{p2}$$

$$\boxed{\frac{m_2 l^2}{3}\ddot{\theta} + \frac{m_2 l\,\ddot{x}}{2}Cos\theta + c_2 l^2\,\dot{\theta} + \frac{m_2 gl}{2}Sin\theta \quad = \quad F_2(t)\,l\,Cos\theta} \qquad \textbf{(F.2-15)}$$

$$\therefore \quad \omega_1 = \sqrt{\frac{k}{m_1 + m_2}} \qquad and \qquad \omega_2 = \sqrt{\frac{3g}{2l}}$$

Case 3 : Forces applied at the free end of the pendulum and to the mass m_1

$$(m_1 + m_2)\,\ddot{x} + \frac{m_2 l\,\ddot{\theta}}{2}Cos\theta - \frac{m_2 l\,\dot{\theta}^2}{2}Sin\theta + k\,x \quad = \quad Q_{b3}$$

$$\boxed{(m_1 + m_2)\,\ddot{x} + \frac{m_2 l\,\ddot{\theta}}{2}Cos\theta + c_1\,\dot{x} + k\,x + h\,x^3 - \frac{m_2 l\,\dot{\theta}^2}{2}Sin\theta \quad = \quad F_1(t) + F_2(t)} \qquad \textbf{(F.2-16)}$$

$$\frac{m_2 l^2}{3}\ddot{\theta} + \frac{m_2 l\,\ddot{x}}{2}Cos\theta + \frac{m_2 gl}{2}Sin\theta \quad = \quad Q_{p2}$$

$$\boxed{\frac{m_2 l^2}{3}\ddot{\theta} + \frac{m_2 l\,\ddot{x}}{2}Cos\theta + c_2 l^2\,\dot{\theta} + \frac{m_2 gl}{2}Sin\theta \quad = \quad F_2(t)\,l\,Cos\theta} \qquad \textbf{(F.2-17)}$$

$$\therefore \quad \omega_1 = \sqrt{\frac{k}{m_1 + m_2}} \qquad and \qquad \omega_2 = \sqrt{\frac{3g}{2l}}$$

For large deflections (i.e. nonlinearities), using the Maclaurin series to expand the trigonometrical functions prior to nondimensionalisation:

$$Sin\theta = \theta - \frac{\theta^3}{3!} + \frac{\theta^5}{5!} + \cdots\cdots$$

$$Cos\theta = 1 - \frac{\theta^2}{2!} + \frac{\theta^4}{4!} + \cdots\cdots$$

By assuming the pendulum rotations to be finite, but not very large, then these become:

$$Sin\theta \approx \theta - \frac{\theta^3}{6} \qquad \textbf{(F.2-18)}$$

$$Cos\theta \approx 1 - \frac{\theta^2}{2} \qquad \textbf{(F.2-19)}$$

GLASGOW UNIVERSITY LIBRARY